Mass Spectrometry-based Metabolomics as a tool for biomarker discovery and diagnosing metabolic health

A thesis submitted in fulfilment of the requirements for the degree of

Doctor of Philosophy

in

Nutritional Science

by

Zhanxuan Wu

School of Health Science

Massy University

Palmerston North

New Zealand

2021

Abstract

Although obesity and prediabetes have been long-established risk factors for type 2 diabetes (T2D), excess fat deposition in visceral and ectopic organ sites (i.e. the “risky” fat depot) has been increasingly recognised as key conduits for T2D. However, quantification of these fat depots relies on expensive and time-consuming imaging techniques. There is a need for identification of biomarkers predictive of risky fat depot levels.

Metabolomics is a promising tool for discovering novel markers and generating mechanistic speculation. This PhD project aims to identify and understand plasma metabolite markers associated with metabolic risk factors including elevated fasting plasma glucose (FPG), fat deposition in visceral (VAT) and ectopic organ sites (liver and pancreas) in non-T2D human. To achieve this, a workflow to select the optimal injected concentration of different sample types for two complementary LC-MS untargeted analyses (polar metabolites and lipidomics) was established and applied to examine the value of measuring the plasma metabolome as a proxy for metabolite concentrations in various tissue sites including adipose tissue, muscle and the liver. Lastly, plasma metabolomic signatures for elevated FPG and VAT were characterised and metabolite markers predictive of VAT and ectopic fat deposition in the liver and pancreas were identified.

This PhD study highlighted the critical importance in optimising injected concentration for LC-MS analysis of different sample types to ensure the maximal number of linear features were obtained, and for the first time showed the plasma metabolomics profile was more reflective of the liver profile than muscle or

adipose tissue. Subsequent metabolomics characterisation of clinical plasma samples reported profound associations between FPG or VAT with changes in several glycerolipid species independent of gender, ethnicity, age and body mass index (BMI). VAT was additionally associated with changes in phospholipid, ether-linked phospholipid and sphingolipid species independent of covariates. Liver fat deposition was predicted by a number of glycerolipid, phosphatidylethanolamine and dihydroceramide lipid species whose plasma concentrations were linearly correlated with the liver counterparts. A novel marker, sulfolithocholic acid, for the prediction of pancreatic fat independent of age, BMI and visceral adiposity was also identified. Finally, the study also reported an improved prediction of ectopic fat deposition by utilising a panel of metabolite markers compared to clinical measurements, and demonstrated the usefulness of the metabolomic signature to identify a subset of normoglycaemic individuals with a worse cardiometabolic profile. Findings from this PhD study highlighted the value of metabolomics as a promising tool to capture metabolic risk, and that candidate markers identified by metabolomics may offer opportunities for improved risk prediction and stratification, disease progression monitoring and to develop alternative means for the measurement of the effectiveness of dietary interventions.

Acknowledgements

First of all, I am deeply grateful to all my supervisors for the incredible amount of support, expertise, guidance and motivation they have provided throughout my PhD journey. They have played irreplaceable roles in guiding me to shape my thinking style, skills and knowledge for conducting research. Dr Karl Fraser, the one who introduced me to the fascinating world of metabolomics, has always been patient, knowledgeable, and open-minded to keep me think both critically and creatively. He was always there for me, to share his knowledge and dissect problems, and with his assistance this challenging subject became much more enticing to me. I would also like to thank Professor Sally Poppitt from the University of Auckland, without whose original idea this research project and position would not have been possible. I appreciate the patience, time and active participation of her into the explanation and discussion of this project. Her challenging questioning style has always guided me to think outside the box and think of the bigger picture. I would also like to express my gratitude to my primary supervisor at Massey University, Professor Marlena Kruger, whose trust in my competence and effort gave me the confidence, determination and motivation required to reach the end of the journey and complete this PhD study.

Secondly, I would like to thank the former technician at AgResearch, Dr Heike Schwendel, for her technical assistance and guidance on the LCMS instrumental analysis. I would also like to thank Dr Arvind Subbaraj, Dr Matthew Barnett, Dr Scott Knowles and Prof Alastair Ross at AgResearch for generously providing comments and suggestions on my research outputs including manuscripts, abstracts, posters, and conference presentations. I am grateful to all co-authors

and collaborators associated with this project (Dr Ivana Sequeira, Mr Wilson Yip, Dr Louise Lu, Dr Lindsay Plank, Dr Rinki Murphy, Prof Garth Cooper, Dr Jean-Charles Martin, Dr Kieren Hollingsworth and Dr Anne-Thea McGill), for their efforts, contributions, inputs and ideas, without whom the completion of this PhD project would not have been possible.

I would also like to extend my appreciation to the Ministry of Business, Innovation and Employment, New Zealand and AgResearch for financially supporting my project and my PhD scholarship.

Finally, I want to thank my family and my loving partner Huan, for always being there for me and providing an incredible amount of support and encouragement, helping me to stay strong and focused when going through rough patches.

Table of Contents

List of figures

List of tables

Abbreviations

2-h PG	2-hour plasma glucose
AA	Amino acids
AAA	Aromatic amino acid
AAT	Abdominal adipose tissue
AC	Acylcarnitine
ADA	American Diabetes Association
AGE	Advanced glycation end-product
ALP	Alkaline phosphatase
ALT	Alanine transaminase
AST	Aspartate transaminase
AT	Adipose tissue
BA	Bile acid
BCAA	Branched chain amino acids
BMI	Body mass index
CE	Cholesteryl ester
Cer	Ceramide
CHO	Carbohydrate
CT	Computed tomography
CV	Coefficient of variation
CVD	Cardiovascular disease
D5D	Delta-5-desaturase
D6D	Delta-6-desaturase
DBP	Diastolic blood pressure
DG	Diglyceride
dhCer	Dihydroceramide
DNL	De novo lipogenesis
DSA	Deep Subcutaneous Abdominal adipose tissue
DXA	Dual energy X-ray absorptiometry
EIC	Extracted ion chromatograms
ER	Endoplasmic reticulum
ESI	Electrospray ionisation
FA	Fatty acid
FAO	Fatty acid oxidation
FFA	Free fatty acid
FOXO1	Forkhead box protein O1
FPG	Fasting plasma glucose
Gcer	Glycosphingolipid
GGT	Gamma-glutamyltransferase
GIP	Gastric inhibitory polypeptide
GL	Glycerolipid
GLP-1	Glucagon-like peptide-1
GM	GM3 ganglioside
GP	Glycerophospholipid
GSIS	Glucose-stimulated insulin secretion

GSK	Glycogen synthase kinase
HbA1c	Hemoglobin A1C
HDL-C	High density lipoprotein-cholesterol
HexCer	Hexosylceramide
HILIC	Hydrophilic interaction chromatography
HMDB	Human metabolome database
HOMA2-IR	Homeostasis model assessment of insulin resistance
HOMA2-β	Homeostasis Model Assessment of β-cell function
HP	High-performance
IAA	Intra-Abdominal Adipose tissue
IDO1	Indoleamine 2,3-dioxygenase-1
IFG	Impaired fasting glucose
IGT	Impaired glucose tolerance
IR	Insulin resistance
IRS	Insulin receptor substrate
JNK	C-Jun amino-terminal kinase
LA	Linoleic acid
LCAC	Long-chain acylcarnitine
LCAT	Lecithin-cholesterol acyltransferase
LC-MS	Liquid chromatography
LDL	Low density lipoprotein
LPC	Lysophosphatidylcholine
LPE	Lysophosphatidylethanolamine
MCAC	Medium-chain acylcarnitine
mIFG	Metabolomics-predicted IFG state
mNFG	Metabolomics-predicted NFG state
MRI	Magnetic resonance imaging
MRS	Magnetic resonance spectroscopy
MS	Mass spectrometry
mTORC1	Mammalian target of rapamycin complex 1
MUFA	Monounsaturated fatty acid
MUVR	Multivariate methods with Unbiased Variable selection in R
Mzdiff	*m/z* difference
n	Number
NAFLD	Non-alcoholic fatty liver disease
NASH	Non-alcoholic steatohepatitis
NFG	Normal fasting glucose
OA	Oleic acid
OGTT	Oral glucose tolerance test
PA	Palmitic acid
PC	Phosphatidylcholine
PDK1	3-phosphoinositide-dependent protein kinase 1
PE	Phosphatidylethnolamine
PE-NMe2	Dimethyl phosphatidylethanolamine
PG	Phosphatidylglycerol
PI	Phosphatidylinositol
PI3K	Phosphatidylinositol-3-kinase
PIP3	Phosphatidylinositol (3,4,5)-triphosphate

PK	Protein kinase
PLA2	Phospholipase A2
PLS	Partial least square
PLS-DA	Partial least squares-discriminant analysis
PPAR	Peroxisome proliferator-activated receptor
PPT	Phosphoprotein phosphatase
PUFA	Polyunsaturated fatty acid
Q2	Goodness of prediction
QC	Quality control
qTOF	Quadrupole Time-of-flight
r	Correlation coefficient
R2Y	Goodness of model fit
RAM	Rectus Abdominis Muscle
rdCV	Repeated-double cross-validation
RF	Random forest
RMSEcv	Root mean square error of cross-validation
ROS	Reactive oxygen species
RP	Reverse phase
RSD	Relative standard deviation
SAA	Subcutaneous Abdominal Adipose tissue
SAT	Subcutaneous adipose tissues
SBP	Systolic blood pressure
SCD	Stearoyl-CoA-desaturase
SFA	Saturated fatty acid
SM	Sphingomyelin
Snthresh	signal-to-noise ratio threshold
STA	Subcutaneous Thigh Adipose tissue
T2D	Type 2 diabetes
TAT	Tyrosine aminotransferase
TBF	Total body fat
TBL	Total body lean
TCA	Tricarboxylic acid cycle
TG	Triglyceride
TIC	Total Ion chromatograms
TMAO	Trimethylamine oxide
TNF	Tumor necrosis factor
TOFI	Thin-on-the-Outside-Fat-on-the-Inside
TRL	Triacylglycerol-rich lipoprotein
UHP	Ultra-high-performance
UP	Ultra-performance
Var	Variable
VAT	Visceral adipose tissue
VL	Vastus Lateralis
VLDL	Very low density lipoprotein
WC	Waist circumference
W-to-H ratio	Waist-to-hip ratio

1. Introduction

1.1 Background and scope

With the growing availability of highly processed less nutritious foods, changes in diet combined with a more sedentary lifestyle are leading to an increasing prevalence of type 2 diabetes (T2D) [1]. T2D is a complex metabolic disorder characterised by a high blood glucose concentration (hyperglycaemia), and it is defined by the American Diabetes Association (ADA) as a disease resulting from a progressive loss of adequate β-cell insulin secretion, frequently with the background of insulin resistance (IR) [2]. Worldwide, the number of people estimated to have diabetes in 2019 is 463 million (9.3% of the world's population), which has doubled since 1980 and is predicted to rise to 578 million (10.2%) by 2030, with T2D accounting for around 90% of the cases [3, 4]. T2D is associated with a cluster of metabolic abnormalities collectively known as cardiometabolic disease, mainly characterised by IR, dysglyceamia, dyslipidemia, hypertension, and central adiposity and predisposes individuals to development of cardiovascular diseases (CVD), as well as certain forms of cancers [5-8]. The long-term complications of T2D are major causes of morbidity, mortality, and exceptional healthcare costs, posing a heavy burden on the economy and healthcare system [9, 10]. The risk of individuals developing cardiometabolic diseases also increases with rising fasting plasma glucose (FPG) levels [11], even before reaching levels sufficient for a diabetes diagnosis (known as the "prediabetic" state [12]). The development of dysglycaemia is noticeably a progressive, preventable, and reversable process [13]. Although prediabetes is an intermediate state of the transition from normoglycaemia to T2D, predicting who will remain asymptomatic for years versus who will rapidly progress towards T2D onset and other CV complications is difficult based on FPG. Thus there is a

need for biomarkers to detect at-risk individuals, so that preventive measures and interventions can be applied to prevent disease onset.

Parallel and likely driving the T2D pandemic is a drastic rise in the prevalence of obesity and overweight, affecting over one-third of the global population [14]. Obesity is a condition where there is an excess accumulation of body fat, defined as having a body mass index (BMI) greater than 30 kg/m^2 (and BMI between 25 and 30 kg/m^2 for overweight) [15]. It is a well-established risk factor for T2D [16], but also independently increases the risk for other metabolic disorders, CVD and certain forms of cancers [17-19]. Physiological perturbations frequently encountered in obesity, including excess plasma free fatty acids (FFA) and chronic low-grade inflammation are causally linked to the development of IR [20], and IR lies central to the development of cardiometabolic diseases [21]. The term “diabesity” has thereafter been coined for to emphasise the strong interdependence between obesity and T2D and a concordant rise of their epidemics [22]. Despite so, many obese individuals remain free of the cardiometabolic disease throughout their life-course, whereas a substantial number of T2D patients are normal weight (BMI < 25) or stably overweight [23]. In addition, there is a large global variation in susceptibility to T2D, with certain ethnic groups like the South and East Asians developing T2D at a younger age and lower BMI compared with Caucasians [1, 24, 25]. These observations collectively challenged the idea that whole body obesity is the main aetiogical cause of T2D [22], and suggested factors other than BMI or total adiposity *per se*, underpin the development of cardiometabolic diseases.

Accumulating evidence revealed a strong association between abdominal adiposity and development of cardiometabolic diseases independent of total

adiposity. With the emergence of more available data and continuous refinement of the hypothesis over the past two decades [26, 27], it is now widely appreciated that excess visceral adipose tissue (i.e. visceral adiposity, VAT) and fat deposition in non-adipose tissue (i.e. ectopic fat deposition in organs such as liver, pancreas, muscle) are the key factors driving poor metabolic health and explaining the obesity heterogeneity [28, 29]. Visceral adiposity has been implicated in both IR and increased risks of developing cardiometabolic diseases independent of BMI [30, 31]. Patients with excess visceral fat have been characterised by poor glycaemic control, improper lipid profiles and inflammatory status regardless of their weights [32], and centrally obese patients at a normal BMI have a similar and possibly higher mortality risk compared with those at the overweight or obese BMI range [33]. Besides, this factor may also explain the inter-ethnic differences in the susceptibility to T2D development [34], with Asians being observed to have greater propensity to deposit fat in the abdominal region and ectopic sites compared with other ethnic groups [35-37]. Although excess visceral/ectopic fat deposition is now recognised as a major contributor to metabolic risk above and beyond BMI, the measurements rely on imaging techniques which are expensive and time-consuming, making its implementation into clinical practice challenging [29]. This again highlights the need for developing tools and new means to estimate levels of the “dangerous” fat depots and identify individuals with increased risk of poor metabolic health outcomes.

Metabolomics is a rapidly growing field in medical research that involves the comprehensive measurements of small molecule metabolites (<1000 Da) in biological specimens including bio-fluids, tissue and cells [38]. It is being used to study the relationship between the metabolomic profile and conditions of interest,

such as biological processes, diseases or interventions. Metabolites are the end-product of cellular processes. The levels and dynamics of metabolites can change substantially in response to subtle changes in genes, transcripts or protein levels, influenced by environmental factors at each cascade and providing an instantaneous snapshot of metabolic status. As such, this technique is well-suited for the study of cardiometabolic diseases which often involve a multitude of metabolic pathways and complex interplay between intrinsic and environmental factors [39]. Metabolomics has been increasingly applied to discover novel biomarkers and understand metabolic alterations in pathophysiological states [40]. Plasma is one of the most widely used sample types for metabolomics analysis as it is less invasive to obtain compared to tissue samples [41]. However, it represents an extracellular pool for different tissues and organs in a body, therefore a major gap in the current field is the relationship between the level of a biomarker in blood and in different tissues, and how reflective the biomarker is of the cellular abnormality. Untangling these relationships may improve the understanding of the biological implications and enhanced interpretability of these biomarkers (Chapters 3 and 4).

Prognostic biomarkers for T2D and discriminating metabolites between T2D/prediabetes and healthy states have been extensively studied and recently summarised in a systematic review [42]. In contrast, the metabolomic characterisation and biomarker discovery for VAT and ectopic fat deposition is still an emerging area. The search for biomarkers is ongoing, with expectations to identify more novel biomarkers, validate those previously reported by others, and gain a more comprehensive understanding of the metabolic pathways associated with VAT and ectopic fat deposition, as well as their molecular links

with the development of dysglycaemia (Chapters 5 and 6). In addition, given the striking observations of an outwardly slimmer T2D population and a greater susceptibility to abdominal obesity in South and East Asians than Caucasians, the underlying metabolic alterations associated with elevated FPG and excess VAT deposition highlights metabolic disparity between the two ethnic groups. The use of ethnicity-specific signatures characteristic for these metabolic traits may identify individuals with a current normoglycaemia state but worse metabolic risks (Chapter 5).

1.2 Aims

The overall aim of this PhD study is to characterise the metabolomic signatures and identify metabolite biomarkers associated with metabolic health. It is hypothesised that untargeted metabolomics can be applied to discover biomarkers correlated with clinical outcomes and metabolic risks including elevated levels of FPG, VAT and ectopic fat deposition; and that some of these metabolite markers are associated with metabolic risks independent of BMI. It is also hypothesised that tissue metabolomes are to some degree correlated with the blood metabolome and thus circulating metabolite markers may be used as a proxy for tissue.

Specific goals addressed in this PhD study include:

1) Optimise sample dilution factors for LC–MS untargeted metabolomics analysis of the tissue metabolome using animal tissues
2) Examine the relationship between the metabolome of plasma and various tissues including adipose tissues, muscle tissue and liver biopsy from humans

3) Identify and compare the ethnicity-specific signatures for fasting plasma glucose (FPG) concentration and the amount of visceral adipose tissue (VAT) assessed by Dual-energy X-ray absorptiometry (DXA) in a cohort of healthy and prediabetic Asian Chinese and Caucasian adults (cross-sectional TOFI_Asia study cohort)
4) Utilise the ethnicity-specific signatures for FPG and VAT to predict FPG state and characterise the cardiometabolic risk profile of the newly stratified groups based on the actual and predicted FPG state (cross-sectional TOFI_Asia study cohort)
5) Identify biomarkers for ectopic fat deposition in pancreas, liver and VAT/SAT ratio assessed by magnetic resonance imaging (MRI) and spectroscopy (MRS) techniques, and compare the performances of metabolite markers with those of clinical markers in a cohort of healthy and prediabetic Asian Chinese and Caucasian female (cross-sectional TOFI_study sub-cohort)

1.3 Thesis Outline

Chapter 1 provides an overview for the background of this PhD study, identifies research gaps attempted to be addressed and describes the overall aim and specific goals of this PhD study.

Chapter 2 reviews the pathophysiology of type 2 diabetes and the role of obesity and visceral adiposity in T2D development, introduces the basics of metabolomics and presents recent findings from its application to study obesity and T2D.

Chapter 3 highlights the need to optimise injected concentration prior to untargeted LC-MS metabolomics analysis and describes a workflow for the

determination of a suitable injected concentration using pig adipose tissue and liver as examples. This chapter addresses specific goal 1.

Manuscript contained in Chapter 3 has been published:

Wu, Z. E., Kruger, M. C., Cooper, G. J., Poppitt, S. D., & Fraser, K. (2019). Tissue-specific sample dilution: An important parameter to optimise prior to untargeted LC-MS metabolomics. Metabolites, 9(7), 124.

Chapter 4 applies the workflow established from the previous chapter to profile human plasma and various tissue types including 4 subtypes of adipose tissue, 2 subtypes of muscle and the liver in obese, non-T2D females, and correlate concentrations of plasma metabolites with the respective metabolites in these tissues to understand whether plasma metabolites can be used as a proxy for the concentration of metabolites in different tissues. This chapter addresses specific goal 2.

Chapter 5 reports and discusses plasma metabolomic signatures for the fasting plasma glucose concentration and visceral adiposity measured by Dual-energy X-ray absorptiometry expressed as % of total body fat for each ethnic group in a mixed gender, Caucasian-Asian Chinese cohort (the TOFI_Asia study). It evaluates the use of a modelling approach to predict FPG state based on the metabolomic signature and identifies a subset of normoglycemic individuals characterised by a worse cardiometabolic risk profile. This chapter addresses specific goal 3 and 4.

Manuscript contained in Chapter 5 has been published:

Wu, Z. E., Fraser, K., Kruger, M. C., Sequeira, I. R., Yip, W., Lu, L. W., ... & Poppitt, S. D. (2020). Metabolomic signatures for visceral adiposity and

dysglycaemia in Asian Chinese and Caucasian European adults: the cross-sectional TOFI_Asia study. Nutrition & metabolism, 17(1), 1-19.

Chapter 6 reports and discusses plasma metabolite markers predictive of the level of pancreatic fat, liver fat and the visceral adipose tissue (VAT)/subcutaneous adipose tissue (SAT) ratio measured by magnetic imaging techniques in a subset of female participants from the TOFI_Asia study, and compares the model performances of these fat depots predicted by metabolite markers with the use of clinical measurements. This chapter addresses specific goal 5.

Manuscript contained in Chapter 6 has been submitted to *International Journal of Obesity* and is under review:

Zhanxuan E. Wu, Karl Fraser, Marlena C. Kruger, Ivana R. Sequeira, Wilson Yip, Louise W. Lu, Lindsay D. Plank, Rinki Murphy, Garth J.S. Cooper, Jean-Charles Martin, Kieren G. Hollingsworth, Sally D. Poppitt. “Untargeted metabolomics reveals plasma biomarkers of ectopic fat in pancreas and liver as assessed by magnetic resonance imaging: the TOFI_Asia study”

Chapter 7 summarises how objectives achieved in the prior scientific chapters (Chapters 3-6) fit into and benefit the research community of metabolomics and metabolic health, and discusses the key findings throughout the PhD study. Finally, conclusions are drawn on the body of the PhD study and future work are suggested.

Chapter 8 contains full list of references.

Chapter 9 contains supplementary data and results that from chapters 3-6 published, submitted, or about to be submitted for journal publication.

2. Literature Review

In this section, the background and pathophysiology of dysglycaemia will be introduced, with a highlight on the role of visceral adiposity and ectopic fat deposition. I then explain why metabolomics is a suitable technique and has achieved widespread use in the study of cardiometabolic disease, along with some fundamentals on metabolomics and the metabolomic process. This will be followed by major findings from recent metabolomics studies applied to dissect metabolic health. Lastly, key considerations for a successful metabolomics study will be detailed, and an overlooked issue for reliable metabolomic profiling is described which will be addressed in the following chapter.

2.1 Pathophysiology of type 2 diabetes (T2D)

2.1.1 Hyperglycaemia: why it matters?

Hyperglycaemia is a characteristic feature for T2D. According to the American Diabetes Association guidelines, individuals with an FPG concentration consistently ranging between 5.6-6.9 mmol/L (known as impaired fasting glucose (IFG)) and/or 2-hour plasma glucose (2-h PG) during an oral glucose tolerance test (OGTT) between 7.8-11 mmol/L (known as impaired glucose tolerance (IGT)) is considered having pre-diabetes, whereas an FPG ≥7 mmol/L and/or 2-h PG ≥11.1 mmol/L is recognised as diabetes [2]. Hyperglycaemia affects over 16% of the global population, with 463 million people estimated to have diabetes and 374 million people diagnosed as prediabetic in 2019 [3]. The rapidly spreading pandemic of the hyperglycaemic condition is concerning as it can lead to cardiometabolic diseases and its complications are a major cause of death. Chronic exposure to a high glucose environment is deleterious to cells and organs [43]. The irreversible damage to cells and organs mediated by chronic hyperglycaemia (referred as glucose toxicity [44]) can happen via a multitude of mechanisms including: overproduction of reactive oxygen species (ROS) and advanced glycation end-products (AGEs), diminishing action of the antioxidant system, modification of biomolecules including proteins, lipids and DNA, and altering activity of numerous cellular pathways [45, 46]. As such, keeping blood glucose level within a normal physiological concentration range is crucial for proper functioning of cells and organs.

2.1.2 Glucose homeostasis

Glucose homeostasis is maintained by a well-controlled balance between glucose appearance (from diet and endogenous production) and disappearance

(through uptake by cells and tissues) in blood. Although blood glucose levels fluctuate throughout the day and transiently surge after a meal, prolonged elevation is prevented through precise hormonal regulation. The principal blood glucose-lowering hormone is insulin, functioning by stimulating glucose uptake by peripheral insulin-responsive tissues through the glucose transporter protein GLUT4, and suppressing glucose output from the liver [47]. GLUT4 is mainly expressed by striated muscle (skeletal and cardiac) and adipose tissue and its activation is insulin-dependent. In addition to its primary function in glycaemic control, insulin also regulates and coordinates the metabolism of carbohydrate, lipid and protein hence playing an important role in regulating systemic energy homeostasis.

2.1.3 Insulin: master regulator of energy homeostasis

Insulin is a glucoregulatory and growth hormone synthesised and secreted by the pancreatic β-cell, and glucose is the principal stimulus for insulin secretion via glucose-stimulated insulin secretion (GSIS) [48]. During fasting, a basal level of insulin is secreted to moderately suppress lipolysis and gluconeogenesis to maintain blood glucose at a normal range [49]. When plasma glucose is elevated, glucose enters β-cell via the bidirectional glucose transporter GLUT2. GLUT2 is an insulin-independent transporter mainly expressed by the liver, pancreatic β-cell and basolateral membrane of small intestine to ensure that the intracellular environment of these cells accurately gauge the blood glucose levels. Glucose influx into the β-cell increases the production of ATP which closes the ATP-sensitive K^+ channels, causing membrane depolarisation and Ca^{2+} influx; the increased cytosolic Ca^{2+} concentration then stimulates exocytosis of insulin-containing vesicles into the circulation (**Figure 2.1**) [48, 50]. Other mediators

including activation of protein kinase C (PKC) and cAMP-dependent protein kinase (PKA) by a number of non-nutrient secretagogues such as neurotransmitters, adipokines and gut-derived peptides hormones i.e. incretins, notably the glucagon-like peptide-1 (GLP-1) and gastric inhibitory polypeptide (GIP) can amplify insulin release and stimulate a decrease in blood glucose levels, whilst certain amino acids have insulinotropic effects (e.g. arginine and ornithine) or act as an insulin secretion enhancer (e.g. leucine) [49]. Plasma free fatty acids (FFAs) also modify insulin secretion, with acute elevation potentiating GSIS whereas chronic elevation decreases GSIS as well as insulin synthesis [51-53].

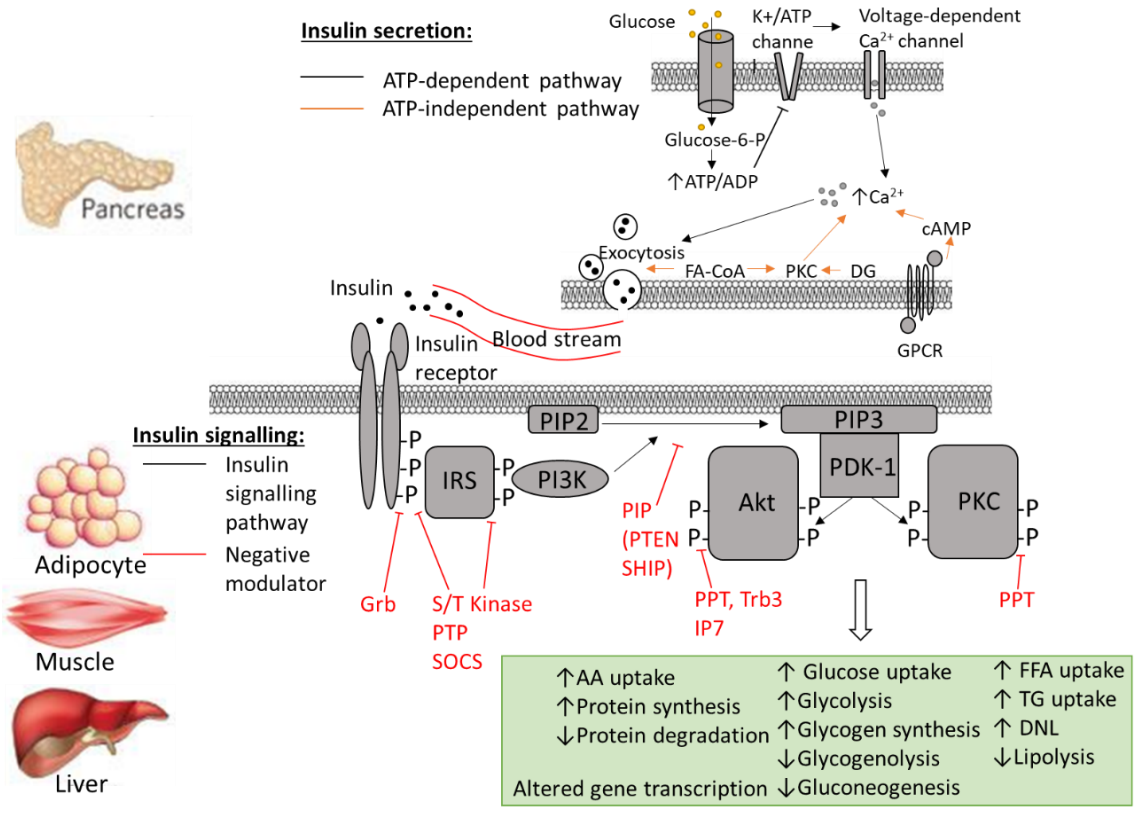

Figure 2.1: Insulin secretion and signalling (redrawn based on [48, 54]). Intracellular pathway mediating the secretion of insulin in the pancreatic β-cell (top) and insulin signalling pathway mediating the metabolic effect in metabolically active tissues (bottom). See the whole section of 2.1.3 for a detailed description.

Insulin binds to cell surface insulin receptors and triggers a cascade of phosphorylation events (**Figure 2.1**) [54]. Insulin receptor substrate (IRS) – protein is the first engaged component upon receptor activation and multiple tyrosine residues are phosphorylated by the activated receptors to form binding sites for phosphatidylinositol-3-kinase (PI3K). PI3K is activated to generate the lipid second messenger phosphatidylinositol (3,4,5)-triphosphate (PIP3), which subsequently recruits and activates 3-phosphoinositide-dependent protein kinase 1 (PDK-1). Known substrates for PDK-1 include protein kinase B (also known as Akt) and atypical protein kinase C (aPKC). The PI3K-Akt pathway provides the critical link of insulin to its metabolic action, as Akt has diverse downstream effectors that regulate cellular metabolism at multiple levels ranging from transcription (e.g. through mTORC1, FOXO family, PGC-1a), protein activity (e.g. via mTORC1, GSK), mitochondrial biogenesis (mTORC1), and transporter translocation (GLUT4) [55]. Alongside Akt, aPKC also mediates insulin-dependent glucose uptake and regulates lipid synthesis [56].

Activation of insulin receptors produces a wide range of downstream effects in adipose tissues, muscles and the liver (**Figure 2.1**) on metabolism of 1) carbohydrate, including increased uptake of glucose, stimulated rate of glycolysis and glycogen synthesis, suppressed rate of glycogenolysis and gluconeogenesis; 2) lipids, including increased uptake of free fatty acids and triglycerides, stimulated *de novo* lipogenesis (DNL) and inhibited lipolysis; and 3) protein, including increased uptake of some amino acids and rate of protein synthesis as well as decreasing rate of protein degradation [57].

Termination of insulin action is equally important in maintaining energy homeostasis. In addition to the internalisation of insulin receptor-insulin complex

and the negative feedback loop by the downstream effectors, various negative regulators to switch off insulin signalling exist: phosphoprotein phosphatase (PPT), lipid phosphatase (PIP), adaptor proteins like Grb10 and SOCS, Ser/Thr kinase (S/T kinase) such as the c-Jun amino-terminal kinase (JNK), conventional and novel PKC etc (**Figure 2.1**) [54]. Modulation of insulin signalling by these pathways/mediators is vital for adaption as individuals progress from the fed to fasted state [54]. However, under pathophysiological conditions some of these inhibitory mechanisms are hyperactive which is tightly linked to development of insulin resistance (IR) [58].

2.1.4 T2D as a disease of insulin resistance and deficiency

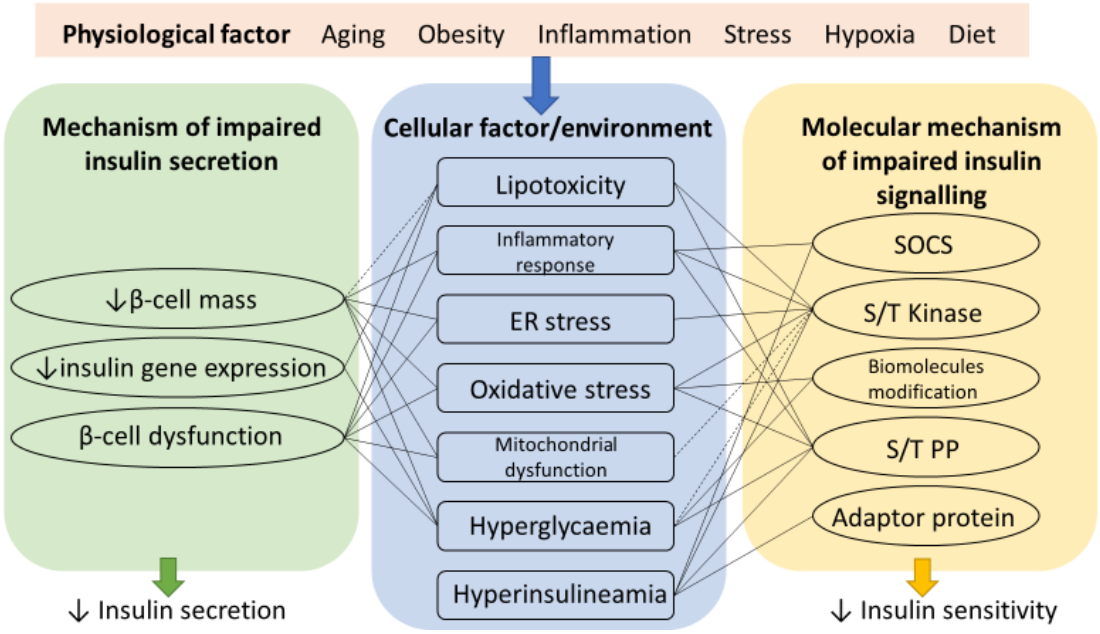

Figure 2.2: Mechanisms of impaired insulin secretion (green) and signalling (yellow) that underly the pathogenesis of T2D, and a multitude of factors at cellular (blue) and physiological levels (orange) contributing to these defects (constructed based on [54, 58-60]). Each connector represents a direct (causal) effect. SOCS: Suppressor of Cytokine Signalling protein; S/T Kinase: Serine/Threonine Protein Kinase; S/T PP: Serine/Threonine Protein Phosphatase.

Given the pivotal role of insulin in stimulating cellular glucose uptake and regulating metabolism, it is not surprising that defects in insulin signalling and

secretion underly T2D pathogenesis (**Figure 2.2**). Whilst inadequate insulin secretion is resultant from β-cell loss and dysfunction, a diminished biological response to insulin by insulin-responsive tissues and organs i.e. IR, is believed to confer/drive persistent hyperglycaemia in the early stage of T2D development. Abnormalities in the insulin signal transduction pathway is fundamental to the molecular mechanisms underlying IR [54]. In addition to the genetic mutations of insulin receptors and signal transducers, which cause rare and severe IR, several extracellular and intracellular factors have been hypothesised to cause IR via direct or indirect activations of negative modulators for insulin signalling. These factors include lipotoxicity (i.e. damage caused by increased lipid flux and generation of lipid intermediates), inflammation, oxidative stress, mitochondrial dysfunction and endoplasmic reticulum (ER) stress [54]. Hyperglycaemia and hyperinsulinemia, though generally considered as consequences of IR, also amplify IR and aggravate dysglycaemia. Notably, each of these factors can independently tune down insulin signalling, but they also impact or trigger each other. For example, excess plasma FFA, palmitic acid (PA) in particular, promotes IR via the production of lipotoxic mediators like diglyceride (DG) and ceramide, which activates PKC-θ leading to IRS-1 Ser307 phosphorylation that blocks the signal transduction of insulin [61]. Decreasing DG levels or inhibiting ceramide synthesis in muscle was shown to protect against lipid-induced IR [62, 63]. Co-infusion of oleic acid (OA) with PA in muscle also reversed PA-induced IR by diverting more PA towards TG synthesis instead of phospholipids and DG [64]. In addition to a direct effect on signal transduction, excess FFA also induces ER stress, which in turn activates stress response and inflammatory pathways leading to cytokine production and Ser/Thr kinase activation [59]. On the other

hand, activation of the inflammatory pathway even without the presence of excess FFA, also elicits insulin resistance via the action of JNK and IKK, which again phosphorylates IRS-1 at serine residuals. The pro-inflammatory cytokine TNF-α also inhibits PPARγ activity and thus lipogenesis, which counteracts the lipogenic effect of insulin and may contribute to lipotoxicity due to excess lipid load. These two simple examples already give a flavour of the complexity in terms of the cellular cross-talk during the development of IR. Likewise, all these factors can drive β-cell dysfunction and apoptosis, leading to decreased insulin secretion. The best characterised factor has been lipoglucotoxicity, in which excess glucose, PA and ceramide impairs insulin production and trafficking [60]. Lipoglucotoxicity can also induce ER stress and mitochondrial dysfunction that ultimately lead to induction of apoptosis [60].

Taken together, IR occurs when the signal transduction is impaired by a cluster of metabolic abnormalities and physiological perturbations, resulting in inability of cells to take up glucose thus hyperglycaemia followed by compensatory hyperinsulinemia. In the meantime, chronic exposure of the β-cell to a lipoglucotoxic environment, stress and inflammation, impairs its function and survival ultimately leading to pancreas failure and onset of T2D.

2.1.5 Obesity and metabolic health

2.1.5.1 The longstanding diabesity theory

The association of obesity (defined as having a body mass index (BMI) greater than 30 kg/m^2) with T2D has been recognised for decades [65]. Chronic low-grade inflammation, excess FFA load, and increased oxidative stress are common traits in obese individuals that are associated with IR and increased risk of T2D development [66, 67]. However, not all overweight/obese individuals

develop T2D, and overweight/obesity is not a prerequisite for IR and T2D development [23]. Individuals with similar BMI show considerable heterogeneity in their susceptibility to T2D development and BMI fails to fully capture cardiometabolic risks. The answer lies at the poor reflection of body composition, total amount of fat and site of fat deposition by BMI alone [27, 29], which is defined by the simple relationship between body weight and height, with no reference to composition of body mass. An extreme example is a lipodystrophy patient, who can have a low BMI whilst exhibiting massive fat deposition in non-adipose tissue rendering higher risks of IR, T2D and CV disorders. In addition, the relationship between BMI range and T2D showed great ethnic disparities, with Asians developing T2D at a lower mean BMI than people from a European descent [25]. Asians were also reported to exhibit the greatest increase in relative risk of T2D for each 5-unit increment in BMI or even modest weight gain compared with Hispanics, whites and blacks [68]. Efforts have been made to adjust these inter-ethnicity disparities when using BMI for risk stratification, and different BMI cut-off values were suggested to be applied for the estimation of cardiometabolic risks in different ethnic groups [69, 70]. Although the twin epidemic of T2D and obesity hold true at the population level, growing evidence from recent epidemiological studies warn of the use of BMI to predict metabolic risks at sub-population and individual levels, and suggest the presence of other factors than an increased BMI *per se* driving poor metabolic health.

2.1.5.2 The era of regional fat distribution

As long ago as 1956, Vague conceptualised the masculine (central) and feminine (peripheral) fat distribution (also known as the apple/pear-shaped nowadays) and hypothesised differentiating risk profiles associated with each of them. Vague

found the android obesity with upper body predominance (i.e. central) led to metabolic disturbances and were associated with premature atherosclerosis and diabetes, whereas the gynoid obesity with lower body predominance (i.e. peripheral) was only linked to mechanical complications [71]. This concept formed the embryo of the abdominal (central) obesity theory which linked body fat distribution to metabolic outcomes. Vague's findings were later confirmed by other cross-sectional studies, in which abdominal obesity was associated with increased hypertension, hypertriglyceridaemia, hyperinsulinaemia and glucose intolerance [72, 73]. The role of abdominal obesity was further reinforced by prospective epidemiological studies showing surface measurements for abdominal obesity such as the waist circumference (WC) or waist-to-hip (W-to-H) ratio predicted development of T2D and CVD independent of BMI [74-77]. However, a meta-analysis found similar associations of BMI, WC and W-to-H ratio with incident diabetes [78]. The inconsistency may be explained by the inability of these surface measurements to distinguish among various fat depots, including VAT (fat depots around organs), subcutaneous adipose tissues (SAT, fat depots underneath skin) and ectopic fat (fat accumulation in the liver, pancreas and muscles) [31]. Essentially SAT and VAT have different properties, as is characterised by different gene expression profiles, adipogenic and inflammatory potentials, and biological processes involving lipolysis/lipogenesis [79, 80]. Fat accumulated in non-adipose tissue such as the liver, pancreas and muscles, on the other hand, can interfere with cellular pathways and impair organ function [81].

Different fat depots can now be separately and accurately assessed using modern measurement technologies such as computed tomography (CT) and

magnetic resonance imaging (MRI), improving the understanding of their contributions to metabolic outcome. Early research performed in the 1980s revealed VAT as a key correlate of metabolic abnormalities [82, 83]. Contradictory, a dominating association of SAT over VAT with obesity-induced IR reported by Abate et al., caused confusion in the interpretation of the role of VAT in metabolic abnormalities [84, 85]. Goodpaster et al., also reported SAT predicted insulin sensitivity independent of VAT, but later found that VAT was the only adiposity parameter predictive of improvement in insulin sensitivity in response to weight loss [86, 87]. One explanation is that relative contributions by SAT or VAT to metabolic abnormalities may be blunted due to VAT being highly correlated with BMI at the population level. At the individual level, there are substantial variations in the level of VAT at any given amount of total adiposity [88]. Studies carefully matching or correcting for total adiposity clearly indicated an independent association of VAT with metabolic disturbances and risk profiles [82, 89-91]. These inter-individual variations have led to the concept of a personal fat threshold, which describes SAT as a metabolic sink for excess TG [92]. When SAT is unable to expand and its lipid storage capacity is exceeded, individuals are predisposed to excess VAT and ectopic fat deposition and thus increased risk of metabolic abnormalities [93].

2.1.5.3 Visceral adiposity

Accumulating evidence from cross-sectional studies found visceral adiposity independently associated with IR, glucose intolerance, T2D and CVD [89]. Meanwhile, prospective studies evaluating baseline visceral adiposity and follow-up metabolic outcomes, provided robust evidence linking VAT to changes in metabolic health status over time. Findings from the Japanese American

Community Diabetes Study in which participants were followed for 10-11 years revealed significant associations of VAT with incident diabetes [94], incident impaired glucose tolerance [95], incident metabolic syndrome [96], and increases in IR over time independent of abdominal SAT and total adiposity [97]. They have also reported that VAT predicted the development of coronary heart disease and hypertension [98]. In a 7-year follow-up study by Lemieux et al, female participants with similar body fat mass gain were divided into groups of small or large increases in VAT, and the greatest deterioration of glucose tolerance and hyperinsulinemia were observed in those with a large increase in VAT [99]. Conversely, when the cohort was split into small or large changes in body fat mass but similar VAT gain, no difference in changes in glucose tolerance and insulin secretion were observed. In several liposuction interventional studies, removal of SAT without loss of VAT did not alter IR, plasma glucose, insulin, adiponectin, or other lipid or inflammatory components of metabolic syndrome, nor did it improve long-term CV risk factors [100, 101]. Unfortunately, there is no surgical procedure to remove only VAT. Nonetheless, a pilot study by Thörne et al., found 2-3 times greater improvements in glycaemic control-related parameters in patients who underwent adjustable gastric banding (AGB) plus removal of VAT than those whom underwent AGB alone despite having similar weight loss at 2-year follow-up [102]. In animal models, transplantation of SAT to the visceral cavity showed improved glucose tolerance, enhanced whole-body insulin sensitivity and reduced hepatic glucose output, suggesting different cell-autonomous properties between SAT and VAT and potentially beneficial metabolic effects of SAT [103, 104]. All these findings coherently highlight an independent role and detrimental effects of excess VAT in T2D pathogenesis. A

recent position statement by Neeland et al., merits attention, in which VAT was highlighted as a key conduit for the adverse effect of obesity on metabolic health [29].

Although the definitive role and causal link of VAT in the aetiology of T2D has yet to be established, several lines of experimental evidence from in vitro and in vivo studies support detrimental effects of excess VAT on metabolic health [27]. Firstly, VAT is more sensitive to catecholamine-induced lipolysis and resistant to insulin-suppressed lipolysis [80]. The VAT-derived FFA are drained by the portal vein which perfuses the liver in a high FFA/glycerol environment. On glucose metabolism, glycerol can be phosphorylated and converted to glucose contributing to elevated gluconeogenesis and hepatic glucose output. On lipid metabolism, increased influx of FFA into the liver upregulates DNL at the transcription level as well as directly increasing substrate availability for re-esterification, resulting in increased intrahepatic TG accumulation and/or very low density lipoprotein (VLDL)-TG secretion. FFA also impair insulin signalling via multiple mechanisms as described in section 2.1.4. Additionally, FFA activate PPAR-α and hepatic nuclear factor which in turn modulates expression of various gene products involved in lipid, carbohydrate, bile and cholesterol metabolism and decreases hepatic insulin clearance. This proposed mechanism is tightly linked to clinical outcomes such as hyperglycaemia, hyperinsulinemia and dyslipidaemia in visceral adiposity patients.

Secondly, chronic inflammation characterised by an altered adipokines/cytokines profile was reported in obese patients and contribute to altered glucose and lipid metabolism and impaired insulin signalling [105]. Both SAT and VAT are remarkable sources of cytokines/adipokines, but they have innately different

inflammatory potentials and profiles [106, 107]. VAT dominates the production of plasminogen activator inhibitor 1 (PAI-1), monocyte chemoattractant protein 1 (MCP-1), interleukin-6 and TNF-α, all of which have well-documented pro-inflammatory effects and whose levels are markedly increased in obese patients, particular among those with abdominal adiposity [108, 109]. In addition, VAT but not SAT, is prominently associated with PAI-1 and high-sensitivity C-reactive protein, a systemic inflammatory marker [110, 111]. Meanwhile, the insulin-sensitising, anti-inflammatory adipokine, adiponectin, is inversely associated with excess VAT, and VAT was shown to be the strongest correlate of adiponectin independent of other adipose tissue parameters [112]. Again, the VAT-derived cytokines/adipokines exposes VAT itself and the liver to a pro-inflammatory environment, but also contributes to the systemic pool and affects distal tissues such as muscle and peripheral adipose tissues [113].

A third, but non-exclusive role of VAT has been postulated by Jean-Pierre Després et al., that is, excess VAT is a marker of the inability of SAT to expand [27]. The impairment of this protective mechanism could subsequently lead to fat accumulation at undesired sites like the liver, muscle and pancreas. Of note, considering excess VAT as a marker of hypertrophied/dysfunctional SAT does not preclude the other two mechanisms (**Figure 2.3**).

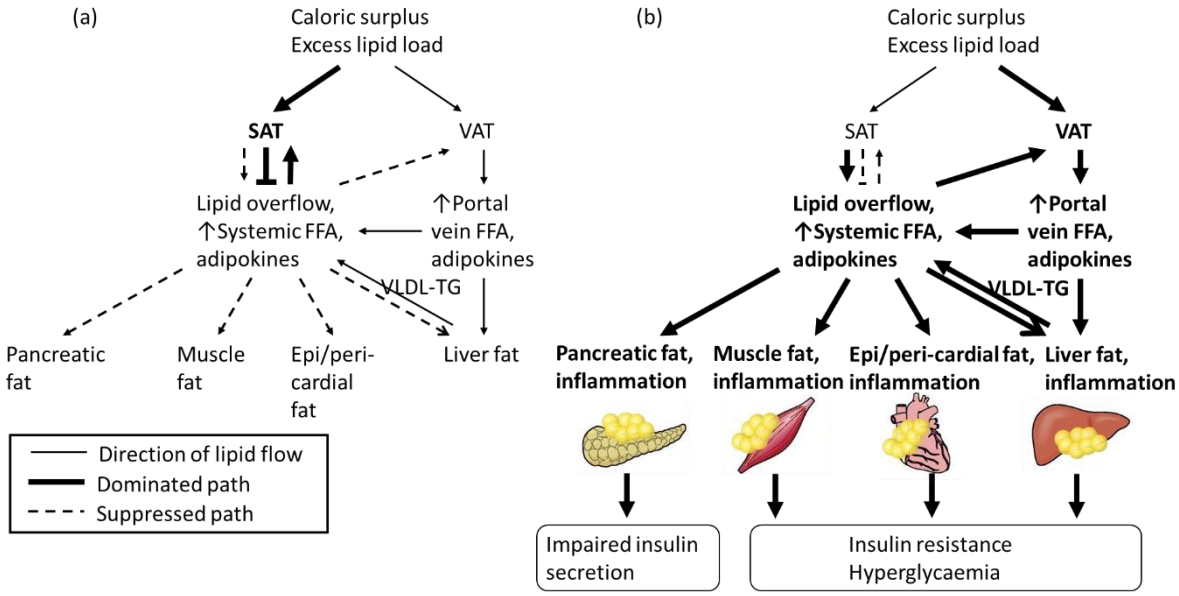

Figure 2.3: An integrated model to show the proposed mechanisms by which visceral adiposity is linked to an impaired glycaemic control (constructed based on [27]). Excess VAT may be a marker of an impaired SAT expandability but also directly mediate effects of caloric surplus at least via an elevated portal FFA and altered inflammatory profile, both of which have direct effects on the liver but also contribute to systemic level of FFA and adipokines/cytokines. In response to chronic caloric surplus, both types of adipose tissues will expand. (a) When SAT is properly functioning with capacity to expand, it acts as a metabolic sink to store excess TG and prevent lipid overflow. (b) In the case of dysfunctional or hypertrophied SAT with impaired expandability, excess fat accumulation in VAT as well as ectopic sites occur.

2.1.5.4 Ectopic fat deposition in the liver and pancreas

In line with the "portal vein theory" described in section 2.1.5.3, non-alcoholic fatty liver disease (NAFLD), characterised by an excess accumulation of liver fat, is strongly associated with visceral adiposity irrespective of BMI category [114-116]. VAT also correlates with inflammation and fibrosis in NAFLD [117]. Hypertriglyceridemia resulting from an increased lipogenesis in the liver and VLDL-TG secretion, is a central correlate of visceral obesity. Clearly excess VAT could be one of the major upstream factors leading to excess liver fat, and excess liver fat mediates many of the metabolic complications associated with visceral adiposity [118]. Other factors such as genetic predisposition and diet can also

contribute to excess liver fat without the presence of visceral adiposity [119]. Mechanistically, excess liver fat is implicated in liver IR, at least via the action of PKCε. Activation of PKCε impairs insulin signalling, leading to defects in insulin-induced activation of liver glycogen synthesis and suppression of gluconeogenesis and hence an elevated glucose output. IR traits including hyperglycaemia and hyperinsulinemia, can also trigger DNL in the liver, exacerbating liver fat deposition and worsening the liver response to insulin.

Whilst liver fat is correlated with VAT and mechanistically linked to IR and dyslipidaemia, the level of fat accumulated in the pancreas has been shown to correlate with age, BMI, abdominal obesity, VAT and associated with metabolic syndrome and T2D [120-123]. It is therefore sensible to speculate that pancreatic fat deposition may be linked to impaired insulin secretion and apoptosis of β-cells. However, clinical evidence is somewhat obscure, with positive, inverse, or no association with insulin secretion being reported by different research groups [122]. In some studies, the association was also subject to diabetic state and observed in either prediabetic/T2D patients [124], or healthy individuals [125]. The lack of consistency may be attributed to the heterogenous fatty infiltration in the pancreas which is made up with intralobular and interlobular fat [126, 127], and different methodologies (histological examination, computed tomography, magnetic resonance imaging, sonography, positron emission tomography etc.) to quantify pancreatic fat [123]. In addition, and probably more biologically relevant, the lipotoxic effect on β-cell function is largely mediated by FFA and other bioactive lipid species such as ceramides and DG [128]. TG may serve as a pool for the generation of FFA and other lipotoxic intermediates, but the accumulated TG itself seems rather inert [129, 130].

Section 2.1.3 briefly introduced that insulin secretion can be modulated by FFA. This happens via the activation of FFA receptor which initiates a series of stress responses and inflammation, ultimately leading to inhibition of glucose-stimulated insulin secretion (GSIS), reduction of insulin gene expression and induction of apoptosis [131]. FFA exposed to the pancreas can be derived locally from infiltrated adipocyte lipolysis and/or systematic elevation of FFA or TG-rich lipoprotein (TRL) like VLDL [128, 132]. PA and hepatokine fetuin-A have been shown to increase pro-inflammatory cytokine production by infiltrated adipocytes in pancreas, causing local inflammation [133]. The activated macrophages inhibit adipocyte differentiation [134], which in turn, may further augment local FFA concentrations. In a more recent study, the negative association of pancreatic fat with insulin secretion in prediabetic individuals was observed, however, only when liver fat and levels of FFA were also markedly elevated, whereas such an inverse relation was absent at median liver fat and FFA levels [135]. Taking this evidence together, it seems logical to suggest that accumulation of pancreatic fat is a consequence of chronic energy surplus, but its association with insulin secretion is dependent on the presence of derangements of lipid metabolism. In this sense, pancreatic fat is merely a marker of increased adiposity rather than a direct cause of impaired insulin secretion. It is the often-accompanying FFA/TRL overflow and other complications in whole body/visceral obesity that lead to β-cell dysfunction.

Whilst robust data support the detrimental consequences of excess VAT, the metabolic abnormalities and long-term complications associated with liver and pancreas fat in isolation remain elusive. In addition, these interesting fat depots are expensive, time-consuming and invasive to measure, raising the need for

alternative tools to quantify these fat depots. Metabolomics may offer opportunity to identify circulating metabolites as candidate biomarkers reflective of levels of VAT and ectopic fat, potentially providing insight into the metabolic abnormalities associated with these fat depots.

2.2 Introducing LC–MS-based untargeted metabolomics

2.2.1 Basics of metabolomics

Metabolomics is an emerging and rapidly growing multi-disciplinary field which employs analytical chemistry techniques and bioinformatics tools to address biological questions [136]. A metabolomics study involves the comprehensive measurement of the complete set of low molecular weight components (also termed “metabolome”) in a biological sample, followed by data pre-processing and subsequent data analysis and modelling to identify set of metabolites associated with condition of interest [38, 137].

2.2.1.1 From a biological aspect

Metabolites are often the end products of complex biochemical processes, therefore metabolomics is the endpoint of the “omics” cascade that links genomics, transcriptomics and proteomics to phenotype [138]. The metabolomic profile of an individual is determined by genetic factors, as the genes encode for all the enzymes and transporters required to carry out biological processes and produce metabolic products. It is also modified by environmental factors and disease states which can alter transcription, translation and protein activity that is subsequently depicted by changes in cellular biochemistry and hence the metabolite concentration [139]. As such, metabolomics has become a popular tool to study complex conditions that often involve interplay between genetic predisposition and environmental modifications with changes in a multitude of

biochemical pathways. Comparison of metabolomic profiles between healthy vs diseased, exposed vs non-exposed, treatment vs placebo etc. informs about the metabolic alterations associated with external stimuli, environmental changes, drug actions and diseases. Integration of metabolomics data with other omics data allows the identification of novel networks and pathways at a multi-layer level and advances the understanding of biological processes [138]. Dissecting the relationship between metabolomic profile and clinical outcomes at a single timepoint (e.g. in cross-sectional study) or being followed up over time (e.g. in longitudinal and prospective studies) facilitates the identification of novel diagnostic/prognostic biomarkers for diseases and may improve risk stratification [140]. On the other hand, linking the baseline metabolomic profile with treatment/intervention outcomes holds promise for the discovery of biomarkers that discriminate non-responders from responders, which in turn helps guide clinical decision making to improve drug safety, efficacy and optimise nutrition and lifestyle management in different individuals [140]. Moreover, metabolomic signatures characteristic for the hallmark features of risk factors (e.g. visceral adiposity, dyslipidaemia, IR) even before the disease can be diagnosed, can provide insight into the metabolic abnormalities associated with the disease development. A major application in the research of cardiometabolic diseases includes biomarker discovery and the understanding of metabolic alterations underlying disease development [141-144].

There are two general approaches adopted by a metabolomics study: targeted and untargeted metabolomics. Targeted metabolomics is a hypothesis-driven approach, which aims at accurately quantifying a subset of metabolites [145]. This approach is used for biomarker validation as well as well-tailored research

questions, usually when a specific class of metabolites or metabolites in one or more specific pathways are of interest, and some prior knowledge is required. By contrast, untargeted metabolomics is an observational, hypothesis-generating, top-down systematic approach to measure as many metabolites as possible from a given specimen regardless the class of metabolites [146]. In this approach, the global metabolite profiles containing hundreds to thousands of metabolites, both known and unknown, are measured and analysed. Only those metabolites significantly different between sample groups or associated with phenotype of interest are reported, and the quantitation of metabolite level is in a relative term (e.g. expressed as fold-change, ratio, and correlation coefficient). Untargeted metabolomics is therefore a true -omic technique that allows serendipitous findings and gives an opportunity to expanding current knowledge.

2.2.1.2 From an analytical chemistry aspect

The metabolic snapshots of a biological sample can be simultaneously measured, owing to recent development of state-of-the-art techniques. Nuclear magnetic resonance spectroscopy (NMR) and mass spectrometry (MS) coupled to a separation technique are the two most commonly used platforms for untargeted metabolomics, although employment of other analytical techniques such as Fourier transform-infrared spectroscopy, surface-based MS and direct infusion MS has been reported. NMR-based metabolomics requires minimal sample preparation, is non-destructive of samples, directly gives structural information of analytes and delivers highly reproducible spectral data. Limitations include a relatively narrow dynamic range (lower detection limit at micro-molar range and sensitive to ~6 orders of magnitude), massive peak overlapping in spectrum and an inability to structurally differentiate among lipid species. Mass

spectrometry is very sensitive and has a much wider dynamic range of detection (pico-molar to milli-molar range) and requires small injection volumes of sample meaning many analyses can be performed. Coupling the MS to a separation technique such as gas-chromatography (GC-MS), liquid-chromatography (LC-MS) or capillary electrophoresis (CE-MS) reduces complexity of the mass spectra and adds another layer of information (retention time) on the physicochemical properties of metabolites [147].

Among MS techniques, LC-MS is the most versatile and the technique of choice for this PhD study. In LC-MS, metabolites are extracted from samples, separated on an LC column, ionised at an ion source, resolved by a mass analyser and detected [148]. Commonly used MS for metabolomics include low-resolution MS such as the triple quadrupole MS for a pre-determined set of ions and high-resolution MS such as Quadrupole Time-of-flight (qTOF) and Orbitrap for a full scan of ions [148]. Triple quadrupole MS monitors fragmentation of a parent ion into a characteristic daughter ion pattern to achieve specificity thus is suitable for targeted analysis. Conversely, high-resolution MS has a high level of precision that resolves ions with very small *m/z* differences to achieve specificity, therefore it is the most straightforward approach for measuring large numbers of metabolites [136, 148, 149]. However, a major challenge in LC-MS-based metabolomics is the lack of a single LC method that can analyse all metabolites due to the enormously diverse physicochemical properties of metabolites [148]. There are different types of LC columns combined with different LC solvent systems (e.g. reversed phase (RP), normal phase) which separate metabolites based on metabolite polarity/solubility [148, 149]. Common practice in the field is

to employ multiple analytical platforms to provide complementary information and increase metabolome coverage [147].

2.2.1.3 From a bioinformatics aspect

Like other ‘omics’ approaches, analysis of metabolomics data requires specialised bioinformatics tools. The raw spectral data undergo extensive pre-processing followed by univariate/multivariate statistical analysis to understand the relationship of metabolites–metabolites (e.g. by network analysis), metabolites–phenotype (clinical data integration), metabolites–other omics layers (e.g. microbiome, transcriptome) [150]. Due to the natural attributes of metabolomics data (hundreds to thousands of variables, high degree of multicollinearity and possibly redundancy as well), advances in machine learning techniques facilitate deep analysis and interpretation of the complex high-dimensional data. Machine learning approaches are mainly categorised as either supervised or unsupervised. In supervised approaches, labelled data is required to guide the model to learn the underlying patterns. The trained model can then recognise these patterns and assign labels in unseen data. In contrast, unsupervised approaches discern unspecified patterns without pre-existing labels in an unbiased manner. Examples of commonly used supervised approaches include random forest, partial least squares regression/discriminant analysis, elastic net, support vector machines etc. Examples of unsupervised approaches include many clustering algorithms and principal component analysis. On the other hand, univariate analysis independently assesses the association of each individual metabolite with a dependent variable (e.g. a clinical outcome, an exposure). Common univariate analysis includes correlation analysis, simple/multiple linear/logistic regression, paired/unpaired t-test, Cox

regression etc. One should keep in mind that the test is repeatedly performed on every metabolite therefore it is important to apply multiple testing correction to avoid false positive findings.

2.2.2 General workflow of LC–MS-based untargeted metabolomics

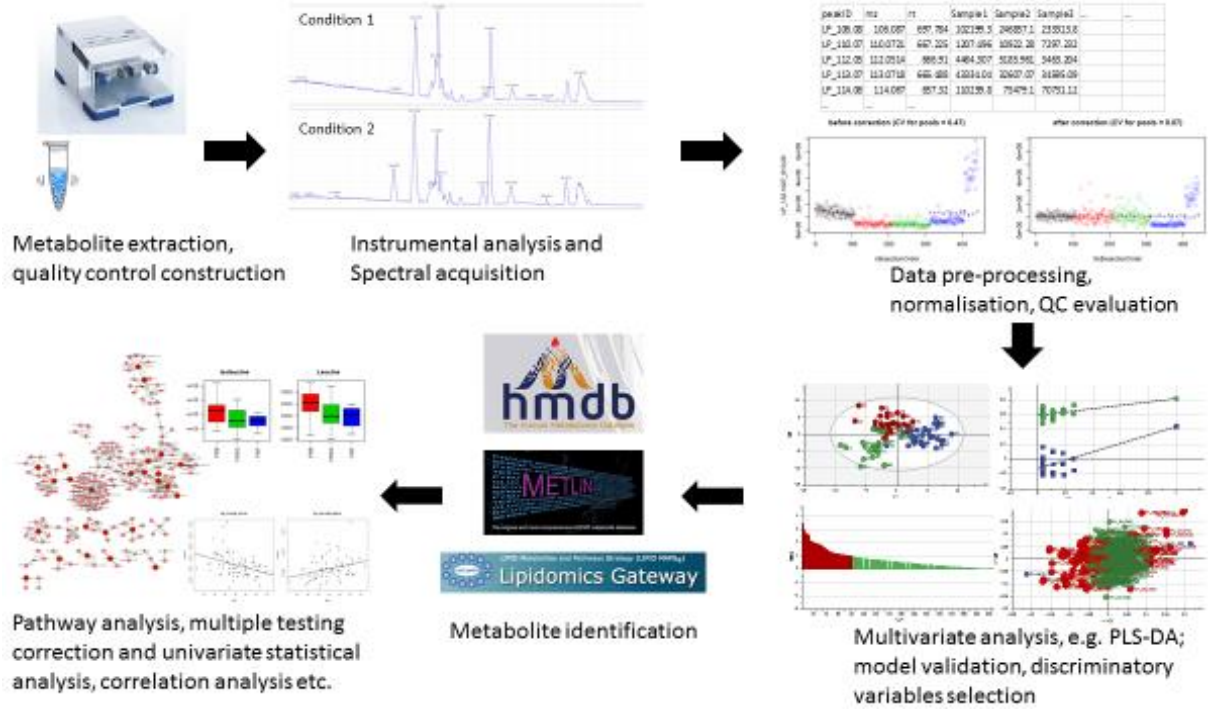

Figure 2.4: General workflow for global metabolomics study.

When measuring by a single analytical platform, liquid chromatography–mass spectrometry (LC–MS) enables the most comprehensive metabolite coverage achievable to date [151]. The general workflow of an LC–MS-based untargeted metabolomics study typically involves steps of sample collection and extraction, data acquisition, processing and analysis and biological interpretation [136, 152], and is summarised in **Figure 2.4**. Briefly, clinical outcomes or conditions of interest (e.g. obese vs lean, normoglycaemic vs prediabetic, intervention vs placebo group) and types of specimen to be collected (e.g. plasma, serum, urine, saliva, cerebrospinal fluid, tissues) should be established prior to sampling. One

should note that confounding factors at biological levels are inevitable, especially in human studies. Confounding factors can overwhelm or mask the effects of the condition of interest on metabolic status and hence the metabolomic profile [153]. The researcher must be aware of these, or the data can be misinterpreted. Therefore, this also needs to be considered before sample collection. Ideally the study groups are well matched/balanced, and data on potential confounding factors should be collected alongside so they can be corrected for where possible [153]. Metabolites in each sample are then extracted and measured by LC–MS. Instrumental analysis of samples produces three-dimensional spectra that contain information of retention time, mass-to-charge ratio (*m/z*) and relative intensity, which can be extracted and converted to a data matrix in the subsequent data pre-processing step. Data pre-processing software or packages such as XCMS and ADAP typically involve steps of peak detection (or peak picking) from each spectrum, retention time correction, peak alignment (or peak matching) across all the acquired spectra across the sample set, and peak filling (re-measurement where missing values exist) [154, 155]. A number of freely available data processing tools covering more and more of the workflow, such as W4M, mzmine, MetaboAnalyst and MS-Dial, have become available over recent years and continue to be enhanced as metabolomics workflows improve [156-159]. Pre-processed data is then normalised, usually using experimental quality control samples, to eliminate or minimise analytical bias such as signal intensity drift and batch effects [160]. Noise, blank features and non-reproducible features are removed before data analysis. Bioinformatics tools and statistical analyses are applied to address a specific goal, for example, identifying discriminatory features between healthy and diseased groups or correlative features with

visceral fat mass. Metabolite annotation is then performed on associated features using online database such as HMDB, Metlin, lipid maps and any in-house libraries developed with pure standard compounds [161-163]. Untargeted metabolomics studies expand the knowledge of potential differential metabolites/mechanisms and subsequently generate hypothesis for new studies. For example, in a biomarker study, validation of the discovered putatively new biomarkers is required in a separate cohort. To answer if these markers will respond to an intervention (e.g. dietary, environmental) or reflect metabolic improvement, then an interventional study should be performed. For metabolites and pathways found to be associated with the condition of interest, mechanistic studies can be conducted in cell- and animal-based models.

2.3 Application of metabolomics on cardiometabolic health research

2.3.1 Metabolomics profiling of obesity and dysglycaemia

Obesity is a whole-body adaptation to chronic energy surplus. It also plays a crucial role in the pathophysiological process of cardiometabolic diseases. Characterisation of metabolomic signature for obesity and its metabolic complications therefore improves understanding of metabolic alterations that occur during the development of obesity and provides insight into the metabolic abnormalities pinpointing adverse metabolic outcomes. Findings from metabolomic studies with a focus on the circulating markers for obesity and T2D identified from human data will be summarised, with underlying mechanisms to explain these associations provided where possible. Since obesity/overweight is simply indicated by BMI, which is convenient to measure, it is the most extensively characterised phenotype compared to other adiposity-related measurements or phenotypes. To date, changes in lipids, AAs and related

metabolites, sugar metabolites and TCA cycle intermediates, nucleotides and related metabolites and microbial metabolites have been reported in both obesity and T2D [42, 164]. Other relevant metabolites that do not fall into these categories have also been occasionally reported.

2.3.1.1 Lipid metabolism

As a condition of “fatness”, lipid derangements associated with obesity have been widely investigated. In a population-based cohort study, BMI adjusted for gender, age, systolic blood pressure (SBP), 2-h post load glucose and smoking status was associated with 17 lipid classes comprising 200 lipid species [165]. Class-association included positive correlations of BMI with dihydroceramide (dhCer), sphingomyelin (SM), phosphatidylcholine (PC), phosphatidylethanolamine (PE), phosphatidylinositol (PI), phosphatidylglycerol (PG), cholesteryl ester (CE), diacylglycerol (DG) and triacylglycerol (TG), and inverse correlations with mono- di- and tri-hexosylceraminde (M/D/THexCer), GM3 ganglioside (GM), ether-linked PC (PC), lysoPC, lysoPE and ether-linked lysoPC. Dysregulation of lipid metabolism is also a characteristic of T2D and suggested to be a metabolic event prior to the onset of dysglycaemia [166]. Meikle et al. have comprehensively measured the lipid profile associated with prevalent prediabetes and T2D and validated in a separate cohort [167]. Using logistic regression adjusted for age, sex, WC and SBP, both prediabetes and T2D were associated with over a hundred of lipid species encompassing 9 lipid classes, including higher levels of dhCer, ceramide (Cer), PE, PI, PG, CE, DG and TG, and lower ether-linked lysoPC compared with healthy controls. 8 out of these 9 class-association were replicable in the validation cohort except ether-linked lysoPC. They also performed linear regression against FPG or 2-h post load glucose adjusted for

covariates and reported additional lipid classes associated with dysglycaemia, including positive correlations of PC and GM, and inverse correlations of DHexCer, THexCer and ether-linked PC in at least one of the cohorts. Lastly, the study showed no significant discrimination of lipid class or species between T2D and prediabetes and highlighted a strikingly similar lipid profile for both conditions, leading the authors to conclude that alterations in the plasma lipid profile were clearly established in the prediabetic state.

The association of obesity with neutral lipids (DGs, TGs and CEs) have been consistently reported in other studies [165, 168, 169]. Abnormal levels of circulating neutral lipids are hallmark features of dyslipidaemia, which is a frequent complication of obesity that links to the development of IR [170]. Increased circulating TGs were also observed in individuals with abdominal obesity, visceral adiposity or fatty liver [171-174]. Notably, the TG signature associated with visceral adiposity or fatty liver were characterised by a low carbon number (≤54C) and double bonds (≤3) [172-174]. In prospective studies, elevated baseline TGs, especially those with low carbon numbers and double bonds, have also been associated with increased risk of T2D and CVD [175, 176]. As FA composition of TGs partly reflects long-term dietary intake and endogenous production, these TG signatures suggested a role of dietary pattern and an altered DNL in regional adiposity and likely contributing to development of cardiometabolic diseases. Interestingly, diet-induced weight loss was associated with predominant decreases and much greater fold changes in TGs species with low carbon number and double bonds [177].

Phospholipids are the major components of membrane bilayers and lipoproteins, among which PC is the most abundant lipid class followed by PE. Whilst an

association of obesity with increased PEs was occasionally observed [178], its association with altered PCs were more frequently reported. However, the direction and pattern of changes, as well as individual species being reported have been heterogenous. For instance, Bachlechner et al., reported that shorter-chained PC (C<40) was positively associated with BMI and WC whereas longer-chained PC (C≥40) was negatively associated [179]. Similar associations of shorter-chained PC including PC (C32:1, C32:2, 34:2, C38:3) with obesity were also observed in other studies [180, 181]. In a recent large cohort study, a majority of shorter-chained PC were also found to be positively correlated with BMI with the exception of C36:3 and C36:4, which were negatively correlated [178]. In contrast, among the 154 lipids measured in another recent large-scale lipidomic study, only PC (C38:3) was reported to be positively correlated with BMI whereas PC (C34:0, C36:0, C36:2, C40:7, C40:8) all showed negative correlations [182]. The author further validated these observations and only the associations with PC (C38:3, C34:0) were replicated. Such high levels of variability suggest the association between PC profile and obesity is likely to be largely confounded by other factors; future studies with more comprehensive data collection such as the dietary data may help disentangle this relationship. Likewise, the relationship between PCs and T2D remains inconclusive. Several PC species were reported to be lower in T2D or prediabetic patients using BMI-adjusted model [183, 184], yet large scale lipidomics study with adjustment for WC and other covariates revealed a mixed associations [167]. Individual PC species were reported to be associated with increased or decreased risk of T2D in prospective studies, but the pattern is elusive [175, 185-188]. On the other hand, elevated PEs have been consistently found to be associated with prevalent

and incident T2D/prediabetes [167, 189, 190]. Although the structural role of phospholipids is well documented, it is less well understood as to why their levels change under pathophysiological conditions. A concordant alteration of phospholipids and glycerolipids may be related to hypertriglyceridaemia and increased VLDL production [191]. In line with this, most of the serum TGs and PCs were reduced by weight loss [177]. Dissecting changes in subclasses and the FA composition in the phospholipids pool may provide further information. Ether-linked phospholipids and lysophospholipids are two phospholipids subclasses frequently reported to be associated with obesity and T2D.

Lower level of ether-linked PCs in obese individuals was reported, and its level was negatively correlated with BMI, total body fat (TBF) and SAT and positively correlated with insulin sensitivity [179, 180, 192, 193]. In another study, the pattern of low levels of circulating PCae and PEae species was shown to be specific to morbid obesity and not discriminatory between healthy and prediabetic state [194]. Contradictory to these observations, Elise et al., reported a significant elevation of circulating ether-linked PC and ether-linked PE in morbidly obese individuals [195]. However, the sample size of this study was small (n=28 in total, compared to tens to thousands subjects from the aforementioned studies) and some participants were on glucose/lipid-lowering medications. The effects of medications were not taken into consideration which can distort the observation as levels of ether-linked phospholipids were shown to be increased by lipid lowering therapy [196]. What has been interesting though is that they used these observations to guide a mechanistic study and demonstrated a stimulatory role of PE-(P-18:0/20:4) to the expression of adhesion molecules in endothelial cells *in vitro.* Intriguingly, a recent large cohort study found negative correlations of

ether-linked phospholipids with BMI and TBF with the exception of those containing a 20:3 or 20:4 acyl chain, which showed positive correlations with TBF [178]. Early studies suggested an anti-oxidative role of this lipid class [196, 197]. Conversely, ether-linked phospholipids containing 20:3 or 20:4 acyl chain may function as lipid reservoir for eicosanoids precursor, which releases arachidonic acid by phospholipase A2 (PLA2) hydrolysis and hence may have pro-inflammatory potential [198]. Ether-linked PCs was also inversely associated with both prevalent and incident T2D [167, 186]. Given the profound association of ether-linked phospholipids with metabolic health but a very limited knowledge of its biological role, this lipid class deserves more attention in future studies.

LPC and LPE are derived from PC and PE respectively via the action of phospholipase or lecithin-cholesterol acyltransferase (LCAT) [199, 200]. Findings on their relations with obesity have been controversial, as are with T2D state. Cross-sectional examination revealed higher LPC (14:0, 16:0, 16:1, 18:1, 18:2, 18:3, 20:5, 22:6), LPE (18:2, 22:6) and lower LPC (18:0), LPE (18:1) in diabetic men [201]; and lower LPC (20:4) in another study [183]. Anthropometric parameters (BMI, WC, TBF) inversely correlated with the global lysoPC and lysoPE profiles i.e. involving multiple species as a general pattern have been reported [165, 178, 202, 203]. Some studies highlighted specific species e.g. LPC (17:0, 18:1, 18:2, 19:0, 20:1, 20:2, 20:4) to be negatively associated with obesity [180, 194, 204-207]. Conversely, positive association of obesity with the global LPC profile or individual species e.g. LPC (14:0, 16:0, 16:1, 18:0), LPE (18:1) were reported by the others [168, 180, 206, 208, 209]. These various findings were in turn interpreted differently. The positive associations have been linked to a previously demonstrated proinflammatory and atherogenic properties of LPC

[209]; such interpretation would lead to the proposition that LPC plays causative role in the pathogenic process of obesity-related metabolic complications such as increased risk of CVD. Conversely, an altered LCAT activity in obesity leading to decreased levels of LPC was suggested to pinpoint the inverse association with global LPC profile [165]. In two short-term intervention studies, overfeeding or hypocaloric diet was associated with weight changes (gain or loss respectively) but not total LPC concentration; however, weight changes in both studies inversely correlated with changes in the level of several LPC species [203, 210]. Clearly, the LPC profile is jointly determined by both the dietary pattern and weight status/obesity; however, resolving the relative contribution by each factor is difficult based on current evidence. Nonetheless, accumulating evidence highlighted LPC (18:2) as a robust, independent negative predictor of incident T2D or dysglycaemia and improved prediction compared with established risk factors [186, 211, 212].

The level of conjugated FA (e.g. in TG, phospholipids) may delineate an altered desaturase activity. As such, the FA product-to-precursor ratio as an estimate for desaturase activity in various blood compartments and lipid fractions has been investigated. Eva et al., reported positive correlations of BMI with index of stearoyl-CoA-desaturase (SCD) (16:1/16:0), delta-6-desaturase (D6D) (20:3/18:2) and negative correlation with delta-5-desaturase (D5D) (20:4/20:3) in serum phospholipids [213]. Concordantly, positive correlations of 16:1, 20:3 whilst negative correlations of 18:2, 20:2 incorporated into plasma phospholipids with BMI were observed in a more recent study, and D6D was greater in obese individuals than lean [214]. Inverse associations of D5D index in phospholipids fraction with BMI, %total body fat and obesity were also noticed by the others

[206, 215]. These studies collectively suggest greater D6D activity and possibly lower D5D activity in obesity [216]. It is worth pointing out that both unconjugated FFA(16:1) and FFA(20:3) were shown to predict future development of metabolic syndrome in obese individuals despite being currently healthy [217], suggesting an altered desaturase activity associated with obesity is pathogenic in the long-term.

There is some evidence for an association between FFA alteration and obesity. Newgard et al., reported significantly higher levels of saturated fatty acids (SFAs), monounsaturated fatty acids (MUFAs) and n-6 polyunsaturated fatty acids (PUFAs) including FFA(14:0, 16:0, 16:1, 18:1 and 20:4) in obese than lean individuals [218]. PA (i.e. FFA(16:0)) was also correlated with visceral fat mass [219]. Conversely, deficiency in n-3 PUFAs including FFA(20:5) and FFA(22:6) was reported in both healthy obese volunteers and CVD male patients compared with healthy controls [220]. However, such associations were not universally observed, for example, a cross-sectional study measuring FFA profile in healthy Asian adults found no association between circulating FFA and obesity [221]. In another study, normal weight and healthy obese groups shared similar FFA profiles, both of which had significantly lower FFA levels than the unhealthy obese group [217]. As for dysglycaemia, there is also some evidence for a cross-sectional association between FFA and IR, prediabetes or T2D, however, the direction of association with individual FFA species were not consistently reported or only reported in one but not in other studies hence the pattern remains elusive [183, 222-224]. Similarly, there is insufficient data to support a prospective association between baseline FFA and T2D risk [225, 226]. Interestingly,

circulating levels of SFAs, MUFAs and n-6 PUFAs were shown to decrease after the weight loss intervention in overweight participants [227, 228].

In addition to the free or conjugated form, an essential role of FAs is to produce energy via beta-oxidation in mitochondria, with carnitine facilitating the transport of FAs across mitochondrial membrane. Medium-chain (MC) and long-chain (LC) acylcarnitines (ACs) as by-product and substrate of fat oxidation may therefore reflect beta-oxidation status and efficiency. Increased ACs (C6, C8:1, C14:1, C16, C18, C18:1, C14-OH and C16-OH) were reported in obesity [206, 208, 218, 229]. However, many of these observations were made in obese patients characterised by other metabolic abnormalities such as higher HOMA-IR and hyperlipidaemia and these potential confounders were not adjusted or matched for in these studies, making it inconclusive as to what extent an altered AC profile is attributed to obesity. To address this question, Mihalik et al., compared the AC profile in obese individuals free of dysglycaemia or with T2D and lean control. Specifically, elevated fasting LCACs were common to both obese individuals with and without T2D, whereas elevated MCACs was only observed in obese T2D individuals [229]. This is further supported by findings from Adams et al., in which MCACs were found strikingly higher in obese T2D compared with BMI- and age-matched obese non-T2D [230]. Increased LCAC may indicate increased FAO flux as a consequence of excess lipid load, whereas increased MCAC has been proposed to arise from incomplete FAO which may be more relevant to an IR state [231, 232]. This latter proposed mechanism is based on observation from *in vitro* and animal models, in which excessive FAO induced by lipid overload coincide with accumulating acylcarnitines, an inability to switch to carbohydrate substrate, and a depletion of TCA intermediates, suggesting discordant FAO and

TCA flux leading to incomplete FAO. Restricting FAO prevents lipid-induced IR in these models. In humans, whether an early, persistent increased FAO flux as in healthy obesity will eventually lead to metabolic inflexibility and IR remains to be established.

Sphingolipids are less abundant than phospholipids but important membrane components of microdomains and lipid rafts that affect receptor organisation and function. Subclasses including SMs, ceramides and sphingosine are also known bioactive molecules that regulate cell growth, differentiation and survival [233]. *In vitro* and animal studies have highlighted dysregulated sphingolipid metabolism in both obesity and during the development of IR, T2D and CVD [234]. In humans, SM species containing SFA chains (C18:0, C20:0, C22:0 and C24:0), but not ceramides, were reported to be higher in the obese group and positively correlated with the parameters for obesity, IR, impaired liver function and lipid metabolism [235]. Likewise, in another study, BMI did not correlate with ceramide but was associated with both the upstream precursor dhCer (positive) and downstream metabolites (positive for SMs, negative for hexosylceramides), suggesting an altered sphingolipids metabolism with upregulated *de novo* biosynthesis and ceramide-to-SM flux in obesity [165]. Increased dhCer and SMs were also associated with abdominal and visceral adiposity [209, 236]. In addition, among prediabetic patients, higher levels of SM (34:1, 36:1, 38:1, 40:1, 40:2, 42:2, 42:3) were observed in those with abdominal obesity compared with the lean group. All these findings collectively suggested an elevation of SMs as a metabolic trait for increased total and/or regional adiposity. Paradoxically, the levels of SMs were reported to be lower in IFG or T2D cases compared with healthy controls [183, 184]. Reduced SMs synthesis has been associated with

increased ROS and reduced insulin secretion therefore may be directly implicated in T2D pathogenesis [237]. Furthermore, the total plasma ceramide concentration and specific species (C18:1, 18:0, 20:0, 24:1, and 24:0) were elevated in T2D subjects and these elevated moieties correlated with the severity of IR and plasma TNF-α level, an inflammatory cytokine that upregulates sphingomyelinase and stimulates ceramide formation [238, 239]. The author then suggested that such an elevated ceramide might be a mediator of IR and inflammation. Given a profound association between obesity and T2D yet very distinct associated sphingolipid profiles, it is plausible that an increased SM biosynthetic flux occurring in obesity is resultant from an increased substrate availability; and the sphingolipid pathway is further modulated by additional factors such as increased pro-inflammatory cytokines during the pathogenesis of T2D, resulting in SM depletion and ceramide accumulation. Results from prospective studies are also obscure. An increased SM (C16:1) was reported to be associated with decreased risk of T2D in one study [186], whereas a more recent large-scale lipidomic study revealed increased T2D risk associated with higher SM(d16:1/18:0) and SM(d18:1/18:0) [240]. One caveat of drawing conclusion based on these findings and linking them to what has been known from mechanistic studies is the lack of a standardised way to report results, since both the sphingosine backbone and the conjugated FA component seems biologically relevant [241, 242].

2.3.1.2 Amino acid metabolism

The association of amino acids with obesity, insulin resistance and T2D has been noticed for more than 40 years [243]. Insulin potently inhibits protein degradation and promotes muscle uptake of amino acids from blood and stimulates protein

synthesis postprandially; thus a more concentrated amino acid pool during post-absorptive state indicates a blunted response to insulin [244]. Emerging evidence suggested alterations in AA metabolism may also be causally linked to pathogenesis of T2D.

Branched-chain amino acids (BCAA) including valine, leucine and isoleucine have been widely reported to be higher in obese individuals and correlated with anthropometric parameters, TBF, VAT and liver fat contents [204-206, 218, 245-249]. Weight loss profoundly reduced circulating BCAAs whose changes were also correlated with reduction in BMI [250, 251]. In addition, a higher level of circulating BCAAs was reported in T2D cases compared with healthy control, and the level of BCAAs predicts future development of T2D and intervention outcomes [186, 252, 253]. BCAAs are essential amino acids, therefore elevated BCAAs reflects excessive protein degradation, which is a consequence of IR. This is supported by a higher levels of BCAAs in metabolically unhealthy obese than metabolically healthy obese individuals and a positive correlation with HOMA-IR and HbA1c [218, 254, 255]. Elevated BCAAs can also result from an abnormal catabolism. Expression of genes encoding for BCAA-catabolising enzymes were reported to be downregulated in visceral and subcutaneous adipose tissues from obese, unhealthy human compared to lean or obese healthy human [254, 256, 257]. On the other hand, mounting evidence has shown not just BCAA, but their metabolites C3- and C5-acylcarnitines, are associated with obesity and strongly correlated with HOMA-IR, suggesting impaired or incomplete BCAA catabolism in obesity and IR state [206, 218, 258, 259]. This is further supported by a concordant reduction in α-ketoglutarate (substrate) and increase in glutamate (product), a paired partner involved in the first step of BCAA

catabolism [218]. The excessive catabolic flux of BCAAs and accumulation of their acylcarnitines metabolites may therefore, and once again (similar to the aforementioned MCAC and LCAC) indicate mitochondrial overload and metabolic inflexibility. Collectively, increased BCAAs may reflect increased protein degradation due to IR, an impaired clearance due to reduced catabolic enzymes, and possibly mitochondrial overload and mismatched TCA and FAO flux leading to incomplete catabolism and thus accumulation of acylcarnitine intermediates.

Higher levels of aromatic amino acids (AAA) including phenylalanine and tyrosine are also associated with obesity, IR and T2D [205, 218, 260-262], discriminatory between metabolically unhealthy obese and metabolically healthy obese individuals [255, 263], and predictive of incident T2D [261, 262]. Elevation of circulating AAA has been suggested in part due to competition for the large neutral amino acid transporter against BCAA [264]. However, AAA, tyrosine in particular, is also associated with visceral adiposity and liver fat content, weight loss and prediction of successful weight loss [207, 248, 250, 251, 265, 266]. Tyrosine is the hydroxylated product of phenylalanine and can be further catabolised by tyrosine aminotransferase (TAT) mainly taking place in the liver. TAT inactivation can be induced by sulphur-containing amino acid L-cysteine or L-cystine *in vitro*, and this takes place via the oxidation of TAT thiol group by thiocysteine, a product of cystine metabolism derived from the transsulfuration pathway [267-270]. Indeed, the transsulfuration pathway in the liver produces precursor for glutathione and an upregulation is tightly linked to oxidative stress [271], which is often implicated in obesity and T2D [272]. Increased flux through the transsulfuration pathways and inactivation of TAT in liver have been reported in experimental diabetes models [273, 274]. An altered AAA metabolism may

therefore be secondary to the protective mechanism to cope with oxidative stress, during which increased production of antioxidant molecules also yield by-products that inactivates TAT. Taken together, accumulation of tyrosine and possibly phenylalanine may indicate perturbed liver metabolism and reveal a status of excessive oxidative stress. This is further supported by a strong association between the level of phenylalanine and ALT [275], a liver dysfunction marker and is correlated with the incidence of cardiovascular disease and metabolic syndrome [276].

In light of the view that an impaired tyrosine catabolism in obesity is consequential to an altered metabolism of sulphur-containing AA, both tyrosine and cysteine have been highlighted as key AA correlates of components of metabolic syndrome, including WC, IR and inflammatory markers independent of age, gender, protein intake, resting metabolic rate and fitness index [277]. In fact, cysteine is hitherto the only AA with cellular, animal and epidemiologic evidence pointed to have an obesogenic effect [278]. Several metabolomic studies provide further evidence for a positive association of cysteine and/or cystine with obesity, IR and T2D [224, 279-281]. Changes of cysteine over time also correlated with changes in BMI and fat mass [282].

Another aromatic AA with a distinct metabolic pathway, tryptophan, and its metabolites including kynurenine and kynurenic acid, were higher in overweight/obese individuals and positively correlated with BMI [202, 204-206, 283, 284]. Kynurenine is also a discriminatory metabolite between metabolically obese and healthy obese individuals [263], and a direct vasodilating effect of kynurenine was reported [285]. Interestingly, expression of the enzyme responsible for tryptophan-kynurenine conversion i.e. indoleamine 2,3-

dioxygenase-1 (IDO1) in adipose tissue and liver was increased in obese individuals and inversely correlated with arterial blood pressure [286]. The kynurenine pathway was reported to be activated by pro-inflammatory cytokines and upregulated in human obesity [287]. The high level of kynurenine and increased kynurenine/tryptophan ratio thus reflect an inflammatory status [288]. In addition, increased kynurenine/tryptophan ratio and a positive correlation with BMI, fat mass, abdominal adipose tissue content and subcutaneous adipocyte size was observed in obese individuals [256, 286, 289]. Alteration of tryptophan metabolism and increased kynurenine pathway may therefore be a marker of low-grade inflammation but also modulate vascular tone that potentially lead to increased macrophage infiltration and nutrient flow towards peripheral tissues in obesity, hence acting as both a consequence of obesity and a contributing factor to its related complications.

In contrast, decreased circulating glycine and acylated glycine metabolites in obese subjects have reported as inversely correlated with BMI [205, 218, 290, 291]. Glycine was also positively correlated with SAT, inversely correlated with intermuscular fat and abdominal adiposity [292]. In addition, glycine is inversely associated with metabolically unhealthy obese phenotype, IR, T2D and prognostic for T2D development, and its level was increased in response to weight loss intervention or exercise program [293]. Glycine is a non-essential AA involved in a multitude of biochemical processes, therefore its depletion in obesity provides little insight into the pathophysiological mechanisms; nevertheless, its robust association with a range of metabolic outcomes makes it a promising candidate marker for diagnosing metabolic health. Data regarding changes of

other AAs and related metabolites has been less pronounced and the direction of changes has been inconsistent.

2.3.1.3 Carbohydrate metabolism

In the world of metabolome, carbohydrate is usually referred to low molecular weight mono- and di-saccharides and downstream metabolites. Elevated plasma glucose is the surrogate marker of prediabetes/T2D, and metabolomics data showing higher glucose in prediabetic/T2D individuals and in obese individuals than healthy control is coherent with conventional measurement [42, 204]. Other hexose sugars (e.g., fructose, mannose, inositol) are associated with prevalent and incident T2D [186, 223, 224, 294]. The major glucose metabolism pathways include glycolysis followed by TCA cycle (under aerobic condition) or production of lactate (under anaerobic condition), glycogenesis and pentose phosphate pathway; whereas the reverse, gluconeogenesis, is responsible for glucose production which mainly takes place in the liver. Increased substrates for gluconeogenesis including lactate and glycerol was associated with increased risks of dysglycaemia [225, 226]. Elevated lactate level is reported in obesity, T2D and NAFLD, and positively correlated with anthropometric parameters and VAT [202, 205, 219, 223, 249, 295]. Glycerol derived from lipolysis was also positively correlated with BMI [202, 205]. Increased circulating levels of citrate, a TCA intermediate, was observed in obese animals but evidence on obese humans are lacking [296, 297]. Positive correlation of other TCA intermediates such as isocitrate and succinyl-carnitine with BMI was occasionally reported [202, 204]. Xylitol is a substrate for the pentose phosphate pathway to generate glycolytic intermediate, and a lower baseline level of xylitol was shown to predict greater weight loss following a 1-year weight loss program [250]. 1,5-anhydroglucitol, a

sugar metabolite proposed as a short-term marker of glycaemic control, was inversely correlated with BMI and consistently reported to be lower in T2D [183, 205, 223, 298]. One should note that many of the carbohydrate-related metabolites were reported in isolated studies; more evidence is required to confirm their relationship with obesity and T2D and understand the underlying pathways.

2.3.2 Tissue metabolomics in obesity

While blood samples are convenient and minimally invasive to obtain from most subjects, thus highly suitable for clinical screening, a major limitation of studying the blood metabolome is that it provides little insight into the tissue site-specific abnormalities, which is usually more biologically relevant to disease pathogenesis. Given that tissue collection is an invasive procedure hence access is more difficult for clinical studies, the number of tissue metabolomics studies of obesity, IR and T2D in human is limited. Several studies compared the tissue metabolite profiles, and reported a range of metabolic changes in several tissues associated with T2D and IR e.g. an altered TG composition in AT [299], increased SFA and MUFA-containing TGs and FFAs, dihydroceramides and ceramides in liver [300], and a lower level of aspartate and higher level of glutamine, histidine, spermidine, SM C16:1, lysoPC (18:0) as well as several PC species in cultured human adipocytes from metabolically unhealthy obese than metabolically healthy obese individuals [301]. Whereas in obesity, increased proportion of certain FFAs (C16:1, C20:4) and ether-linked PE in adipose tissue was reported [193]. ex vivo AT profiling from obese individuals also revealed an increased AAs release and diminished uptake of essential AA by VAT [302].

A few studies report between-group comparisons of metabolite profiles of tissues alongside the plasma/serum sample data. Blachnio et al., profiled the sphingolipids in plasma and AT from obese and lean participants, and showed that AT total ceramide content, sphinganine, sphingosine, sphingosine-1-phosphate (S1P), Cer (C14, C16, C24) were greater in obese than lean participants in both genders. Plasma data showed similar trend, with total ceramide content, S1P, Cer (C14, C16, C18, C18:1, C24:1) observed to be significantly greater in obese than in their lean counterparts in both genders [303]. These data support that plasma provide a window into tissue-specific metabolites and show concordance/discordance with metabolic alterations in tissue site. However, such data did not provide direct evidence for plasma metabolite to act as surrogate markers of tissue metabolites. Only a few studies correlated circulating metabolites with their counterparts in different tissue zones and these studies were conducted in a targeted manner. Plasma FFA composition has been hypothesised to be indicators for AT FFA composition since AT lipolysis is a major source of plasma FFA. Hellmuth et al., reported a strong positive correlation of some plasma and AT (both SAT and VAT) FFA (15:0, 22:6, 18:2, 20:5) in obese non-T2D females [304]. However, a 12-month intervention study involving 204 male and female participants showed poor-to moderate correlation between plasma and SAT FFA at baseline, and changes in plasma n-3 PUFAs failed to predict changes in SAT in response to increased n-3 PUFA intake [305]. Acylcarnitines are FAO metabolites therefore it has been speculated whether metabolically active organ/tissues are sources of plasma acylcarnines. Plasma acylcarnitines did not correlate with muscle acylcarnitines [306]; data on other tissues/organs are lacking. On the other hand, several plasma steroid hormones

such as estrone, testosterone and dihydrotestosterone were found to be correlated with their concentrations in omental and SAT [307]. To bridge tissue metabolomics and biomarker research, a thorough investigation of the relationship between plasma and tissue metabolites is required. To date, no study employs untargeted metabolomics approach to gain a wide picture of the relationship between plasma and tissue metabolome. This lack of data comparing blood metabolome with tissue metabolome profiles in obesity/T2D studies highlights a potential gap in the understanding of more detailed metabolic phenotyping and altered metabolism in a specific tissue site. Relying on blood metabolites in a large circulating pool may hide the site-specific mechanisms being perturbed by metabolic disorders. Therefore, it is important to address this gap, in doing so it may improve the interpretability and the understanding of implication of plasma biomarkers identified by metabolomics approach. That brings out a current challenge in the field of untargeted metabolomics, that is, there is no single method able to measure the full metabolome in various sample types that contain very different metabolites compositions and abundances. Sample preparation is a crucial step to ensure metabolome coverage and data quality. In the next section, key considerations of sample preparation for untargeted metabolomics will be discussed.

2.4 Sample preparation for LC–MS-based untargeted metabolomics

2.4.1 The critical importance of sample preparation

Prior to instrumental analysis, metabolites must be liberated from complex biological matrices and presented in a form that is compatible with the analytical technique. Unlike other omics cascades which have uniform building blocks (nucleotides for DNA and RNA; amino acids for protein), the endogenous

metabolome constituents span a broad spectrum of physicochemical properties, ranging from very polar metabolites e.g. sugars and amino acids, to amphiphilic metabolites e.g. acylcarnitines and lysophospholipids, to the very hydrophobic end e.g. triacylglycerides and cholesteryl esters. As such, no single extraction solvent nor analytical platform can cover the full metabolome. The choice of sample preparation protocols highly depends on the analytical platform and the sample type, and the sample preparation step is critical for determining how comprehensive and reliable the profile collected is for subsequent data analysis. The relative levels of metabolites could be distorted by the sample-preparation methods or extraction methods, leading to contradictory biological interpretation and erroneous conclusions [308, 309]. Choosing and optimising an appropriate sample preparation method is therefore essential for metabolomics to succeed. Key elements in the success of an untargeted metabolomics study include wide metabolome coverage and reliable quantification, biological- rather than analytical-driven data variance, and ideally, even subtle changes detectable between groups.

2.4.2 Requirement for sample type-specific pre-treatment

Plasma and serum are the blood compartments widely used for clinical chemistry diagnoses and contain a broad range of metabolites, making them important targets for metabolomics study [41]. These samples are protein-rich biological matrices (6-8 g/L) and require pre-treatment to reduce protein contents to a tolerable level [310]. Presence of proteins can severely hamper the quality of the analysis (by binding and sequestering metabolites, suppressing ionisation efficiency, precipitating during analysis and blocking the LC column, modifying the stationary phase in the column etc.). Denaturation methods such as

aggregation by heat, salt, and acid is not ideal for metabolomics as they usually trap the metabolites in the aggregate resulting in loss of metabolites in the aqueous extract [310, 311]. In contrast, protein precipitation using organic solvents has been shown to have better reproducibility and metabolite coverage while efficiently removing proteins, among which methanol was reported to have superior performance [311]. The use of methanol has dominated the field. Over 50% of studies carry out plasma/serum extraction using pure methanol or methanol/water mixture (proportion varied from lab to lab) [41]. Acetonitrile is also used in some studies, but only achieved sub-optimal proteins removal compared with methanol-treated samples. Metabolite profile derived from methanol-treated samples was also reported to produce better group separation than acetonitrile-treated samples in the subsequent data analysis [312]. The use of other organic solvents or miscible solvents (methanol, ethanol, isopropanol, acetone, acetonitrile, chloroform and water etc.) with different proportions have also been reported but few of them have been widely used or validated [41].

Tissue metabolites provide larger amounts of biologically relevant information than biofluids as well as valuable insights into the biochemistry of disease. Intact tissues contain heterogenous cell types as well as extracellular matrix and cellular membrane that prevents direct contact of the organic solvent to intracellular contents [313]. Hence, tissue samples need to be physically disrupted and homogenised to increase reproducibility and extraction efficiency [314, 315]. Tissue grinding in liquid nitrogen or bead-based smashing with a tissue-lyser are common practice for tissue pre-treatment. The latter technique provides an advantage in that it allows simultaneous and high-throughput homogenisation of multiple samples, is convenient and eliminates any sample carry-over effect

[313]. A comprehensive comparison among different sample preparation strategies with C. elegans suggested bead-beating as a highly desirable tissue disruption technique over manual grinding or rotatory homogenisation [316]. For animal tissues, bead-beating was found to effectively homogenise brain, bone marrow, kidney, spleen and liver tissues whereas collagenase treatment followed by bead-beating was the best for lung and heart tissues [317].

2.4.3 Considerations on choice of extraction solvents

Metabolites are usually extracted by single phases or biphasic solvent systems, and the choice of extraction solvents can considerably affect the metabolite profile. For example, Reis et al., showed different extraction solvents have negligible effects on predominant lipid classes but significantly influenced the extraction efficiency for low abundant lipids from the human plasma LDL fraction [318]. In another study, protein precipitation with acetonitrile/isopropanol/water or acetone/methanol produced similar polar metabolite profiles but different from those obtained using biphasic extraction methods [319]. In monophasic extraction, proteins are precipitated by the addition of a single type or miscible organic solvent as introduced in the previous section. This is followed by centrifugation and the supernatant can be directly analysed. Monophasic extraction is the simplest form of extraction that requires minimal number of steps therefore is less prone to experimental variability. On the downside, a monophasic solvent is incapable of extracting metabolites with very different polarities. For instance, methanol is efficient in extracting polar metabolites but poor in solubilising neutral lipids, whereas hexane or chloroform favours hydrophobic molecules but poorly interacts with polar metabolites. Moreover, injection of a monophasic extract containing metabolites with a variety of

physicochemical properties may compromise the chromatographic separation. For example, metabolites strongly interacting with the separation column can modify the stationary phase such that it affects stability and retention of other metabolites. Metabolites which do not or weakly bind to the column can co-elute at the solvent front which is usually not reproducibly measured. In this regard the biphasic solvent system offers several advantages over monophasic solvent systems. This was firstly demonstrated by Folch and lately modified by Bligh and Dyer, a chloroform/methanol/water based-extraction solvent that produces an upper aqueous layer and bottom organic layer that is superior in recovering lipid fractions from tissues [320, 321]. Later this method was also demonstrated to be able to efficiently extract polar metabolites [322]. This method has become popular since the polar and non-polar metabolites partition into two different phases and are simultaneously extracted, which can then be analysed separately. It has been successfully used to extract a variety of sample types including heart, liver, brain, adipose tissue, muscle, plasma and serum [323-325]. Other studies have proposed using methyl-tert-butyl-ether (MTBE) or dichloromethane in replacing chloroform because of low toxicity and efficient recovery of both polar and non-polar metabolites [326-328]. The MTBE method is desirable for a lipidomics study since the organic phase sits at the top of the sample extraction tube and is easily accessible. Both the polar and lipid profiles obtained from the MTBE method are similar to those obtained from the Folch method, however, the Folch method has been reported to produce a slightly better lipid recovery [319].

2.4.4 Evaporation/reconstitution

To ensure data quality, metabolites extract needs to be presented in an analysis-compatible solvent and at an injected concentration that fits in the linear range of the analytical platform as much as possible. An evaporation/reconstitution step can be incorporated to achieve these goals.

A compatible injection solvent with the LC system is essential for optimal chromatographic separation. In some cases, the extraction solvents are incompatible with the initial mobile phase composition which can result in poor chromatographic peak shape. The use of organic solvents of high solvent strength generally improves lipids solubilisation but may interfere with a proper equilibration of the injected sample between column stationary phase (peak retention) and the mobile phase, leading to compounds smearing and peak distortion. To overcome these issues, the metabolite extract can be evaporated and resuspended in an appropriate solvent that suits the LC column and mobile phase. Optimising the reconstitution solvent has been shown to improve data quality, reproducibility and metabolome coverage. For example, Anna et al., showed RPLC−MS analysis of methanol-extracted samples reconstituted in 100% water produced the highest number of detected features as well as discriminatory metabolites between lymphoma vs healthy controls in the subsequent data analysis, over the use of 50% or 100% methanol for reconstitution [329].

A robust metabolomics method requires not just that a maximum number of metabolites is detected, but also that they fall within the linear dynamic range of the method so that the relative intensity reflects the inter-sample difference [148]. Not accounting for nonlinearity of the measurements will affect the biological interpretation of the results e.g. over- or underestimating the relative fold change

or distorting the relationship with a clinical measurement. Notably, different sample types are inherently different in metabolite composition and abundance. For example, glycerolipids account for more than 90% of the total lipid contents in adipose tissue whereas phospholipids and sphingolipids are less than 5% [330]. Triglycerides account for 50-70% of the total lipid contents in pork muscle, whereas the phospholipid can be present at a level as high as 50% depending on the metabolic subtypes of muscle tissues [331]. Concentrations of some amino acids and phospholipids species can occur at 5-10 or even 50 times higher in some tissues than others e.g. level of glycine in liver (3700 nmol/g) vs fat (425 nmo/g), level of phosphatidylcholine C38:6 in liver (1289 nmol/g) vs brain (126 nmol/g) vs fat (19.9 nmol/g) [332]. The large variability means different sample types extracted using a standardised protocol may not always be compatible with the loading capacity of the separation column or the linear dynamic range of the mass spectrometer. Signal response often becomes sublinear at high concentrations due to detector saturation or trap filling leading to space-charge effect. In an attempt to detect low abundant metabolites, it is common to overload LC-MS systems, compromising quantitative performance. The injected concentration of the same tissue type in the literature has varied considerably, for example, lipid extracts from cardiac tissue has been injected at 10 mg/ml or even lower [333, 334], whilst in another study the injected concentration was more than 10 times higher [335]. This lack of consistency is not unexpected, as it is due to, in part, different choices of reconstitution solvents, LC columns and separation methods as well as MS detector instrumentation type and sensitivity. However, the decision on a suitable injected concentration, as well as a strategy to ensure maximal number of features falling within the linear range of LC–MS in

the existing literature is rarely reasoned or described. This issue will be addressed in Chapter 3.

The take home message is that, no single analytical technique or extraction solvent can cover the full metabolome, and there is always compromise in a metabolomics study. It is very important to understand the strength and limitation of each technique, and the experimental strategy should be well adjusted to answer the research question.

3. Tissue-Specific Sample Dilution: An Important Parameter to Optimise Prior to Untargeted LC-MS Metabolomics

In an effort to draw biological meaningful conclusions, the data has to first be reliable, especially when the quantification of metabolites are in a relative terms i.e. within experiment. In spite of extensive research done to advance instrumental methodology and optimise metabolite extraction, the choice of a suitable injected concentration is often overlooked. This optimal concentration is not of a single metabolite, but is the overall injected concentration of a sample extract containing hundreds to thousands of metabolites, and needs to be carefully considered in order to ensure as many metabolites as possible can be reliably measured. However, the optimisation of this parameter is rarely looked at or discussed in the literature and is particularly relevant when measuring different sample matrices. Since the injected concentration is a factor that can affect data quality and reproducibility and given that this study works on multiple sample types, this section demonstrates a simple and fast workflow for the determination of this parameter.

Abstract

When developing a sample preparation protocol for LC–MS untargeted metabolomics of a new sample matrix unfamiliar to the laboratory, selection of a suitable injection concentration is rarely described. Here we developed a simple workflow to address this issue prior to untargeted LC–MS metabolomics using fresh pig adipose tissue and liver tissue. Bi-phasic extraction was performed to enable simultaneous optimisation of parameters for analysis of both lipids and polar extracts. A series of diluted pooled samples were analysed by LC system coupled to high resolution orbitrap MS instrument and used to evaluate signal linearity. Suitable injected concentrations were determined based on both the number of reproducible features and linear features. With our laboratory settings, the optimum concentrations of fresh tissue mass to reconstitution solvent extract concentration (mg tissue/ml reconstitution solvent) of liver and adipose tissue lipid fractions were found to be 125 mg/mL and 7.81 mg/mL respectively, producing 2811 (ESI+) and 4326 (ESI−) linear features from liver, 698 (ESI+) and 498 (ESI−) linear features from adipose tissue. For analysis of the polar fraction of both tissues, 250 mg/mL was suitable, producing 403 (ESI+) and 235 (ESI−) linear features from liver, 114 (ESI+) and 108 (ESI−) linear features from adipose tissue. Incorrect reconstitution volumes resulted in either severe overloading or poor linearity in our lipid data, while too dilute polar fractions resulted in a low number of reproducible features (<50) compared to hundreds of reproducible features from the optimum concentration used. Our study highlights on multiple matrices and multiple extract and chromatography types, the critical importance of determining a suitable injected concentration prior to untargeted LC–MS

metabolomics, with the described workflow applicable to any matrix and LC–MS system.

3.1 Introduction

Untargeted metabolomics is becoming more widespread as a powerful tool for biomarker discovery and determination of metabolic changes associated with exposure, diet, and disease at a system level [141, 336-339]. This involves measuring as many metabolites as possible, both the known and unknown molecules present in a biological sample, followed by data pre-processing to extract chemometric information and relative intensities of features from the spectral data, and subsequent analysis with multivariate/univariate statistical methods to identify discriminant features between groups of interest [38]. To date, liquid chromatography–mass spectrometry (LC–MS) is the preferred technique for untargeted metabolomics, enabling the most comprehensive metabolite coverage due to the compatibility of most metabolites with LC along with the sensitivity and selectivity of MS [151, 340, 341]. Although validated extraction methods suitable for various analytical platforms, tissue types and biofluids are available [313, 318, 326, 342-344], careful selection of a suitable injected concentration (or sample loading amount) for each particular LC-MS system are sometimes overlooked or less considered when developing a sample preparation protocol. Injected concentration can be associated with overloading, signal saturation or features falling below detection limit and, hence, is a factor that can affect data quality and reproducibility [345]. A robust metabolomics method requires not just that a maximum number of metabolites is detected, but also that they fall within the linear dynamic range of the method to allow direct comparison

of metabolites between samples [38]. Not accounting for nonlinearity of the measurements will severely affect the biological interpretation of the results.

With recent technological advances, a diverse range of LC–MS systems are available for untargeted metabolomics, spanning from the already commonly used systems such as high- or ultra-performance LC systems coupled to Q-TOF, orbitrap or triple quadrupole MS instruments [346], to more recently emerging analytical systems such as chemical isotope labelling (CIL)-nanoLC–MS [347]. The performance of different vendors LC–MS instruments systems can vary largely through factors such as ion source ionisation efficiency, ion extraction and focusing, and linear dynamic range of the MS detection system, as well as external variables such as the loading capacity of different LC separation columns. In a recent study by Cajka et al., the optimum loading amount of plasma extracts for lipidomics analysis was found to be instrument-dependent, and the author highlighted that avoiding ion saturation is the key to harmonise results across different laboratories [348]. The presence of sample-specific matrix effects could add further complexity with regards to ionisation mechanisms and interfering molecules impacting signal responses of individual metabolic features in a less predictable way [349]. Moreover, metabolite composition and abundance can vary widely for different sample types, hence, optimum injected concentration is also sample type-dependent and needs to be individually adjusted for.

In an untargeted metabolomics study, it is extremely difficult to use standard compounds to monitor signal linearity for every single feature due to the presence of unknowns [160]. Nonetheless, evaluation of the linear dynamic range can been performed using a serial diluted pooled quality control (QC) sample [348]. A

strategy that included a serial diluted pooled QC in an analytical run sequence along with the analysis of experimental samples, followed by removal of features that did not follow proper linear trends during data pre-processing step, has been previously proposed to improve data robustness and quality [350, 351]. Despite its usefulness in discriminating true biological signals from non-biological origin features, this strategy could also discard biological features that are already at a suboptimal concentration in the samples due to incorrect sample reconstitution. Carefully adjusting the reconstitution volume and determining a suitable injected concentration prior to the analysis of real experimental samples will help to ensure the optimum number of reproducible and linear features in a single analytical run of experimental samples are measured.

The goal of this study was to develop a strategy for the determination of optimal injected concentrations for untargeted LC–MS metabolomics analysis of multiple tissue and extract types. The approach includes LC–MS analysis of serial diluted pooled extracts, chromatographic visualisation, reproducibility assessment and concentration-intensity correlation calculation, and should be carried out before analysing any experimental samples. Our study highlights that the reconstitution volume (thus sample concentration injected into the LC-MS) must be carefully adjusted to avoid overloading and signal saturation, and that injected concentration affects feature reproducibility and, hence, is a critical and independent factor to check to ensure accurate and reliable data. The usefulness of the developed strategy is not limited to the animal samples exemplified in the present study but can be applied to a variety of other sample types and LC–MS systems.

3.2 Materials and methods

3.2.1. Animal Tissues for Sample Preparation Optimisation

Pig tissues were purchased from commercial butcheries (Palmerston North, New Zealand). The samples comprised a fresh section of subcutaneous adipose tissue from the loin area and liver.

3.2.2. Chemicals

All organic solvents for metabolite extraction, reconstitution and LC–MS analysis (chloroform, methanol, acetonitrile isopropanol and formic acid) were obtained from Thermo Fisher Scientific (Auckland, New Zealand) and were of LC–MS grade except chloroform, which was of analytical grade; Milli-Q® ultrapure water was obtained from Merck Millipore (Bedford, MA, USA). Ammonium formate (Fluka™, HPLC grade) was obtained from Sigma-Aldrich (Auckland, New Zealand). Lipid internal standard 1-palmitoyl(D_{31})-2-oleoyl-sn-glycero-3-phosphoethanolamine (16:0 d_{31}-18:1-PE) was purchased from Avanti® (Avanti Polar Lipids, Alabaster, AL, USA).

3.2.3. Metabolite Extraction

The tissue extraction protocol has been previously described [352]. Each tissue type was divided into 20 samples weighing 50 mg each. To extract metabolites, 50 mg tissue (adipose tissue, liver) was homogenised in 800 µL pre-chilled (-20 °C) $CHCl_3$:MeOH (50:50, v/v) with a 5 mm zirconium bead per plastic tube for 2 × 60 s at 30 Hz using a TissueLyser (Qiagen, Hilden, Germany), followed by addition of 400 µL water, vortex-mixing (2 × 15 s) and centrifugation (Eppendorf Centrifuge 5427 R, Germany). Centrifuge parameters were set at 11,000 rpm, 4 °C, 10 min. Two blank samples were prepared following exactly the same protocol except that there was no tissue present. For each tissue type, 200 µL of the lower organic layer from each sample was transferred into a glass tube,

combined and gently mixed to generate an organic extract pool, which was subsequently aliquoted into 200 µL samples, evaporated to dryness under a stream of nitrogen and stored at −80 °C until analysis. Similarly, pooled polar extract was made by combining 200 µL aliquots of the upper aqueous layer from each sample from the same tissue type, mixing and then dividing the pooled extract into 200 µL aliquots, and again evaporating to dryness under a stream of nitrogen and stored at −80 °C until analysis.

3.2.4. Serial Dilution Experiment for Reconstitution Volume Determination

Dried organic extracts from 200 µL aliquot of the pooled sample for each tissue type were re-dissolved in different volumes (ranging from 100–6400 µL) of a modified Folch solution ($CHCl_3$:MeOH:H_2O, 66:33:1, v/v/v) containing pre-dissolved 0.01% 16:0 d_{31}-18:1-PE internal standard [0.01% (%w/v)]. Dried aqueous extracts from 200 µL aliquot were re-dissolved in different volumes (ranged from 50 µL to 800 µL) of acetonitrile:H_2O (50:50, v/v). The reconstitution solvent volumes and full range of tested injected concentration for the organic and aqueous extracts from each tissue type was summarised in **Table 3.1**. Note: Higher reconstitution volumes were utilised for adipose lipid extracts as a preliminary study utilising the same reconstitution volumes as liver produced severe overloading. Concentration of the extract injected was calculated as in the equation below:

$$Concentration\ (mg/ml) = \frac{\frac{50mg\ tissue}{Extraction\ solvent\ volume\ (ml)\ \dagger} * 0.2\ ml\ aliquot}{\frac{Reconstitution\ solvent\ volume\ (\mu l)}{1000}}$$

† Extraction solvent for polar metabolite = 0.8 ml; Extraction solvent for lipid = 0.4 ml

Table 3.1: Reconstitution volume and concentrations of the analysed samples.

Lipid	Reconstitution volume (µL)	Concentration (mg/mL)*
Liver	100	250
	200	125
	400	62.5
	800	31.25
	1600	15.63
Adipose	1600	15.63
	2000	12.5
	3200	7.81
	4000	6.25
	6400	3.91
Polar Metabolite	**Reconstitution Volume (µL)**	**Concentration (mg/mL)***
Liver	50	250
	100	125
	200	62.5
	400	31.25
	800	15.63
Adipose	50	250
	100	125
	200	62.5
	400	31.25
	800	15.63

extract concentration* is expressed as mg fresh tissue before extraction per ml reconstitution solvent

3.2.5. Ultra-Performance Liquid Chromatography (UPLC)-Mass Spectrometry Analysis of Lipids

LC–MS conditions were slightly modified from a previously described method by Samuelsson et al. [353]. Lipid analyses were performed using an Accela 1250 quaternary UHPLC system coupled to Q Exactive hybrid quadrupole-Orbitrap mass spectrometer (Thermo Fisher Scientific, Waltham, MA, USA). An Acquity CSH™ C18 column 1.7 µm, 2.1 mm × 100 mm (Waters, USA) was used for lipid separation with a column temperature of 65 °C and mobile phase flow rate at 600

µL/min. The mobile phases consisted of acetonitrile/H_2O (60:40) with 10 mM ammonium formate and 0.1% formic acid (A), and isopropanol/acetonitrile (90:10) with 10 mM ammonium formate and 0.1% formic acid (B). Analytes were eluted from the column with the following gradient program: 15–30% B (0.0–2.0 min), 30–48% B (2.0–2.5 min), 48–82% B (2.5–11.0 min), 82–99% B (11.0–11.5 min), 99% B was maintained for 3.5 min followed by re-equilibration with 15% B for 5 min. Two microliter reconstituted samples were injected. Each sample was injected six times; three technical replicates with the mass spectrometer operating in positive and three technical replicates operating in negative ionisation mode with a heated electrospray ionisation source set to 370 °C. External mass calibration of the Orbitrap prior to sample analysis was performed by flow injection of the calibration mix solution according to the manufacturer's instructions. High resolution data (resolution 70,000 at 2 scans/s) was acquired by full scan from *m/z* 200–2000 with source voltage of 3500 V electrospray ionisation positive mode (ESI+) or −3600 V ESI negative mode (ESI−), capillary temperature of 275 °C, and sheath, auxiliary and sweep gas flow rates of 40, 10 and 5 arbitrary units, respectively.

3.2.6. Liquid Chromatography (LC)-Mass Spectrometry Analysis of Polar Metabolites

The LC–MS conditions used in this study were as previously described [354]. Briefly, polar metabolites were analysed with an Accela 1250 quaternary UHPLC pump coupled to an Exactive Orbitrap mass spectrometry (Thermo Fisher Scientific, Waltham, MA, USA). Chromatographic separation was carried out at 25 °C on a SeQuant® ZIC®-pHILIC 5 µm, 2.1 mm × 100 mm column (Merck, Germany) with the following solvent system: A = 10 mM ammonium formate in

water, B = 0.1% formic acid in acetonitrile. A gradient program was used at a flow rate of 250 µL/min: 3–3% A (0.0–1.0 min), 3–30% A (1.0–12.0 min), 30–90% A (12.0–14.5 min), 90% A was maintained for 3.5 min followed by re-equilibration with 3% A for 7 min. An injection volume of 2 µL was used and each sample was injected six times; three technical replicates with the mass spectrometer operating in positive and three technical replicates operating in negative electrospray ionisation mode. The electrospray probe was operated unheated at room temperature (20 °C) to avoid degradation of thermally labile compounds. External mass calibration of the Orbitrap prior to sample analysis was performed by flow injection of the calibration mix solution according to the manufacturer's instruction. High resolution data (resolution 25,000 at 4scans/s) was acquired by full scan from *m/z* 55 to 1100 with source voltage of 4000 V for ESI+ and −4000 V for ESI−, capillary temperature of 325 °C, and sheath, auxiliary, and sweep gas flow rates of 40, 10, and five arbitrary units, respectively.

3.2.7. Data Processing

The acquired spectral data were converted with the ProteoWizard tool MSConvert (v 3.0.1818) to mzXML format and pre-processed with the XCMS package (v3.0.2) in the R environment (v3.2.2) [154], to extract chemometric information (metabolic features) and integrate the peak area (intensity) of the detected metabolic features. Solvent front (retention time < 2mins) was removed from analysis. Chromatographic visualisation was performed using Xcalibur™ Software (Thermo Fisher Scientific, USA). Total ion chromatograms (TIC) were visually examined to investigate the overall changes of total ion intensity as well as metabolite/lipid profiles. The extracted ion chromatograms (EIC) of peaks selected from highly apparent/abundant elution regions along with low abundant

peaks from the baseline region were also assessed for Gaussian shape and visual trends of signal response relative to the injected concentration. XCMS parameters for peak detection in lipid and HILIC data are provided in **Table 3.2**. The pre-processed data was subjected to blank features filtering based on tstat and p-values (sample vs. blank tstat < 1 or those with tstat >1 but p-value ≥ 0.05) generated by the diffreport function from the XCMS package. Subsequent analyses were conducted on non-blank features and all results and discussion were based on non-blank features only, defined as having a sample vs. blank tstat > 1 and p-value < 0.05. The relative standard deviation (RSD) of each injected concentration for every feature was calculated based on the triplicate injections. Peak areas were log10 transformed and used to calculate the Pearson correlation coefficient (r) between intensity and concentration to provide an estimate of linearity. The mean intensity-concentration relationship cut-off value selected to represent good linearity was r > 0.95 for lipid features and r > 0.9 for HILIC features. Linearity calculations were repeated five times, firstly covering the full concentration range, and then excluding the lowest, two lowest, highest and two highest concentrations sequentially. The resulting features meeting the linearity requirements utilising the correlation and exclusion procedure described above were then gathered to yield the maximum number of linear features, thus determining the optimal concentration to be used for analysis.

Table 3.2: XCMS settings for peak detection in lipid data and HILIC data obtained from each ionisation mode

	Method	Ppm	Mzdiff	Peakwidth	Prefilter	Snthresh	Noise
Lipid ESI+	centwave	10	0.001	5, 30	6, 20000	20	10000
Lipid ESI-	centwave	10	0.001	5, 30	6, 20000	20	10000
HILIC ESI+	centwave	10	0.001	12, 48	3, 2000	20	1000
HILIC ESI-	centwave	10	0.001	12, 48	3, 2000	20	1000

Ppm: maxmial tolerated m/z deviation in consecutive scans, in ppm (parts per million)
Mzdiff: minimum difference in m/z for peaks with overlapping retention times, can be negative to allow overlap

Peakwidth: Chromatographic peak width, given as range (min,max) in seconds
Prefilter: prefilter=c(k,I). Prefilter step for the first phase. Mass traces are only retained if they contain at least k peaks with intensity >= I.
Snthresh: signal to noise ratio cutoff, definition see below.
Noise: optional argument which is useful for data that was centroided without any intensity threshold, centroids with intensity < noise are omitted from ROI detection

3.3 Results and Discussion

3.3.1. Workflow Summary and General Considerations

A step of solvent evaporation and reconstitution has become commonly used in untargeted metabolomics, allowing for changes in injection solvent composition and the injected concentration of the sample extracts, ensuring optimal chromatography along with maximal metabolome coverage and/or minimal saturation is achieved [355]. It has been previously reported that optimum loading amount for plasma lipidomics analysis was instrument-dependent [348, 356]. The present study highlights that the optimum injected concentration is also sample type-dependent and should, therefore, be adjusted individually for each tissue matrix and analytical stream. We developed a simple workflow for the determination of suitable injected concentrations for animal tissues metabolomics and lipidomics analyses, to maximise the number of features that fall within the linear range of analysis.

The developed workflow consisted of four steps: serial dilution and analysis of a pooled sample, brief visual chromatographic examination, data processing to summarise the number of features and their measured peak areas, followed by peak area response linearity assessment using calculated correlation coefficients. The selection of an initial concentration range to test began with the highest possible concentrations as it was likely to allow more low abundant metabolites to be detected [357]; however, this sample pre-concentration was also most likely to produce overloading and ion suppression and potentially

introduce changes in the matrix [160]. To ensure injections causing excessive system overloading were quickly eliminated from the process visual chromatogram examination was initially carried out before entering the more time-consuming data pre-processing step. This step provided a quick view of the systematic effect of injected sample dilution on the acquired profile, peak shape, and linear trend. To perform this visualisation step, stacked or overlaid TIC and selected EIC of small, medium, and large peaks on a fixed intensity scale were examined. Peaks with height and area in the TIC and selected EICs increased as the concentration increased in response (e.g., peak height, ion abundance, peak area) to concentrations whilst maintaining Gaussian shapes without severe distortion (e.g., widening, shoulder peak split peak, flattened apex) were considered as acceptable and the tested concentration ranges were passed onto the next step for further data processing. If the visual inspection was not passed, the serial dilution experiment could be repeated with a higher or lower concentration range if there were no practical limitations, e.g., available sample amount. Once the visual chromatographic examination was satisfied, data processing was carried out to examine the effects of injected concentration on the number of detected features and their reproducibility. Correlation coefficients for the concentration-dependent response of every feature were calculated. This step covered the full range of testing concentrations as well as excluding one or two concentrations at either the higher or the lower end. When the highest (one or more) concentrations were excluded and the correlation calculations produced more linear features than that from the full concentration range, it was considered that there was a considerable number of chromatographically overloading features or features undergoing signal saturation or suppression. Likewise,

excluding the lowest (few) concentrations produced more linear features, signifying that several features are under the detection limit when a low concentration is injected. This evaluation step informed how high or low the injected concentration may go without causing too much overloading/saturation or information loss. The general rule we followed to determine the suitable injected concentration for the analysis of our (or any) sample type was that the highest possible concentration within the concentration range that produced the maximum number of linear features should be selected.

3.3.2. Chromatographic Examination

Lipid extracts from liver and polar metabolite extracts from both adipose tissue and liver were injected at a concentration range between 15.63–250 mg/mL, whereas lipid extracts from adipose tissue were injected at a much lower concentration range between 3.91–15.63 mg/mL. This was due to severe chromatographic overloading of adipose lipid profile between 10–13 min analysed in ESI+, and supressed signal intensities between 5–9 min in ESI− that we observed in a preliminary study with a concentration range between 15.63–250 mg/mL (**Appendix: Figure 9.1**). Incorrect reconstitution volumes, i.e., too concentrated lipid fractions from adipose tissue in this case, resulted in severe overloading and poor dilution responses, and this was improved by diluting the samples further (**Figure 3.1**). Examination of TICs and EICs of adipose tissue lipid profiles injected at 3.91–15.63 mg/mL showed overall good dilution responses and Gaussian peak shapes in ESI+ (**Figure 3.2**) and ESI− (**Figure 3.3**). Although trends of saturation at the higher concentrations were still observed and lower concentrations likely resulted in signal loss, these issues were further addressed and appraised using the subsequent step of linearity

calculation and evaluation described below. It was also noted the importance of combining TICs and EICs for this step since relying solely on TICs examination could sometimes be misleading especially for regions with medium-to-low ionic intensities. For example, *m/z* 732.5528 from **Figure 3.2** showed no apparent peak in the TIC, so performing EIC allowed testing of the dilution response for a concentration range of peaks. This highlighted that for the chromatographic examination step, it was important to examine not only regions of high intensity peaks, but also the baseline region. The three other tissue extracts (lipid for liver tissue, HILIC (polar metabolites) for liver tissue and adipose tissue) also passed both TICs and selected EICs evaluation step, showing overall good concentration-dependent responses and Gaussian peak shapes of the EICs (**Appendix: Figure 9.2–9.4**) and, thus, were passed through to the XCMS data processing step.

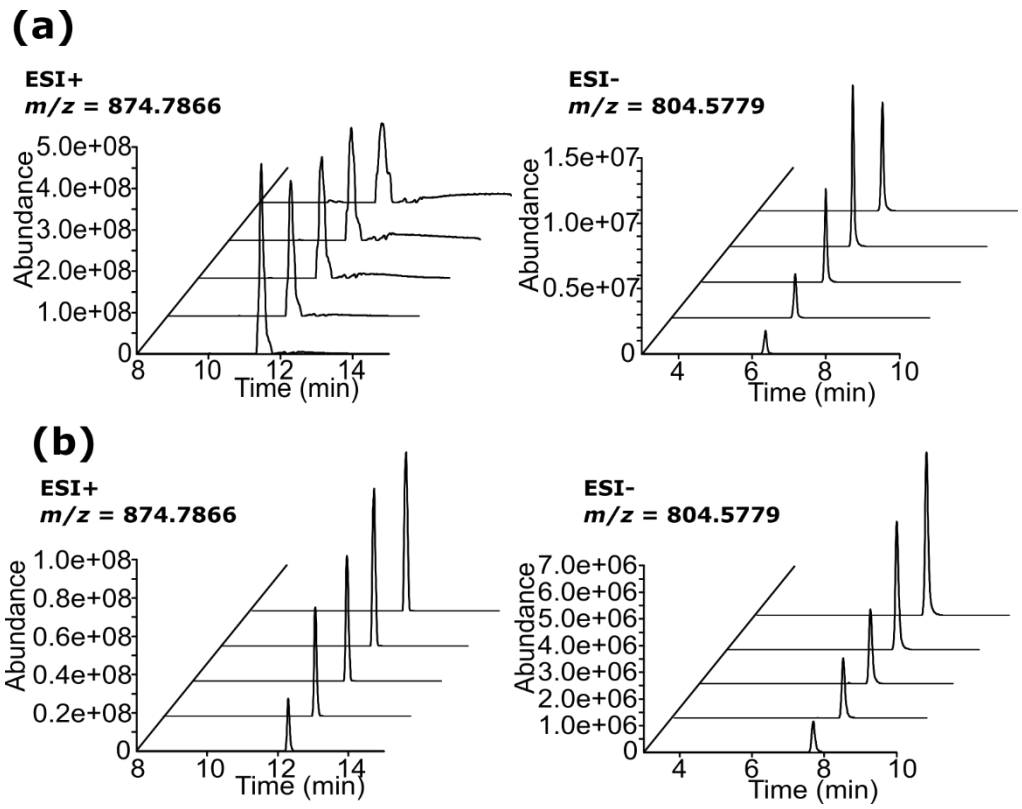

Figure 3.1: Extracted ion chromatogram (EIC) of selected features from adipose tissue lipid profile on a fixed scale of absolute intensity. EIC at (a) high injected concentrations (15.63–250 mg/mL) showed overloading in ESI+ and suppressed signal intensities in ESI−; data was from unpublished preliminary study and can be found in S1. This was improved by injecting at (b) lower concentration range (3.91–15.63 mg/mL) with higher dilution factors. The EIC along the z-axis starts from the lowest injected concentration at the front towards the highest concentration at the back.

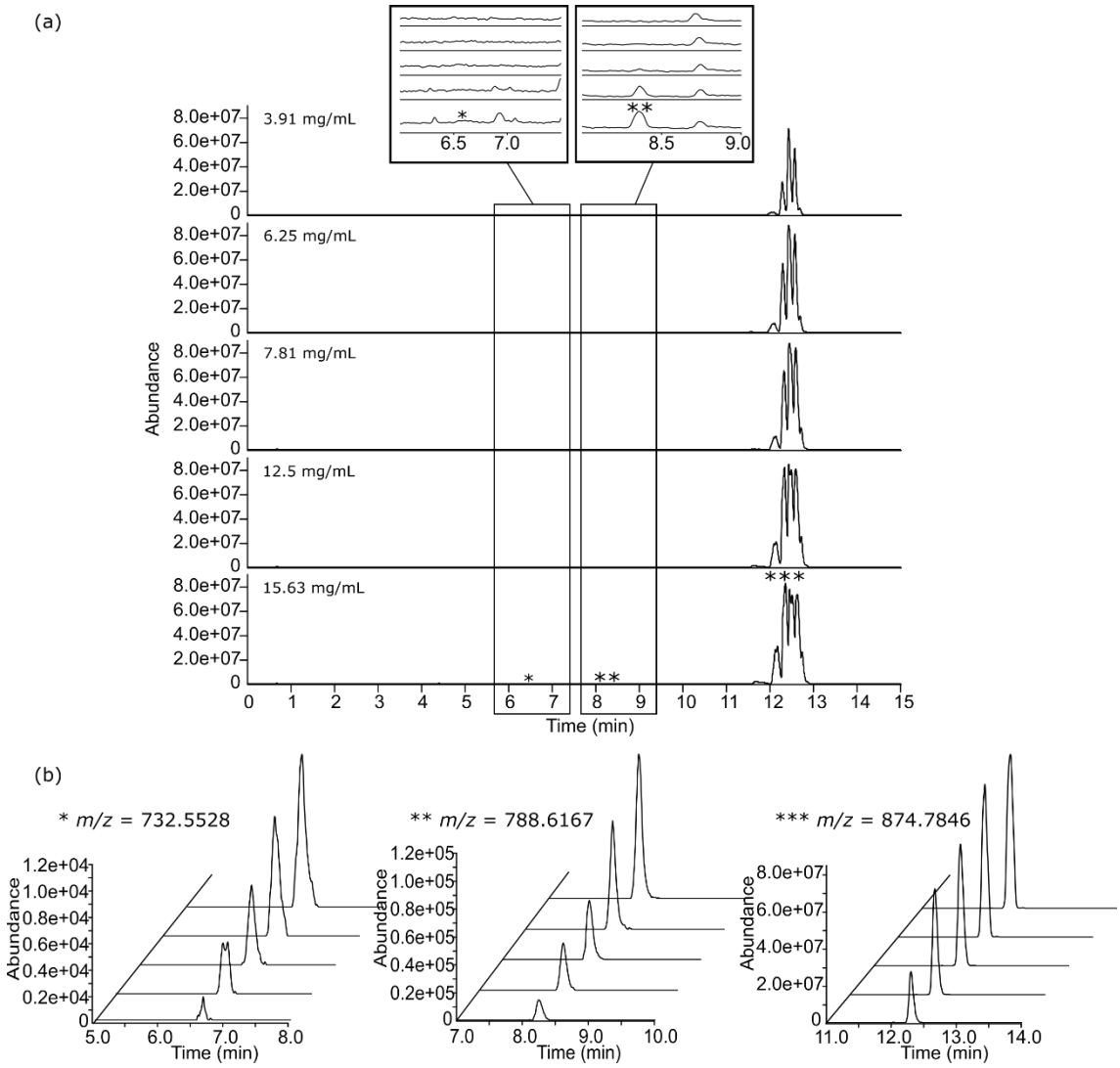

Figure 3.2: (a) Total ion chromatogram (TIC) of lipid extracts from 50 mg adipose tissue at low (3.91 mg/mL), intermediate (7.81 mg/mL) and high (15.63 mg/mL) injected concentration analysed by ESI+ and (b) examples for selected EIC of peaks representative of low, medium and high intensity features are indicated in the TIC with *, **, and *, respectively, on a fixed scale of absolute intensity to evaluate peak shape and the concentration-dependent response. The EIC along the z-axis starts from the lowest injected concentration at the front towards the highest concentration at the back.**

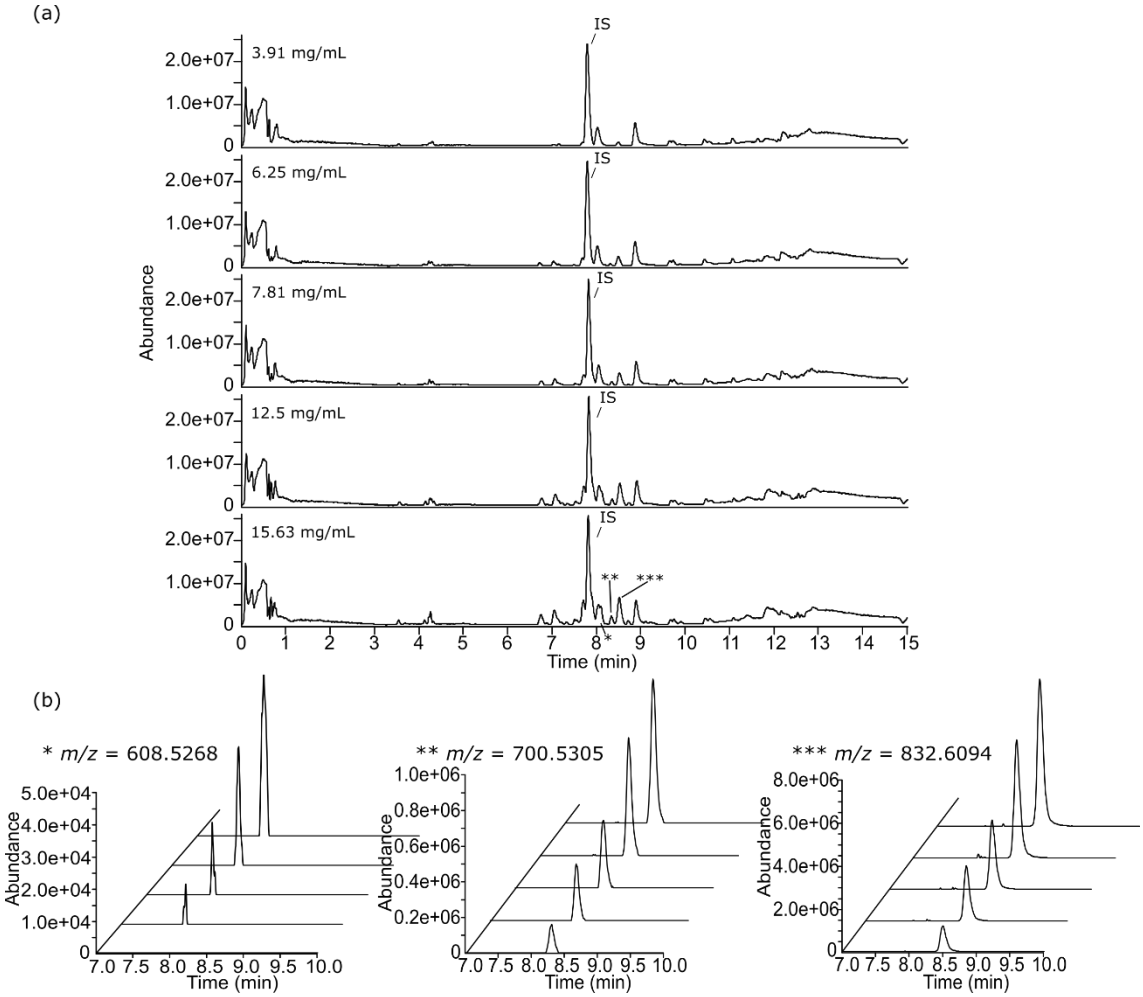

Figure 3.3: (a) Total ion chromatogram (TIC) of lipid extracts from 50mg adipose tissue at low (3.91 mg/mL), intermediate (7.81 mg/mL) and high (15.63 mg/mL) injected concentration analysed by ESI− and (b) examples for selected EIC of peaks representative of low, medium and high intensity features are indicated in the TIC with *, **, and *, respectively, on a fixed scale of absolute intensity to evaluate peak shape and the concentration-dependent response. The EIC along the z-axis starts from the lowest injected concentration at the front towards the highest concentration at the back. IS: Internal standard peak.**

3.3.3. Feature Summary and Reproducibility

An increased number of features detected by XCMS was observed as injected concentration increased in both the lipid and HILIC analyses for ESI+ and ESI− of adipose tissue and liver tissue (**Table 3.3**). This was expected as lower injected concentrations tended to result in loss of signal of the lower abundant metabolites [358]. In the lipid data for both tissues, over 80% of the detected features in every

tested concentration in both ionisation modes exhibited good reproducibility (relative standard deviation (RSD) < 30%), indicating that increasing the injected concentration did not impair reproducibility under conditions applied in this study.

Table 3.3: Number of total detected non-blank features, number of non-blank reproducible features and percentage (%) reproducible features of total features at each concentration in lipid and polar (HILIC) fraction of adipose tissue and liver extracts.

-	Concentration (mg/mL)	ESI (+)			ESI (−)		
		#Non-Blank Features (tstat > 1, p < 0.05)	#Non-Blank Features with RSD < 30	%	#Non-Blank Features (tstat > 1, p < 0.05)	#Non-Blank Features With RSD < 30	%
Adipose lipids	3.91	856	814	95.1	441	420	95.2
	6.25	921	895	97.2	628	605	96.3
	7.81	939	914	97.3	751	710	94.5
	12.5	955	934	97.8	972	935	96.2
	15.63	985	942	95.6	1160	1127	97.2
Liver lipids	15.63	1339	1189	88.8	2984	2789	93.5
	31.25	1784	1510	84.6	4038	3820	94.6
	62.5	2634	2418	91.8	5122	4824	94.2
	125	3098	3047	98.4	5952	5659	95.1
	250	3210	3110	96.9	6576	6186	94.1
Adipose HILIC	15.63	20	17	85.0	30	29	96.7
	31.25	25	21	84.0	57	55	96.5
	62.5	77	72	93.5	72	62	86.1
	125	209	203	97.1	114	101	88.6
	250	239	217	90.8	176	154	87.5
Liver HILIC	15.63	53	47	88.7	39	11	28.2
	31.25	82	74	90.2	83	38	45.8
	62.5	435	413	94.9	236	221	93.6
	125	480	443	92.3	304	276	90.8
	250	553	496	89.7	380	349	91.8

Similarly, over 80% of the detected features in every tested concentration of both tissues analysed by HILIC ESI+ exhibited good reproducibility (RSD < 30%), whereas HILIC ESI− analysis produced less features as well as a generally larger RSD, especially at lower injected concentrations (≤31.25 mg/mL). Despite a generally good RSD analysed by HILIC ESI+, the total number of features and percentage of reproducible features were much lower at low concentrations (≤31.25 mg/mL). Our data showed that when injected concentrations were less than 31.25 mg/mL, a large portion of polar metabolic features from both adipose and liver tissues were not stably and reproducibly measured, and thus should be avoided. This highlighted that the injected concentration considerably impacted

both the number of detected features and features reproducibility, especially with the HPLC HILIC analysis system, and therefore should be taken into consideration when selecting for a suitable injection concentration for LC–MS analysis.

3.3.4. Feature Linearity Testing for Selection of Suitable Injection Concentration

Linearity assessment was performed on all features present in the highest injection concentration in each dataset, including those that might fall outside the detection limit when injected at a lower concentration. After careful assessment of the linear relationship between concentration and peak area response, a correlation coefficient (r) cut-off value of 0.95 for the lipid and 0.9 for the HPLC HILIC analysis was considered optimal for the two analytical datasets. The difference in cut-off value for lipid and HILIC analyses was due to an overall different data reproducibility by the two analytical platforms. RSDs were better for the UPLC lipid analysis than the HPLC HILIC analysis potentially due to higher signal-to-noise ratios and improved peak integration of the UPLC peaks [359, 360], with the reproducibility of the peak measurement likely impacting the correlation coefficient. For example, the highest r value in the ESI− analysis of liver lipid and HILIC were 1 and 0.97, respectively, despite they were graphically similar in the degree of linearity (**Figure 3.4**). Figure 3.4 showed how progressive drops in r value corresponded to changes in the linear relationship between concentration and ion intensity on a correlation plot and provides (some visual) references as to how an optimal cut-off value for linearity assessment was determined. As expected, a clear linear relationship was observed at the highest r value to start with. At the first few units drop in the r value, e.g., from 1–0.96 in lipid and 0.97–0.93 in HILIC analyses, the linear relationship was preserved. As

r value dropped further, the linear relationship started to slightly distort or curve. A cut-off value was set at the margin of the well-preserved linearity and where subtle curvature may occur. In the following context, features that passed the cut-off value will be referred as linear features and the rest as non-linear features.

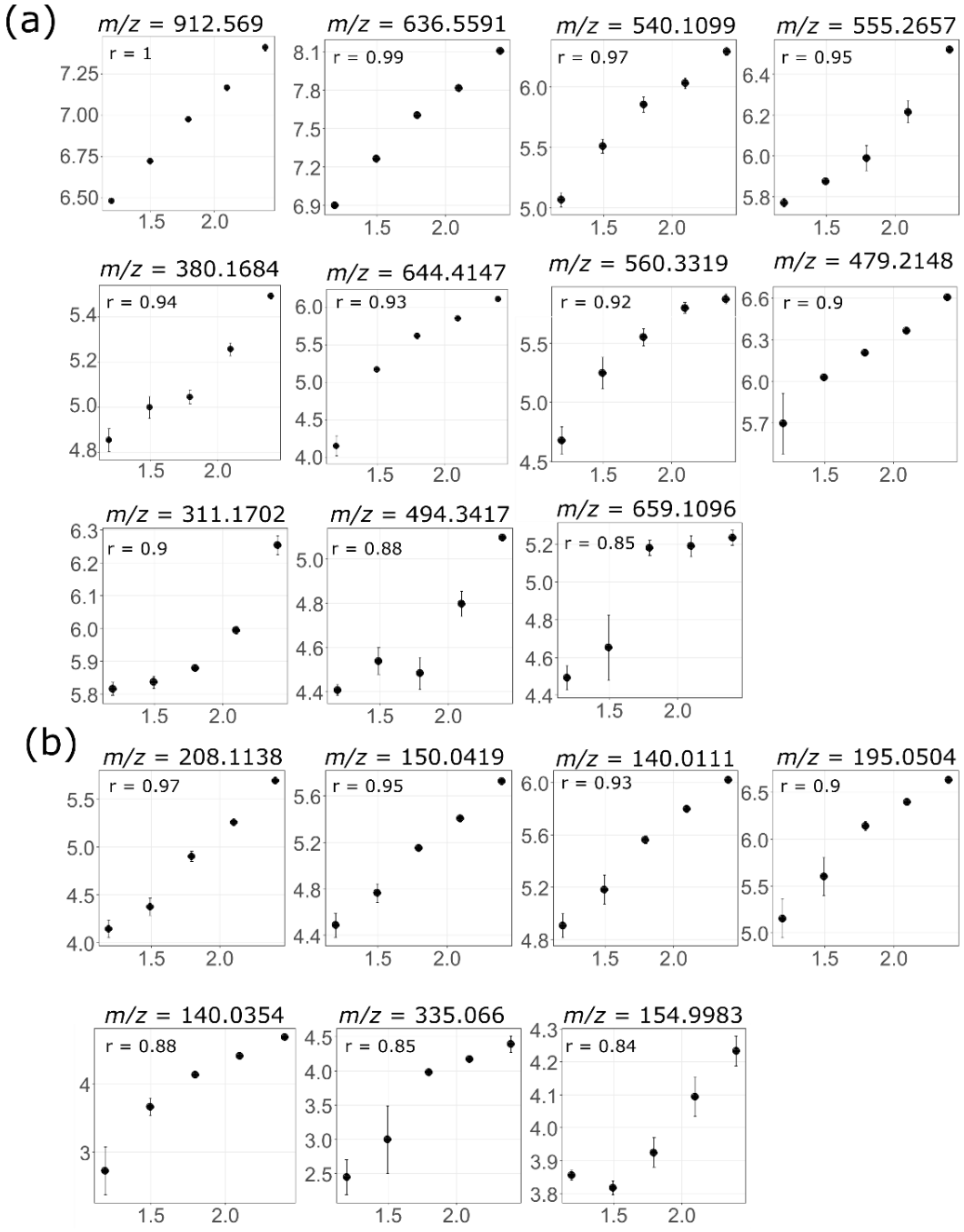

Figure 3.4: Examples for correlation plots of features in liver lipid ESI− (a) and liver HILIC ESI− (b), highlighting a linear-to-non-linear transformation from the above to the below of the cut-off r value (0.95 for lipid and 0.9 for HILIC). X-axis: log-transformed concentration; y-axis: log-transformed intensity.

Non-linear features were mainly due to: 1) Large RSD in one or more concentrations at either the higher or lower concentration end; 2) Near plateau at either the higher or lower concentration range; and 3) Processing artefacts, matrix effect and substances from non-biological origin. Non-linear features due to the last reason above would have random trends or an inverse correlation for the signal-to-injection concentration response [361]. Whilst processing artefacts are inevitable, the number of features attributed to this category should be similar for the same tissue extract type across the five tested concentrations because the extraction protocol, instrument settings, and XCMS data pre-processing settings were kept identical. Non-linear features due to the first two reasons above would still produce a concentration-dependent trend and removal of the distortion region was expected to resume linearity. As such, the correlation coefficient was recalculated with the exclusion of one or two concentrations at either end of the injected concentration range. Non-linear features that became linear after exclusion of one or two concentrations would be assigned to one of the “exclude” categories; for example, if excluding the highest concentration made a non-linear feature become linear it was assigned/categorised as “exclude h1”. The number in each category was then compared to investigate how many non-linear features were due to higher end or lower end issues (e.g., overloading, below detection limit, high RSD, etc.). and the result for all datasets were summarised in **Table 3.4**.

Table 3.4: Number of features exhibiting linear trend from correlation analysis with full range of tested injected concentrations (r > 0.95 for lipids, r > 0.9 for HILIC) and number of additional features exhibiting linear trend after excluding the lowest concentration (exclude l1), excluding the lowest two concentrations (exclude l2), excluding the highest concentration (exclude h1) and excluding the highest two concentrations (exclude h2).

Lipids									
Mode	Tissue	#Feature	r > 0.95	Exclude l1	Exclude l2	Exclude h1	Exclude h2	Remain r < 0.95	Undefined
ESI+	Adipose	985	428	23	5	56	188	235	50
	Liver	3210	2119	422	299	20	25	314	11
ESI-	Adipose	1160	304	121	42	25	47	576	45
	Liver	6576	3022	654	587	181	325	1683	124
HILIC									
Mode	Tissue	#Feature	r > 0.9	Exclude l1	Exclude l2	Exclude h1	Exclude h2	Remain r < 0.9	Undefined
ESI+	Adipose	239	94	6	14	1	2	122	0
	Liver	553	349	16	38	9	7	134	0
ESI-	Adipose	176	70	26	12	0	1	67	0
	Liver	380	136	39	60	2	1	142	0

Figure 3.5 utilised liver lipid ESI− as an example to demonstrate this approach. Among the 6576 features detected, 3022 features exhibited linear response, and 3554 features were categorised as non-linear features when the dilution trend of full concentration range was used. Among these 3554 non-linear features, 654 features became linear after excluding the lowest concentration, and an additional 587 features became linear after excluding the lowest two concentrations, indicating a large number of features were problematic if injected at low concentration (<31.25 mg/mL). Possible reasons included samples were too dilute to be reproducibly measured or completely below the detection limit at these concentrations. On the other side, 181 and an additional 325 features became linear after excluding the highest and second highest concentrations respectively. The higher concentration end issue was likely to be associated with column overloading, saturation, signal suppression and/or samples became too concentrated to be reproducibly measured. A total of 1683 features remained non-linear even after excluding the higher or lower end datapoints. This can be attributed to several reasons, such as processing artefacts, signals from non-

biological origin, incomplete removal of noise, or simply because the testing range did not cover the linear range of the feature. There was also a small amount of features falling in a category called “undefined” and only lipid data in the present study appeared to show this phenomenon. These features were non-linear in the full range but became linear both after excluding higher end and low end, primarily due to dual end issues for which the exact reasons were difficult to identify and the responses were less predictable. As the number of features falling in this category was tolerable in all four lipid datasets (<10% of total features), they were treated as non-linear features, rather than being assigned to any of the “exclude” categories. Collectively, the interpretation of this step indicated that in liver lipid ESI−, it was favourable to inject higher than 31.25 mg/mL. Similarly, in liver lipid ESI+ excluding l1 and l2 increased the number of linear features by 422 and an additional 299 respectively, whereas excluding h1 or h2 only slightly increased the number of linear features by 20 and an additional 25, respectively, suggesting an injected concentration higher than 31.25 mg/mL was favourable. Adipose lipid ESI− favoured an injected concentration higher than 3.91 mg/mL but ESI+ data indicated a considerable amount of overloading features if injected beyond 12.5 mg/mL, with excluded h2 increasing the number of linear features by 188. Therefore, it was desirable to also avoid an injected concentration higher than 12.5 mg/mL. All four HILIC datasets suggested an injected concentration no less than 31.25 mg/mL should be used for polar metabolites analysis.

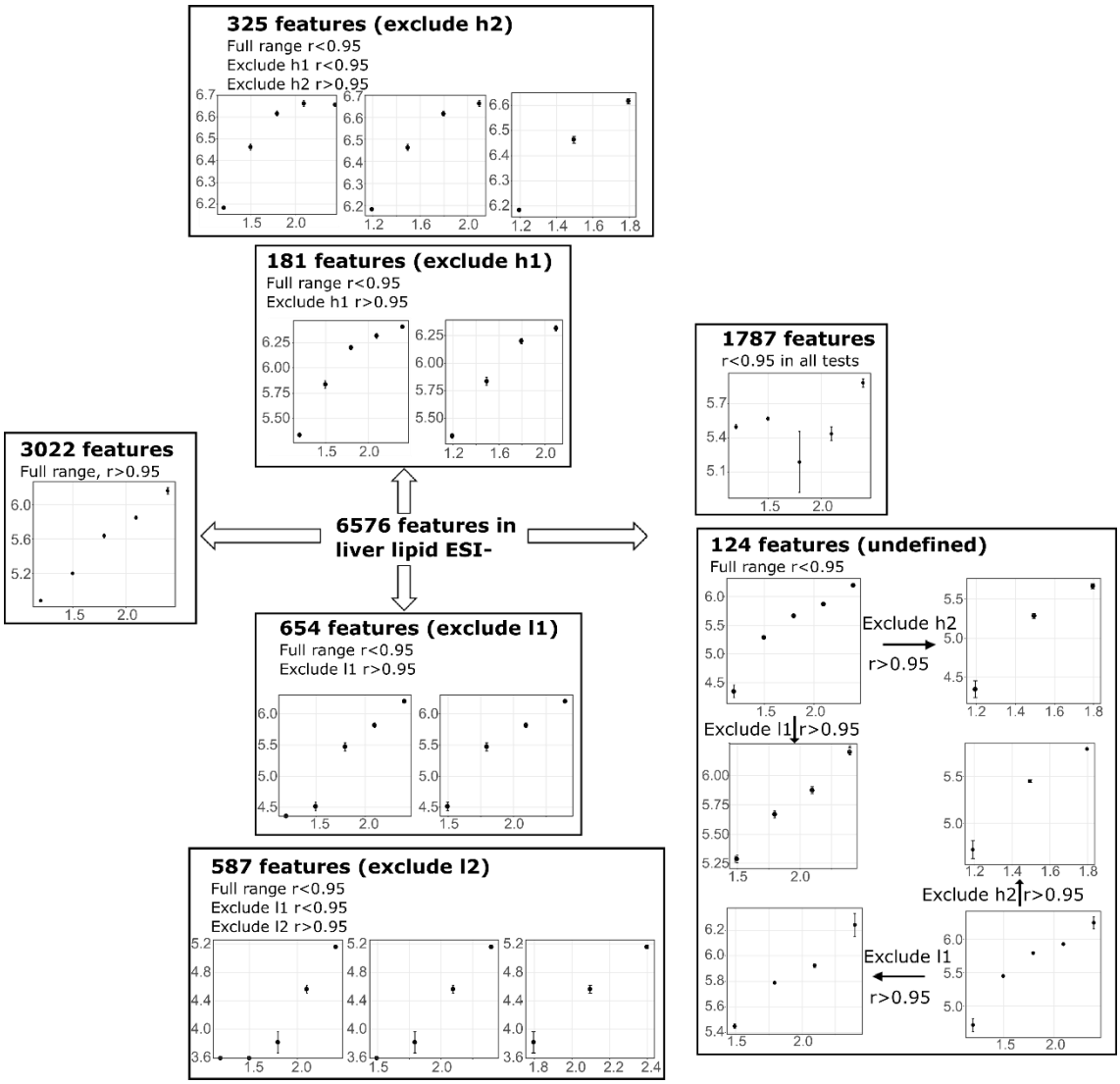

Figure 3.5: Features assigned to different category using liver lipid ESI− as an example. Excludedh1, h2, l1, l2 means excluding the highest one, highest two, lowest one, or lowest two concentrations. Excluding these concentrations improved r values of non-linear features to above the cut-off threshold respectively. X-axis: log-transformed concentration; y-axis: log-transformed intensity.

Table 3.4 characterised feature linearity using the maximum number of detected features in each dataset and informed about the concentrations that should be avoided. Yet it did not inform the number of linear features at each concentration that fell into the linear range. To this end, the total number of features at each concentration needed to be taken into account. Noted that the correlation coefficient was calculated based on all features detected in the highest

concentration, this did not rule out the fact that some linear features might not meet the criteria of non-blank features at lower concentrations, i.e., although linear trend was observed, the signal-to-noise ratio, or integrated peak area, in the low concentration samples were not significantly different from blank samples. To calculate the number of linear features at each concentration, the data was first filtered based on the number of non-blank features at each concentration, followed by summing up/gathering the number of linear features at that concentration. The number of features that fell into the linear range at each concentration was summarised in **Table 3.5**. Again with liver lipid ESI− as an example, 1339 non-blank features detected in liver lipid ESI+ at the lowest concentration (15.63 mg/mL), among which 1285 were linear based on the full range calculation, 13 were linear in exclude h1, 16 were linear in exclude h2 and thus a total 1312 linear features out of the 1339 detected non-blank features were detected in the 15.63 mg/mL concentration sample. Linear features from exclude l1 and exclude l2 (i.e., non-linear became linear after excluding the lowest or lowest two concentrations) would not be counted as a linear feature for this concentration as they fell outside of the linear range when injected at 15.63 mg/mL. With this approach, it was concluded that an injected concentration of 7.81 mg/mL was suitable for lipid analysis of adipose tissue, yielding 698 (ESI+) and 498 (ESI−) linear features. An injected concentration of 125 mg/mL was suitable for lipid analysis of the liver, yielding 2811 (ESI+) and 4326 (ESI−) linear features, whereas in HPLC HILIC analysis it was optimal to inject at 250 mg/mL for both tissue types to maximise the number of linear features yield (**Table 3.5**).

Table 3.5: The number of linear features that falls within the linear range and the number of linear features of the total detected non-blank features at each tested injected concentration in lipid and polar (HILIC) fractions of adipose tissue and liver extracts.

		Concentration	Non-Blank Features	r > 0.95 (Full)	r > 0.95 (Exclude l1)	r > 0.95 (Exclude l2)	r > 0.95 (Exclude h1)	r > 0.95 (Exclude h2)	Total Linear Features
Adipose lipids	ESI+	3.91	856	415	-	-	56	183	654
		6.25	921	426	22	-	56	187	691
		7.81	939	428	22	5	56	187	698
		12.5	955	428	22	5	56	-	511
		15.63	985	428	23	5	-	-	456
	ESI−	3.91	441	264	-	-	25	31	320
		6.25	628	290	95	-	25	35	445
		7.81	751	296	107	35	25	35	498
		12.5	972	302	119	41	25	-	487
		15.63	1160	304	121	42	-	-	467
Liver lipids	ESI+	15.63	1339	1285	-	-	13	14	1312
		31.25	1784	1570	145	-	15	16	1746
		62.5	2634	1939	344	198	18	21	2520
		125	3098	2083	414	295	19	-	2811
		250	3210	2119	422	299	-	-	2840
	ESI−	15.63	2984	2178	-	-	111	173	2462
		31.25	4038	2517	441	-	138	203	3299
		62.5	5122	2817	558	420	174	235	4204
		125	5952	2955	635	556	180	-	4326
		250	6576	3022	654	587	-	-	4263
Adipose HILIC	ESI+	15.63	20	4	-	-	0	1	5
		31.25	25	5	0	-	0	1	6
		62.5	77	29	0	7	1	1	38
		125	209	89	4	14	1	-	108
		250	239	94	6	14	-	-	114
	ESI−	15.63	30	27	-	-	0	0	27
		31.25	57	42	12	-	0	0	54
		62.5	72	49	17	3	0	0	69
		125	114	59	23	8	0	-	90
		250	176	70	26	12	-	-	108
Liver HILIC	ESI+	15.63	53	29	-	-	1	3	33
		31.25	82	42	2	-	3	5	52
		62.5	435	311	11	26	9	6	363
		125	480	331	14	30	9	-	384
		250	553	349	16	38	-	-	403
	ESI−	15.63	39	34	-	-	0	0	34
		31.25	83	60	5	-	2	0	67
		62.5	236	118	22	44	2	0	186
		125	304	126	35	51	2	-	214
		250	380	136	39	60	-	-	235

Highest absolute number is highlighted by bold and underlined.

3.3.5. Strength and Limitation of This Study

This study addressed an often-overlooked topic on the choice of suitable injected concentration for analysing samples in an untargeted metabolomics study. Reconstitution has been a way to alter sample concentration to suit the analytical platform and condition. The metabolite profile of different sample types can be very different in abundance of particular lipid species or metabolites due to the different biological processes and functions they carry out [332]. For example,

lipid concentrations and compositions vary considerably between different tissues, such as adipose compared to muscle tissue. Even with the same extraction protocol and analytical platform, the injected concentration between differing tissues was an important parameter to check for as it affected both the profile and the amount of reliably measured features. Due to the different instrument sensitivities and column loading capacities equipped in different laboratories, in combination with the very different nature of the sample types of interest, the so-called suitable concentration could vary considerably. Few studies have detailed the decision on the suitable injected concentration when performing untargeted metabolomics, potentially for the reason that this decision could be subjective. This study attempted to demonstrate a workflow to this end. We have provided some references and guidelines as to how injected concentration could impact number of detected features, reproducible features and non-linear features. We have also provided examples to demonstrate potential detrimental consequences of not carefully checking the tissue-specific sample dilution prior to the analysis of real samples, hence highlighting the importance of this step.

Signal response to sample dilution can be used to evaluate signal linearity in untargeted metabolomics [351]. The use of serial diluted samples along with real samples at analytical and post-analytical stages to remove non-linearly scaled features to improve data quality has been previously reported [350, 361, 362]. Serial diluted samples can also be used to determine a suitable injection concentration for metabolomics analysis as a step of sample preparation protocol optimisation, which has yet to be described in existing literature. Here we are the first to describe a workflow with fine details for the determination of a suitable,

sample type- and analytical stream-specific, injection concentration for metabolomics analysis. The described strategy was performed with a pooled sample to ensure the procedure was executed on a sample that will have the representative metabolite composition of the sample type and study condition. Whilst the study samples can be extracted, dried and briefly stored under optimal conditions [363], the pooled sample is used to run a serial dilution experiment; once the suitable injected concentration is determined, dried extracts from study samples can then be reconstituted and analysed at the optimum concentrations, although long-term storage of samples should be avoided as this could lead to sample degradation/poor resolubilisation and changes in profiles [364]. There are both pros and cons of this workflow. The process of data acquisition for the serial diluted pooled samples is identical to that for the study samples, hence, the signal responses to different injected concentration will reflect how study samples would behave. If a sample type is naturally abundant in certain class of metabolite, e.g., glycerolipids in adipose tissue [330], sample dilution can help to avoid column overloading, signal saturation and potentially ion suppression as well [365, 366]. Sample pre-concentration, on the other hand, would allow more low abundant metabolites to be detected and reliably measured. On the downside, dilution of injected samples can cause signal loss of low abundant metabolites and hence a decrease of total detected features whereas sample preconcentration could cause overloading of abundant metabolites/lipid species. A higher dilution factor may also impair data reproducibility and increase RSDs as shown in this study. Given the wide concentration range of endogenous metabolites in samples and the goal of untargeted metabolomics is to reliably measure as many of them as possible it is, therefore, important to find the balance between data quality and

metabolome coverage. This workflow, instead of looking at responses of individual lipid species or metabolites which would be not realistic in untargeted metabolomics, focused on the effect of injected concentration on metabolomic profile and feature properties on a global scale, and favoured the selection of concentration with the highest amount of linear features relative to the other tested concentrations. Another point worth noting is that increasing the number of reliably measured features did not necessarily mean an increased number of detected metabolites. Redundant features derived from isotopic masses, adduct formation and source-induced fragmentation could be presented without adding biological information to the data. Nonetheless, capturing extra chemometric information and maintaining data integrity might facilitate metabolite identification in the later stage of a metabolomics study. Lastly, this strategy has no means to optimise metabolome coverage or reproducibility from the aspect of extraction and reconstitution solvents as well as instrument settings, therefore, some knowledge on or a pre-optimised analytical workflow with regards to the choice of extraction and reconstitution solvents as well as the type of instrument and columns, elution programme, mobile phase, etc., should be established. There are many studies investigating extraction solvents and conditions for most commonly used sample types [326, 343, 346, 363, 367, 368]. Nonetheless, our study highlights the critical importance of assessing the effect of injected sample concentration as an independent parameter on the acquired metabolomic profile, feature characterisation and linearity, and provides a feasible way to determine a suitable concentration prior to the analysis of real samples.

3.4 Conclusions

The present study utilised lipid and polar metabolite extracts (bi-phasic solvent extraction to generate extracts of polar metabolites and lipids) from two different tissues as examples to demonstrate a workflow for the selection of injected concentration for LC–MS analysis. We report under our laboratory and analysis conditions that an injected concentration at 125 mg/mL and 7.81 mg/mL is suitable for lipid analyses from liver and adipose tissue, respectively. Over 90% of the detected features were reproducible in each dataset, producing 2811 (ESI+) and 4326 (ESI−) linear features in liver and 698 (ESI+) and 498 (ESI−) linear features in adipose tissue. An injected concentration at 250 mg/mL was suitable for the analyses of polar extracts from both types of tissues. Over 85% of the detected features were reproducible in each dataset, producing 403 (ESI+) and 235 (ESI−) linear features in liver and 114 (ESI+) and 108 (ESI−) linear features in adipose tissue. We highlight that the injected concentration can be associated with overloading, saturation, or features under the detection limit, and affect data quality and reproducibility, as well as the number of detected and linear features. Therefore, the injected concentration is a critical parameter to check for and should be carefully adjusted prior to the analysis of real samples. The optimum injected concentration could vary depending on various factors, such as extraction protocol, solvent compatibility, column type, instrument type and sample type, and we have demonstrated a general workflow to determine this important parameter. The developed workflow is also applicable to a variety of other sample types and LC–MS systems, and should be considered fundamental to LC–MS-based untargeted metabolomics analysis.

3.5 Contributions and acknowledgements

This Chapter has been formally published in *Metabolites*:

Wu, Zhanxuan E., Marlena C. Kruger, Garth JS Cooper, Sally D. Poppitt, and Karl Fraser. "Tissue-specific sample dilution: An important parameter to optimise prior to untargeted LC-MS metabolomics." Metabolites 9, no. 7 (2019): 124.

Author Contributions:

Conceptualization, Garth J.S. Cooper; Methodology, Zhanxuan E. Wu and Garth J.S. Cooper; Sample preparation and extraction, Zhanxuan E. Wu; Metabolomics data acquisition, Zhanxuan E. Wu; Data analysis, Zhanxuan E. Wu; Data visualization and presentation, Zhanxuan E. Wu; Writing – original draft, Zhanxuan E. Wu; Writing – review & editing, Karl Fraser; Supervision, Marlena Kruger, Sally D. Poppitt and Karl Fraser; Funding acquisition, Sally D. Poppitt. All authors reviewed the final manuscript

MASSEY UNIVERSITY
TE KUNENGA KI PŪREHUROA
UNIVERSITY OF NEW ZEALAND

GRADUATE RESEARCH SCHOOL

STATEMENT OF CONTRIBUTION
DOCTORATE WITH PUBLICATIONS/MANUSCRIPTS

We, the candidate and the candidate's Primary Supervisor, certify that all co-authors have consented to their work being included in the thesis and they have accepted the candidate's contribution as indicated below in the *Statement of Originality*.

Name of candidate:	Zhanxuan Wu
Name/title of Primary Supervisor:	Marlena Kruger
In which chapter is the manuscript /published work:	3

Please select one of the following three options:

(●) The manuscript/published work is published or in press

- Please provide the full reference of the Research Output:

Wu, Zhanxuan E., et al. "Tissue-specific sample dilution: An important parameter to optimise prior to untargeted LC-MS metabolomics." Metabolites 9.7 (2019): 124.

( ) The manuscript is currently under review for publication – please indicate:

- The name of the journal:
- The percentage of the manuscript/published work that was contributed by the candidate: 90
- Describe the contribution that the candidate has made to the manuscript/published work:

Methodology development; experiment; writing: figures & tables generation.

( ) It is intended that the manuscript will be published, but it has not yet been submitted to a journal

Candidate's Signature:	Zhanxuan Wu Digitally signed by Zhanxuan Wu Date: 2020.08.31 15:37:40 +1200'
Date:	31-Aug-2020
Primary Supervisor's Signature:	Marlena Kruger Digitally signed by Marlena Kruger DN: cn=Marlena Kruger, c=NZ, o=Massey University, email=m.l.kruger@massey.ac.nz Date: 2020.09.01 08:40:08 +12'00'
Date:	1/9/2020

This form should appear at the end of each thesis chapter/section/appendix submitted as a manuscript/ publication or collected as an appendix at the end of the thesis.

GRS Version 5 – 13 December 2019
DRC 19/09/10

4. A metabolomics study to dissect the relationship between plasma and adipose, muscle and liver tissue metabolomes in a cohort of obese, non-diabetic women

After establishing a workflow to determine the optimal injected concentration for the LC-MS analysis of different sample types and extracts from the previous chapter, the method was applied to profile human plasma, 4 subtypes of adipose tissues, 2 subtypes of muscle and the liver biopsy, and the correlation between plasma and tissue metabolome was examined. To date, this is the first study measuring a wide range of metabolites and lipid species in an untargeted manner and investigating whether certain (set of) plasma metabolites can effectively act as a proxy for the metabolite concentration in a specific tissue site.

Abstract

Untargeted metabolomics has become widely applied to study the metabolic alterations underpinning human disease development and to identify candidate biomarkers for disease diagnosis and prognosis. Although blood samples are metabolite-rich, easily accessible and less invasive to obtain than tissue, translating and understanding the relevance of a blood metabolite marker can be challenging if it is unknown whether such a marker reflects its concentration in different tissues. To explore this field, metabolomic and lipidomic profiles of plasma, 4 subtypes of adipose tissue (AT), 2 subtypes of muscle and liver biopsy from a group of obese, non-diabetic females (n=26) scheduled to undergo bariatric surgery were measured by liquid chromatography coupled with mass spectrometry (LC–MS). Relationships between plasma and tissue profiles were examined using Pearson correlation analysis subject to Benjamin-Hochberg (BH) correction. Plasma polar metabolites and lipid species showed the highest number of significantly positive correlations with their corresponding concentrations in liver tissue, including lipid species of ceramide, mono- and di-hexosylceramide, sphingomyelin, phosphatidylcholine (PC), phosphatidylethanolamine (PE), lysophosphatidylethanolamine (LPE), dimethyl phosphatidylethanolamine (PE-NMe2), ether-linked PC, ether-linked PE, free fatty acid (FFA), cholesteryl ester, diacylglycerol and triacylglycerol (TG), and polar metabolites linked to metabolism of amino acids (AA), energy, fatty acids and gut microbial metabolites. Plasma also showed significant positive correlations with muscle for PC, ether-linked PE and ether-linked PC species, and polar metabolites linked to AA and energy metabolism and gut microbial metabolites. Plasma polar metabolites were poorly correlated with concentrations

in the various AT sites, whilst plasma lipids showed positive correlations with AT for TG species. In conclusion, plasma metabolomic and lipidomic profiles were reflective more of the liver profile than any of the muscle or AT sites. Our study highlighted that when interpreting plasma metabolite levels as a proxy for abnormal tissue metabolism associated with disease development, considerations on their relationships with different tissues are needed to allow for mechanistic speculation in the correct sample type.

4.1 Introduction

Untargeted metabolomics involves the comprehensive measurement of metabolites in a biological sample and has become an emerging tool for biomarker discovery and the understanding of metabolic alterations associated with diseases [39]. Since metabolites are produced during complex biochemical processes, metabolomics is the final measurement linking genomics, transcriptomics and proteomics to phenotype, whilst the metabolite profile provides a signature for biochemical activity jointly determined by intrinsic and external factors [38]. As such, this technique is well-suited for the study of cardiometabolic diseases which often involve a multitude of metabolic pathways and complex interplay between intrinsic and environmental factors [39].

Among various human clinical sample types available for measurement, plasma and serum are the blood compartments which are convenient and minimally invasive to obtain and as such are widely used for clinical chemistry diagnoses and risk screening [41]. Blood samples contain a broad range of metabolites: the Human Metabolome Project has identified and quantified over 4200 metabolites in human serum [369], while the lipid composition in human plasma also contains remarkable diversity, with more than 500 lipid species quantified [370]. Given the rich complexity of metabolites that can be measured in blood, correlating the circulating metabolite profile with phenotype or clinical outcomes becomes potentially highly informative and descriptive of any health issues, making the circulating metabolites in blood important targets in clinical studies. To date, metabolomics has been successfully applied to identify circulating markers that have the potential to diagnose cardiometabolic diseases at an early stage or provide additional prognostic value [186, 212, 371-373]. Metabolomic profiling of

blood samples has also provided a systemic snapshot of metabolic alterations under pathophysiological conditions, hence opening a window for mechanistic investigation of the underpinning pathways during disease development [374]. Despite this, a major limitation of studying the blood metabolome is that it may provide little insight into tissue site-specific abnormalities, which are usually more biologically relevant to disease pathogenesis [313]. A current gap in the clinical-metabolomic research field is that it has not been established whether the metabolite biomarkers detected in the circulation can be used as a proxy for tissue metabolite concentration abnormalities.

Due to the invasiveness of tissue collection procedures, the availability of tissue samples is more difficult to achieve for clinical studies and hence the number of tissue metabolomics studies in humans is limited. Characterisation of the metabolomic profiles from various tissue types have demonstrated a different composition and abundance of metabolites in different tissue samples. For example, higher levels of ceramides, sphingomyelins, phosphatidylcholine, phosphatidylethanolamines, lysophospholipids but lower triacylglycerols and ether-linked phosphatidylcholines were detected in the liver compared with AT [330, 375]. Given the heterogeneity of various tissues and that blood represents a dynamic extracellular pool for tissues/organs, it is not clear to what extent the metabolic constituents and their levels in local tissue sites can be reflected in the blood metabolome.

Several studies characterising the metabolomic profile of tissues alongside blood-derived samples supported that plasma/serum provide a window into tissue-specific metabolites [376, 377]. These studies also provided evidence for concordant metabolic changes in both the circulation and local tissue sites

associated with diseases or interventions. However, few studies have investigated the relationship between concentrations of circulating metabolites and their counterparts in different tissue types, and these studies were conducted using more traditional targeted analyses, including free fatty acids (FFA), acylcarnitines and steroid hormones [304-307]. Moreover, several lipid classes and polar metabolites such as ceramides, sphingomyelins, phospholipids and ether-linked phospholipids, branched-chain amino acids (BCAAs) and aromatic AAs, were frequently reported to be associated with obesity, T2D and CVD [42, 164, 378]; yet it is unknown whether these circulating metabolites can act as surrogate indicators for their concentrations in metabolically active sites, including AT depots, muscle compartments and liver.

To date, there has been no study employing an untargeted metabolomics approach to gain a wide picture of the relationship between the metabolomic profile of human plasma and a range of tissues. To address these limitations in knowledge, a thorough investigation of the relationship between plasma and multiple AT and muscle sites in addition to liver metabolites measured by two complementary LC-MS platforms in an untargeted manner was carried out. Findings from the present study may enhance the interpretability and accelerate the translation of plasma candidate markers identified by a metabolomics approach to be useful for clinical screening, and potentially highlight where erroneous assumptions for some metabolites and their tissue metabolism may occur by only measuring the plasma metabolome as a proxy.

4.2 Materials and methods

4.2.1 Study subjects and samples

Obese, non-T2D females were recruited from patients scheduled for bariatric surgery (n = 21, mean body mass index, BMI = 40.9 kg/m^2) or general upper gastrointestinal (GI) surgery (n = 5, mean BMI = 38.6 kg/m^2). Participants undergoing bariatric surgery completed a 14-day low energy diet (LED, 4MJ/day intake) in order to achieve ≥10% body weight loss prior to the surgery. All participants were free of diagnosed cardiovascular or other metabolic disease and underwent surgery after an overnight fast during the surgical procedure, biopsies of 4 subtypes of AT (Subcutaneous Thigh Adipose tissue, STA; Subcutaneous Abdominal Adipose tissue, SAA; Deep Subcutaneous Abdominal adipose tissue, DSA; Intra-Abdominal Adipose tissue, IAA), two subtypes of muscle tissue (Vastus Lateralis, VL; Rectus Abdominis Muscle, RAM) and liver (at the wedge of large lobe) were collected (**Figure 4.1**).

Participants were recruited at Auckland City Hospital, Auckland, New Zealand. Informed written consent was obtained at the Greenlane Clinical Centre or the University of Auckland Human Nutrition Unit (ethics approval-NTX/08/10/103).

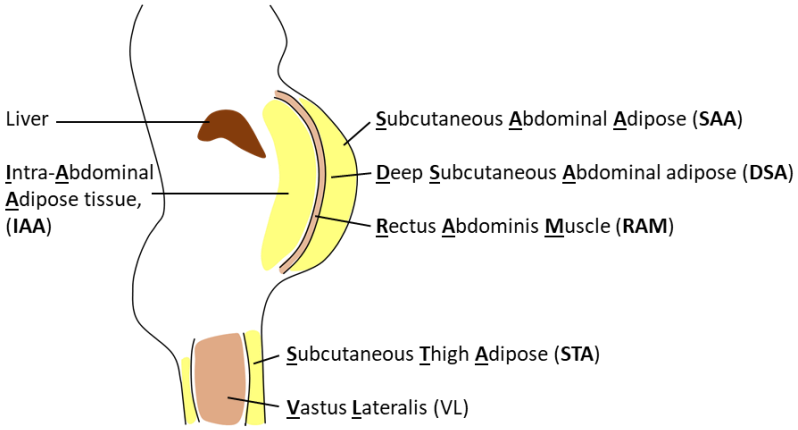

Figure 4.1: Schematic of the location of sites from which the 7 tissue samples were collected for metabolomics analysis.

4.2.2 Materials

All organic solvents for metabolite extraction, reconstitution and LC–MS analysis (chloroform, methanol, acetonitrile isopropanol and formic acid) were obtained from Thermo Fisher Scientific (Auckland, New Zealand) and were of LC–MS grade except chloroform, which was of analytical grade. Milli-Q® ultrapure water was obtained from Merck Millipore (Bedford, MA, USA). Ammonium formate (Fluka™, HPLC grade) was obtained from Sigma-Aldrich (Auckland, New Zealand). Lipid internal standard 1-palmitoyl(D_{31})-2-oleoyl-sn-glycero-3-phosphoethanolamine (16:0 d_{31}-18:1-PE) was purchased from Avanti® (Avanti Polar Lipids, Alabaster, AL, USA). The extraction solvent of chloroform/methanol (v/v, 50:50) containing 16mg/L pre-dissolved internal standards (d_5-L-tryptophan, d_4-citric acid, d_{10}-leucine, d_2-tyrosine, d_{35}-stearic acid, d_5-benzoic acid, 13C-glucose, d_7-alanine) was stored at -20 ^{o}C. A modified Folch solution (chloroform/methanol/water, v/v/v, 66:33:1) containing 0.01% (%w/v) pre-dissolved 16:0 d_{31}-18:1-Phosphoethanolamine internal standard for reconstitution of organic extract was also stored at -20 ^{o}C freezer. Acetonitrile/water (v/v, 50:50) for reconstitution of the polar extract was stored at 4 ^{o}C fridge.

4.2.3 Metabolomics analysis

Metabolite extraction was performed with 100 µl plasma or 25 mg frozen tissue using a bi-phasic extraction method previously described (Chapter 3) [379]. Briefly, tissue was homogenised in 800 µl pre-chilled extraction solvent with a single bead per tube for 2x60s at 30Hz, followed by addition of 400 µl water, vortex-mixing (2x15s) and centrifugation (11000 rpm, 4 ^{o}C, 10min). The plasma samples were mixed with 800 µl pre-chilled extraction solvent, agitated for 30s and placed in -20 ^{o}C freezer for 60 min to allow protein precipitation, followed by

addition of 400 µl water, vortex-mixing (2x15s) and centrifugation (11000 rpm, 4 ^{o}C, 10min). Finally, 200 µl of the upper aqueous layer and 200 µl of the bottom organic layer were transferred into two separate 2 ml microcentrifuge tubes separately, evaporated under a stream of nitrogen and stored at -80 ^{o}C until analysis. All remaining upper phase or lower phase from the same sample type were combined to construct an aqueous or organic pool respectively for each sample matrix, aliquoted into 200µl and evaporated under a stream of nitrogen for QC sample construction. Blank samples were prepared following the same protocol but without the presence of tissue or plasma samples.

On the day of analysis, dried extracts were reconstituted in appropriate volume of reconstitution solvent and analysed as previously described. Briefly, dried polar extracts were reconstituted in 800 µl reconstitution solvent were separated on a SeQuant® ZIC®-pHILIC 5 µm, 2.1 mm × 100 mm column (Merck, Germany) and analysed by a Thermo LC–MS system consisting of an Accela 1250 quaternary UHPLC pump coupled to an Exactive Orbitrap mass spectrometer (Thermo Fisher Scientific, Waltham, MA, USA). Samples were analysed in both positive electrospray ionisation (ESI+) and negative electrospray ionisation (ESI-). Dried organic extracts (lipidome) reconstituted in 200 µl (plasma), 400 µl (liver), 800 µl (muscle) and 2000 µl (AT) reconstitution solvent were separated on an Acquity CSH™ C18 column 1.7 µm, 2.1 mm × 100 mm (Waters, USA) and analysed by a Thermo LC–MS system comprising an Accela 1250 quaternary UHPLC system coupled to a Q Exactive hybrid quadrupole-Orbitrap mass spectrometer (Thermo Fisher Scientific, Waltham, MA, USA) using both ESI+ and ESI- modes.

Raw datafiles were converted to mzXML format with the ProteoWizard tool MSconvert (v 3.0.1818 [380]) and pre-processed with XCMS (v3.0.2) altogether

in R (v3.2.2) [154] so that the feature names could be aligned across the different sample types. The mega data matrix was then divided into subsets based on sample type and normalised by the same sample type pooled QC in the W4M Galaxy environment [381]. Blank features (defined as [nQC = 0], or [nQC≠0, nBlank≠0, tstat < 1 and p < 0.05 of QC over Blank generated by XCMS diffreport function]) and non-reproducible features (% coefficient of variation < 30% in QC) were filtered out. Lipids were annotated using LipidSearch software v4.1.16 on representative MS^2 datafiles (Thermo Fisher Scientific, USA). Polar metabolites were annotated using an in-house library based on authentic standards (AgResearch) analysed through HILIC LC–MS analysis under conditions identical to the current study. Unidentified features were searched against online databases including HMDB (http://www.hmdb.ca/), Metlin (http://metlin.scripps.edu/) and Lipid Maps (http://www.lipidmaps.org/) based on *m/z* with less than 10 ppm (for lipid features) or 15 ppm (for polar metabolite features) mass error.

4.2.4 Statistical analyses

For each ESI mode of each analytical platform (polar and organic), data analyses were performed in the following 4 steps:

A data matrix of paired plasma-tissue profiles containing annotated features common to both plasma and the tissue matrix (i.e. non-blank, reproducibly measured features) were constructed. Several participants did not have all tissue sites collected and participants with a plasma sample collected but no tissue sampled were excluded from analysis for that specific plasma-tissue matrix. A total number of 22 (STA), 22 (IAA), 19 (SAA), 26 (DSA), 20 (VL), 19 (RAM) and 24 (liver) datapoints were available for each plasma-tissue data matrix.

All profiles were normalised by BMI, log-transformed and mean-centred (auto-scaled) based on sample type. Pearson correlation analysis was applied on every paired feature in each plasma-tissue comparison.

To account for false positive discoveries (due to multiple comparison or processing artefacts), the p-value from the Pearson correlations were subjected to Benjamini-Hochberg multiple testing correction (BH-corrected) for each paired plasma-tissue data matrix. A BH-corrected p-value < 0.05 was considered statistically significant. Extracted ion chromatograms (EIC) from significantly correlated features were visually examined to further remove poorly integrated or misaligned features.

Any redundant features representing the same putative metabolite or lipid were also removed to report only individual lipid species/metabolites.

For polar metabolites measured, up to 3 metabolic pathways/functions were assigned to each significantly correlated metabolite between plasma and muscle or the liver. Designation of pathways/functions was based on online (HMDB, https://hmdb.ca/; pubchem, https://pubchem.ncbi.nlm.nih.gov/; KEGG, https://www.genome.jp/) and in-house database [382]. The frequency of metabolic pathways/functions to which the metabolites were linked was displayed using wordcloud (https://worditout.com/word-cloud/create).

4.3 Results

4.3.1 Lipidomic profiling and identification of significantly correlated lipids between plasma and 7 tissue types

Results for ESI+ lipidomic analysis are summarised in **Figure 4.2**. A total number of 843 (ESI+) lipid features were annotated. Among the annotated lipid features analysed by ESI+ mode, 553 (Plasma), 414 (STA), 455 (IAA), 449 (SAA), 447

(DSA), 388 (VL), 332 (RAM) and 482 (liver) features were detected in each tissue matrix. Of these measured features, 265 (STA), 261 (IAA), 285 (SAA), 289 (DSA), 307 (VL), 280 (RAM) and 377 (liver) features were common between plasma and each corresponding tissue. For each plasma-tissue pair, 2 (STA), 16 (IAA), 4 (SAA), 5 (DSA) and 202 (liver) features showed significant positive correlation between the plasma level and the tissue counterpart level (BH-corrected $p < 0.05$). No muscle lipid species measured by the ESI+ mode was correlated with plasma (**Figure 4.2a**). Plasma lipid species correlated with AT depots were all triglycerides (TG) with the exception of SAA, which also showed a positive correlation for 1 ether-linked phosphatidylcholine (PC) species. Those correlated with the liver encompassed cholesterol esters (CE), diglycerides (DG), TG, PC, phosphatidylethanolamines (PE), ether-linked PC, ether-linked PE, ceramide (Cer) and sphingomyelins (SM) (**Figure 4.2b**).

A total number of 472 (ESI-) lipid features were annotated (**Figure 4.3a**). 355 (Plasma), 83 (STA), 80 (IAA), 70 (SAA), 64 (DSA), 158 (VL), 150 (RAM) and 382 (liver) features were detected in each tissue matrix. Of these, 76 (STA), 73 (IAA), 66 (SAA), 61 (DSA), 137 (VL), 133 (RAM) and 279 (liver) features were common to plasma and each corresponding tissue. For each plasma-tissue pair, 4 (STA), 4 (IAA), 2 (SAA), 10 (VL), 12 (RAM) and 143 (liver) features showed significant positive correlation between the plasma level and the tissue counterpart level (BH-corrected $p < 0.05$). No DSA lipid species measured by the ESI- mode were correlated with plasma. Plasma lipids showed positive correlations with 3 subtypes of AT and both subtypes of muscle for a range of phospholipids, while 2 ceramide species and 1 FFA in plasma were also correlated with SAT and VL, respectively. Plasma lipid species encompassing ceramides, SM, mono- and di-

hexosylceramides, PC, PE, ether-linked PC, ether-linked PE, lysophosphatidylethanolamine (LPE), dimethyl-PE (PE-NMe2) and bilirubin were positively correlated with levels in the liver (**figure 4.3b**).

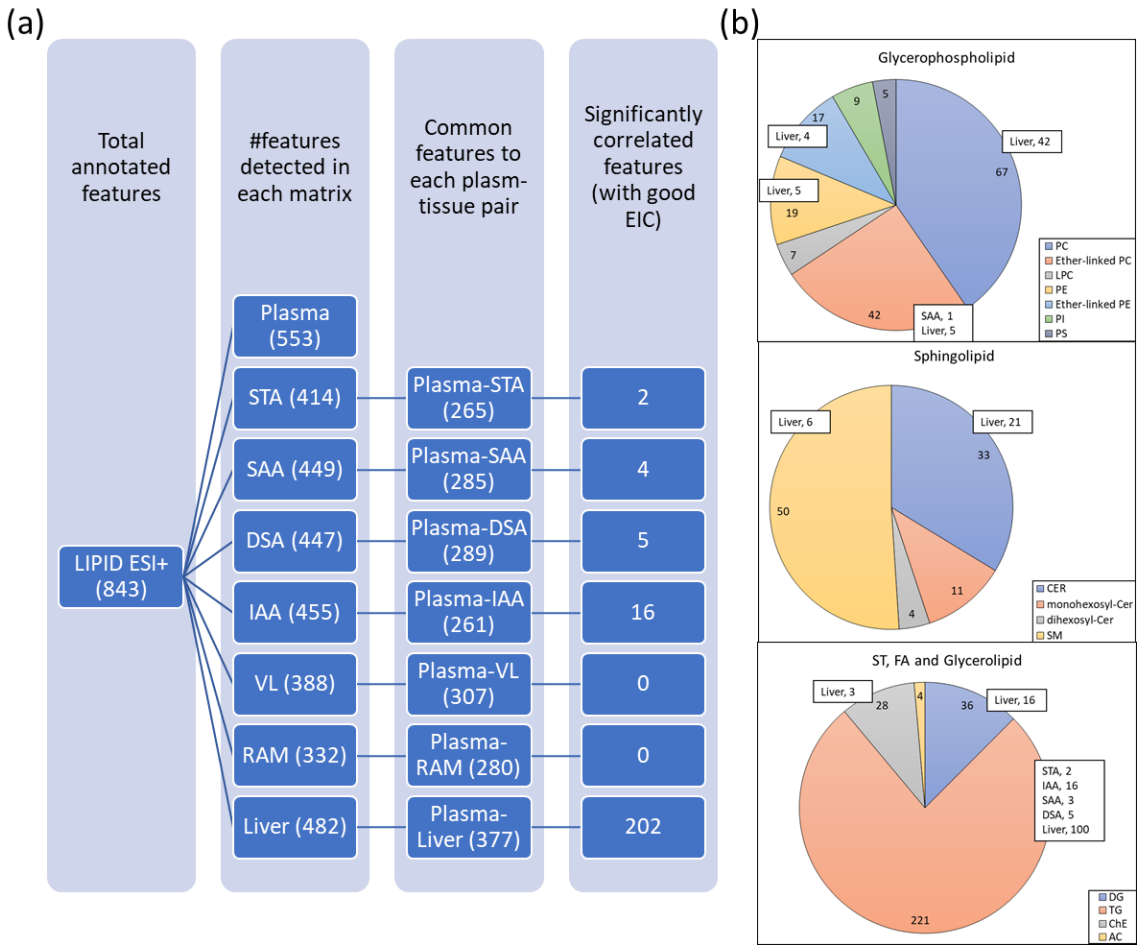

Figure 4.2: Characterisation of lipid features measured by ESI+. (a) number of features in each sample type and correlated features between plasma and each tissue type. (b) number of annotated features in plasma (pie chart) and correlated features with their counterparts in different tissues (box). STA: Subcutaneous Thigh Adipose tissue; SAA: Subcutaneous Abdominal Adipose tissue; DSA: Deep Subcutaneous Abdominal adipose tissue; IAA: Intra-Abdominal Adipose tissue, IAA); VL: Vastus Lateralis, VL; RAM: Rectus Abdominis Muscle.

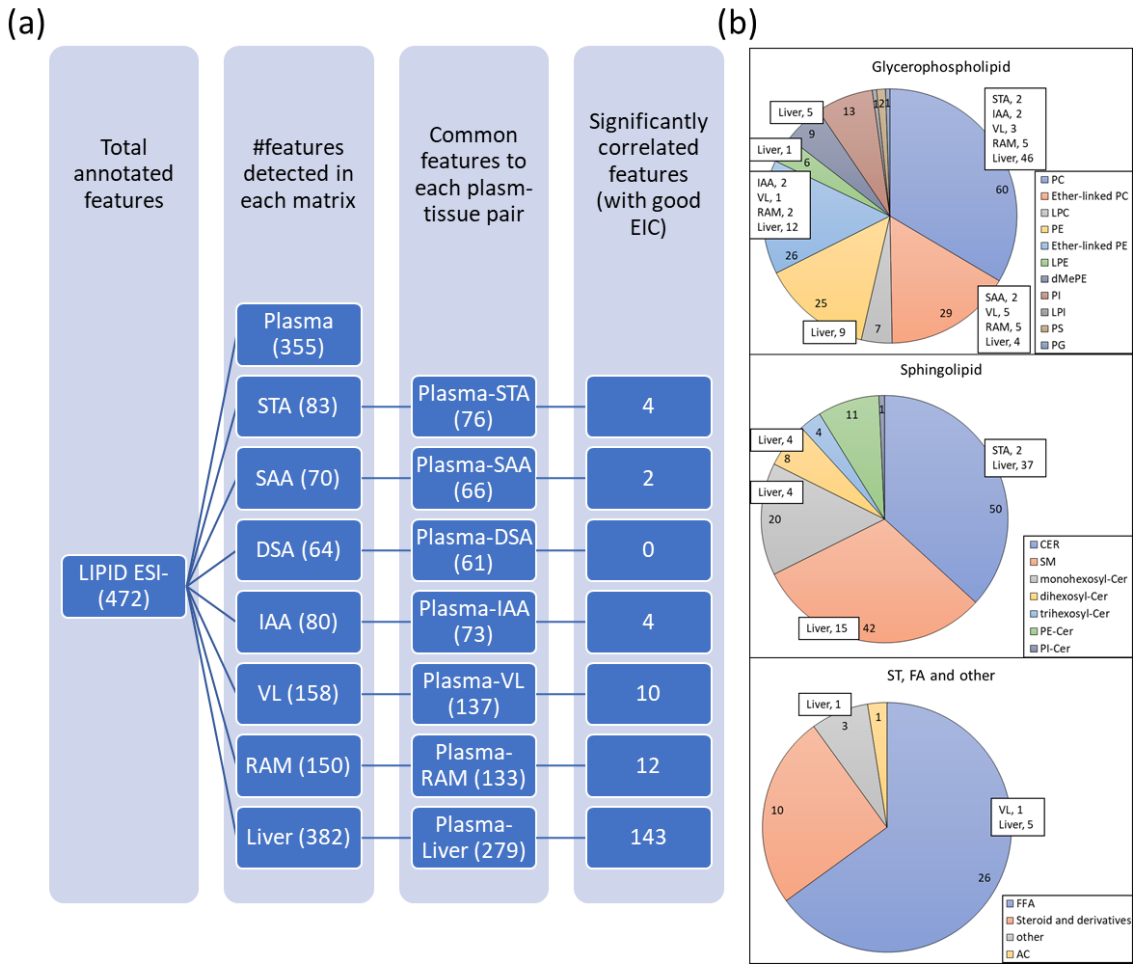

Figure 4.3: Characterisation of lipid features measured by ESI-. (a) number of features in each sample type and correlated features between plasma and each tissue type. (b) number of annotated features in plasma (pie chart) and correlated features with their counterparts in different tissues (box). STA: Subcutaneous Thigh Adipose tissue; SAA: Subcutaneous Abdominal Adipose tissue; DSA: Deep Subcutaneous Abdominal adipose tissue; IAA: Intra-Abdominal Adipose tissue, IAA); VL: Vastus Lateralis, VL; RAM: Rectus Abdominis Muscle.

By merging the significantly correlated lipid features identified by ESI+ and ESI- analyses together, plasma compared to liver provided the largest number of correlated lipid species (215 putative lipid species), followed by the IAA and the 2 subtypes of muscle tissue (IAA > RAM > VL, between 10-20 lipid species). Plasma lipids were poorly correlated with their respective lipids in subcutaneous AT depots including STA, SAA and DSA (<10 lipid species). Individual correlated lipid species and the statistical descriptions are provided in **Appendix: Table 9.1**.

Saturated and monounsaturated TGs in plasma were exclusively correlated with their levels in the liver. TGs of a lower degree of saturation (2-3 double bonds) were correlated with their levels in liver and SAA, whereas polyunsaturated TGs containing larger numbers of carbons (C ≥54, double bond ≥6) were correlated with their levels in the liver and AT depots including STA, IAA and DSA (**Figure 4.4**). Among the 74 plasma TGs species correlated with liver, the top 3 most correlated TGs were all saturated species (TG 48:0, r = 0.88; TG 53:0, r = 0.87; TG 46:0, r = 0.85).

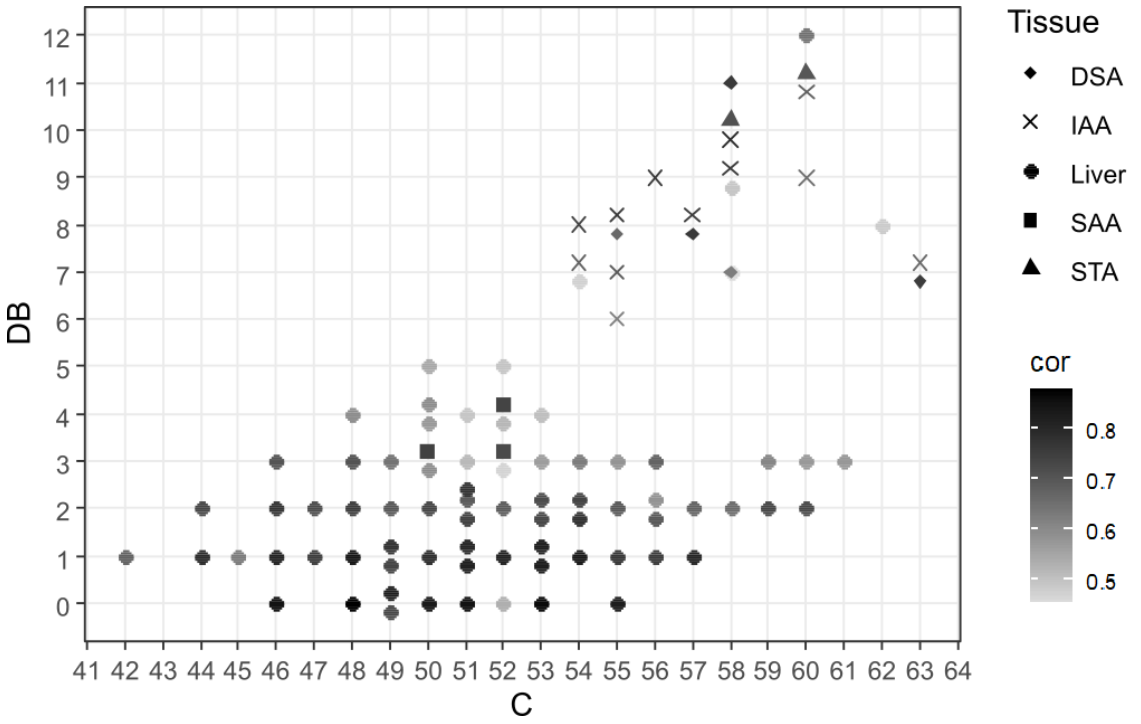

Figure 4.4: composition of TG species in plasma showing significant correlations (BH p < 0.05) with the corresponding species in the liver or AT depots. DB: total number of double bonds; C: total number of carbons. STA: Subcutaneous Thigh Adipose tissue; SAA: Subcutaneous Abdominal Adipose tissue; DSA: Deep Subcutaneous Abdominal adipose tissue; IAA: Intra-Abdominal Adipose tissue, IAA). Cor: correlation coefficient.

Several plasma sphingolipids encompassing subclasses of (dihydro)sphingomyelins, (dihydro)ceramides, deoxy-(dihydro)ceramides, were correlated with their levels in the liver. Ceramides containing 36-43 carbons and double bonds ≤1 were highly correlated between plasma and the liver (r 0.6-0.84),

whereas those containing very long chain (C = 44) and/or 2 double bonds were moderately correlated (r 0.45-0.6). Likewise, the most highly correlated sphingomyelins between plasma and the liver were those containing 36-43 carbons and double bonds ≤1 (r 0.5-0.84); while the least correlated (yet still significantly) sphingomyelins were those containing shorter chain (carbon <36) and/or 2 double bonds (r 0.45-0.5). Two plasma ceramides also correlated with STA ceramides (Cer(d40:1), Cer(m42:2)).

Plasma FFA showed positive correlations with the liver for FFA (18:0) and FFA (20:5), and with the VL muscle for FFA (18:1). No correlation was observed between plasma and AT FFA levels. Plasma phospholipids (PC, PE, ether-linked PC and ether-linked PE) showed positive correlations with all 7 tissue types, however the individual species differed.

Bilirubin and several lipid species belonging to CE, DGs, mono- and di-hexosylceramides, LPE and PE-NMe2 in plasma were only correlated with the corresponding species in the liver.

4.3.2 Metabolomic profiling and identification of significantly correlated polar metabolites between plasma and 7 tissue types

Results for the polar metabolite (HILIC) data are summarised in **figure 4.5**. A total number of 162 (ESI+) polar metabolite features were annotated. Of these, 73 (Plasma), 59 (STA), 62 (IAA), 42 (SAA), 41 (DSA), 108 (VL), 94 (RAM) and 119 (liver) features were detected in each tissue matrix. Among features common to plasma and each corresponding tissue, 3 (STA), 4 (IAA), 1 (SAA), 6 (DSA), 16 (VL), 15 (RAM) and 27 (liver) features showed significant correlation between its plasma level and the tissue counterpart (BH-corrected $p < 0.05$). For ESI- analysis of polar metabolites, 31 features were annotated, and plasma

metabolites only displayed positive correlations for 1 (STA), 3 (VL) and 1 (liver) features.

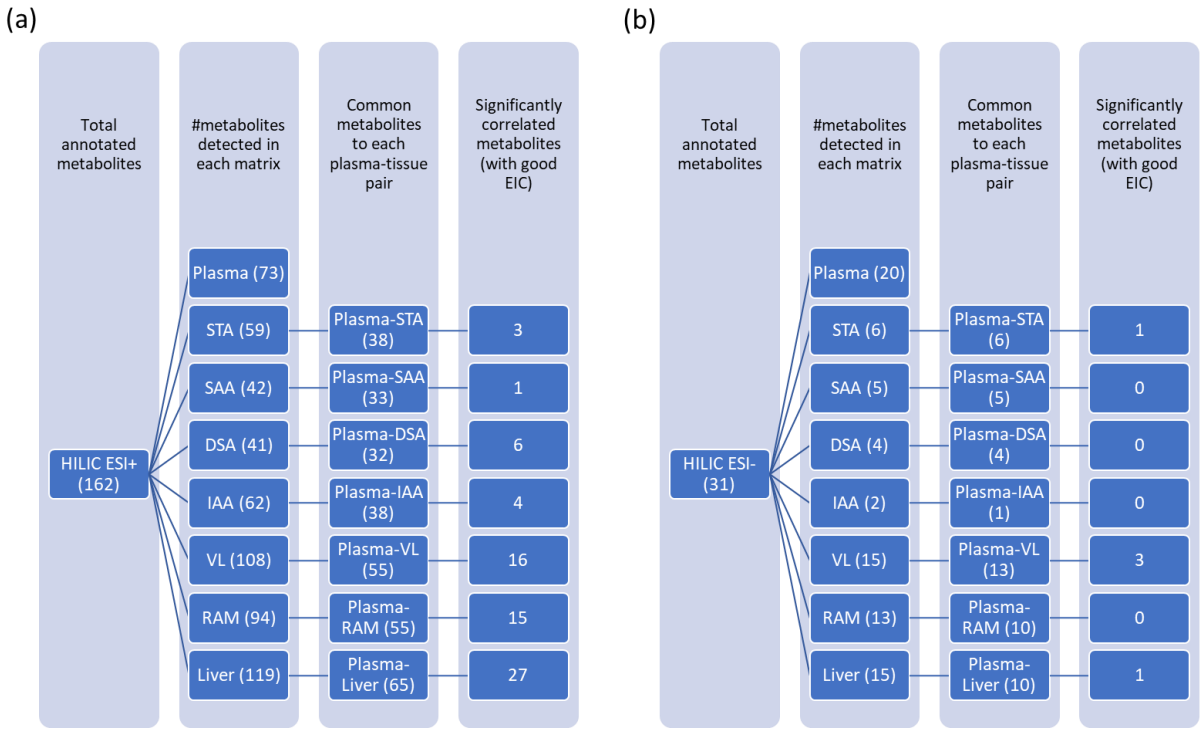

Figure 4.5: Number of polar metabolite (HILIC) features in each sample type and correlated features between plasma and each tissue type measured by ESI+ (a) and ESI- (b). STA: Subcutaneous Thigh Adipose tissue; SAA: Subcutaneous Abdominal Adipose tissue; DSA: Deep Subcutaneous Abdominal adipose tissue; IAA: Intra-Abdominal Adipose tissue, IAA); VL: Vastus Lateralis, VL; RAM: Rectus Abdominis Muscle.

By collating the significantly correlated polar metabolite features identified by ESI+ and ESI- analyses together, the greatest number of plasma metabolites were correlated with its liver counterpart (28 features accounting for 28 putative metabolites), followed by the two subtypes of muscle tissue (between 10-20 metabolites); while plasma polar metabolites were poorly correlated with their levels in AT depots (<10 metabolites). Individual correlated metabolites and the statistical descriptions are provided in **Appendix: Table 9.2**.

Plasma showed significantly positive correlations with liver for metabolites linked with amino acid (AA) metabolism, energy metabolism, fatty acid metabolism,

microbiota metabolism, cysteine and homocysteine metabolism and metabolic disorders (**Figure 4.6**). Positive correlations were also identified between plasma and muscle for metabolites linked with energy metabolism, AA metabolism, cysteine and homocysteine metabolism, metabolic disorders and neurotransmitter (VL) or AA metabolism, energy metabolism, BCAA metabolism and metabolic disorders (RAM) (**Figure 4.6**).

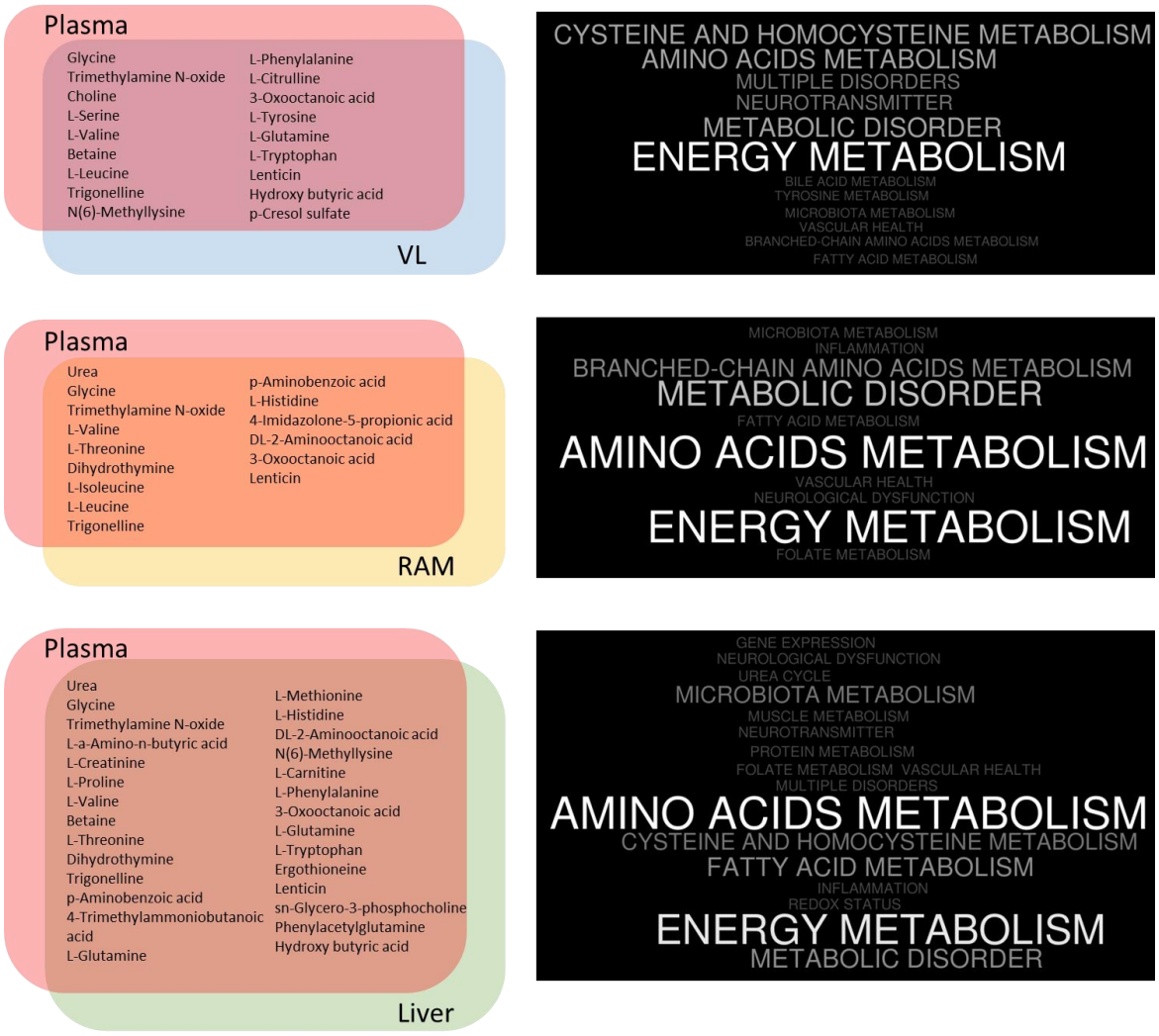

Figure 4.6: Individual polar metabolites showing significant correlation between plasma and VL, RAM or liver (BH p<0.05), and the metabolic pathway/function in which these metabolites are linked to, generated using wordcloud based on frequency of the pathway/function being assigned. The size and colour intensity of the wordcloud figure reflects frequency of each pathway/function being assigned. VL: Vastus Lateralis, VL; RAM: Rectus Abdominis Muscle.

4.4 Discussion

Metabolomics has become widely applied to study the relationship between the blood metabolome and various diseases, however translating/understanding the relevance of a blood metabolite marker can be challenging if it is unknown to what extent it reflects tissue abnormalities. The present study sought to identify plasma metabolites that were reflective of levels in different human tissue types. Because of limited access to samples of human liver, muscle and AT, the samples analysed were obtained from obese subjects undergoing bariatric or upper GI surgery. We chose to apply untargeted metabolomics to study these samples because the relationship between metabolomic profiles of plasma and various tissues has been poorly characterised and a gap remains to be addressed. The profiling and correlation of a broad range of metabolite classes (instead of focusing on a specific class) would allow for generation of novel and highly informative results from this observational study. Two LC-MS platforms were adopted to increase metabolome coverage, i.e. HILIC chromatography for polar metabolites and lipidomics for non-polar metabolites. Both ESI+ and ESI- modes were carried out to obtain complementary and more complete datasets, as using only one ionisation mode may limit the measure of particular metabolite/lipid classes. Without prior knowledge or assumptions, our study found that the plasma lipidome is more reflective of the liver than other tissue types examined. Two hundred and two lipid features accounting for 151 putative lipid species measured by ESI+, and 143 lipid features accounting for 115 lipid species measured by ESI- showed significant positive correlations between plasma and liver. These lipid species collectively encompassed the lipid classes of ceramide, mono- and di-hexosylceramide, sphingomyelin, PC, PE, LPE, PE-NMe2, ether-

linked PC, ether-linked PE, FFA, CE, DG and TG. Likewise, the greatest number of plasma polar metabolites measured by the HILIC LC–MS platform were found to be correlated with concentrations in the liver. This included numerous AAs (e.g. valine, threonine, tryptophan), metabolites linked with energy metabolism (e.g. creatinine, carnitine), FA metabolism (e.g. 3-oxooctanoic acid, hydroxybutyric acid), cysteine and homocysteine metabolism (e.g. betaine, methionine), and gut microbial metabolites (e.g. trimethylamine oxide (TMAO), p-aminobenzoic acid, ergothioneine).

Further to the profound association between the plasma and liver metabolite profiles, a modest number of plasma polar metabolites were also found to be correlated with concentrations in muscle tissues, including a range of AAs and related metabolites, gut microbial metabolites and xenobiotics that were mainly involved in AA metabolism and energy metabolism. In contrast, plasma polar metabolites were poorly correlated with AT depots, likely owing to the less aqueous cellular environment of AT. Conversely, plasma lipids showed positive correlations with muscle tissues for phospholipids, and with ATs mainly for TGs. Interestingly, despite being at different locations, both muscle subtypes showed positive correlations with plasma for several long chain polyunsaturated fatty acid (LCPUFA)-containing PC, ether-linked PC and ether-linked PE. Likewise, regardless of the location, plasma showed positive correlations with all 4 AT subtypes for several PUFA-containing TGs with total carbon number ≥50. However, the number of correlated TGs notably decreased as the location of AT shifted from a more central site towards peripheral site (i.e. IAA>DSA>SAA>STA), suggesting regional differences of AT contributing to the plasma TG pool.

Plasma bilirubin is a metabolite that reflects liver function, metabolism and excretion of bile and has been an important component to calculate a prognostic score for liver disease [383]. A model comprising plasma levels of bilirubin and creatinine (along with the prothrombin time) to predict mortality at the end-stage of liver disease was developed [384]. Our results of direct linear relationships between liver and plasma concentrations of bilirubin and creatinine provided further confirmation to support the validity and robustness of these metabolites as potential biomarkers for diagnosis and prognosis of liver disease.

Elevated total blood TG is a characteristic of dyslipidaemia. However, previous lipidomics studies have highlighted differential cardiometabolic risks associated with different sets of TG species, with those TG containing a lower total carbon number and unsaturated bonds being more detrimental and prominently associated with fatty liver diseases and incident CVD [173, 174, 176]. In another study, TG species with both low carbon number and degree of unsaturation were associated with increased risk of T2D, whereas those with high carbon number and degree of unsaturation were associated with a decreased risk of T2D [175]. These studies collectively emphasised the need for dissecting the relationship between individual TG species and cardiometabolic risk and understanding them at a molecular level. In the present study, the concentration of plasma TG species was found to be correlated with both liver and AT. Levels of saturated and monounsaturated TGs in plasma were exclusively correlated with their levels in the liver, the metabolically active site of TG synthesis and secretion, whereas levels of PUFA-containing TGs were correlated with their levels in ATs, the sites of TG storage. Complementary to biomarker discovery studies, our results indicated that the specific set of plasma TGs identified as potential predictors for

poor cardiometabolic health are indeed likely reflective of an abnormal level in the liver, possibly attributing to a higher rate of *de novo* lipogenesis, TG synthesis and very low density lipoprotein (VLDL) secretion. On the contrary, TG species potentially acting as negative predictors for cardiometabolic risk, reflect their storage in ATs which may be linked to the dietary intake of PUFA.

In addition to TG, disruption of the lipid balance involved in sphingolipid metabolism was frequently reported to be associated with T2D. Circulating ceramide has been correlated with insulin resistance (IR), fasting plasma glucose and markers of inflammation [182, 238, 239, 385], and was found to be increased in individuals with T2D [167]. Increased dihydroceramide, the precursor of ceramide biosynthesis, was also associated with prevalent and incident T2D [167, 386]. Conversely, downstream ceramide metabolites including sphingomyelin and glycosphingolipid species were found to be lower in T2D [167, 184]. However, there is still a lack of consensus across numerous datasets, with some other studies reporting the opposite or no changes [167, 182, 387]. The inconsistent findings on the exact relationship between the sphingolipid signature and clinical endpoint may be due to ceramide being an intermediate of sphingolipid metabolism, thus a central molecule at a branching point for pathways of different metabolic fates [388]. Several lines of evidence have demonstrated a role of ceramide as a lipid mediator whose production is regulated by several factors such as lipid supply and the inflammatory pathway, and ceramide exerts several downstream effects such as lipid raft formation, impaired insulin signalling, induction of endoplasmic reticulum (ER) stress, inflammatory pathway activation and apoptosis [388]. As such, changes in the level of various sphingolipid species in plasma associated with metabolic

diseases and conditions have been frequently postulated to be linked with inflammation, IR and oxidative stress [184, 238, 389]. Yet a deeper understanding and interpretation remains challenging without knowing whether the altered metabolism is confined within local tissue sites or can be readily detectable in the circulation. Herein, we reported that a majority of plasma sphingolipids, on a broad scale, including ceramide, sphingomyelins and glycosphingomyelins, show strong correlation with the concentration of corresponding species in the liver. We have also observed that the correlated sphingomyelins and ceramides between plasma and liver showed chain length-specificity, mainly for those containing a very long acyl chain fatty acids (VLCFA) such as C22:0, C24:0 and C24:1, in line with the previous finding of CerS2, a ceramide synthase showing substrate specificity for longer acyl chain species, being predominantly expressed in the liver [390, 391]. Our result provided evidence supporting the liver to be a major source of plasma VLCFA-containing ceramides and SMs. Given the concentrations were well correlated, changes in this subset of sphingolipids in plasma is likely capturing an abnormal handling and metabolism of sphingolipids in the liver.

DG is an intermediate of TG metabolism and has also been long recognised as a mediator of IR in the liver and muscle [392]. High intracellular levels of DG are associated with activation of protein kinase C (PKC) which subsequently phosphorylates insulin receptor substrate (IRS)-1 and suppresses the insulin signalling pathway [393, 394]. Increased circulating DG was also reported to be associated with prediabetes and T2D [167]. Herein, we observed positive correlations of DG between plasma and the liver, but not muscle or AT depots,

therefore highlighting abnormally high levels of circulating DG reported in dysglycaemia may be indicative of development of liver IR.

Plasma FFA composition has been hypothesised to be an indicator of AT FFA composition since AT lipolysis is a major source of plasma FFA. However, findings from existing studies have been inconsistent. Hellmuth et al., reported a strong positive correlation of plasma FFA (15:0, 22:6, 18:2, 20:5) with concentrations in both SAT and VAT in obese non-T2D females [304]. In another 12-month intervention study, poor-to moderate correlations between plasma and SAT FFA were reported, and changes in plasma n-3 PUFAs failed to predict changes in SAT in response to increased n-3 PUFA intake [305]. In the present study, we did not observe any correlations between plasma and ATs FFA levels. Instead, plasma FFA were found to be correlated with FFA contents in the liver (FA 18:0, 20:5) and VL muscle (FA 18:1). Likewise, acylcarnitines are fatty acid oxidation (FAO) metabolites and therefore it has been speculated whether metabolically active organ/tissues are actually sources of plasma acylcarnines. Plasma acylcarnitines did not correlate with muscle acylcarnitines in human [306], and data on other tissues/organs are lacking. Herein, our study was able to detect 4 long chain acylcarnitines in plasma, yet none of them showed correlations with any examined tissue types.

Positive correlations for several plasma PC species with multiple tissues, including some AT depots (STA, IAA), muscle (VL, RAM) and liver were detected. PCs are a major component of cellular membranes and therefore are ubiquitous throughout the body. Altered levels of circulating PCs have previously been associated with T2D, although the composition and direction of changes have been inconsistent to date [167, 183, 184]. This may be due to the plasma PC

profile being determined by several factors e.g. composition of FA intake, desaturase activity, and the balance between fission and fusion of biological membranes in the circulation and local tissue sites. Nonetheless, interesting patterns for the correlated PC species were noticed in the present study. Correlations with a broad scale of tissue sites (STA, IAA, VL, RAM and liver) were found for plasma PUFA-containing PC species with a total carbon number of 36 or 38. Plasma PC species that contained a lower even total carbon number (C≤34) and a MUFA chain were correlated with the more central tissue sites (IAA, RAM and liver). Plasma saturated PC species, as well as PC species that contained an odd total carbon number or higher even total carbon number (C≥40) with varying degrees of unsaturation were correlated with concentrations in the liver only. Plasma PCs did not correlate with abdominal subcutaneous AT depots (SAA and DSA). Our results highlighted potential differential contributions from different tissue sites to the plasma PC profile. Interpretation of plasma PC species as markers for cardiometabolic disease will require consideration of their relationship with tissue levels, and our findings provide some reference for this.

Accumulating evidence from recent metabolomics studies have shown an inverse association between plasma ether-linked phospholipids and cardiometabolic diseases [167, 168, 181, 186]. Ether-linked phospholipids are peroxisome-derived moieties and play a structural role as a membrane component [395]. They may also act as signalling molecules and have antioxidant properties [395]. However, the source and implication of plasma ether-linked phospholipids are less well understood. Our results revealed that several plasma ether-linked PC species reflected levels in the liver, SAA and both muscle subtypes, whilst plasma

ether-linked PE species reflected levels in the liver, IAA and both muscle subtypes.

In addition to various plasma lipid species found to be reflective of concentrations in different tissue sites, some interesting findings on plasma polar metabolites were also observed. Numerous plasma AAs were found to be positively correlated with concentrations in the muscles and liver. This is as expected since protein turnover in the muscle and liver is increased during fasting and thus likely to act as major contributor to the plasma AA pool during fasting state when the samples were obtained [396-398].

Glycero-3-phosphocholine, the lipid backbone of PCs showed positive correlation between plasma and liver, in agreement with our lipid data showing a wide range of PC species to be correlated between plasma and the liver.

Dysregulation of cysteine and homocysteine metabolism (also known as the transmethylation and transsulfuration pathway) has been implicated in the development of fatty liver diseases [399], and this pathway plays a critical role in maintaining liver health [400, 401]. Unsurprisingly, concentrations of several metabolites linked to this pathway such as methyl donor replenisher (e.g. betaine and methionine), and methylated products (e.g. N(6)-Methyllysine and trigonelline) also showed positive correlation between plasma and liver.

Trimethylamine (TMA) is produced by the gut microbiota and the liver is the site of first pass metabolism that oxidises TMA to TMAO [402]. Therefore, liver is the primary source for TMAO in the circulation and a strong correlation is expected. Interestingly, TMAO was also positively correlated with concentrations in the muscle. A TMAO transporter has been recently identified and characterised therefore its accumulation in tissues is possible [403] and the strong positive

correlations of plasma TMAO with muscles, but not ATs, might be due to a higher peripheral blood flow through the muscle tissues. Concentrations of several other microbial metabolites in plasma (e.g. p-aminobenzoic acid, p-cresol sulfate, ergothioneine) were also found to be correlated with ATs, muscles and/or the liver, however, the metabolism, distribution and biological implication of these microbial metabolites are less well characterised. Nonetheless, untargeted metabolomics adopted by the present study confirmed the accumulation of these metabolites in various tissue sites. Future pharmacokinetics and in vitro studies may help explain and understand these relationships. Likewise, lenticin is a xenobiotic and our result showed its accumulation in muscle and the liver, of which concentrations were also correlated with plasma level. Given the strong correlations between various non-endogenous compounds in muscle or liver and the circulation and the current view that gut microbiota impact metabolic health, whether these metabolites play a biological role and mediate the association between gut microbiota and host health could warrant future research.

4.5 Conclusion

In conclusion, the plasma lipidomic profile from obese but otherwise healthy females is mostly reflective of the liver profile, while several plasma phospholipid species and TG species were also correlated with concentrations in the muscle and AT, respectively. The plasma polar metabolite profile is more reflective of the liver and muscle for metabolites mainly linked to amino acid and energy metabolism, but poorly correlated with AT profile. Our study confirms that the overall plasma metabolomic profile provides a window for monitoring metabolites in multiple tissue types, and various constituents of the plasma profile can be used as a proxy for tissue metabolites. Given that the plasma metabolomics

profile is more reflective of some tissues (e.g. the liver) but not the others (e.g. AT), our study also highlighted the critical importance of understanding to what degree and which tissue site(s) the concentration of a plasma metabolite reflects when linking a plasma metabolite to the potential underlying mechanism occurring in a specific tissue. Miss-interpretation of a plasma candidate marker with regards to the site of metabolic abnormalities may lead to incorrect mechanistic speculation.

4.6 Contributions and acknowledgements

This Chapter is written with the intention to be submitted to the journal *FASEB*.

Zhanxuan E. Wu, Marlena C. Kruger, Ivana R. Sequeira, McGill, Anne-Thea, Sally D. Poppitt and Karl Fraser. “A metabolomics study to dissect the relationship between plasma and adipose, muscle and liver tissue metabolomes in a cohort of obese, non-diabetic women.”

Author Contributions:

Conceptualization, Sally D. Poppitt; Methodology, Zhanxuan E. Wu; Sample collection, storage and handling, McGill, Anne-Thea, Ivana R. Sequeira; Sample preparation and extraction, Zhanxuan E. Wu; Metabolomics data acquisition, Zhanxuan E. Wu; Data analysis, Zhanxuan E. Wu; Data visualization and presentation, Zhanxuan E. Wu; Writing – original draft, Zhanxuan E. Wu; Writing – review & editing, Marlena Kruger, Sally D. Poppitt and Karl Fraser; Supervision, Marlena Kruger, Sally D. Poppitt and Karl Fraser; Funding acquisition, Sally D. Poppitt.

MASSEY UNIVERSITY
TE KUNENGA KI PŪREHUROA
UNIVERSITY OF NEW ZEALAND

GRADUATE RESEARCH SCHOOL

STATEMENT OF CONTRIBUTION
DOCTORATE WITH PUBLICATIONS/MANUSCRIPTS

We, the candidate and the candidate's Primary Supervisor, certify that all co-authors have consented to their work being included in the thesis and they have accepted the candidate's contribution as indicated below in the *Statement of Originality*.

Name of candidate:	Zhanxuan Wu
Name/title of Primary Supervisor:	Marlena Kruger
In which chapter is the manuscript /published work:	4

Please select one of the following three options:

○ The manuscript/published work is published or in press

- Please provide the full reference of the Research Output:

○ The manuscript is currently under review for publication – please indicate:

- The name of the journal:
- The percentage of the manuscript/published work that was contributed by the candidate:
- Describe the contribution that the candidate has made to the manuscript/published work:

◉ It is intended that the manuscript will be published, but it has not yet been submitted to a journal

Candidate's Signature:	Zhanxuan Wu
Date:	31-Aug-2020
Primary Supervisor's Signature:	Marlena Kruger
Date:	1/9/2020

This form should appear at the end of each thesis chapter/section/appendix submitted as a manuscript/ publication or collected as an appendix at the end of the thesis.

GRS Version 5 – 13 December 2019
DRC 19/09/10

5. Differential metabolomic signature for fasting glucose and visceral adiposity by ethnicity in a cohort of healthy and prediabetic Asian Chinese and Caucasian adults: the TOFI_Asia study

This chapter characterised the plasma metabolomic signature for elevated FPG and VAT, both of which are risk factors for development of T2D in each of the two ethnicities: Caucasian and Asian Chinese. The plasma signature was then used to predict the FPG state and the cardiometabolic risk profile of the predicted FPG groups were compared.

Abstract

Asian Chinese are more susceptible to deposition of visceral adipose tissue (VAT) and type 2 diabetes (T2D) development than European Caucasians when matched for gender, age and body mass index (BMI). Our aims were: (i) characterise the ethnicity-specific metabolomic signature of visceral adiposity measured by dual energy X-ray absorptiometry (DXA) and fasting plasma glucose (FPG), and (ii) identify individuals susceptible to worse metabolic health outcomes. Fasting plasma samples from normoglycaemic (n=274) and prediabetic (n=83) participants were analysed with liquid chromatography–mass spectrometry using untargeted metabolomics. Multiple linear regression adjusting for age, gender and BMI was performed to identify metabolites associated with FPG and VAT calculated as percentage of total body fat ($\%VAT_{TBF}$) in each ethnic group. Metabolic risk groups in each ethnicity were stratified based on the joint metabolomic signature for FPG and $\%VAT_{TBF}$ and clinically characterised using partial least squares-discriminant analysis (PLS-DA) and t-tests. FPG was correlated with 40 and 110 metabolites in Caucasians and Chinese respectively, with diglyceride DG(38:5) (adjusted $\beta = 0.29$, $p = 3.00E-05$) in Caucasians and triglyceride TG(54:4) (adjusted $\beta = 0.28$, $p = 2.02E-07$) in Chinese being the most significantly correlated metabolite based on the p-value. $\%VAT_{TBF}$ was correlated with 85 and 119 metabolites in Caucasians and Chinese respectively, with TG(56:2) (adjusted $\beta = 0.3$, $p = 8.25E-09$) in Caucasians and TG(58:3) (adjusted $\beta = 0.25$, $p = 2.34E-08$) in Chinese being the most significantly correlated. 24 metabolites associated with FPG were common to both ethnicities including glycerolipid species. 69 metabolites associated with $\%VAT_{TBF}$ were common to both ethnicities including positive correlations with dihydroceramide,

sphingomyelin, glycerolipid, phosphatidylcholine, phosphatidylethnolamine, and inverse correlations with ether-linked phosphatidylcholine. Participant re-stratification found greater total and central adiposity, worse clinical lipid profiles, higher serum glucoregulatory peptides and liver enzymes in normal fasting glucose (NFG) individuals with a prediabetic metabolomic profile than NFG individuals with a normoglycaemic metabolomic profile in both ethnicities. Untargeted metabolomics identified common and disparate metabolites associated with FPG and $\%VAT_{TBF}$, with an ethnic-dimorphic signature for these metabolic traits. These signatures could improve risk stratification and identify NFG individuals with an adverse cardiometabolic and T2D risk profile.

5.1 Introduction

The prevalence of type 2 diabetes (T2D) has witnessed a drastic surge in China over recent decades. There are now 110 million people with T2D in China [404], reaching epidemic proportions and predicted to continue on this trajectory [405]. Whilst the accelerated rise of the T2D prevalence is likely due to a rapid transition to a westernised diet and lifestyle [34, 406], striking observations of younger and outwardly slimmer individuals with diabetes in South and East Asia highlights the role of ethnicity in T2D risk [25]. Although high BMI has been a well-established risk factors for T2D [16], it is evident that even modest weight gain greatly increases T2D risk in Asians compared to modest increases in other ethnicities [68]. The mechanisms underpinning the greater risk of poor metabolic health in Asian populations have not yet been elucidated, but it is clear that site of fat deposition plays an important role [35, 407, 408], and Asian populations are more prone to abdominal and visceral adiposity as well as ectopic fat deposition into key organs including pancreas and liver [35-37]. Excess visceral adipose tissue (VAT) and ectopic fat deposition are associated with higher risks of cardiometabolic diseases and complications [81, 409, 410]. It has been hypothesised that poor adipose expandability in 'safer' subcutaneous sites may promote this 'lipid overspill' and ectopic storage [411-413]. The TOFI (Thin-on-the-Outside-Fat-on-the-Inside) profile has been coined for these individuals who may have hidden risks of cardiometabolic disease [414].

Current measurements of VAT and ectopic organ fat rely on imaging techniques which are expensive and time-consuming. Whilst blood glucose and HbA_{1c} both provide simple and cost-effective markers of prediabetes, predicting individuals who remain in the prediabetic state for many years vs those progressing rapidly

to T2D is difficult from these single markers. Metabolomics provides a useful means to advance the understanding of disease pathophysiology, and may facilitate the identification of at-risk individuals before dysglycaemia occurs and/or predict those who will rapidly worsen to T2D [415, 416]. For example, metabolic shifts in branched-chain amino acids (BCAAs) are the most prominent changes associated with insulin resistance (IR) and predictive of future T2D development to date [39]. Increased levels of circulating BCAAs can be due to increased protein degradation in IR [417], while evidence for higher levels of C3- and C5-acylcarnitine, the catabolic intermediates of BCAAs, associated with IR and T2D have also been reported, suggesting that higher levels of circulating BCAA may also be due to an impaired catabolism resulting from mitochondrial overload and metabolic inflexibility [218]. Higher levels of medium-chain acylcarnitines (MCAC) were reported in T2D patients, which has been postulated as a consequence of incomplete fatty acid oxidation (FAO) [230]. However, higher levels of long-chain AC (LCAC) , which may be indicative of an excessive lipid load and FAO flux, were found to be predictive of incident T2D [418]. Mechanistic investigation suggested accumulation of LCAC and MCAC was due to mitochondrial overload and discordant FAO and citric acid cycle (TCA) activity [231, 232]. Other metabolites such as those involved in sugar metabolism, purine metabolism and the urea cycle have been occasionally reported [42], and the identification and understanding of metabolite markers for T2D is ongoing. There are few studies investigating the metabolomic profile associated with the increased VAT depots. To date, several AAs, organic acids, ether-linked phosphatidylcholines (PCs), lysoPCs-to-PCs ratio have been reported as markers for VAT [219, 249, 266, 419].

Given that increased VAT deposition is a risk factor for T2D development and may underlie an increased propensity for poor metabolic health in specific populations such as Asians, a major gap in the field remains as to how characteristic plasma signatures for VAT calculated as percentage of total body fat ($\%VAT_{TBF}$) and glycaemia are related to each other, and whether the metabolite markers for these two metabolic traits are common or unique to different ethnic groups. Herein, we simultaneously profiled the plasma samples from non-diabetic individuals across a range of FPG and VAT content from 2 ethnic groups (Asian Chinese and age- and BMI-matched Caucasian Europeans). FPG was focused on in this study as it is one of the 3 measurements (along with HbA1c and oral glucose tolerance test) for prediabetes/T2D diagnosis according to the American diabetes association (ADA) criteria [2]. FPG and HbA1c are convenient and less time-consuming to obtain thus are suitable for large-scale studies. The level of FPG is less subject to haemoglobin variants or certain conditions e.g. sickle cell disease or recent blood transfusion as opposed to HbA1c [2], hence was chosen as an outcome variable to be investigated in this study. The goals of this study were 1) to determine whether plasma metabolomic profiles measured using an unbiased untargeted approach differed between ethnicities; 2) to characterise the metabolomic signatures associated with $\%VAT_{TBF}$ and FPG in each ethnic group; 3) to predict FPG state using the metabolomic signature (i.e. metabolic FPG state) and characterise the clinical profiles of the metabolic FPG state.

5.2 Materials and methods

5.2.1 Ethics approval and consent to participate

The study received ethical approval from the Health and Disabilities Ethics Committee (HDEC), Auckland, New Zealand (16/STH/23) and is registered with the Australian New Zealand Clinical Trials Registry ACTRN: 12616000362493. All participants gave written informed consent at the time of study enrolment.

5.2.2 Study Cohort

The TOFI-Asia study is a cross-sectional study conducted at the Human Nutrition Unit (HNU), University of Auckland, New Zealand. All participants self-reported both parents of the same ethnic descent, i.e. European Caucasian or Asian Chinese according to ethnic group profiles by Stats New Zealand, Tatauranga Aotearoa) [420]. Participants were recruited for both genders across a wide range of ages (20-70 years) and BMI (20-45 kg/m^2), and were either normoglycaemic or prediabetic based on ADA criteria [421]. They had no significant weight gain or loss (>10%) in the previous 3 months, no prior bariatric surgery, were not pregnant, breastfeeding, or currently taking glucose-related medications (e.g. glucocorticoids) or had a significant current or prior history of disease including T2D. A detailed description of the study population and protocol can be found elsewhere [422]. In total, 199 Asian Chinese and 158 European Caucasian participants were enrolled in the study. All participants attended the study visit following an overnight fast.

5.2.3 Phenotypic Characterisation and Laboratory Measurements

Body weight, height, waist and hip circumference, and blood pressure were recorded at HNU at the study visit. Fasting venous blood samples were collected, separated, and stored at -80°C until analysis. FPG was measured using the hexokinase method. HbA_{1c} was determined by capillary electrophoresis. Plasma glucoregulatory peptides (insulin, C-peptide, glucagon, total amylin, gastric

inhibitory polypeptide (GIP) and glucagon-like peptide-1 (GLP-1)) were analysed by multiplex immunoassay. Serum liver enzymes (alanine transaminase (ALT), aspartate transaminase (AST), alkaline phosphatase (ALP), gamma-glutamyltransferase (GGT)) and lipids (total cholesterol, total triglyceride (TG), HDL-cholesterol) were analysed using internationally accredited methods. Details of sampling procedures and blood measurements have been reported elsewhere [422].

5.2.4 Body Composition

Dual energy X-ray absorptiometry (DXA) (iDXA, GE Healthcare, WI, USA) scanning was used to obtain total body fat (TBF), abdominal adipose tissue (AAT) and VAT mass as previously described [422]. One participant did not attend DXA scanning therefore 356 body composition profiles were available.

Region-specific percentage measures were obtained;

%TBF = 100 x TBF mass/(total body lean mass + TBF mass);

%AAT = 100 x AAT mass/(abdominal lean mass + AAT mass)

Visceral adipose tissue was calculated in 2 ways:

(i) $\%VAT_{TBF}$ = (100 x VAT mass / TBF mass

(ii) $\%VAT_{AAT}$ = 100 x VAT mass /AAT mass

$\%VAT_{TBF}$ is used as a measure of visceral adiposity in this manuscript and the dependent variable to be characterise by metabolomics. This is because it considers both total body fat mass (i.e. outside the viscera) and VAT mass (i.e. inside the viscera), and hence is representative of the “TOFI” phenotype of interest to the present study.

5.2.5 Sample Preparation for LC–MS Untargeted Metabolomics

Samples were randomised into 4 batches and extracted on 4 consecutive days. The protocol for metabolite extraction was adapted from a previously reported method [352]. Briefly, 100 µL plasma was mixed with 800 µL pre-chilled (-20 °C) $CHCl_3$:MeOH (50:50, v/v) containing internal standard compounds (detail provided in **Appendix: Table 9.3**), agitated for 30s and placed in a -20 °C freezer for 60 min to allow protein precipitation, followed by addition of 400 µL H_20, vortex-mixing for 30 s and centrifugation (Eppendorf Centrifuge 5427 R, Eppendorf, Hamburg, Germany). Centrifuge parameters were set at 11,000 rpm, 4 °C, 10 min. Two blank samples were prepared following the same protocol replacing plasma with H_20. 200 µL of the upper aqueous layer and 200 µL of the lower organic layer were transferred into two 2 mL microcentrifuge tubes separately, dried down under a nitrogen stream and stored at -80 °C. To account for intra- and inter-batch variation, pooled QC samples were prepared by combining an aliquot of the upper or lower phase from every sample extracted on the same day in a clean glass tube and stored at -80 °C. At the end of all sample extractions, the pooled samples on each day were then combined, dispensed into separate 200 µl aliquots and dried down under the nitrogen stream and stored at -80 °C. On the day of instrumental analysis, dried polar and lipid extracts were reconstituted in 200 µL acetonitrile:H_2O (50:50, v/v) and modified Folch solution ($CHCl_3$:MeOH:H_2O, 66:33:1, v/v/v) containing pre-dissolved 0.01% 16:0 d_{31}-18:1-PE internal standard [0.01% (%w/v)] for polar metabolite and lipid analysis respectively. The reconstitution volume was determined using a previously described workflow [379].

5.2.6 Ultra-Performance Liquid Chromatography (UPLC)-Mass Spectrometry Analysis of Lipids

Lipid analyses were performed using an Accela 1250 quaternary UHPLC system coupled to a Q Exactive hybrid quadrupole-Orbitrap mass spectrometer (Thermo Fisher Scientific, Waltham, MA, USA) with a heated electrospray ionisation source set to 370 °C. An Acquity CSH™ C18 column 1.7 µm, 2.1 mm × 100 mm (Waters, Milford, MA, USA) was used for lipid separation with a column temperature of 65 °C and mobile phase flow rate at 600 µL/min. The mobile phases consisted of acetonitrile/H_2O (60:40) with 10 mM ammonium formate and 0.1% formic acid (A), and isopropanol/acetonitrile (90:10) with 10 mM ammonium formate and 0.1% formic acid (B). Analytes were eluted from the column with the following gradient program: 15–30% B (0.0–2.0 min), 30–48% B (2.0–2.5 min), 48–82% B (2.5–11.0 min), 82–99% B (11.0–11.5 min), 99% B was maintained for 3.5 min followed by re-equilibration with 15% B for 3 min. Two microliter reconstituted samples were injected. External mass calibration of the Orbitrap prior to sample analysis was performed by flow injection of the calibration mix solution according to the manufacturer's instructions. High resolution data (resolution 70,000) was acquired by full scan from *m/z* 200–2000 with source voltage of 3500 V electrospray ionisation positive mode (ESI+) or −3600 V ESI negative mode (ESI−), capillary temperature of 275 °C, and sheath, auxiliary and sweep gas flow rates of 40, 10 and 5 arbitrary units, respectively. Data-dependent MS^2 data were collected with a mass resolution set to 35,000 recording a mass range of *m/z* 200-2000 and maximum trap fill time of 250 ms (full scan mode) or 120 ms (MS^2 scan mode). The isolation window of selected MS^1 scans was ± 1.5 *m/z* with a normalised collision energy of 30 units.

5.2.7 Liquid Chromatography (LC)-Mass Spectrometry Analysis of Polar Metabolites

Polar metabolites were analysed with an Accela 1250 quaternary UHPLC pump coupled to an Exactive Orbitrap mass spectrometry (Thermo Fisher Scientific, USA). Chromatographic separation was carried out at 25 °C on a SeQuant® ZIC®-pHILIC 5 µm, 2.1 mm × 100 mm column (Merck, Darmstadt, Germany) with the following solvent system: A = 10 mM ammonium formate in water, B = 0.1% formic acid in acetonitrile. A gradient program was used at a flow rate of 250 µL/min: 3–3% A (0.0–1.0 min), 3–30% A (1.0–12.0 min), 30–90% A (12.0–14.5 min), 90% A was maintained for 3.5 min followed by re-equilibration with 3% A for 7 min. An injection volume of 2 µL was used. The electrospray probe was operated unheated at room temperature (20 °C) to avoid degradation of thermally labile compounds. External mass calibration of the Orbitrap prior to sample analysis was performed by flow injection of the calibration mix solution according to the manufacturer's instruction. High resolution data (resolution 25,000) were acquired by full scan from *m/z* 55 to 1100 with source voltage of 4000 V for ESI+ and −4000 V for ESI−, capillary temperature of 325 °C, and sheath, auxiliary, and sweep gas flow rates of 40, 10, and five arbitrary units, respectively.

5.2.8 Data processing

Raw data files were converted to mzXML format with MSconvert (v 3.0.1818) and pre-processed. Three lipid datafiles were corrupted and excluded from analysis. Lipid data were preprocessed with the XCMS package (v3.0.2) in the R programming environment (v3.2.2) [154], whereas polar metabolite data were preprocessed with the ADAP algorithm in mzMINE (v2.31) (processing parameters provided in **Appendix: Table 9.4-9.5**) [155, 423]. Features not detected in 100% of the QC samples were excluded. For polar metabolite data, features detected in at least one blank sample before peak filling step were

removed. For lipid data, blank features were filtered out based on tstat and p-values (sample vs. blank tstat < 1 or those with tstat >1 but p-value ≥ 0.05) generated by the diffreport function from the XCMS package. Manual examination of EIC was conducted to filter out poorly integrated peaks, using build-in function in mzMINE for the polar metabolite data and the EICs generated by the diffreport function in the XCMS package for lipid data. After data cleaning, signal drift and batch effects were corrected by LOESS in the W4M Galaxy environment [381], and features with QC %CV>30 were removed. Lipid identification was performed using LipidSearch software v4.1.16 on MS^2 datafiles (Thermo Fisher Scientific, USA) as previously described to generate a MS^2-annotated lipid ID library and matched against the processed lipid data matrices based on parent mass and retention times [424]. Lipid features without an MS^2-annotated lipid ID were searched against online database including HMDB (http://www.hmdb.ca/), Metlin (http://metlin.scripps.edu/) and Lipid Maps (http://www.lipidmaps.org/) based on *m/z* with less than 10 ppm mass error. Polar metabolites were annotated using an in-house library based on authentic standards (AgResearch) analysed through HILIC LCMS analysis under conditions identical to the current study. Metabolic features without a hit in the library were searched against online database including HMDB and Metlin based on *m/z* with less than 15 ppm error.

5.2.9 Statistical analyses

Multivariate analysis using partial least squares-discriminant analysis (PLS-DA) was initially applied to investigate differences in baseline profiles of the two ethnic groups (SIMCA version 16, Umeå, Sweden). Logistic regression was subsequently performed to allow for adjustment for age, gender, HDL-C, insulin,

FPG, HbA_{1c}, BMI and $\%VAT_{TBF}$ in identifying discriminatory lipids and metabolites between the two ethnicities (with Caucasian as reference level and Asian Chinese as level 1). To characterise the metabolomic and lipidomic signatures for FPG or $\%VAT_{TBF}$ (as the outcome variable), multiple linear regression was performed on every feature adjusting for age, gender and BMI in an ethnicity-specific manner. All univariate statistical analyses were carried out in R (v3.5.1) and subjected to FDR correction (Benjamini Hochberg procedure) [425]. Up till this point the lipid profiles and polar metabolites profiles were analysed separately due to different number of available profiles (3 lipid profiles were corrupted), but the list of associated metabolites (both lipids and polar metabolites) were combined into a single table for each trait of interest for reporting purpose.

The prediction model of FPG state by a panel of metabolites associated with FPG and $\%VAT_{TBF}$ in each ethnicity was built using random forest (RF) [426] in MetaboAnalyst v4.0 [427]. In detail, the datamatrix containing intensities of all metabolites associated with FPG and/or $\%VAT_{TBF}$ in each ethnicity identified by the aforementioned multiple linear regression, were extracted and imported to MetaboAnalyst for biomarker analysis. Three samples were excluded from the re-stratification due to the absence of their lipidomic profiles. RF analysis was performed on the 100 most important variables ranked by decreases in accuracy through 30 repeats of 3-fold random sub-sampling cross-validation. Individuals who were predicted as NFG by the metabolomic-based RF model were designated as “mNFG”, whereas those predicted as IFG were designated as “mIFG”. The predicted FPG state was further combined with their actual FPG state as determined by the ADA FPG criteria to create a new stratification system consisted of 4 groups: NFG-mNFG (NFG individuals predicted to be NFG based

on their metabolomic profile), NFG-mIFG (NFG individuals predicted to be IFG), IFG-mNFG (IFG individuals predicted to be NFG) and IFG-mIFG (IFG individuals predicted to be IFG). The clinical profile (including HbA_{1c}, HOMA2-IR, BMI, age, waist-to-hip ratio, SBP, DBP, ALT, AST, ALP, GGT, total cholesterol, HDL-C, total TG, LDL-C, amylin, C-Peptide, GIP, GLP-1, glucagon, insulin) of the metabolic FPG state and the 4 sub-phenotype were then characterised using multivariate PLS-DA (SIMCA 16, Umetrics) and univariate t-test (R (v3.5.1)).

5.3 Results

Characteristics of the study population are summarised in **Table 5.1**. Asian Chinese had higher body weight, DBP, %AAT, $\%VAT_{TBF}$, $\%VAT_{AAT}$, HbA_{1c}, FPG, fasting insulin, total TG, ALT, GGT, amylin, GLP-1 and glucagon, and lower HDL-cholesterol than Caucasians.

Table 5.1: Metabolic risk factors in Caucasian European (N=158) and Asian Chinese (N=199) enrolled in the TOFI_Asia Study.

	Caucasian European	Asian Chinese	*P value*
n	158	199	
% female	59	54	
Age (yr)	41.7 ± 16.1	40.5 ± 13.3	0.47
Anthropometry			
Weight (kg)	79.9 ± 15.7	75.6 ± 14.4	0.007
Height (m)	1.72 ± 0.09	1.66 ± 0.08	< 0.0001
BMI (kg/m^2)	26.9 ± 4.6	27.2 ± 3.9	0.53
Waist circumference (cm)	90.3 ± 14.1	90.0 ± 10.8	0.79
Hip circumference (cm)	101.1 ± 11.8	99.1 ± 10.2	0.07
[a] Systolic blood pressure (mmHg)	120 ± 15	122 ± 17	0.23
[a] Diastolic blood pressure (mmHg)	66 ± 8	69 ± 11	0.002
Body composition - [b] DXA			
Total body fat (TBF) mass (kg)	26.6 ± 11.4	25.5 ± 7.8	0.33
%TBF	33.8 ± 10.2	35.0 ± 7.2	0.21
Abdominal adipose tissue (AAT) mass (kg)	2.3 ± 1.4	2.4 ± 1.0	0.65
AAT (% of abdominal tissue mass)	36.8 ± 14.1	40.8 ± 9.1	0.003
Visceral adipose tissue (VAT) mass (kg)	0.9 ± 0.8	1.0 ± 0.6	0.07

Table 5.1 (continued)

$\%VAT_{TBF}$	2.86 ± 2.19	3.73 ± 1.98	0.0001
$\%VAT_{AAT}$	32.2 ± 19.9	39.7 ± 16.4	0.0002
Blood biochemistry			
[c] HbA_{1c}	33.3 ± 3.6	35.8 ± 3.9	< 0.0001
Fasting plasma glucose, FPG (mmol/L)	5.0 ± 0.6	5.3 ± 0.5	< 0.0001
Fasting plasma insulin (pg/ml)	430.4 ± 316.5	570.6 ± 359.9	0.0001
HOMA2-IR	1.8 ± 2.0	1.9 ± 1.2	0.8
HOMA2-β	140.4 ± 122.7	126.2 ± 61.4	0.18
[d] Total cholesterol (mmol/L)	5.0 ± 1.0	4.8 ± 0.9	0.19
[d] Triglycerides (mmol/L), TAG	1.1 ± 0.6	1.4 ± 0.9	0.0001
[d] HDL-Cholesterol (mmol/L)	1.6 ± 0.4	1.4 ± 0.4	< 0.0001
[d] LDL-Cholesterol (mmol/L)	2.9 ± 0.9	2.8 ± 0.8	0.49
[e] Alanine amino transferase, ALT (U/L)	15.8 ± 10.4	19.3 ± 14.0	0.008
[e] Aspartate amino transferase, AST (U/L)	20.9 ± 8.7	19.9 ± 6.4	0.23
[e] Alkaline phosphatase, ALP(U/L)	97.2 ± 27.2	96.2 ± 23.5	0.68
[e] Gamma glutamyl transferase, GGT (U/L)	23.6 ± 18.2	30.2 ± 23.8	0.003
Amylin (pg/ml)	28.8 ± 15.2	33.8 ± 17.4	0.005
C-peptide (pg/ml)	939.7 ± 554.5	935.3 ± 460.7	0.94
Gastric inhibitory peptide, GIP (pg/ml)	72.4 ± 58.2	79.0 ± 48.0	0.25
Glucagon like peptide – 1, GLP-1 (pg/ml)	146.6 ± 62.0	165.4 ± 87.6	0.02
Glucagon (pg/ml)	59.2 ± 35.3	71.1 ± 35.1	0.002

Results are mean ± SD. Numbers were as stated above each column except for bracketed values [a] Systolic and diastolic blood pressure were measured in 198 Asian Chinese; [b] Body composition was assessed in 157 Caucasian European; [c] HbA1c was measured in 157 Caucasian European; [d] lipid profile and [e] liver function were assessed in 198 Asian Chinese. Nonstandard abbreviations: DXA, dual energy x-ray absorptiometry; HbA1c, haemoglobin A1c; HOMA2-IR, Homeostasis Model Assessment of insulin resistance; HOMA2-β: Homeostasis Model Assessment of β-cell function.

5.3.1 Characterisation of fasting plasma profile associated with ethnicity differences

The score plots from the PLS-DA models for both lipid and polar metabolite profiles showed clear and robust separation between Asian Chinese and Caucasian cohorts (Q2 values of 0.502 for lipids and 0.593 for polar metabolites, confirming that the models had acceptable validity), indicating ethnicity influences the fasting plasma metabolome (**Figure 5.1**).

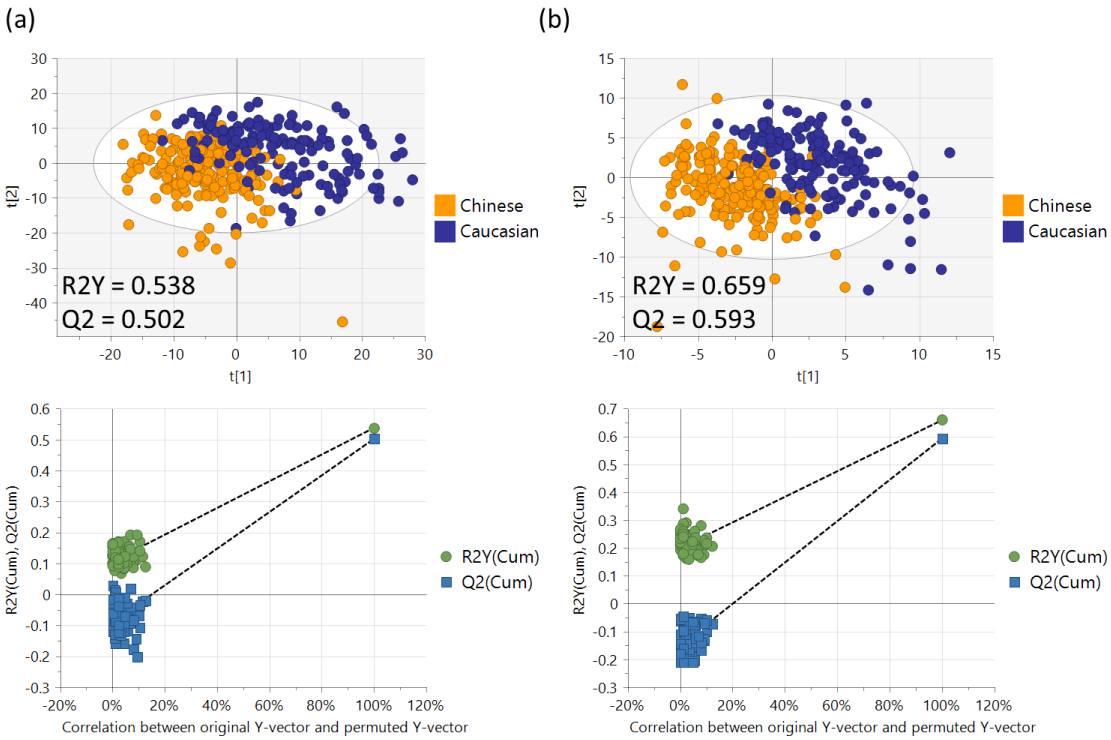

Figure 5.1: PLS-DA analysis for metabolomics differences between Caucasians and Asian Chinese. PLS-DA score plot (top) and 100 permutation tests (bottom) showing good separation and robust model for: (a) lipid profile and (b) polar metabolite profile, between Asian Chinese and Caucasian.

Logistic regression was applied to identify metabolites associated with ethnicity independent of potential covariates. Of the 629 lipid features measured by LC-MS, 170 identified lipid species over 15 lipid subclasses in addition to 25 unknowns were significantly associated with ethnicity, independent of potential covariates (BH adjusted $p < 0.05$) **(Figure 5.2 and Appendix: Table 9.6)**. Levels of lipid species belonging to lipid classes lysophosphatidylcholine (lysoPC), lysophosphatidylethanolamine (lysoPE), phosphatidylethanolamine (PE), phosphatidylinositol (PI), ceramide (Cer), glycosphingolipids (GCer), sphingomyelin (SM) and cholesteryl ester (CE) were exclusively higher in Caucasians, whereas those belonging to free fatty acid (FFA) and diacylglycerol (DG) classes were exclusively higher in Asian Chinese **(Figure 5.2a)**. Although triacylglycerol (TG), phosphatidylcholine (PC), ether-linked PC and ether-linked

PE did not display unidirectional association with either ethnic group, some characteristic patterns were observed. TGs containing carbon chains between C12-C18 and with a higher degree of saturation were associated with Caucasians whereas TGs enriched in long and very long chains between C16-C22 and with a higher degree of unsaturation were associated with Asian Chinese **(Figure 5.2b)**. The majority of discriminatory PCs and ether-linked PCs were at higher levels in Caucasians with the exception of PC(40:6), PC(p-38:6) and PC(p-40:6) which were higher in Asian Chinese, which again, contained a polyunsaturated fatty acid (PUFA). Ether-linked PEs associated with Asian Chinese also tended to contain more PUFA **(Figure 5.2b and Appendix: Table 9.6)**. Despite significantly higher total fasting TG as measured by biochemical assay in Asian Chinese **(Table 5.1)**, lipidomics indicated that the molecular makeup of plasma glycerolipid is discriminatory between the two ethnic groups.

A number of endogenous and exogenous polar metabolites were discriminatory between Caucasians and Asian Chinese **(Appendix: Table 9.7)**. These metabolites spanned a wide range of biological functions and pathways such as AA metabolism, carbohydrate (CHO) metabolism, energy production, fatty acid (FA) metabolism, nucleotide metabolism, protein metabolism and modification and the methyl transfer pathway **(Figure 5.3)**.

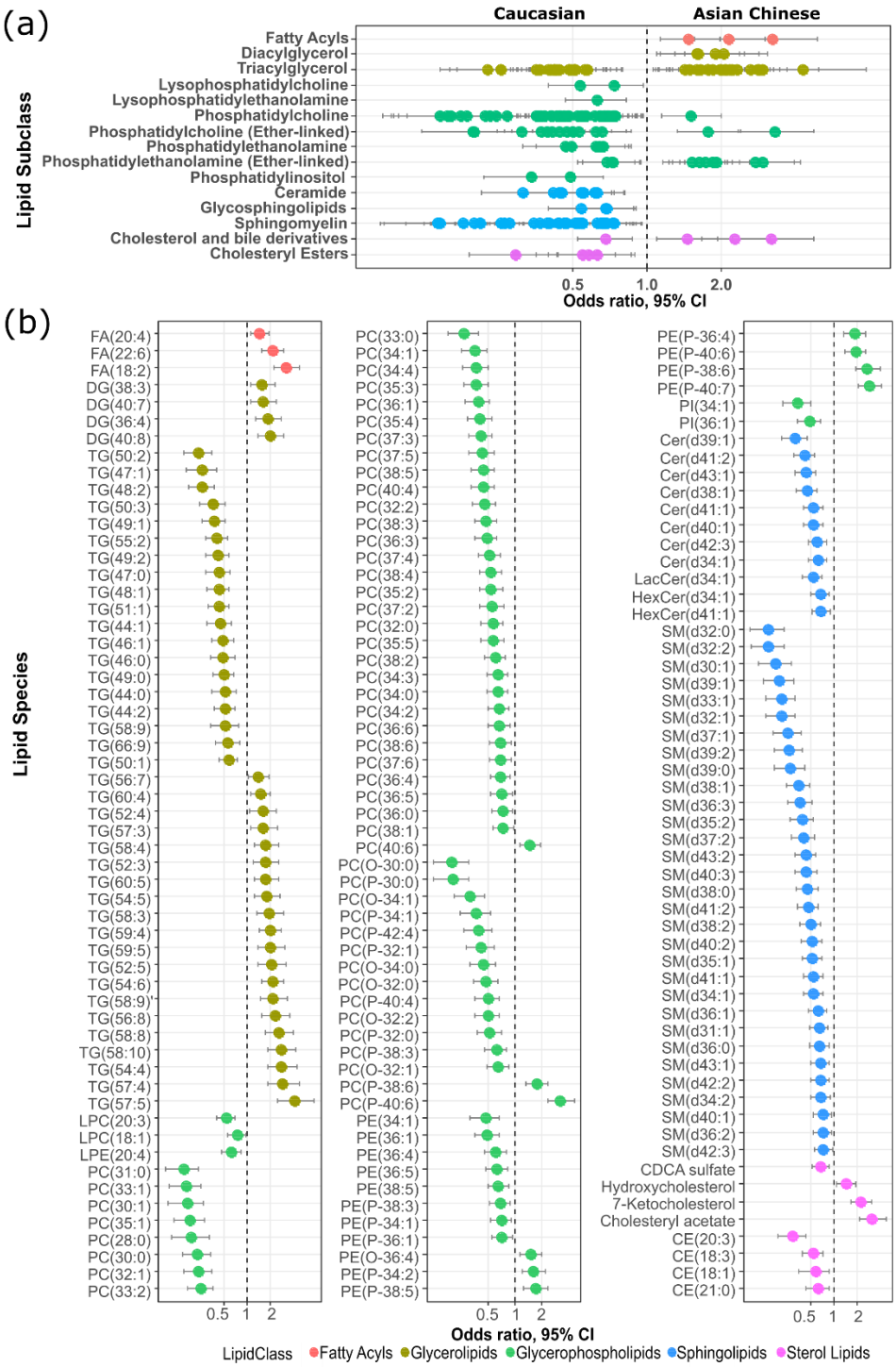

Figure 5.2: Association of lipid profile with ethnicity. Lipids associated with ethnicity at the level of (a) lipid subclasses and (b) individual lipid species following adjustment for age, gender, HDL-C, Insulin, FPG, HbA1c, BMI and %VAT$_{TBF}$. All the displayed lipids have statistically significant p value (BH-corrected p < 0.05). FA: fatty acid; DG: diacylglycerol; TG: triacylglycerol; LPC: lysophosphatidylcholine; LPE: lysophosphatidylethanolamine; PC: phosphatidylcholine; PC(O-/P-): ether-linked (plasmenyl/plasmanyl) PC; PE: phosphatidylethanolamine; PE(O-/P-): ether-linked (plasmenyl/plasmanyl) PE; PI: phosphatidylinositol; Cer: ceradmie; Lac: lactosylceramide; HexCer: glucosylceramide; SM: sphingomyelin; CE: cholesteryl ester; CDCA sulfate: Chenodeoxycholic acid sulfate

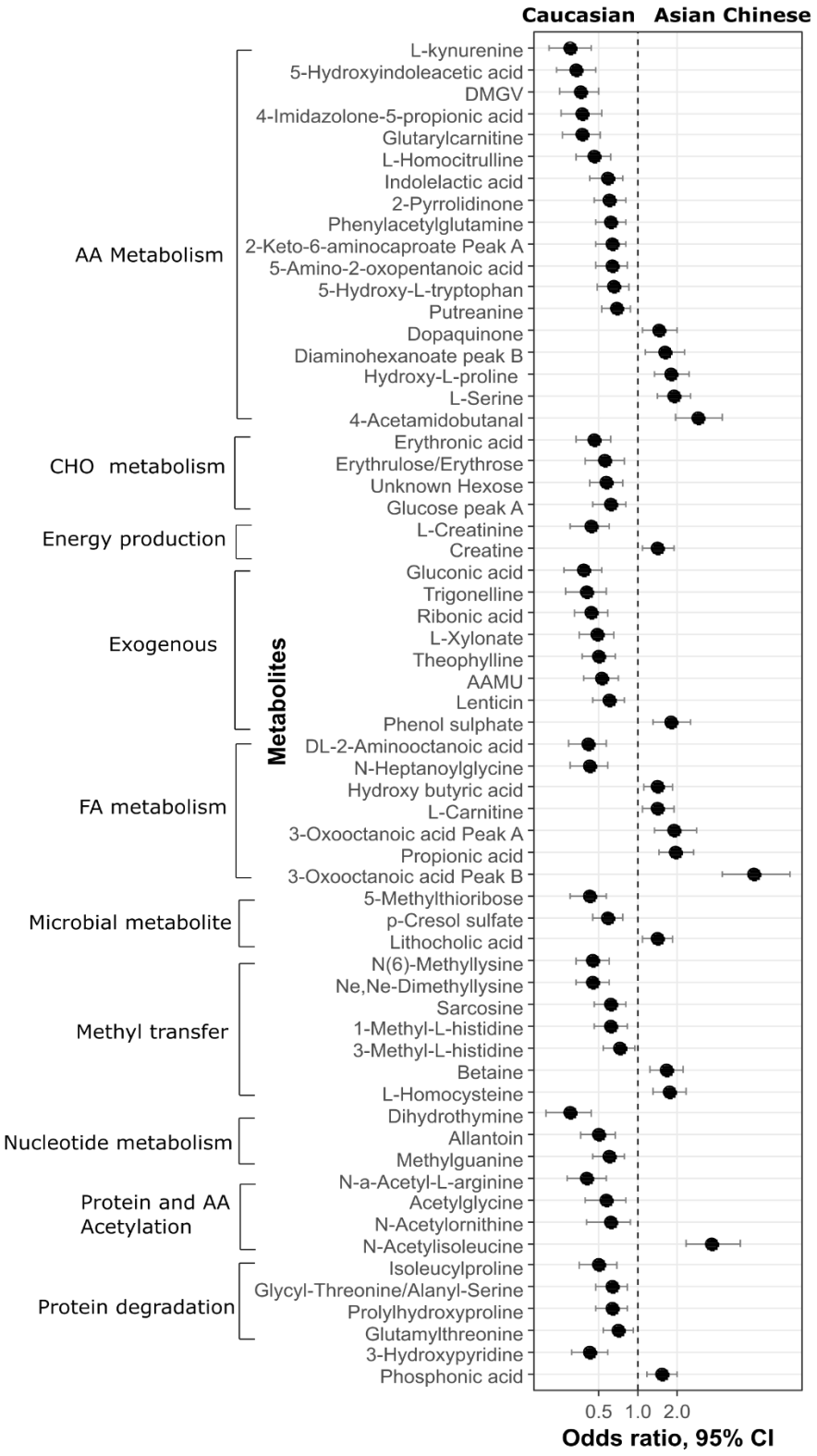

Figure 5.3: Association of polar metabolite profiles with ethnicity. Differentially expressed polar metabolites in Caucasian and Asian, after adjusting for age, gender, HDL-C, Insulin, FPG, HbA_{1c}, BMI and $\%VAT_{TBF}$. All the displayed metabolites have statistically significant p value (BH-corrected p < 0.05). AAMU: 5-Acetylamino-6-amino-3-methyluracil; DMGV: (alpha-keto-dimethyl-delta-N,N-Dimethylguanidynol) valeric acid

5.3.2 Ethnicity-specific metabolomic signatures of FPG and $\%VAT_{TBF}$

Metabolic features associated with FPG that are common to both ethnic groups or unique to each ethnic group were summarised in **Figure 5.4a and Appendix: Table 9.8**. After adjusting for gender, age and BMI, FPG in Caucasians was associated with 40 non-redundant features yielding 33 identified metabolites, including positive correlations with 4 DG species, 17 TGs, 2 ether-linked PCs, 4 ether-linked PEs, 3 PCs, 2 hexoses (both likely to be glucose peaks as confirmed by internal standard, **Appendix: Figure 9.5**) and erythronic acid. The phospholipids and ether-linked phospholipids notably contained an arachidonic acyl chain n20:4 (confirmed with MS^2 spectral data). The strongest marker for FPG other than the MS-measured glucose (in terms of having the lowest p-value) in Caucasians was DG(38:5) (adjusted beta-coefficient = 0.29 [95% CI 0.16-0.42], p = 3.00E-05). FPG in Asian Chinese was associated with 110 non-redundant features yielding 101 identified metabolites, including positive correlations with 6 ceramides, 10 DGs, 59 TGs, 4 PCs, 3 PEs, 2 hexoses (MS-measured glucose) and an unknown hexose, and negative correlations with 2 CE, 2 FFAs, 8 SMs, 2 ether-linked PCs, HexCer(d42:2) and L-acetylcarnitine. The strongest marker was TG(54:4) (0.28 [95% CI 0.18-0.38], p = 2.02E-07). Only MS-measured glucose, 4 DG species, 16 TG species plus 2 unknowns were common makers for FPG in both ethnic groups (19% overlapped), and many of them contained an oleate moiety (**Figure 5.4a**).

$\%VAT_{TBF}$ was associated with many lipid species in both Caucasians and Asian Chinese, whilst no polar metabolites measured by HILIC remained significantly associated with $\%VAT_{TBF}$ after multiple testing correction (BH-corrected $p<0.05$). The $\%VAT_{TBF}$-associated lipid features, either unique to each, or common to both

ethnic groups, have been provided in **Figure 5.4b and Appendix: Table 9.9**. Independent of gender, age and BMI, %VAT_{TBF} in Caucasians was associated with 85 non-redundant features (96% identified), including positive correlations with Cer(d40:0), SM(d36:0), 8 DGs, 4 PCs, 4 PEs and 60 TGs, and negative correlations with 2 ether-linked PCs and 2 SMs. The most strongly associated lipid species based on p-value was TG(56:2) (0.3 [95% CI 0.2-0.4], p = 8.25E-09). %VAT_{TBF} in Asian Chinese was associated with 119 non-redundant features (92% identified), including positive correlations with PC(38:3), SM(d36:0), SM(d40:0), 4 ceramides, 10 DGs, 8 PEs and 59 TGs, and negative correlations with PC(38:7), PE(P-36:1), 2 CEs, 13 ether-linked PCs and 9 SMs, with TG(58:3) being the most significantly correlated marker (0.25 [95% CI 0.17-0.34], p = 2.34E-08). 67 lipid species were common markers for %VAT_{TBF} in both ethnic groups, encompassing lipid species of ceramide, SM, PC, PEs, ether-linked PCs, DGs and TGs (51.8% overlapped), and many of them notably contained a linoleate moiety (**Figure 5.4b**).

Among the 105 variables associated with either FPG or %VAT_{TBF} in Caucasians, 20 were common markers for both FPG and %VAT_{TBF} (19% overlap) after adjusting for age, gender and BMI. These included DG(36:2), DG(38:2) and 17 TG species plus one unknown lipid species (*m/z* = 933.8665) **(Figure 5.5a and Appendix: Table 9.10)**. Whereas in Asian Chinese, 69 out of 160 variables associated with either trait were common markers for FPG and %VAT_{TBF} (43.9% overlap) independent of age, gender and BMI, including CE(22:4), Cer(d40:1), Cer(d42:1), PE(36:1), PE(36:2), SM(d42:3), SM(d43:2), SM(t34:1) in addition to 10 DG and 50 TG species plus one unknown lipid species (*m/z* = 924.8006) **(Figure 5.5b and Appendix: Table 9.11)**.

(a) FPG

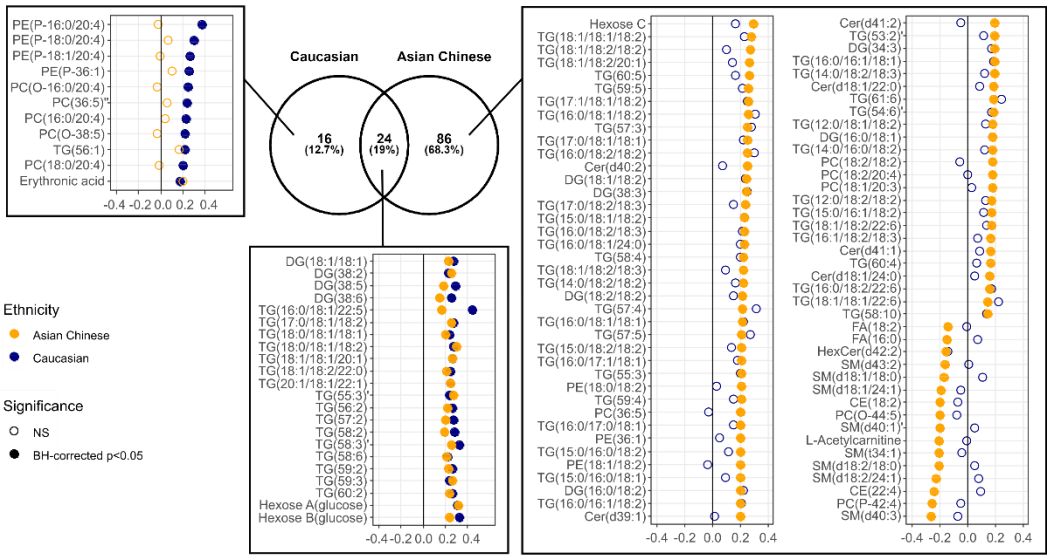

(b) %VAT$_{TBF}$

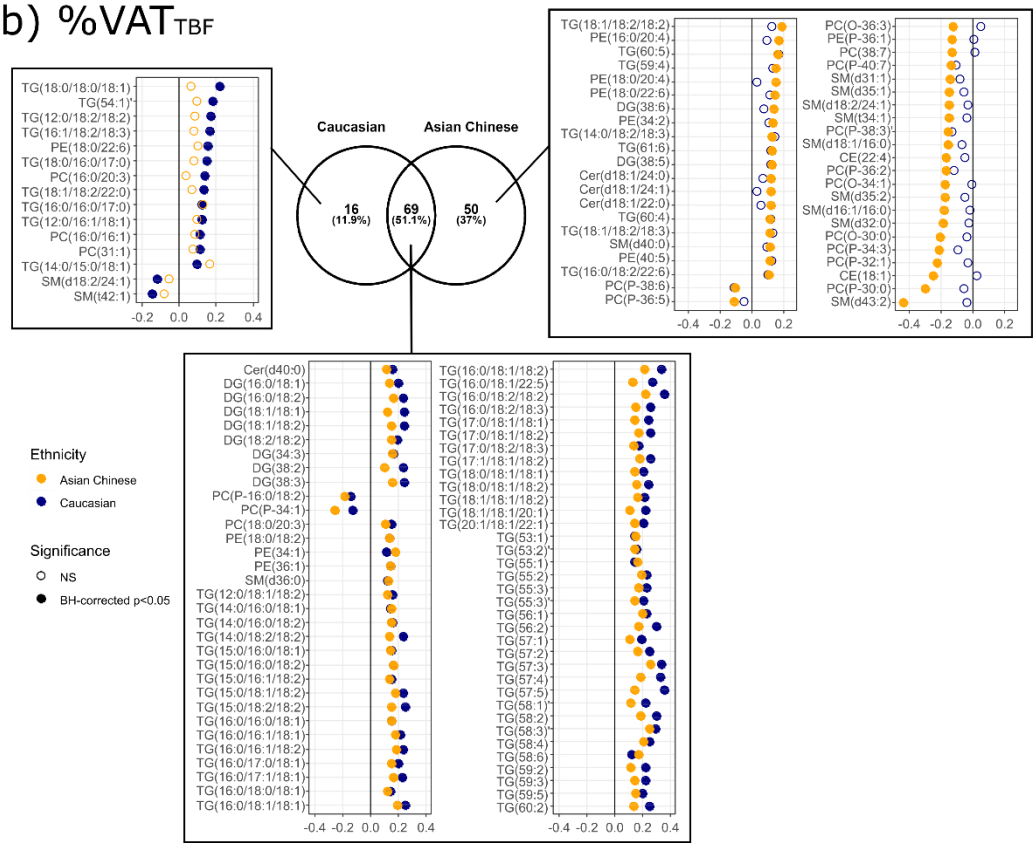

Figure 5.4: Metabolites significantly associated with FPG and %VAT$_{TBF}$, after adjusting for gender, age and BMI. The Venn diagram showed the number of variables common or unique to Caucasian and Asian Chinese, including both annotated metabolites and unknowns; the adjusted beta-coefficient of every annotated metabolites in Caucasian (blue) and Asian Chinese (orange), were displayed in the coefficient plot.

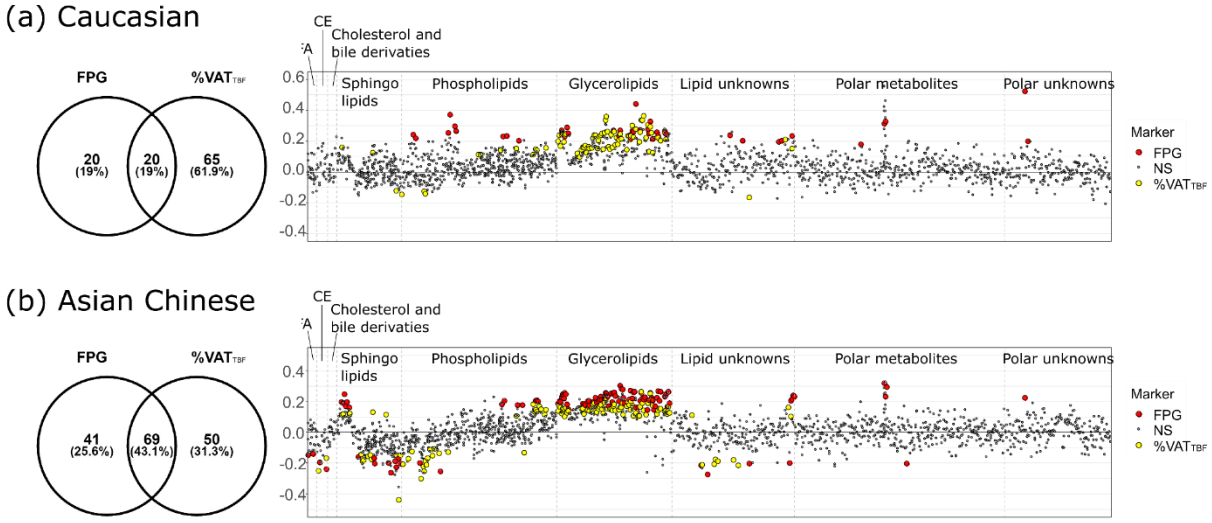

Figure 5.5: Overlaid metabolomic signature for FPG and %VAT$_{TBF}$ in Caucasians and Asian Chinese. The Venn diagram showed the number of variables common or unique to FPG and %VAT$_{TBF}$, including both annotated metabolites and unknowns; the overlaid coefficient plot on the right displayed adjusted beta-coefficient of all metabolic features, with those being significantly associated with FPG (red) or VA (yellow) highlighted (BH-corrected p < 0.05). NS: non-significant.

5.3.3 Predicting FPG state using the metabolomic signature

We have identified individual metabolites significantly associated with FPG and/or %VAT$_{TBF}$. Next, a random forest model for predicting IFG state from these metabolites as a set of predictors was constructed. To do so, we combined the list of metabolites associated with FPG or %VAT$_{TBF}$ from the previous step but removed the two MS-measured glucose features (i.e. 160-2=158 variables for Asian Chinese and 105-2=103 variables for Caucasians), and built RF based on 100 top-ranked metabolites for each ethnicity (**Appendix: Table 9.10-9.11**). The reason for excluding the MS-measured glucose from the re-stratification step is that it is of interest to determine the metabotype using biologically relevant information other than glucose itself, and including glucose may confound the variable selection and sample re-stratification. The RF models achieved a prediction accuracy with an area under receiver operating characteristic (ROC)

curve of 0.79 (95% CI 0.704-0.882) in Caucasians and 0.76 (95% CI 0.646-0.847) in Asian Chinese **(Appendix: Figure 9.6)**. These models were then used to define mFPG state, the predicted FPG state based on the metabolomic signature.

5.3.4 Characterisation of clinical profiles of the metabolic FPG state

After establishing a model to predict metabolic FPG state using the metabolomic signature (i.e. designated as either mNFG or mIFG), participants were stratified into 4 groups for each ethnicity: 2 had predicted FPG states concordant to the actual state (NFG-mNFG, IFG-mIGF), and 2 had a discordant metabolic FPG state from the actual state (NFG-mIFG, IFG-mNFG). Seventy four percent of NFG and 77% of IFG individuals had a concordant predicted FPG state (i.e. NFG-mNFG and IFG-mIFG, respectively) in Caucasian; 26% of NFG individuals were predicted to be mIFG (NFG-mIFG) and 23% of IFG individuals were predicted as mNFG (IFG-mNFG). In Asian Chinese, 70% of NFG and 74% of IFG individuals were predicted to have an mNFG and mIFG state, respectively; 30% of NFG individuals had an mIFG state and 26% of IFG individuals had an mNFG state.

The clinical and anthropometric profiles between these newly designated groups were then compared using a multivariate PLS-DA or univariate t-test approach. For the PLS-DA model, we first constructed and compared models using 21 clinical and anthropometric measurements as explanatory variables and mNFG vs mIFG as predicted by the metabolomic signature or NFG vs IFG as stratified by ADA FPG criteria (**Figure 5.6**). Both models of mNFG vs mIFG and NFG vs IFG were robust and revealed good separation between sample groups (mNFG vs mIFG model, R2Y = 0.428, Q2=0.384 for Caucasians and R2Y = 0.284, Q2=0.254 for Asian Chinese; NFG vs IFG model, R2Y = 0.316, Q2=0.282 for Caucasians and R2Y = 0.22, Q2=0.179 for Asian Chinese), with mNFG vs mIFG

model outperforming NFG vs IFG in both ethnicities (**Figure 5.6**). This highlighted the clinical profile was correlated better with the predicted FPG state by metabolomic than the actual FPG state.

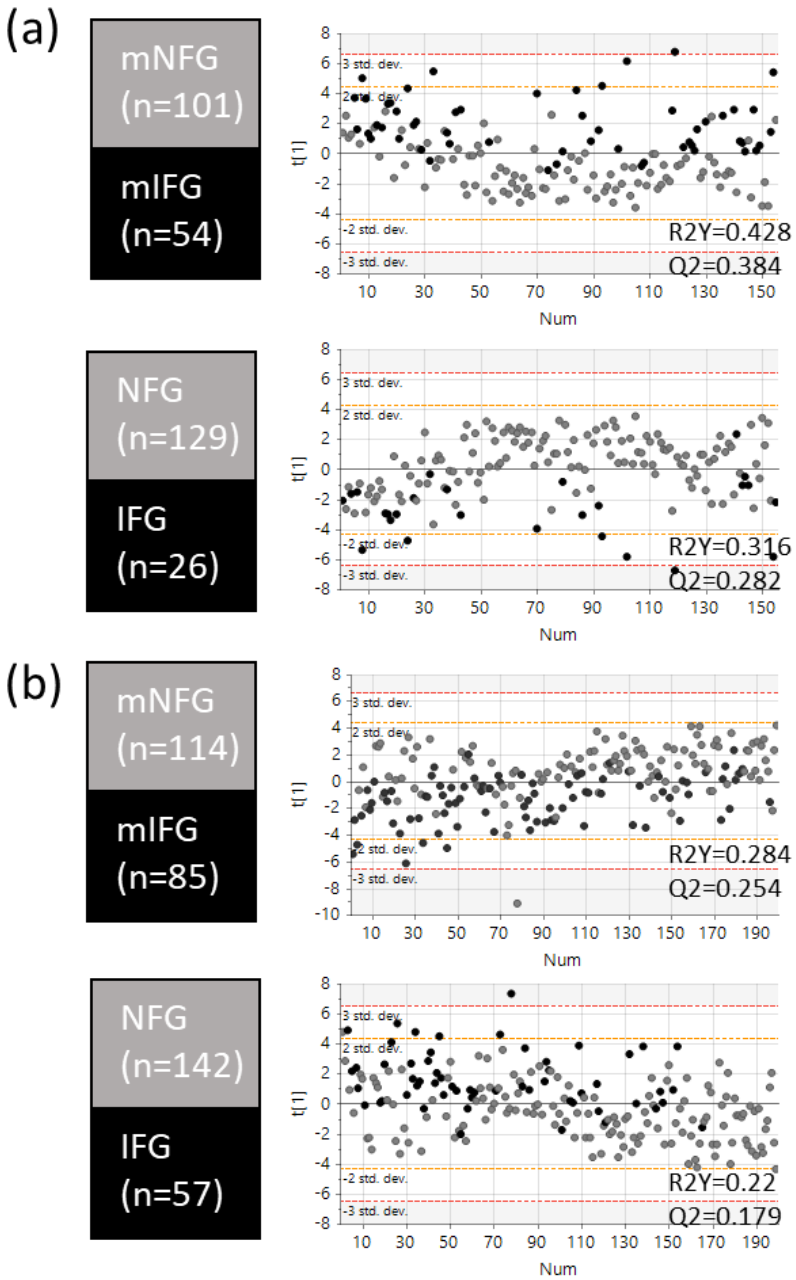

Figure 5.6: PLS-DA model based on clinical variables associated with cardiometabolic risks as independent variables. Score plots and model performances for PLS-DA models of NFG vs IFG or mNFG vs mIFG in (a) Caucasian and (b) Asian Chinese. Clinical variables including HbA_{1c}, HOMA2-IR, BMI, age, waist-to-hip ratio, SBP, DBP, ALT, AST, ALP, GGT, total cholesterol, HDL-C, total TG, LDL-C, amylin, C-Peptide, GIP, GLP-1, glucagon, insulin were use as x-variable in the PLS-DA model. Red and yellow dash line represent 3 and 2 standard deviation boundary of the score plot, respectively.

From the 4-group PLS-DA analysis, component 1 clearly separated NFG-mNFG from all 3 IFG groups (NFG-mIFG, IFG-mNFG and IFG-mIFG) in both ethnic groups, and the centre of NFG-mIFG was projected even closer to IFG-mIFG than to NFG-mNFG **(Figure 5.7)**. These results collectively indicated a similar clinical risk profile of individuals delineated by the metabolic FPG state.

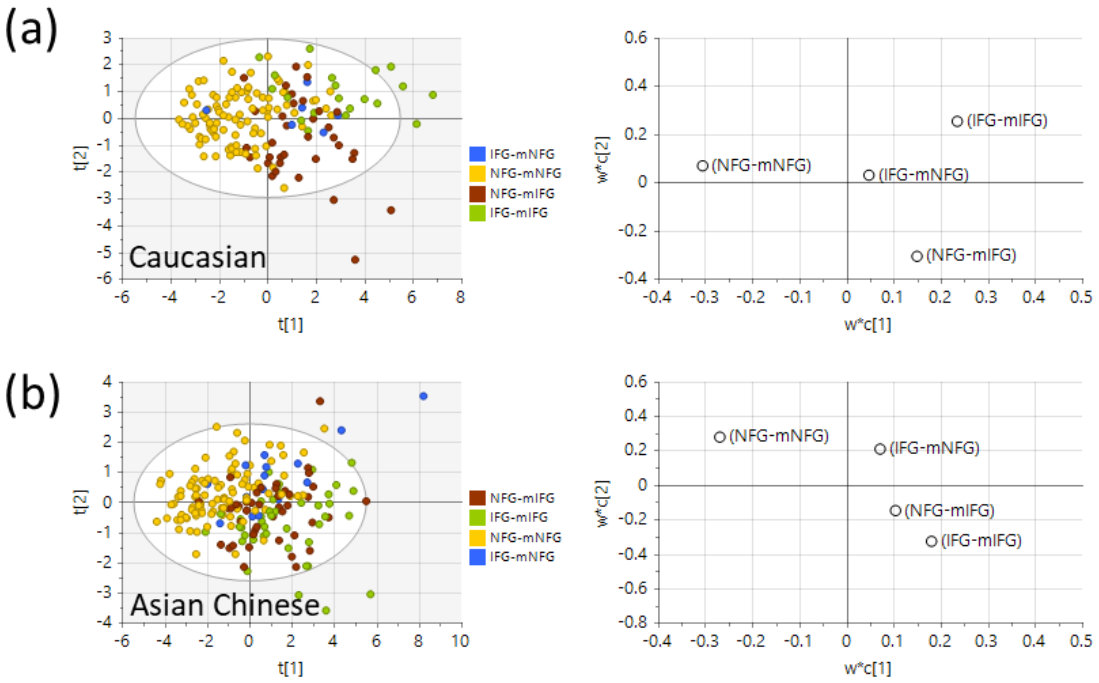

Figure 5.7: PLS-DA model based on parameters associated with cardiometabolic risks as independent variables. Score plots and loading plots with projected centre from each group for PLS-DA of four level analysis (NFG-mNFG, NFG-mIFG, IFG-mNFG and IFG-mIFG) in (a) Caucasian and (b) Asian Chinese.

Comparison of clinical and anthropometric measurements associated with cardiometabolic risk using a univariate approach based on this new stratification revealed a worse cardiometabolic risk profile of NFG-mIFG individuals compared to the NFG-mNFG, despite all currently having a 'normal' fasting glucose level. This included higher adiposity-related parameters (BMI, waist-to-hip ratio), liver enzyme (ALP, GGT), total cholesterol, total TG, LDL-C, glucoregulatory hormones (amylin, C-peptide, GLP-1, glucagon, insulin), and lower HDL-C in Caucasians ($p < 0.05$) **(Figure 5.8a)**. In Asian Chinese, NFG-mIFG individuals

were characterised by higher blood pressure (SBP, DBP), adiposity-related parameters (BMI, waist-to-hip ratio), liver enzymes (ALT, AST, GGT), total cholesterol, total TG, glucoregulatory hormones (amylin, C-peptide, insulin), and lower HDL-C than NFG-mNFG individuals ($p < 0.05$) **(Figure 5.8b)**. Conversely, Caucasian IFG-mNFG individuals tended to be younger and had lower total TG, and Asian Chinese IFG-mNFG individuals had lower total TG and higher HDL-C than their IFG-mIFG counterparts ($p < 0.05$).

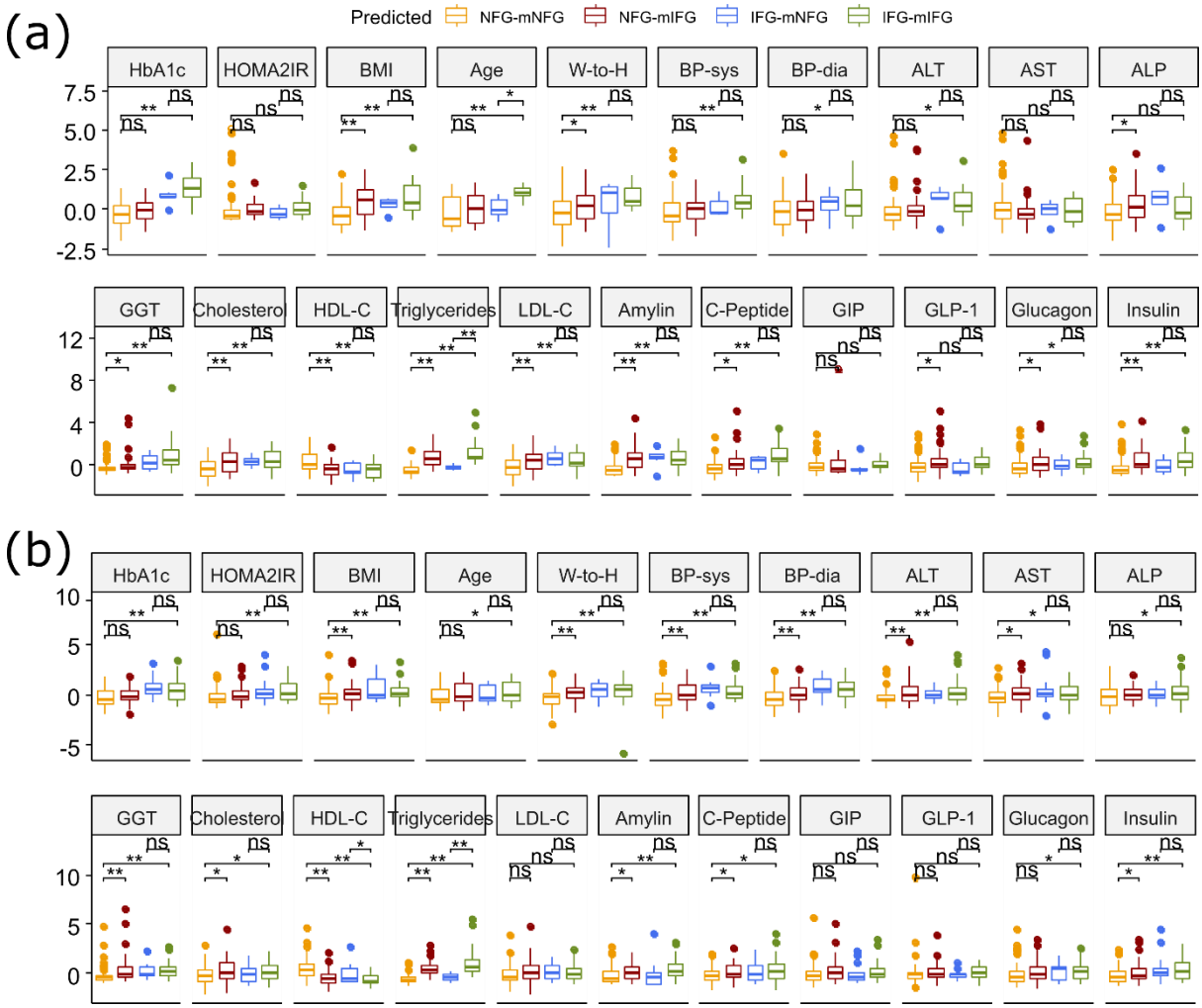

Figure 5.8: Clinical characterisation the newly assigned metabotype groups. Boxplot showed different levels of parameters associated with cardiometabolic health among healthy (NFG-mNFG), normoglycaemic with "prediabetic" metabolomic signature (NFG-mIFG), impaired fasting glucose with normoglycaemic metabolomic signature (IFG-mNFG), and prediabetic (IFG-mIFG) individual in (a) Caucasian and (b) Asian Chinese. T-test was carried out on each pair of NFG-mNFG vs NFG-mIFG, IFG-mNFG vs IFG-mIFG, NFG-mNFG vs IFG-mIFG (*p<0.05, **p<0.01, ns: p>0.05). All measured values were scaled to mean = 0, standard deviation = 1 (y-axis).

5.4 Discussion

T2D is a progressive disease that may be prevented if at-risk individuals can be identified before disease onset and managed through lifestyle and dietary intervention [428]. As such, prediabetes has attracted considerable attention as it represents a stage where individuals have a suboptimal glycaemic profile and a higher risk of proceeding to T2D onset [429]. Metabolite markers identified using metabolomics may provide insights into the metabolic perturbation contributing to T2D development and help to identify at-risk individuals. Notably most metabolomics studies screening for biomarkers have focused on a single population, however ethnicity is also a key risk factor for T2D that requires investigation. The greater susceptibility of specific populations to T2D with higher propensity of visceral fat deposition suggests metabolic alterations contributing to T2D development are likely to differ between ethnicities [430]. Our study provides compelling evidence for a highly discriminatory fasting plasma metabolome between Asian Chinese and Caucasians. The major differences included a number of AA-related metabolites involved in tryptophan and histidine metabolism, methyl transfer pathway, sugar derivatives, gut microbial metabolites and exogenous compounds, as well as lipid species encompassing 15 lipid subclasses. These results highlighted the need for investigating metabolic alterations and biomarkers associated with T2D development in each ethnicity separately. Subsequently, the ethnicity-stratified analysis showed that FPG was associated with a wide range of lipid species and fewer polar metabolites in both ethnic groups, emphasising a prominent shift in lipid metabolism associated with T2D development. Common markers for FPG across both ethnic groups included DG and TG species and the MS-measured glucose. The association between

elevated glycerolipids and development of T2D has been well documented, and our results are in line with other metabolomics studies [167, 189, 431]. FPG was additionally associated with 3 lipid classes and erythronic acid in Caucasian, and 8 lipid classes, acetylcarnitine and an unknown hexose in Asian Chinese. These associations were unique to each ethnic group and might underlie different metabolic perturbation contributing to development of dysglycaemia. Notably, more lipid markers remained significantly associated with FPG in Asian Chinese after adjustment for age, gender and BMI than in Caucasians, and a larger portion of markers for FPG overlapped with those for $\%VAT_{TBF}$ in Asian Chinese (43.9% overlap) than in Caucasians (19% overlap), suggesting visceral adiposity was more closely related to the development of dysglycaemia in Asian Chinese independent of total adiposity.

With limited studies investigating metabolic alterations associate with VAT deposition, we here provided evidence demonstrating visceral adiposity profoundly affected lipid metabolism whilst changes of polar metabolites were only weakly associated (i.e. no metabolites passed the significance level after multiple testing correction). 85 lipid species belonging to 7 classes were common $\%VAT_{TBF}$ markers to both ethnic groups, and $\%VAT_{TBF}$ was specifically associated with 2 additional lipid classes in Asian Chinese. Both ethnic groups had a TG species (TG(58:2) for Caucasians and TG(58:3) for Asian Chinese) as the most significant marker (i.e. lowest p-value) correlated with $\%VAT_{TBF}$. The similar pattern of lipid profiles associated with $\%VAT_{TBF}$ across the 2 ethnic groups suggested a homogenous metabolic adaptation to visceral adiposity irrespective of ethnic background.

Dysregulation of lipid metabolism is a characteristic of T2D and suggested to be a metabolic event prior to the onset of dysglycaemia [166]. Meikle et al. have comprehensively measured the lipid profile associated with prevalent prediabetes and T2D [167]. Many of their observations were replicated in our Asian Chinese group, including association with glycerolipids, ceramides, PEs and ether-linked PCs. Ceramides have been implicated in insulin resistance (IR) as mediators of lipotoxicity and strong associations between high levels of plasma ceramides and reduced insulin sensitivity, prediabetes (glucose intolerance as determined by oral glucose tolerance test) and T2D have been previously reported [238]. In addition, we detected an inverse association between levels of FPG and SMs and hexosylceramide. In a previous cross-sectional study comprising 111 Asian participants, levels of SMs were also markedly lower in IFG/T2D individuals than controls [184]. SMs also inversely correlated with T2D risk in prospective studies including the European Prospective Investigation into Cancer and Nutrition (EPIC)-Potsdam and PREDIMED trials [186, 189]. The positive correlation of ceramides concomitant with negative correlation of SM species and hexosylceramide with FPG observed in the present study reinforced a role of altered sphingolipid metabolism in T2D pathogenesis. Interestingly, $\%VAT_{TBF}$ also correlated with several ceramide species and dihydroceramide Cer(d40:0), and negatively correlated with SM species in Asian Chinese, highlighting a link between visceral adiposity and altered sphingolipid metabolism. Remarkably, all ceramide species correlated with $\%VAT_{TBF}$ observed in our study contained a very long acyl chain (C22:0, C24:0 and C24:1), all of which are likely to be products of CerS2, a ceramide synthase showing substrate specificity for longer acyl chain species which is predominantly expressed in liver [390, 391].

Collectively, visceral adiposity might be associated with an altered sphingolipid metabolism that might partly contribute to hepatic IR and confer early dysglycaemia in Asian Chinese. An altered sphingolipid profile was also associated with visceral adiposity but not FPG in Caucasians, suggesting an altered sphingolipid metabolism was a consistent trait for increased VAT deposition across both ethnicities but not directly implicated in early dysglycaemia in Caucasians.

Our results confirmed a metabolic shift in the phospholipid profile implicated in T2D development [432]. However, the molecular makeup segregated between the two ethnic groups. FPG positively correlated with a number of PCs in both ethnic groups, and additionally correlated with PEs in Asian Chinese. We also observed elevated PCs and PEs associated with $\%VAT_{TBF}$ in both ethnic groups. The association between PEs and prediabetes/T2D was highlighted in Meikle's study as well as in another study conducted in a Chinese cohort [167, 190]. Both PEs and PCs were also reported to be associated with incident T2D [186, 189]. A concordant alteration of phospholipids and glycerolipids has been suggested to relate to hypertriglyceridaemia and increased VLDL production [191].

We have intriguingly observed an inverse correlation of FA(16:0) and FA(18:2) with FPG in Asian Chinese, as opposed to several studies reporting associations of elevated FFA with IR and development of T2D [184, 222, 433]. One explanation might be an increased uptake and utilisation of FFA by the liver to fuel TG re-esterification and VLDL secretion [434, 435]. In fact, a recent study has shown a U-shaped instead of linear relationship between plasma FFA and insulin resistance in Chinese, and this trend was more prominent in non-obese individuals [436]. As elevated plasma FFA is a characteristic of adipose tissue IR

[437], our data did not support adipose tissue IR as a primary factor associated with early dysglycaemia in our Asian Chinese cohort; instead, hepatic IR or hyperinsulinaemia leading to increased hepatic uptake and utilisation of FFA might explain such an inverse association. In addition, we observed an inverse correlation between acetylcarnitine and FPG in Asian Chinese. Acetylcarnitine is the product of complete beta-oxidation as well as a substrate for lipogenesis, and an inverse correlation may reflect impairment in complete FAO or an increased utilisation for lipogenesis. Our method did not detect other acylcarnitines, thus it is difficult to conclude whether such an inverse correlation was due to incomplete FAO. Profiling of acylcarnitines with a targeted approach in the future may help to explain this association.

We observed a negative correlation between FPG and an ether-linked PC in Asian Chinese, consistent with other reports of an inverse association of this lipid class with prevalent and incident T2D, obesity and IR [167, 186, 189, 209]. In addition, an inverse association between ether-linked PC and $\%VAT_{TBF}$ was observed in both ethnic groups, in good agreement with a previous finding of an ether lipid signature characteristic for VAT deposition [266]. Little is known about the biological role of ether-linked PC despite accumulating evidence showing its association with metabolic health. It might act as a free radical scavenger and protect against LDL oxidation [196, 198]. In contrast to Asian Chinese, a mixture of ether-linked PC and ether-linked PE positively correlated with FPG in Caucasians, all of which contained an arachidonic acyl chain. Ether-linked phospholipids are also sources of arachidonic acid and arachidonic acid is a precursor of the production of pro-inflammatory eicosanoids [198, 438]. Our result suggested an elevated FPG in Caucasians was concurrent with an increased lipid

reservoir for secondary messengers with pro-inflammatory potential, which might accelerate insulin resistance and the development of T2D.

Contrary to several studies demonstrating a positive association between CE and prediabetes/T2D, we have unexpectedly found an inverse association. However, the PREDIMED trial has reported an inverse association between CEs and risks of T2D and CVD [189, 439], and the authors linked this observation to the "atherogenic lipoprotein phenotype" (characterised by increasing atypically small and dense LDL, usually accompanied by elevated plasma TG and reduced HDL [440]). The small and dense LDL particles are packed with TG instead of CEs [441], and are suggested to be preferentially cleared from plasma via a receptor-independent pathway and therefore exhibit enhanced atherogenic potential [442]. A previous intervention study has shown a high CHO diet is a primary dietary factor driving the atherogenic lipoprotein pattern whereas a restricted CHO diet attenuated this expression [443]. Without dietary record in the present study it is hard to comment beyond this point; but considering the cultural background of Asian Chinese tending to consume large amount of refined grain (e.g. rice), our interesting finding prompts the hypothesis that the association between CE and risk factors for T2D development may be interrelated with diet.

In addition to the MS-measured glucose itself, FPG was correlated with erythronic acid in Caucasians and an unknown hexose in Asian Chinese. Erythronic acid is a novel hitherto-unreported marker that will require further validation, whereas increased hexose (other than glucose) associated with prediabetes and T2D was in line with the others [184, 223].

Taking the metabolomic signature jointly determined by $\%VAT_{TBF}$ - and FPG-associated metabolomic profiles, we were able to create a novel stratification with

a subset of normoglycaemic individuals whose metabolomic signature resembled that of prediabetes (termed NFG-mIFG). In both ethnicities they were characterised by higher BMI and W-to-H ratio, and worse lipid (higher total cholesterol and TG, lower HDL-C), liver enzyme and hormone (amylin, C-peptide and insulin) profiles compared to NFG-mNFG counterparts. Of particular interest were the higher liver enzymes, which are indicators of inflamed or damaged liver cells. The liver is a key organ in the regulation of energy homeostasis and metabolism, and is proposed as the primary site affected by excess VAT deposition [409]. Hepatic IR may result from release by VAT into the portal vein of lipolytic products such as FFA and adipokines, as well as inflammatory cytokines by infiltrated macrophages [444]. Importantly, the multivariate statistical modelling revealed improved discrimination between mNFG and mIFG metabotypes than clinical NFG and IFG classification, suggesting a metabolomics-derived signature was more reflective of the integrated changes across a broad range of cardiometabolic risk factors. NFG-mIFG individuals maybe more susceptible to rapid development of T2D than NFG-mNFG despite current normoglycaemia. Validation of these predictions are required through a longitudinal follow up study, or retrospectively on already existing longitudinal public datasets.

One strength of our study is the simultaneous measurement of metabolomic profiles from two co-located ethnic groups with the same extraction protocol and analytical platform, allowing direct comparison whilst minimising environmental confounding factors to inform ethnicity-specific changes in metabolism associated with T2D development. The use of unbiased, highly sensitive and complementary methods enabled a more holistic view of metabolic perturbation

associated with increased visceral adiposity and FPG. In addition, we have utilised the metabolomic signature characteristics to develop a possible risk prediction of T2D development, identifying individuals with a worse cardiometabolic profile despite having normoglycaemia. Limitations include the nature of cross-sectional studies which precludes conclusion on causality and requires follow-up to confirm our findings. In spite of a wide range of metabolites and lipids measured by untargeted metabolomics, this approach may not be optimal if a particular class of metabolites/lipids is of interest, hence it is inevitable that some of the findings by others using metabolite class-optimised targeted approaches such as the analysis for acylcarnitines were not observed in our study.

5.5 Conclusion

Our study has revealed a broad spectrum of lipid species associated with FPG and $\%VAT_{TBF}$ in both Caucasian and Asian Chinese independent of age, gender and BMI. We have shown plasma metabolomic profile to be profoundly influenced by ethnicity and are the first to compare an ethnicity-specific signature for T2D risk factors including FPG and visceral adiposity. A similar signature for $\%VAT_{TBF}$ across both ethnicities but a very different signature for FPG observed in the present study highlighted homogeneous metabolic adaptations and alterations in response to VAT deposition, yet a distinct underlying pathogenesis of dysglycaemia. Predictive modelling using the joint metabolomic signature of FPG and $\%VAT_{TBF}$ has identified a subset of individuals with worse cardiometabolic risk despite current healthy normoglycaemia. This novel approach of re-stratification using the metabolomic signature aids early identification of those at-

risk of T2D. This modelling approach could be applied to a wide range of diseases.

5.6 Contributions and acknowledgements

This Chapter has been submitted to *BMC Nutrition & Metabolism* and is under review.

Zhanxuan E. Wu, Karl Fraser, Marlena C. Kruger, Ivana R. Sequeira, Wilson Yip, Louise W. Lu, Lindsay D. Plank, Rinki Murphy, Garth J.S. Cooper, Jean-Charles Martin, Sally D. Poppitt. “Metabolomic signatures for visceral adiposity and dysglycaemia in Asian Chinese and Caucasian European adults: The cross-sectional TOFI_Asia study”.

Author Contributions:

IRS led the clinical part of this study; IRS, WY and LWL contributed to participants recruitment, sample collection and the clinical data; IRS, WY, LDP and RM contributed to body composition measurement. KF led and supervised the metabolomics part of this study. ZEW conducted sample extraction, metabolomics profile acquisition, data analyses and results interpretation. MCK provided supervision. GJSC provided the protocol for sample extraction and advised on results interpretation. JCM advised on the metabolomics data analyses and results interpretation. ZEW drafted the manuscript and coordinated updates following inputs from co-authors. KF, SDP, IRS, JCM, GJSC, LDP and RM critically reviewed and commented on the manuscript. SDP was the principal investigator for the Metabolic Health platform within the National Science Challenge High Value Nutrition (HVN) program, who conceptualised and designed this study. All authors read and approved the final version of the manuscript.

MASSEY UNIVERSITY
TE KUNENGA KI PŪREHUROA
UNIVERSITY OF NEW ZEALAND

GRADUATE RESEARCH SCHOOL

STATEMENT OF CONTRIBUTION
DOCTORATE WITH PUBLICATIONS/MANUSCRIPTS

We, the candidate and the candidate's Primary Supervisor, certify that all co-authors have consented to their work being included in the thesis and they have accepted the candidate's contribution as indicated below in the *Statement of Originality*.

Name of candidate:	Zhanxuan Wu
Name/title of Primary Supervisor:	Marlena Kruger
In which chapter is the manuscript /published work:	5

Please select one of the following three options:

○ The manuscript/published work is published or in press

- Please provide the full reference of the Research Output:

◉ The manuscript is currently under review for publication – please indicate:

- The name of the journal:
BMC Metabolism & Nutrition
- The percentage of the manuscript/published work that was contributed by the candidate: 90
- Describe the contribution that the candidate has made to the manuscript/published work:
Metabolomics data acquisition; metabolomics data analysis; writing; figures & tables generation.

○ It is intended that the manuscript will be published, but it has not yet been submitted to a journal

Candidate's Signature:	Zhanxuan Wu Digitally signed by Zhanxuan Wu Date: 2020.08.31 15:38:27 +1200
Date:	31-Aug-2020
Primary Supervisor's Signature:	Marlena Kruger Digitally signed by Marlena Kruger DN: cn=Marlena Kruger, c=NZ, o=Massey University, email=m.c.kruger@massey.ac.nz Date: 2020.09.01 08:44:08 +1200
Date:	1/9/2020

This form should appear at the end of each thesis chapter/section/appendix submitted as a manuscript/ publication or collected as an appendix at the end of the thesis.

GRS Version 5 – 13 December 2019
DRC 19/09/10

6. Biomarkers for ectopic deposition in Asian Chinese and Caucasian females: the TOFI_Asia study

This chapter sought to identify plasma metabolite markers that are predictive of the level of ectopic fat deposition in the liver, pancreas and visceral site which are otherwise expensive to measure. This chapter also compared the use of candidate metabolite markers for the prediction of ectopic fat with the use of a range of clinical measurements such as blood pressure, FPG and the lipid profile, and have demonstrated the potential value and robustness of measuring a handful of metabolites to estimate the level of ectopic fat deposition.

Abstract

Excess visceral obesity and ectopic organ fat is associated with increased risk of cardiometabolic disease. However, circulating markers for early detection of ectopic fat, particularly pancreas and liver, are lacking. Lipid storage in pancreas, liver, abdominal subcutaneous adipose tissue (SAT) and visceral adipose tissue (VAT) from 68 healthy or pre-diabetic Caucasian and Chinese women enrolled in the TOFI_Asia study was assessed by magnetic resonance imaging/spectroscopy (MRI/S). Plasma metabolites were measured with untargeted liquid chromatography–mass spectroscopy (LC–MS). Multivariate partial least squares (PLS) regression identified biomarkers of VAT/SAT and ectopic fat; univariate multiple linear regression (MLR) identified individual metabolites associated with VAT/SAT (adjusting for ethnicity and total adiposity), and ectopic fat (adjusting for ethnicity, total adiposity, and VAT/SAT); MLR adjusted for ethnicity identified clinical and anthropometric correlates for each fat depot. PLS identified 56, 64 and 31 metabolites which jointly predicted pancreatic fat (R2Y = 0.81, Q2 = 0.69), liver fat (RY2 = 0.8, Q2 = 0.66) and VAT/SAT ((R2Y = 0.7, Q2 = 0.62) respectively. Among the PLS-identified markers, only bile acid sulfolithocholic acid was significantly associated with pancreatic fat in the MLR, adjusting for ethnicity and adiposity covariates. Dihydrosphingomyelin (dhSM(d36:0)), 3 phosphatidylethanolamines, 5 diacylglycerols (DG) and 40 triacylglycerols (TG) were associated with liver fat independent of covariates. L-cystine, ceramide (Cer(d41:1)), 3 DGs and 20 TGs were associated with VAT/SAT independent of covariates. Notably, comparison with clinical correlates showed better predictivity of ectopic fat by these PLS-identified plasma metabolite markers. Untargeted metabolomics identified biomarkers of visceral

and ectopic fat that improved fat level prediction over clinical markers. Whilst several plasma metabolites associated with liver fat independent of total and visceral adiposity, only bile acid sulfolithocholic acid was an independent plasma marker of pancreas fat.

6.1 Introduction

Although obesity has been long recognised as a risk factor for cardiometabolic disease and subsequent complications [445], individuals within each body mass index (BMI) category show considerable heterogeneity in their cardiometabolic manifestations and clinical risk profiles [28]. Notably specific populations, e.g. South and East Asians, develop type 2 diabetes (T2D) at lower BMI and younger age [25], with risk of T2D increased by even modest weight gain compared to more resilient populations such as Caucasians [68]. One factor purported to drive these risks among individuals with comparable BMI is deposition of visceral and non-adipose ectopic organ fat [88], likely a contributor to ethnicity differences in progression to T2D [34]. Asians have been observed to have greater propensity for abdominal and ectopic fat deposition, compared with other ethnicities [35-37]. Visceral adiposity and ectopic fat are in turn implicated in insulin resistance (IR) and dyslipidaemia [409], and associated with increased risk of metabolic syndrome, T2D and cardiovascular disease (CVD), independent of BMI [446-448].

Despite the important role that it may play, current assessment and accurate quantification of ectopic fat relies on either advanced imaging techniques or histologic examination of biopsied tissue, which are both time consuming and expensive, or invasive. Circulating biomarkers for early detection of visceral adiposity and ectopic fat deposition in key organs of liver and pancreas prior to the onset of metabolic disease are lacking. Notably, the critical importance of identifying such biomarkers has recently been highlighted by Neeland and colleagues in a position statement from the International Atherosclerosis Society

and International Chair on Cardiometabolic Risk Working Group on Visceral Obesity [29].

With advanced metabolomics techniques, comprehensive measurements of plasma small molecules in combination with machine learning approaches may allow identification of novel biomarkers to estimate VAT and organ fat content from a single fasting blood sample. These markers may also reflect perturbed metabolism and point to underpinning mechanisms driving development of poor metabolic health. Systemic metabolomic profiling of non-alcoholic fatty liver disease (NAFLD) has identified biomarker candidates such as taurocholate, glutamyl dipeptides, mannose and lactate, carnitine and several acylcarnitines, FFA, lysophosphatidylcholine, glycerolipids (GL) as markers of NAFLD progression [449]. However, most biomarkers were identified in the context of diagnosed NAFLD cases, whereas biomarkers for early detection of asymptomatic liver fat deposition remain to be determined. Importantly, no circulating biomarkers of pancreas fat have yet been identified. To date only the targeted metabolomics study by Jaghutriz et al., have reported this data, in a study which was unable to identify plasma metabolites that characterised high vs. low pancreatic fat, in a group of prediabetic European Caucasians with impaired glucose tolerance [450]. More studies are required to determine whether markers of pancreatic fat deposition are detectable in circulation.

Our current cross-sectional study explored the relationship between plasma metabolome and fat deposition in the pancreas, liver and visceral sites, assessed by magnetic resonance imaging (MRI) and spectroscopy (MRS), in Caucasian and Chinese participants enrolled in the TOFI Asia study. The goals were firstly to identify candidate metabolite markers that predict pancreas, liver and visceral

fat, and elucidate the associated metabolic changes; and secondly to compare the predictive performance of these metabolite markers with a range of clinical measurements associated with each fat depot identified from the present cohort.

6.2 Materials and methods

6.2.1 Ethical approval

This study received ethical approval from the Health and Disabilities Ethics Committee, Auckland, New Zealand (16/STH/23) and is registered with the Australian New Zealand Clinical Trials Registry ACTRN:12616000362493. All participants provided written informed consent.

6.2.2 Study participants and protocol

This investigation is part of the cross-sectional TOFI_Asia study described elsewhere [422]. Female participants aged 20-70 years, BMI 20-45 kg/m^2, fasting plasma glucose (FPG) ≤ 6.9 mmol/L, who self-reported both parents of same ethnicity (European Caucasian or Asian Chinese) were eligible. Exclusions were significant weight change (>10%) in prior 3 months, bariatric surgery, glucose-related medications, current/prior history of disease including T2D, pregnancy, breastfeeding. Sixty eight female participants (34 Chinese, 34 Caucasian) were enrolled in the study. Fasting venous blood samples were collected in clinic and stored at -80^{o}C for later batch analyses. Total body fat (TBF) was determined by dual-energy X-ray absorptiometry (DXA) (iDXA, GE Healthcare, WI, USA) at the Body Composition Laboratory, University of Auckland. Magnetic resonance imaging (MRI) for pancreas and spectroscopy (MRS) for liver was conducted fasted within 1 week of clinic visit using a 3T Magnetom Skyra Siemens scanner, VE 11A (Erlangen, Germany) at the Centre for Advanced MRI (CAMRI), University of Auckland.

6.2.3 Anthropometric and clinical measurements

Height, weight, waist and hip circumferences, systolic (SBP) and diastolic (DBP) blood pressure were recorded at clinic. Fasting plasma glucose was analysed by hexokinase method, HbA_{1c} by capillary electrophoresis (Cap2FP, IDF, France), liver function tests and lipid profile were analysed using standard clinical methods. Glucoregulatory peptides (insulin, C-peptide, glucagon, amylin, gastric inhibitory peptide (GIP), total glucagon-like peptide-1 (GLP-1)) were analysed using MILLIPLEX®MAP Human Metabolic Hormone Magnetic Bead Panel (Merck, HE, Germany) from BD P800 vacutainers.

6.2.4 Assessment and analysis of body composition for visceral and organ fat

TBF and total body lean (TBL, fat-free soft tissue) mass were obtained from full body DXA scan, measured supine. TBF was expressed as % of total soft tissue mass:

%TBF = TBF mass*100/(TBL mass + TBF mass)

Detailed MRI/MRS methods for abdomen (VAT, SAT), pancreas and liver are described elsewhere [451]. Briefly, the abdominal cavity was scanned in the sagittal direction from diaphragm to pelvis. A 2-point Dixon imaging technique was used for fat-water separation. Three blocks of forty 5-mm axial slices were acquired during an 11-s breath-hold. Pancreas was located, and fourteen axial images of 5-mm thickness acquired. For the MRS scan of liver, a 2*2*2 cm^3 voxel was placed in the right lobe avoiding blood vessels and biliary tree; spectra were obtained in transverse, coronal and sagittal planes +/- water suppression. Fat fraction (FF) map corrected for noise bias at L4-L5 intervertebral disc space was constructed using custom Matlab R2017a software (The Mathworks, Inc., Massachusetts, US), and abdominal adipose tissue from FF map segmented into

VAT and SAT compartments (Image J [452]), multiplied by the slice thickness to obtain fat volume, and VAT/SAT ratio calculated. Pancreatic fat was estimated as mean of 2 candidate pancreas FF maps, with 3 regions of interest (ROIs) head, body, tail [453]. For MRS, area under the curve (AUC) of water and fat peaks from spectra without water suppression were obtained (SIVIC software [454]), and liver fat expressed as % calculated vol/vol of fat and water. Pancreas FF maps from 3 Caucasians contained artefact, and MRS from 1 Caucasian could not be analysed due to inverse spectral signal; hence 65 pancreas, 67 liver fat, and 68 VAT/SAT ratios were analysed.

6.2.5 Metabolomics analysis and data processing

Metabolite extraction, data acquisition and processing of samples from TOFI_Asia cohort have been previously described (Chapter 5). The processed metabolomic profile from samples in this current MRI cohort were isolated to construct a new dataset for statistical analyses. Briefly, metabolites were extracted using a bi-phasic approach and the aqueous and organic phases were analysed separately by two LC–MS platforms using a method published elsewhere [455]. Raw datafiles were converted to mzXML format with the ProteoWizard tool MSconvert (v 3.0.1818 [380]). Data preprocessing, cleaning, normalisation (by LOESS algorithm in the W4M Galaxy environment [381]), feature filtering (% coefficient of variation < 30 in QC) and metabolites annotation were carried out as described in Chapter 5.

6.2.6 Determination and exclusion of biological outliers

A partial least square (PLS) regression model was initially applied to examine the relationship between the level of each fat depot measured by MRI and the plasma metabolome (lipids + polar metabolic features) in the whole MRI cohort. In our

preliminary exploration, a significant PLS model was only observed for VAT/SAT ratio ($p < 0.05$) (**Appendix: Table 9.12**). Examination of residuals suggested the presence of biological outliers (i.e. the relationship between the level of fat depot and the metabolomic profile of these samples did not follow the general pattern of the rest of the cohort) (**Appendix: Figure 9.7**). Exclusion of outliers improved the residual normality (assessed with the Kurtosis test (R v3.5.1)) [456]) and goodness of the PLS model fit, suggesting the poor model performances, particularly of pancreatic fat and liver fat, were driven by these few outliers (**Appendix: Table 9.12**). As such, for the subsequent analysis outliers were excluded (3 samples for pancreatic fat, 0% Caucasian; 5 samples for liver fat, 60% Caucasian; 1 sample for VAT/SAT, 100% Caucasian).

6.2.7 Data analysis

Multivariate methods with Unbiased Variable selection in R (MUVR) [457] were performed on the full metabolome (polar metabolites + lipids) to select important variables associated with pancreatic fat, liver fat, or VAT/SAT (continuous Y variable) in a PLS regression model (R v3.5.1). To ensure the model was not over-fitted before or after variable selection, 100 permutation tests were run on each PLS model with repeated-double cross-validation (PLS-rdCV) built on either full metabolome or MUVR-selected variables (R v3.5.1). Variables selected by MUVR were annotated and redundant chemometric features (e.g. isotopes, multiple adducts) representing the same metabolites were removed to constitute the post-selection data-matrix. Performances of PLS models built on full metabolome vs MUVR post-selection for each fat depot were compared, and coefficients of variables obtained (SIMCA 16, Umeå, Sweden). An optimal number of components were chosen to minimise root the mean square error of

cross-validation (RMSEcv). The prediction accuracy was estimated by Pearson's correlation coefficients (r) calculated between predicted vs measured Y values. To evaluate the predictive power of the set of metabolite markers and for comparison with potential clinical markers (including anthropometric parameters), sigfinicantly associated clinical markers with each fat depot were identified using linear regression (adjusting for ethnicity) and then combined to construct a panel for comparison of predictive power. Performance of PLS models built on (a) the panel of clinical markers, (b) the panel of metabolite markers, and (c) the panel of combined clinical and metabolite markers, were assessed and compared (SIMCA 16).To understand how individual metabolite markers related to each of pancreas, liver and VAT/SAT, multiple linear regression with multiple testing correction (Benjamini Hochberg procedure (BH) [425]) was applied. The association between each fat depot and metabolite markers was corrected for ethnicity (model (M)1), then further for total adiposity-related parameters including BMI and %TBF (M2). For pancreatic and liver fat, the model was further adjusted for VAT/SAT (M3). The statistical workflow is summarised in **Figure 6.1**.

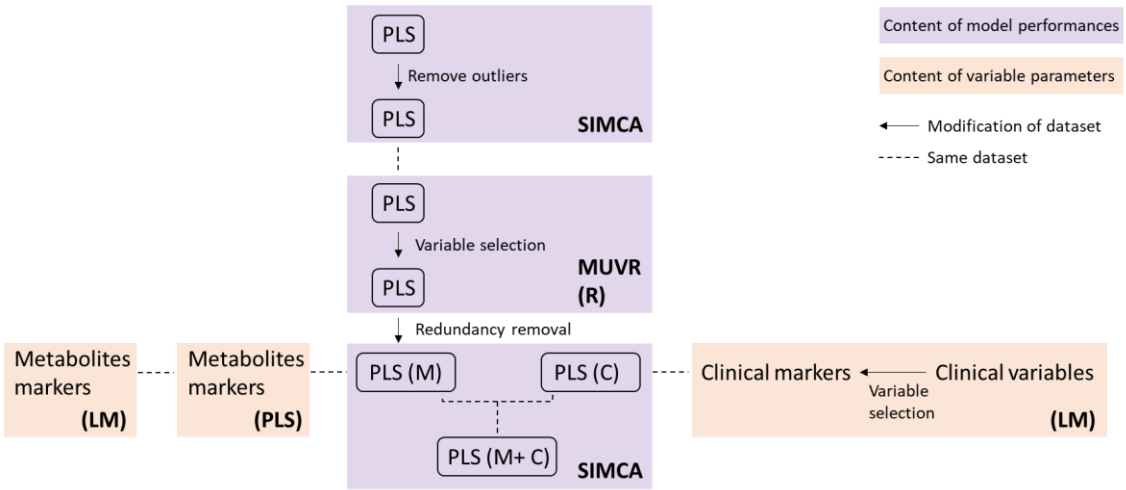

Figure 6.1: Workflow for data analysis in this study. SIMCA: SIMCA software v16; LM: linear regression; PLS: partial least squared regression; MUVR: Unbiased Variable selection in R.

6.3 Results

6.3.1 Identifying novel biomarkers of visceral and organ fat with a multivariate statistical approach

After metabolite selection by MUVR and removal of redundant features, 56 (91% identified), 64 (95% identified), and 31 (100% identified) variables were associated with pancreatic fat, liver fat, and VAT/SAT respectively. Comparison of model performances before and after variable selection are summarised in **Table 6.1**. In all 3 models, variable selection improved goodness of model fit (R2Y) and predictivity (Q2) whilst reducing the number of variables in the model. The fitted Y values using the selected variables were better correlated with the measured Y values (correlation coefficient r) than using the full metabolome. The number of components in each PLS model was selected such that it achieved minimum prediction error, determined by assessing model prediction accuracy and average error (Q2 and RMSEcv) (**Appendix: Figure 9.8**). Overfitting of models was avoided by assessing model performances with rdCV as an alternative validation scheme with 100 permutations (**Appendix: Table 9.13**).

Table 6.1: comparison of model performances of PLS with 7-fold cross-validation between full metabolome vs post-selection.

		Full metabolome					post-selection					
	nVar	nComp	R2Y	Q2	$P_{CV\text{-}ANOVA}$	r	nVar	nComp	R2Y	Q2	$P_{CV\text{-}ANOVA}$	r
Pancreatic fat	910	1	0.39	0.25	2.43E-04	0.63	56	3	0.81	0.69	2.12E-12	0.90
Liver fat	910	1	0.52	0.33	6.86E-06	0.72	64	3	0.80	0.66	6.11E-12	0.89
VAT/SAT	910	1	0.47	0.30	1.32E-05	0.69	31	2	0.70	0.62	1.88E-12	0.83

nVar: number of variables; nComp: number of components; R2Y: goodness of model fit; Q2: predictivity; Pcv-anova: statistical significance of the PLS model; r: Pearson correlation coefficient

Pancreatic fat was associated with sulfolithocholic acid, cholesteryl ester (CE(20:3)), fatty acid (FA(16:1)), LC-MS measured glucose, urea, phosphorylcholine, kynurenic acid, 5 amino acids (AA) and lipid species encompassing 26 glycerolipids (GL), 9 glycerophospholipids (GP) and 3

sphingolipids (SP) (**Figure 6.2a**). These metabolites jointly explained 81% of the variance of pancreatic fat in a 3 component-PLS model and estimated levels of pancreatic fat with a high correlation with measured levels (r = 0.90). Liver fat was associated with homocitrulline, lactate, lactosylceramide (LacCer(d34:1)), dihydrosphingomyelin (dhSM(d36:0)), 5 FAs, 47 GLs and 5 GPs (**Figure 6.2b**). These metabolites jointly explained 80% of the variance of liver fat in a 3 component-PLS model and estimated levels of liver fat with a high correlation with measured levels (r = 0.89). Notably, the TG species associated with liver fat were highly saturated (all containing ≤ 3 unsaturated bonds); among the 27 MS2-annotated TGs, 75% contained at least one C16:0 palmitic acid (PA), while 63% contained at least one C18:1 oleic acid (OA). VAT/SAT was associated with L-cystine, ceramide (Cer(d41:1)), ether linked phosphatidylcholine (PC(O-38:6)), 3 FAs and 25 GLs (**Figure 6.2c**). These metabolites jointly explained 70% of the variance of VAT/SAT in a 2 component-PLS model and estimated levels of VAT/SAT with a high correlation with measured levels (r = 0.83). Among the 11 MS^2-annotated TGs associated with VAT/SAT, 82% contained at least one C18:2 linoleic acid (LA), and 73% contained at least one C18:1 OA.

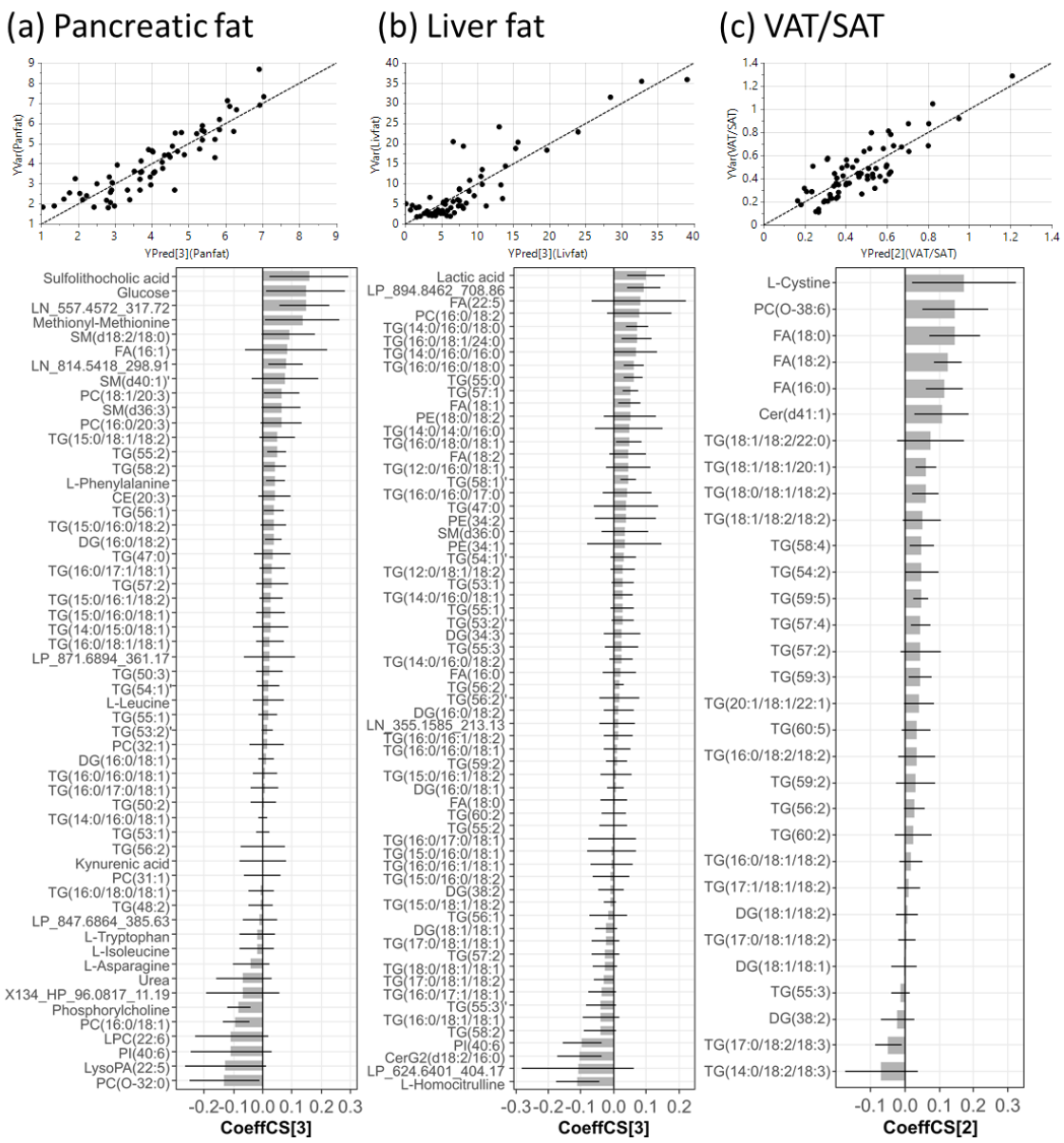

Figure 6.2: Scatter plots of measured vs PLS-estimated value of (a) pancreatic fat, (b) liver fat and (c) VAT/SAT ratio, and bar plots showing the coeffCS (centered and scaled coefficient) with error bars indicating cross-validation confidence interval (95% CI) of variables in each corresponding PLS model used for estimation. The numbers in the bracket beside YPred and CoeffCS denotes the number of components in the PLS model.

6.3.2 Estimating visceral and organ fat deposition using clinical and metabolite biomarkers

Pancreatic fat was associated with FPG, HbA_{1c}, BMI, %TBF, age, SBP, DBP, total cholesterol (TC), triglyceride (TG) and LDL-C (**Figure 6.3a**), which jointly produced a PLS model with R2Y = 0.51, Q2 = 0.46 (**Table 6.2**). Liver fat was

associated with BMI, % TBF, age, SBP, DBP, ALT, ALP, GGT, TC and TG (**Figure 6.3b**), yielding a PLS model with R2Y = 0.48, Q2 = 0.4 (**Table 6.2**). VAT/SAT was associated with FPG, HbA_{1c}, BMI, age, SBP, DBP, GGT, TC, TG and LDL-C (**Figure 6.3c**), producing a PLS model with R2Y = 0.56, Q2 = 0.44 (**Table 6.2**). Metabolite markers explained the presence of pancreatic fat (R2Y = 0.81, Q2 = 0.69), liver fat (RY2 = 0.8, Q2 = 0.66) and VAT/SAT (R2Y = 0.7, Q2 = 0.62) better than clinical markers; while combining clinical markers and metabolite markers yielded a similar model performance compared to the use of metabolite markers alone (**Table 6.2**).

Table 6.2: comparison of model performances of PLS with 7-fold cross-validation among models built on metabolites markers (M), clinical markers (C) or combination of metabolite and clinical markers (C+M)

Dataset	Biomarker panel	nComp	R2Y	Q2	$P_{CV\text{-}ANOVA}$	RMSEE	RMSEcv	r
Pancreatic fat	M	3	0.81	0.69	2.12E-12	0.72	0.89	0.90
	C	1	0.51	0.46	1.15E-08	1.14	1.18	0.71
	C+M	3	0.81	0.67	1.12E-11	0.72	0.92	0.90
Liver fat	M	3	0.80	0.66	6.11E-12	3.84	4.65	0.89
	C	1	0.48	0.40	3.51E-07	5.98	6.37	0.70
	C+M	2	0.74	0.63	5.49E-12	4.25	4.94	0.86
VAT/SAT	M	2	0.70	0.62	1.88E-12	0.13	0.14	0.83
	C	2	0.56	0.44	1.42E-07	0.16	0.17	0.74
	C+M	2	0.74	0.67	3.98E-14	0.12	0.13	0.86

nComp: number of components; RMSEE: roo mean square error of estimation; RMSEcv: root mean square error of cross-validation; r: Pearson correlation coefficient

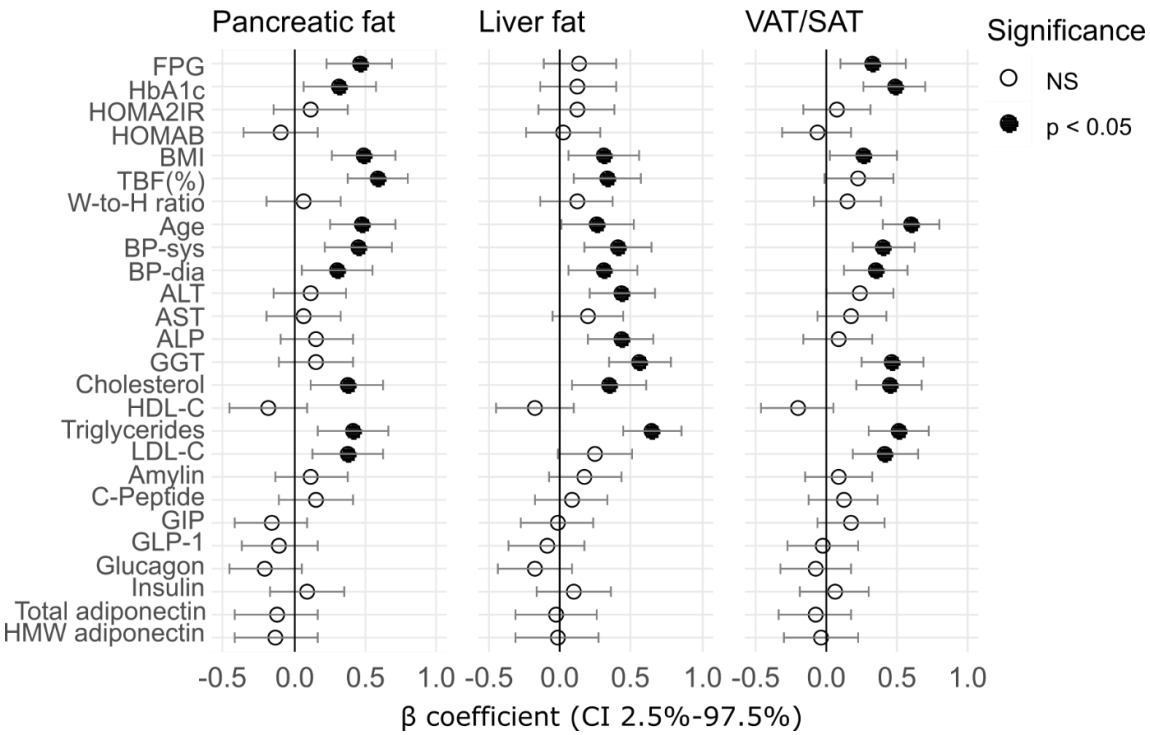

Figure 6.3: Adjusted β coefficient with 95% CI of each individual clinical variable regressed on level of (a) pancreatic fat, (b) liver fat and (c) VAT/SAT ratio in linear regression models adjusting for ethnicity. Significantly associated clinical variables (p < 0.05) are displayed in solid filled circle.

6.3.3 Characterising the association of individual metabolite markers with visceral and organ fat

Of the 56 metabolites associated with pancreatic fat, 44 were independent of ethnicity (BH-corrected p < 0.05). Further adjustment for total adiposity yielded a list of lipid species of PC, DG and TG, CE(20:3), methionyl-methionine and sulfolithocholic acid as significantly associated metabolites (BH-corrected p < 0.05); only the bile acid sulfolithocholic acid remained significantly associated after further adjustment for VAT/SAT (M3) (**Figure 6.4a and Appendix: Table 9.14**). Among the 64 metabolite markers for liver fat, 54 were independent of ethnicity (BH-corrected p < 0.05). None of these associations was influenced by further adjustment for total adiposity in terms of effect size or level of significance; only lactic acid, PC(34:2), TG(52:2) and TG(58:2) became non-significant after further adjustment for VAT/SAT (**Figure 6.4b and Appendix: Table 9.15**).

Among the 31 metabolite markers for VAT/SAT, 27 were independent of ethnicity. All metabolites except FA(18:0) and TG(53:5) remained significantly associated after further adjustment for total adiposity (BH-corrected p < 0.05) (**Figure 6.4c and Appendix: Table 9.16**).

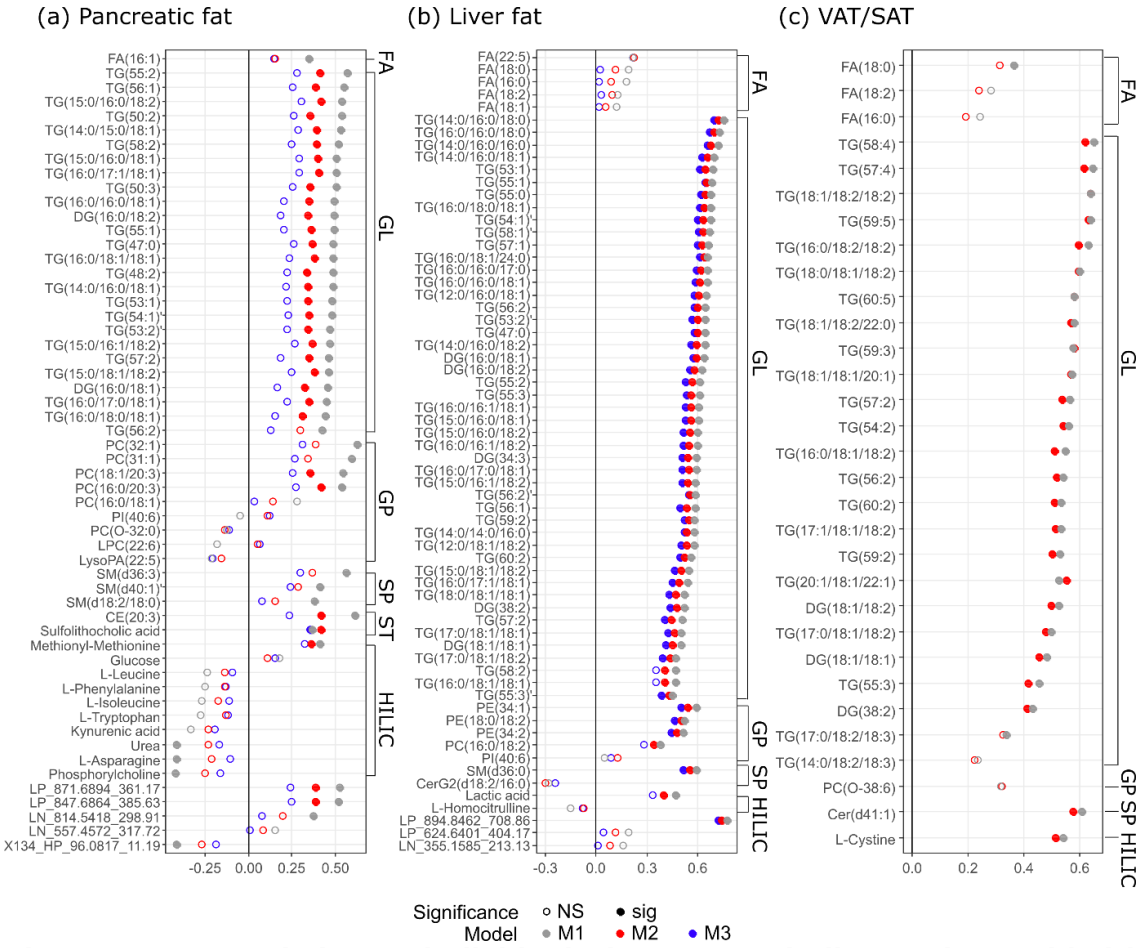

Figure 6.4: Association of individual plasma metabolite markers with (a) pancreatic fat, (b) liver fat, (c) VAT/SAT ratio assessed by multiple linear regression, with adjustment for ethnicity (M1), ethnicity + BMI + TBF(%) (M2); pancreatic fat and liver fat were further adjusted for VAT/SAT (M3). Significance tests were after multiple testing correction (p < 0.05). Markers were categorised by classes and within each class, ordered by coefficient in M1 from the highest to the lowest. FA: fatty acyls; GL: glycerolipids; GP: glycerophospholipids; SP: sphingolipids; ST: sterol lipids; HILIC: HILIC-measured polar metabolites.

6.4 Discussion

In this study we identified plasma metabolites associated with visceral and ectopic fat deposition in a cohort of European Caucasian and Asian Chinese females, in alignment with recent international position statements for the need

for identification of such biomarkers in clinical practice [29]. With a robust metabolite selection technique and PLS modelling approach, novel metabolite markers that jointly explain over 70% variance (i.e.R2Y) in pancreatic fat, liver fat and VAT/SAT ratio have been identified. The estimated levels of these fat depots by metabolite markers were highly correlated with the measured values ($r > 0.8$). We also assessed the associations of a range of commonly used clinical and anthropometric measurements with these fat depots. Several traditional CVD risk factors, including age, BP (SBP, DBP) and dyslipidaemia (TC and TG), were common correlates for all three fat depots. Despite this, these CVD risk factors alone with other significant clinical correlates for each fat depot, only moderately captured levels of ectopic fat (R2Y at around 0.5) and did not add to the metabolite prediction of ectopic fat. Our study highlighted the value of biomarker exploration using an untargeted metabolomics approach. These markers hold promise for developing new means to predict levels of ectopic fat which is otherwise expensive and time-consuming to obtain, but also provide insight into metabolic alterations that might be linked to dietary pattern and disease development thus generating hypothesis for future intervention or mechanistic studies. Furthermore, these metabolite markers can be a fast and cheap substitute for the MRI/MRS-assessed ectopic fat to be included for an improved prediction of cardiometabolic disease outcomes, which will need to be evaluated in future prospective studies.

To our best knowledge, this is the first study reporting novel metabolite markers predictive of pancreatic fat content, among which the bile acid, sulfolithocholic acid, remained significantly associated with pancreatic fat independent of total and visceral adiposity. Sulfolithocholic acid is the sulphated product of lithocholic

acid (LCA), a secondary bile acid (BA) produced by microbiota [458]. Altered BA metabolism and signalling are implicated in both T2D development and bariatric surgery-induced metabolic improvements [459, 460]. Levels of secondary BAs were observed to increase after bariatric surgery and associated with improved glycaemic control [461, 462]. Since both adipocytes and pancreatic cells expressed BA receptors [459], the profound association of sulfolithocholic acid with pancreatic fat observed in the present study sheds new light on potentially novel mechanisms of fatty infiltration modulated by the enterohepatic circulation and BA metabolism. A future targeted metabolomics study is warranted to confirm this association as well as to explore the relationship between other BAs with pancreatic fat deposition.

Other markers predictive of pancreatic fat identified in the present study included a number of metabolites previously reported as markers of obesity (palmitoleic acid, monounsaturated PCs and SMs, asparagine, phosphorylcholine and urea) [180, 205, 239, 463-465]. Concordantly, depot-specific investigation of these markers in our current study indicates that their associations with pancreatic fat were, indeed, largely due to increased total adiposity. Other markers including CE(20:3), C20:3-containing PCs, DGs, TGs and methionyl-methionine were independent of BMI and %TBF, but explained by increased VAT/SAT. Since both increased total adiposity and visceral adiposity are upstream factors predisposing individuals to an increased risk of ectopic fat deposition, our results suggest that these markers for pancreatic fat mainly reflect increased total and visceral adiposity.

We observed a TG signature characterised by low double bonds (≤3) and mainly lower carbon number (≤54 C) to be associated with liver fat content. TG species

with low double bonds and carbon number were found to be markedly increased in NAFLD patients and have the strongest predictive value in the classification of incident CVD, whilst monounsaturated TG was a significant predictor of non-alcoholic steatohepatitis (NASH) [173, 176, 466]. Our findings suggested that such a CVD risk- and NAFLD-related TG signature to some degree captured an elevated liver fat content and is already detectable even before NAFLD diagnosis, again highlighting the potential of metabolomics to facilitate risk screening.

Interestingly, several saturated TG species such as TG(44:0), TG(46:0), TG(48:0) and TG(50:0) are markers exclusively for liver fat but not visceral or pancreatic fat. These markers may reflect consumption of a high saturated fat diet [467]. Many liver fat-associated TG species contained PA and/or OA, both are hallmarks of *de novo* lipogenesis (DNL). Higher rate of DNL, fractional contribution to VLDL-FA and VLDL-TG from DNL were previously observed in patients with higher liver fat contents, and DNL rate positively correlated with the amount of intrahepatic TG [468]. In agreement, our data clearly indicated that accumulation of liver fat can be manifested by an elevation of a consortium of TG species in the circulation that likely originated from DNL, independent of the total and visceral adiposity. Our results support a tight link between increased DNL and development of fatty liver, as well as potential beneficial effects of dietary intervention targeting lipogenesis, possibly including restricted mono/disaccharide carbohydrate or elimination of fructose-containing diets alongside restricted fat diets [469, 470].

Liver fat was also associated with dhSM(d36:0) and 3 PE species (PE(34:1), PE(34:2) and PE(36:2)) independent of total adiposity and visceral adiposity. Evidence from an *in vitro* study suggested PEs to be a strong modulator of

membrane disruption induced by amylin, an amyloidogenic protein key to development of T2D [471]. On the other hand, dhSM has been associated with obesity and dysglycaemia [182]. Our finding of a positive correlation of dhSM(d36:0) with liver fat could be due to an increased substrate availability leading to increased synthesis of this lipid species, supporting the aforementioned increased DNL associated with excess liver fat deposition.

Two other markers, PC(34:2) and lactate, were also strongly associated with and predictive of, but not site-specific to, liver fat content. This is not unexpected as these metabolites are localised in many tissues, abundant in plasma and sensitive to several conditions and diseases. Increased plasma lactate has been associated with impaired oxidative capacity, obesity, IR and T2D, and its level progressively decreased in response to weight loss [472-475]. PC(34:2) has been identified as a marker for metabolic syndrome [476]. It is also associated with vascular complications in NAFLD patients [477]. Herein we provided evidence for an association of these markers with increased liver fat and in conjunction with other metabolites markers, predictive of liver fat content.

VAT/SAT is associated with a number of GLs enriched in LA. LA is an n-6 FA proposed to be obesogenic and may contribute to a chronic inflammatory state due to competition with the n-3 FA alpha-linolenic acid (ALA) for Δ-6 desaturase [478]. Whilst n-6 FAs are precursors for pro-inflammatory mediators, the n-3 FAs products have lower inflammatory or even anti-inflammatory properties. Interestingly, 2 ALA-containing TG species were observed to be the strongest negative estimators for the level of VAT/SAT in the multivariate PLS model, as opposed to several LA-containing TGs that are positively associated. Furthermore, LA along with 2 saturated FAs appeared to be strong estimators for

the level of VAT/SAT in the PLS model as their coefficients were high (ranked 3rd-5th). Since the plasma TG signature may also reflect long-term dietary patterns, such associations suggest a possible link between long-term consumption of LA-rich diets and increased visceral adiposity.

L-cystine is a significant predictor for and strongly correlated with VAT/SAT as revealed by both the PLS and MLR analysis. Similar to our study, plasma levels of cystine taken as an indicator of oxidative stress, was shown to be associated with android (visceral) fat at baseline in a cohort of patients with a cardiometabolic disorders [479]. Cystine is the major extracellular form of cysteine, and its plasma level may be associated with dietary methionine consumption [480, 481]. It would be necessary to investigate through a randomised controlled trial (RCT) whether a methionine-restricted diet can reduce circulating cystine level and simultaneously reduce visceral adiposity and improve metabolic health.

A strength of the present study is the use of a robust variable selection technique to select biomarkers. Performing model fitting and variable selection on the same dataset can introduce bias; model over-fitting could also be a concern due to a large number of variables and small number of observations. The MUVR algorithm simultaneously performs metabolite selection (on the inner segments) and assessment of model performance (on the outer loop that does not participate in model construction and variable selection), effectively reducing the risk of overfitting, biased selection and false positive discoveries [457]. A data-driven manner of MUVR to determine the optimal number of associated variables makes it an efficient tool for metabolite selection and not subjective to intuition or artefacts. Secondly, this study was conducted on a cohort free of severe metabolic diseases or medications, thus maximally eliminating potential

confounding effects of metabolic diseases on the blood metabolome, allowing the identification of biomarkers for early detection of increased risk of poor metabolic health prior to disease onset. With both DXA and MRI/MRS data available we were able to adjust the association for TBF, enhancing the understanding of the site-specificity of these markers. Limitations of this study include the relatively small cohort size and the lack of an external validation cohort, which must be addressed in future studies. Although the predicted Y value can be theoretically calculated using solely the coefficients provided in the PLS model, these coefficients are not transferable across platforms and laboratories. Thus, translation of these markers to potential clinical biomarkers will require accurate quantification of absolute concentration by other techniques e.g. targeted LC-MS/MS.

6.5 Conclusion

In conclusion, we have identified metabolites predictive of ectopic fat deposition (pancreas and liver fat, and VAT/SAT ratio) and shown these biomarkers to outperform the use of anthropometric and clinical measurements, including several CVD risk factors. Importantly, sulfolithocholic acid is a novel marker for pancreatic fat which requires validation in the future. Other markers are consistent with findings from previous metabolomics studies in the context of obesity, fatty liver diseases, T2D and CVD. Noteworthy, our cohort is devoid of cardiometabolic diseases therefore these markers held promise for developing alternative approach for detection of increased ectopic fat deposition and risk screnning prior to disease onset. Moreover, the metabolite markers provide evidence at the molecular level potentially linking ectopic fat to dietary intake, generating hypotheses for future investigation. These markers may also provide

an alternative means to measure the effectiveness of dietary interventions. Whether these markers add value to the prediction of cardiovascular risk will require further study and validation in separate cohorts.

6.6 Contributions and acknowledgements

This Chapter has been submitted to *International Journal of Obesity* and is under review.

Zhanxuan E. Wu, Karl Fraser, Marlena C. Kruger, Ivana R. Sequeira, Wilson Yip, Louise W. Lu, Lindsay D. Plank, Rinki Murphy, Garth J.S. Cooper, Jean-Charles Martin, Kieren G. Hollingsworth, Sally D. Poppitt. “Untargeted metabolomics reveals plasma biomarkers of ectopic fat in pancreas and liver as assessed by magnetic resonance imaging: the TOFI_Asia study”

Author Contributions:

IRS, WY and LWL contributed to participants recruitment, sample collection and the clinical data; IRS, WY, LDP and RM contributed to body composition measurement. IRS and KGH contributed to ectopic fat measurement and quantification. ZEW conducted sample extraction, metabolomics profile acquisition, data analyses and results interpretation. KF and MCK provided supervision. GJSC provided the protocol for sample extraction and advised on results interpretation. JCM advised on results interpretation. ZEW drafted the manuscript and coordinated updates following inputs from co-authors. KF, LDP, RM, SDP, JCM and GJSC critically reviewed and commented on the manuscript. SDP was the principal investigator for the Metabolic Health platform within the National Science Challenge High Value Nutrition (HVN) program, who conceptualised and designed this study. All authors read and approved the final version of the manuscript.

MASSEY UNIVERSITY
TE KUNENGA KI PŪREHUROA
UNIVERSITY OF NEW ZEALAND

GRADUATE RESEARCH SCHOOL

STATEMENT OF CONTRIBUTION
DOCTORATE WITH PUBLICATIONS/MANUSCRIPTS

We, the candidate and the candidate's Primary Supervisor, certify that all co-authors have consented to their work being included in the thesis and they have accepted the candidate's contribution as indicated below in the *Statement of Originality*.

Name of candidate:	Zhanxuan Wu
Name/title of Primary Supervisor:	Marlena Kruger
In which chapter is the manuscript /published work:	6

Please select one of the following three options:

○ The manuscript/published work is published or in press

- Please provide the full reference of the Research Output:

◉ The manuscript is currently under review for publication – please indicate:

- The name of the journal:
International Journal of Obesity
- The percentage of the manuscript/published work that was contributed by the candidate: 90
- Describe the contribution that the candidate has made to the manuscript/published work:
Metabolomics data acquisition; metabolomics data analysis; writing; figures & tables generation.

○ It is intended that the manuscript will be published, but it has not yet been submitted to a journal

Candidate's Signature:	Zhanxuan Wu
Date:	31-Aug-2020
Primary Supervisor's Signature:	Marlena Kruger
Date:	1/9/2020

This form should appear at the end of each thesis chapter/section/appendix submitted as a manuscript/ publication or collected as an appendix at the end of the thesis.

GRS Version 5 – 13 December 2019
DRC 19/09/10

7. Discussion and Conclusion

7.1 Discussion

The overall aim of this PhD project was to apply metabolomics to identify and understand plasma biomarkers for risks factors associated with T2D development and link these markers to underlying biochemical pathways of key metabolically active tissues. Findings from Chapter 4 supported the hypothesis that tissue metabolomes are to some degree correlated with the blood metabolome. Findings from Chapter 5 and 6 also provided robust evidence for the hypothesis that untargeted metabolomics can be applied to discover biomarkers correlated with clinical outcomes and metabolic risks independent of BMI, as stated in section 1.2.

T2D is a metabolic disease characterised by chronic dysregulation of blood glucose homeostasis, which exposes tissues and organs to a glucotoxic environment, aggravating cellular dysfunction and leading to development of various complications such as microvascular and macrovascular disorders, CVD and renal diseases [45]. However, dysglycaemia is the endpoint to define T2D. Development of T2D involves more than dysregulation of glucose homeostasis, notably profound alterations in the metabolism of lipids, fatty acids and amino acids as reported previously, with these metabolic abnormalities often taking place long before the onset of T2D [175, 252]. Given that development of T2D is a progressive, multi-factorial and potentially reversible process, identification of individuals at higher risk of T2D development well before the disease onset has remained a research focus to tackle the T2D pandemic. Although obesity has been long recognised as a risk factor for T2D development, recent evidence from human and animal models has highlighted visceral adiposity and ectopic fat deposition as key conduits for T2D [29]. Unlike obesity which is commonly

presented as the index of adiposity, BMI, derived from a mathematic calculation based on height and body weight, the amount of fat deposited in the visceral region, around and within organs is easily mis-estimated by total adiposity and requires expensive, time-consuming and sometimes invasive approaches to measure [482]. As such, there is a need to discover and understand biomarkers for early detection of visceral adiposity and ectopic fat deposition, which can potentially enhance our knowledge of T2D development and improve risk stratification.

Untargeted metabolomics has emerged as a promising tool for biomarker discovery as well as the understanding of metabolic alterations associated with pathophysiological processes. Over the past two decades, the metabolomics community has advanced the analytical and computational tools and generated a wealth of data for disease diagnosis, prognosis and mechanistic investigation [42, 144, 483]. However, several fundamental issues from both the analytical and biological aspects have yet to be adequately addressed. An often-overlooked issue during the metabolomic profile acquisition by LC-MS is the choice of suitable injection concentrations for the analyses of different sample types, which has proven to impact on the reliability and reproducibility of the profile (Chapter 3). As such, a workflow for the selection of optimal injection concentrations for different sample types including adipose tissue and liver was developed using animal tissues (Chapter 3), addressing the specific goal 1 mentioned in section 1.2.This chapter highlighted considerable differences in the optimal injection concentration across the different tissues and analysis modes, which must be accounted for on any metabolomic analytical LCMS platform.

To address the specific goal 2 in section 1.2, the established workflow from Chapter 3 was subsequently applied to profile human tissues (Chapter 4) and plasma (Chapters 4-6). To our best knowledge, the research conducted in Chapter 4 was the first to comprehensively measure metabolomic profiles of plasma and multiple adipose tissue depots, muscle types and liver, and then correlate concentrations of plasma metabolites with the respective metabolites in these tissues. Findings from Chapter 4 helped dissect which tissue site(s) the concentration of a circulating metabolite was reflective of, and hence provided evidence for or against the capacity of circulating metabolites to act as a surrogate marker for its respective tissue concentrations. Noteworthy, results from Chapter 4 provide a general reference for not just metabolite markers reported in the current thesis, but also a range of plasma metabolites associated with various disease contexts or intervention outcomes.

Work covered in Chapter 5 and 6 has addressed goals 3-5 in section 1.2. Research from the current PhD study has successfully characterised the plasma metabolomic signature for visceral adiposity assessed by DXA in a cohort of 365 individuals (Chapter 5). This was then further investigated to identify circulating metabolite markers predictive of the amount of ectopic fat deposition in the liver, pancreas and VAT/SAT ratio assessed by magnetic resonance imaging techniques (Chapter 6) in a subgroup of 68 individuals. Candidate markers identified in Chapter 5 and 6 may serve as alternative biomarkers for visceral and organ fat deposition or a complement to established risk factors for T2D risk screening, likely improving accuracy for risk estimation. Findings from this PhD study hold promise for increasing the accuracy of T2D risk prediction in the future,

reinforcing the applicability and usefulness of metabolomics in biomarker research.

7.1.1: Metabolomics as a tool for profiling tissue and circulating metabolites

The validity of a metabolomics-drawn conclusion is based on the assumption that the relative abundance of metabolites being quantified is proportional to their differences in concentrations across samples [148]. This requires the signal intensity of measured metabolites to fall within the linear range of the analytical technique being used to measure them. Not accounting for nonlinearity of the measurements can lead to over- or under-estimation of the variation between samples and distort association. Unlike targeted metabolomics in which the measurement of metabolites can be monitored with standard compounds and a linear calibration curve, evaluation of the linear dynamic range for untargeted analysis can been performed using a serial diluted pooled quality control (QC) sample [348]. The developed methodology in Chapter 3 reported LC–MS analysis of serial diluted pooled extracts, chromatographic visualisation, reproducibility assessment and concentration-intensity correlation calculation to determine the suitable injected concentration, for each sample type and analysis type, based on both the number of reproducible features and linear features. Chapter 3 found that incorrect reconstitution volumes (and thus injection concentration) can result in either severe overloading or poor linearity, whilst too diluted samples resulted in a low number of reproducible features. It also highlighted that different injection concentrations are required for the analyses of different sample types (exemplified by adipose tissue and liver) as well as metabolite polarity extracts to ensure that the maximal number of metabolites are measured in the linear response range of the instrumentation.

After establishing a workflow to select a suitable injected concentration for accurate and reliable profiling applicable for an array of sample types, human samples were analysed with this methodology in order to provide insight into plasma metabolite levels and the relationship to their respective levels in tissue. The plasma metabolomic profile was reflective more of the liver profile than muscle or adipose tissues. For example, elevated DG and ceramide contents in the liver have been observed in T2D animal models and were implicated/causally linked to liver IR [484]. However, it is unknown whether such metabolic alterations were confined within the liver or can be readily captured by the plasma metabolomic profile. Findings from Chapter 4 provided direct evidence for a linear correlation for the concentrations of several plasma DG and ceramide species with their liver counterparts. Intermediates involved in metabolic pathways that actively take place in the liver such as the phosphatidylethanolamine N-methyltransferase (PEMT)-pathway (e.g. dimethylphosphatidylethanolamine species) and transmethylation and transulfuration pathways (e.g. betaine, methionine), also showed positive correlations between liver and plasma as expected. Liver is also an active site of de novo lipogenesis (DNL) during fasting that synthesise palmitic acid (PA) as initial major product [485]. An upregulated DNL in the liver is likely to be a key driver for the metabolic complications of obesity [486]. PA can be esterified to TG that is either accumulated inside the liver or secreted into the circulation, and Chapter 4 highlighted that several saturated TG (notably those containing the PA chain) in plasma positively correlated with their liver counterparts. Several polar metabolites linked to amino acids, energy metabolism and microbial metabolites/xenobiotics were found to show positive correlations between plasma and muscle as well as the liver. In

contrast, plasma polar metabolites were poorly correlated with their adipose tissue counterparts, likely owing to a less aqueous environment of these tissues. These findings are unique and critical to understand the value of measuring metabolites in plasma for capturing metabolic alterations that might be occurring in biologically active tissue sites.

7.1.2 Metabolomics as a promising tool to capture metabolic risk

In clinical studies, metabolomics has been widely applied to identify metabolites associated with clinical outcomes or endpoints. However, other potential advantages of metabolomics to advance medical research still needs to be exploited. Recently Cirullin et al., developed a modelling approach based on the metabolomic signature for obesity to re-stratify participants, and identified a subset of individuals whose predicted BMI by metabolomic signature was much higher than their actual BMI [204]. These individuals were characterised by phenotypes of metabolic health similar to obese individuals with obese metabolomes. The authors nonetheless pointed out investigation on other metabolic traits might offer greater utility [204]. Inspired by this study, metabolomic signatures characteristic for elevated FPG and %VAT reported in Chapter 5 were further extended to build a model to predict an individual's FPG states, and the clinical and anthropometric measurements associated with metabolic risks of these newly designated groups (i.e. NFG-mNFG, NFG-mIFG, IFG-mNFG and IFG-mIFG) were characterised and compared. Interestingly, NFG individuals predicted to have an IFG state based on their metabolomic signature were characterised by a higher BMI and W-to-H ratio, and worse lipid profile, liver enzyme profile and glucoregulatory hormone profile compared with NFG-mNFG counterparts. This finding highlighted the potential for metabolomics

results measured from a single fasting blood sample combined with computational tools can capture a range of metabolic risk factors, enabling early detection of individuals at higher risk of T2D so that informed lifestyle choices can be made.

Chapter 6 applied untargeted metabolomics combined with computational tools to identify sets of metabolite markers predictive of levels of ectopic fat including liver fat, pancreas fat and VAT/SAT ratio, and reported predicted values being highly correlated with those measured by magnetic resonance imaging techniques. In addition, predictive models of ectopic fat deposition by a panel of metabolite markers (measured using metabolomics) outperformed predictions from clinical variables including several metabolic risk factors, and the variance of ectopic fat deposition was better explained by metabolite markers than clinical variables. These findings once again highlighted the usefulness of metabolomics as a promising tool to capture metabolic risk, and that candidate markers identified by metabolomics can potentially be implemented into routine practice for risk screening.

7.1.3 Metabolite markers for visceral adiposity and ectopic fat deposition

This PhD study has included two visceral adiposity-related parameters as outcome variables correlated with metabolomic profile using regression methods: amount of visceral fat expressed as % of total body fat assessed using DXA scanning methods (Chapter 5), and the ratio of visceral adipose tissue to subcutaneous adipose tissue measured using magnetic resonance techniques (Chapter 6). Although the DXA measurement was conducted on a large cohort of mixed genders, whereas the MRI measurement was conducted on a single gender subset of this cohort of females only, and different modelling approaches

were used to analyse the two datasets, a number of plasma lipid markers were consistently found to be associated with visceral adiposity. These markers included DG(36:2), DG(36:3), DG(38:2) and 18 TG species with 52-60 total number of carbons and varying degree of unsaturation (2-5 double bonds). Interestingly, plasma levels of these DG and TG species did not correlate with their intra-abdominal adipose tissue counterparts but reflected levels in the liver instead (Chapter 4). This suggested that plasma lipid markers for excess VAT did not reflect FA composition of TG storage in this fat depot, but the FFA derived from VAT lipolysis, delivered to the liver via the portal vein, re-esterified to TG molecules and accumulated/secreted into the circulation in VLDL.

In line with the previous findings of marked increases of TG species with low double bonds and carbon number in NAFLD patients and monounsaturated TG species as significant predictors for NASH [173, 466], Chapter 6 reported several TG species with low double bonds and carbon number as predictors of liver fat deposition. These TG species, including several saturated and monounsaturated TG species, were found to show significant positive correlations between plasma and liver (Chapter 4), suggesting the liver as a major source of these TG species in the circulation and that dysregulated TG metabolism in the liver was directly linked to the development of fatty liver disease.

In addition to the aforementioned TG species, a number of plasma lipid markers predictive of liver fat content, including dihydroceramide, PE and DG species reported in Chapter 6 were found to be linearly correlated with their corresponding concentrations in the liver (Chapter 4). These findings coherently suggested that the plasma markers predictive of liver fat accumulation were able to capture and were directly linked to perturbed lipid metabolism occurring in the liver.

7.2 Conclusion

The present PhD study applied untargeted metabolomics to identify plasma biomarkers for risks factors associated with T2D development including elevated FPG, visceral adiposity and ectopic fat deposition in the liver and pancreas. Research from this PhD study showed a significant discriminatory metabolomic profile between Caucasians and Asian Chinese and reported plasma signatures for elevated FPG or visceral adiposity in each ethnic group independent of age, gender and BMI. Common to both ethnic groups, elevated FPG was associated with perturbations in several glycerolipid species, whereas elevated visceral fat was associated with increased levels of dihydroceramide, SM, DG, TG, PC and PE species, and decreased levels of ether-linked PC species. Metabolic associations unique to each ethnic group were also observed, and the use of ethnic-specific plasma signatures was able to identify individuals with the corresponding ethnicity potentially at higher risk of T2D development. These individuals were characterised by a worse cardiometabolic profile despite being currently normoglycaemic. This PhD study also identified sets of plasma candidate markers that jointly predict levels of liver fat or pancreatic fat quantified by magnetic resonance imaging techniques, which were shown to achieve better prediction of these fat depots than the use of clinical and anthropometric measurements. Individual plasma metabolites associated with accumulation of liver fat or pancreatic fat independent of ethnicity, total adiposity and visceral adiposity were also reported, among which sulfolithocholic acid (a bile acid) was found to be a novel predictor for pancreatic fat. Liver fat deposition was independently associated with increased dihydrosphingomyelin, PE, DG and TG species in plasma, and the plasma concentrations of most of these metabolites

were linearly correlated with their concentrations in the liver tissue. The plasma candidate markers associated with risk factors for T2D development identified by the present PhD study may offer opportunities for improved risk prediction and stratification, disease progression monitoring and to develop alternative means for the measurement of the effectiveness of dietary interventions. These markers may also provide insights into the metabolic perturbation contributing to T2D development and facilitate hypothesis generation for mechanistic speculation, highlighting the potential of untargeted metabolomics in advancing knowledge in T2D pathophysiology and improving risk screening for T2D.

7.3 Future perspectives

An advantage of untargeted metabolomics is that it is not constrained to a particular class of metabolite, therefore offering opportunities to capture a more comprehensive snapshot of the systemic variation associated with phenotype. This PhD study has generated a wealth of data for the metabolic association with body composition, and FPG level, both of which are risk factors for T2D. However, a major limitation is that all these associations were observed cross-sectionally from a single cohort, in the absence of follow-up data. Translating these candidate markers from bench to routine practice still requires considerable research, which involves at least 3 key steps: validation of these markers as suitable substitutes for ectopic fat deposition in a separate cohort; confirmation of associations of these markers with incident T2D in prospective studies; and development of a predictive model with weighted scores of these metabolites in the risk assessment with targeted analysis approach.

Several diet-related metabolites have been reported to be associated with ectopic and visceral fat deposition. To eliminate potential confounding effects of diet on

the observed associations, future studies including a controlled-diet design is warranted for a better understanding of the relationships between diet-risk factors.

This PhD study also reported several unknown metabolites associated with risk factors for T2D. The identity of these unknown metabolites could be resolved using a combination of advanced MS methodology and subsequent targeted approaches e.g. the use of standard compounds or generation of fragmentation (MS^2) spectra of the unknown compound to elucidate structure.

Stemming from the rationale behind these workpieces, identification of metabolite markers for other ectopic fat depots e.g. cardiac, epicardial and perivascular fat, which are likely directly implicated in development of CVD, can become another direction for the research community of cardiometabolic health.

The current study also showed that the plasma metabolomic profile is reflective more of the liver profile than muscle or adipose tissues, supporting the premise that several plasma metabolites can serve as surrogate indicators for the concentrations of liver metabolites. The study cohort for this study (Chapter 4) was nonetheless relatively small and contained obese, non-T2D females only. Therefore, these findings need to be validated in a larger cohort. Whether such tissue-plasma relationships are universally true or modified by diseases will also need to be clarified in future studies. Considering that the plasma metabolomics profile is reflective of some tissues but not the others, examination of the relationship between plasma and other tissues such as the spleen, pancreas and kidney in the future can potentially enhance the knowledge of plasma metabolites in relation to the multi-tissue metabolic profiles and reinforce the value of

measuring the plasma metabolomic profile for the understanding of disease pathophysiology.

8. References

1. Unnikrishnan R, Pradeepa R, Joshi SR, Mohan V. Type 2 diabetes: demystifying the global epidemic. Diabetes. 2017;66(6):1432-42.
2. Association AD. 2. Classification and Diagnosis of Diabetes: Standards of Medical Care in Diabetes—2020. Diabetes Care. 2020;43(Supplement 1):S14-S31.
3. Saeedi P, Petersohn I, Salpea P, Malanda B, Karuranga S, Unwin N, et al. Global and regional diabetes prevalence estimates for 2019 and projections for 2030 and 2045: Results from the International Diabetes Federation Diabetes Atlas. Diabetes Res Clin Pract. 2019;157:107843.
4. Zhou B, Lu Y, Hajifathalian K, Bentham J, Di Cesare M, Danaei G, et al. Worldwide trends in diabetes since 1980: a pooled analysis of 751 population-based studies with 4· 4 million participants. The Lancet. 2016;387(10027):1513-30.
5. Einarson TR, Acs A, Ludwig C, Panton UH. Prevalence of cardiovascular disease in type 2 diabetes: a systematic literature review of scientific evidence from across the world in 2007–2017. Cardiovasc Diabetol. 2018;17(1):1-19.
6. Leon BM, Maddox TM. Diabetes and cardiovascular disease: Epidemiology, biological mechanisms, treatment recommendations and future research. World journal of diabetes. 2015;6(13):1246-58.
7. Collaboration ERF. Diabetes mellitus, fasting glucose, and risk of cause-specific death. N Engl J Med. 2011;364(9):829-41.
8. Shah AD, Langenberg C, Rapsomaniki E, Denaxas S, Pujades-Rodriguez M, Gale CP, et al. Type 2 diabetes and incidence of cardiovascular diseases: a cohort study in 1· 9 million people. Lancet Diabetes Endocrinol. 2015;3(2):105-13.
9. Bhupathiraju SN, Hu FB. Epidemiology of obesity and diabetes and their cardiovascular complications. Circ Res. 2016;118(11):1723-35.
10. Gomes MdB. Impact of diabetes on cardiovascular disease: an update. International journal of hypertension. 2013;2013.
11. Singh GM, Danaei G, Farzadfar F, Stevens GA, Woodward M, Wormser D, et al. The age-specific quantitative effects of metabolic risk factors on cardiovascular diseases and diabetes: a pooled analysis. PLoS ONE. 2013;8(7):e65174.
12. Tabák AG, Herder C, Rathmann W, Brunner EJ, Kivimäki M. Prediabetes: a high-risk state for diabetes development. The Lancet. 2012;379(9833):2279-90.
13. Association AD. 3. Prevention or Delay of Type 2 Diabetes: Standards of Medical Care in Diabetes-2019. Diabetes Care. 2019;42(Suppl 1):S29.
14. Ng M, Fleming T, Robinson M, Thomson B, Graetz N, Margono C, et al. Global, regional, and national prevalence of overweight and obesity in children and adults during 1980–2013: a systematic analysis for the Global Burden of Disease Study 2013. The lancet. 2014;384(9945):766-81.
15. Collaboration PS. Body-mass index and cause-specific mortality in 900 000 adults: collaborative analyses of 57 prospective studies. The Lancet. 2009;373(9669):1083-96.

16. Sanada H, Yokokawa H, Yoneda M, Yatabe J, Yatabe MS, Williams SM, et al. High body mass index is an important risk factor for the development of type 2 diabetes. Intern Med. 2012;51(14):1821-6.
17. Bray G, Kim K, Wilding J, Federation WO. Obesity: a chronic relapsing progressive disease process. A position statement of the World Obesity Federation. Obes Rev. 2017;18(7):715-23.
18. Field AE, Coakley EH, Must A, Spadano JL, Laird N, Dietz WH, et al. Impact of overweight on the risk of developing common chronic diseases during a 10-year period. Arch Intern Med. 2001;161(13):1581-6.
19. Visscher TL, Seidell JC. The public health impact of obesity. Annu Rev Public Health. 2001;22(1):355-75.
20. Chadt A, Scherneck S, Joost H-G, Al-Hasani H. Molecular links between obesity and diabetes:“diabesity”. Endotext [Internet]: MDText. com, Inc.; 2018.
21. Ormazabal V, Nair S, Elfeky O, Aguayo C, Salomon C, Zuñiga FA. Association between insulin resistance and the development of cardiovascular disease. Cardiovasc Diabetol. 2018;17(1):1-14.
22. Astrup A, Finer N. Redefining type 2 diabetes:‘diabesity’or ‘obesity dependent diabetes mellitus’? Obes Rev. 2000;1(2):57-9.
23. Wildman RP, Muntner P, Reynolds K, McGinn AP, Rajpathak S, Wylie-Rosett J, et al. The obese without cardiometabolic risk factor clustering and the normal weight with cardiometabolic risk factor clustering: prevalence and correlates of 2 phenotypes among the US population (NHANES 1999-2004). Arch Intern Med. 2008;168(15):1617-24.
24. Chan JC, Malik V, Jia W, Kadowaki T, Yajnik CS, Yoon K-H, et al. Diabetes in Asia: epidemiology, risk factors, and pathophysiology. JAMA. 2009;301(20):2129-40.
25. Yoon K-H, Lee J-H, Kim J-W, Cho JH, Choi Y-H, Ko S-H, et al. Epidemic obesity and type 2 diabetes in Asia. The Lancet. 2006;368(9548):1681-8.
26. Després J-P, Lemieux I, Bergeron J, Pibarot P, Mathieu P, Larose E, et al. Abdominal obesity and the metabolic syndrome: contribution to global cardiometabolic risk. Arterioscler Thromb Vasc Biol. 2008;28(6):1039-49.
27. Tchernof A, Després J-P. Pathophysiology of human visceral obesity: an update. Physiol Rev. 2013;93(1):359-404.
28. Neeland IJ, Poirier P, Després J-P. Cardiovascular and metabolic heterogeneity of obesity: clinical challenges and implications for management. Circulation. 2018;137(13):1391-406.
29. Neeland IJ, Ross R, Després J-P, Matsuzawa Y, Yamashita S, Shai I, et al. Visceral and ectopic fat, atherosclerosis, and cardiometabolic disease: a position statement. Lancet Diabetes Endocrinol. 2019;7(9):715-25.
30. Lebovitz HE, Banerji MA. Point: visceral adiposity is causally related to insulin resistance. Diabetes Care. 2005;28(9):2322-5.
31. Hanley AJ, Wagenknecht LE. Abdominal adiposity and diabetes risk: the importance of precise measures and longitudinal studies. Diabetes. 2008;57(5):1153-5.
32. Cembrowska P, Stefańska A, Odrowąż-Sypniewska G. Obesity phenotypes: normal-weight individuals with metabolic disorders versus metabolically healthy obese. Medical research journal. 2016;1(3):95-9.
33. Bosomworth NJ. Normal-weight central obesity: Unique hazard of the toxic waist. Can Fam Physician. 2019;65(6):399-408.

34. Ma RC, Chan JC. Type 2 diabetes in East Asians: similarities and differences with populations in Europe and the United States. Ann N Y Acad Sci. 2013;1281(1):64-91.
35. Rattarasarn C. Dysregulated lipid storage and its relationship with insulin resistance and cardiovascular risk factors in non-obese Asian patients with type 2 diabetes. Adipocyte. 2018;7(2):71-80.
36. Lear SA, Humphries KH, Kohli S, Chockalingam A, Frohlich JJ, Birmingham CL. Visceral adipose tissue accumulation differs according to ethnic background: results of the Multicultural Community Health Assessment Trial (M-CHAT). Am J Clin Nutr. 2007;86(2):353-9.
37. Wulan S, Westerterp K, Plasqui G. Ethnic differences in body composition and the associated metabolic profile: a comparative study between Asians and Caucasians. Maturitas. 2010;65(4):315-9.
38. Fiehn O. Metabolomics—the link between genotypes and phenotypes. Functional genomics: Springer; 2002. p. 155-71.
39. Newgard CB. Metabolomics and metabolic diseases: where do we stand? Cell Metab. 2017;25(1):43-56.
40. Brunius C, Shi L, Landberg R. Metabolomics for improved understanding and prediction of cardiometabolic diseases—Recent findings from human studies. Current Nutrition Reports. 2015;4(4):348-64.
41. Gika H, Theodoridis G. Sample preparation prior to the LC–MS-based metabolomics/metabonomics of blood-derived samples. Bioanalysis. 2011;3(14):1647-61.
42. Guasch-Ferré M, Hruby A, Toledo E, Clish CB, Martínez-González MA, Salas-Salvadó J, et al. Metabolomics in prediabetes and diabetes: a systematic review and meta-analysis. Diabetes Care. 2016;39(5):833-46.
43. Campos C. Chronic hyperglycemia and glucose toxicity: pathology and clinical sequelae. Postgrad Med. 2012;124(6):90-7.
44. Yki-Järvinen H. Glucose toxicity. Endocr Rev. 1992;13(3):415-31.
45. Giri B, Dey S, Das T, Sarkar M, Banerjee J, Dash SK. Chronic hyperglycemia mediated physiological alteration and metabolic distortion leads to organ dysfunction, infection, cancer progression and other pathophysiological consequences: an update on glucose toxicity. Biomedicine & Pharmacotherapy. 2018;107:306-28.
46. Kawahito S, Kitahata H, Oshita S. Problems associated with glucose toxicity: role of hyperglycemia-induced oxidative stress. World journal of gastroenterology: WJG. 2009;15(33):4137-42.
47. Dunger D. Insulin and insulin-like growth factors in diabetes mellitus. Arch Dis Child. 1995;72(6):469-71.
48. Henquin J-C, Ravier M, Nenquin M, Jonas J-C, Gilon P. Hierarchy of the β - cell signals controlling insulin secretion. Eur J Clin Invest. 2003;33(9):742-50.
49. Wilcox G. Insulin and insulin resistance. Clinical biochemist reviews. 2005;26(2):19-39.
50. Rorsman P, Braun M. Regulation of insulin secretion in human pancreatic islets. Annu Rev Physiol. 2013;75:155-79.
51. Cen J, Sargsyan E, Bergsten P. Fatty acids stimulate insulin secretion from human pancreatic islets at fasting glucose concentrations via mitochondria-dependent and-independent mechanisms. Nutr Metab (Lond). 2016;13(1):1-9.

52. Paolisso G, Gambardella A, Amato L, Tortoriello R, D'amore A, Varricchio M, et al. Opposite effects of short-and long-term fatty acid infusion on insulin secretion in healthy subjects. Diabetologia. 1995;38(11):1295-9.
53. Grill V, Qvigstad E. Fatty acids and insulin secretion. Br J Nutr. 2000;83(S1):S79-S84.
54. Boucher J, Kleinridders A, Kahn CR. Insulin receptor signaling in normal and insulin-resistant states. Cold Spring Harbor perspectives in biology. 2014;6(1):a009191.
55. Huang X, Liu G, Guo J, Su Z. The PI3K/AKT pathway in obesity and type 2 diabetes. International journal of biological sciences. 2018;14(11):1483-96.
56. Farese RV, Sajan MP. Metabolic functions of atypical protein kinase C:“good” and “bad” as defined by nutritional status. American Journal of Physiology-Endocrinology and Metabolism. 2010;298(3):E385-E94.
57. Dimitriadis G, Mitrou P, Lambadiari V, Maratou E, Raptis SA. Insulin effects in muscle and adipose tissue. Diabetes Res Clin Pract. 2011;93:S52-S9.
58. Kowluru A, Matti A. Hyperactivation of protein phosphatase 2A in models of glucolipotoxicity and diabetes: potential mechanisms and functional consequences. Biochem Pharmacol. 2012;84(5):591-7.
59. Yung JHM, Giacca A. Role of c-Jun N-terminal Kinase (JNK) in Obesity and Type 2 Diabetes. Cells. 2020;9(3):706.
60. Lytrivi M, Castell A-L, Poitout V, Cnop M. Recent insights into mechanisms of β-cell lipo-and glucolipotoxicity in type 2 diabetes. J Mol Biol. 2020;432(5):1514-34.
61. Yu C, Chen Y, Cline GW, Zhang D, Zong H, Wang Y, et al. Mechanism by which fatty acids inhibit insulin activation of insulin receptor substrate-1 (IRS-1)-associated phosphatidylinositol 3-kinase activity in muscle. J Biol Chem. 2002;277(52):50230-6.
62. Liu L, Zhang Y, Chen N, Shi X, Tsang B, Yu Y-H. Upregulation of myocellular DGAT1 augments triglyceride synthesis in skeletal muscle and protects against fat-induced insulin resistance. The Journal of clinical investigation. 2007;117(6):1679-89.
63. Holland WL, Brozinick JT, Wang L-P, Hawkins ED, Sargent KM, Liu Y, et al. Inhibition of ceramide synthesis ameliorates glucocorticoid-, saturated-fat-, and obesity-induced insulin resistance. Cell Metab. 2007;5(3):167-79.
64. Peng G, Li L, Liu Y, Pu J, Zhang S, Yu J, et al. Oleate blocks palmitate-induced abnormal lipid distribution, endoplasmic reticulum expansion and stress, and insulin resistance in skeletal muscle. Endocrinology. 2011;152(6):2206-18.
65. Mokdad AH, Ford ES, Bowman BA, Dietz WH, Vinicor F, Bales VS, et al. Prevalence of obesity, diabetes, and obesity-related health risk factors, 2001. JAMA. 2003;289(1):76-9.
66. Manna P, Jain SK. Obesity, oxidative stress, adipose tissue dysfunction, and the associated health risks: causes and therapeutic strategies. Metabolic syndrome and related disorders. 2015;13(10):423-44.
67. Boden G. Obesity and free fatty acids. Endocrinol Metab Clin North Am. 2008;37(3):635-46.
68. Shai I, Jiang R, Manson JE, Stampfer MJ, Willett WC, Colditz GA, et al. Ethnicity, obesity, and risk of type 2 diabetes in women: a 20-year follow-up study. Diabetes Care. 2006;29(7):1585-90.
69. Chiu M, Austin PC, Manuel DG, Shah BR, Tu JV. Deriving ethnic-specific BMI cutoff points for assessing diabetes risk. Diabetes Care. 2011;34(8):1741-8.

70. Tillin T, Sattar N, Godsland I, Hughes A, Chaturvedi N, Forouhi N. Ethnicity‐specific obesity cut‐points in the development of Type 2 diabetes–a prospective study including three ethnic groups in the United Kingdom. Diabet Med. 2015;32(2):226-34.
71. Vague J. The degree of masculine differentiation of obesities: a factor determining predisposition to diabetes, atherosclerosis, gout, and uric calculous disease. Am J Clin Nutr. 1956;4(1):20-34.
72. Kissebah AH, Vydelingum N, Murray R, Evans DJ, Kalkhoff RK, Adams PW. Relation of body fat distribution to metabolic complications of obesity. J Clin Endocrinol Metab. 1982;54(2):254-60.
73. Krotkiewski M, Björntorp P, Sjöström L, Smith U. Impact of obesity on metabolism in men and women. Importance of regional adipose tissue distribution. The Journal of clinical investigation. 1983;72(3):1150-62.
74. Ohlson L-O, Larsson B, Svärdsudd K, Welin L, Eriksson H, Wilhelmsen L, et al. The influence of body fat distribution on the incidence of diabetes mellitus: 13.5 years of follow-up of the participants in the study of men born in 1913. Diabetes. 1985;34(10):1055-8.
75. Lapidus L, Bengtsson C, Larsson B, Pennert K, Rybo E, Sjöström L. Distribution of adipose tissue and risk of cardiovascular disease and death: a 12 year follow up of participants in the population study of women in Gothenburg, Sweden. Br Med J (Clin Res Ed). 1984;289(6454):1257-61.
76. Carey VJ, Walters EE, Colditz GA, Solomon CG, Willet WC, Rosner BA, et al. Body fat distribution and risk of non-insulin-dependent diabetes mellitus in women: the Nurses' Health Study. Am J Epidemiol. 1997;145(7):614-9.
77. Lundgren H, Bengtsson C, Blohme G, Lapidus L, Sjöström L. Adiposity and adipose tissue distribution in relation to incidence of diabetes in women: results from a prospective population study in Gothenburg, Sweden. Int J Obes. 1989;13(4):413-23.
78. Vazquez G, Duval S, Jacobs Jr DR, Silventoinen K. Comparison of body mass index, waist circumference, and waist/hip ratio in predicting incident diabetes: a meta-analysis. Epidemiol Rev. 2007;29(1):115-28.
79. Baglioni S, Cantini G, Poli G, Francalanci M, Squecco R, Di Franco A, et al. Functional differences in visceral and subcutaneous fat pads originate from differences in the adipose stem cell. PLoS ONE. 2012;7(5):e36569.
80. Lafontan M, Berlan M. Do regional differences in adipocyte biology provide new pathophysiological insights? Trends Pharmacol Sci. 2003;24(6):276-83.
81. Trouwborst I, Bowser SM, Goossens GH, Blaak EE. Ectopic fat accumulation in distinct insulin resistant phenotypes; targets for personalized nutritional interventions. Front Nutr. 2018;5:77.
82. Després J-P, Nadeau A, Tremblay A, Ferland M, Moorjani S, Lupien PJ, et al. Role of deep abdominal fat in the association between regional adipose tissue distribution and glucose tolerance in obese women. Diabetes. 1989;38(3):304-9.
83. Fujioka S, Matsuzawa Y, Tokunaga K, Tarui S. Contribution of intra-abdominal fat accumulation to the impairment of glucose and lipid metabolism in human obesity. Metabolism-Clinical and Experimental. 1987;36(1):54-9.
84. Abate N, Garg A, Peshock RM, Stray-Gundersen J, Grundy SM. Relationships of generalized and regional adiposity to insulin sensitivity in men. The Journal of clinical investigation. 1995;96(1):88-98.

85. Garg A. Regional adiposity and insulin resistance. J Clin Endocrinol Metab. 2004;89(9):4206-10.
86. Goodpaster BH, Thaete FL, Simoneau J-A, Kelley DE. Subcutaneous abdominal fat and thigh muscle composition predict insulin sensitivity independently of visceral fat. Diabetes. 1997;46(10):1579-85.
87. Goodpaster BH, Kelley DE, Wing RR, Meier A, Thaete FL. Effects of weight loss on regional fat distribution and insulin sensitivity in obesity. Diabetes. 1999;48(4):839-47.
88. Nazare J-A, Smith J, Borel A-L, Aschner P, Barter P, Van Gaal L, et al. Usefulness of measuring both body mass index and waist circumference for the estimation of visceral adiposity and related cardiometabolic risk profile (from the INSPIRE ME IAA study). Am J Cardiol. 2015;115(3):307-15.
89. Pouliot M-C, Després J-P, Nadeau A, Moorjani S, Prud'Homme D, Lupien PJ, et al. Visceral obesity in men: associations with glucose tolerance, plasma insulin, and lipoprotein levels. Diabetes. 1992;41(7):826-34.
90. Ross R, Aru J, Freeman J, Hudson R, Janssen I. Abdominal adiposity and insulin resistance in obese men. American Journal of Physiology-Endocrinology And Metabolism. 2002;282(3):E657-E63.
91. Ross R, Freeman J, Hudson R, Janssen I. Abdominal obesity, muscle composition, and insulin resistance in premenopausal women. J Clin Endocrinol Metab. 2002;87(11):5044-51.
92. Taylor R, Holman RR. Normal weight individuals who develop type 2 diabetes: the personal fat threshold. Clin Sci. 2015;128(7):405-10.
93. Cuthbertson DJ, Steele T, Wilding JP, Halford J, Harrold JA, Hamer M, et al. What have human experimental overfeeding studies taught us about adipose tissue expansion and susceptibility to obesity and metabolic complications? Int J Obes. 2017;41(6):853-65.
94. Boyko EJ, Fujimoto WY, Leonetti DL, Newell-Morris L. Visceral adiposity and risk of type 2 diabetes: a prospective study among Japanese Americans. Diabetes Care. 2000;23(4):465-71.
95. Hayashi T, Boyko EJ, Leonetti DL, McNeely MJ, Newell-Morris L, Kahn SE, et al. Visceral adiposity and the risk of impaired glucose tolerance: a prospective study among Japanese Americans. Diabetes Care. 2003;26(3):650-5.
96. Tong J, Boyko E, Utzschneider K, McNeely M, Hayashi T, Carr D, et al. Intra-abdominal fat accumulation predicts the development of the metabolic syndrome in non-diabetic Japanese-Americans. Diabetologia. 2007;50(6):1156-60.
97. Hayashi T, Boyko EJ, McNeely MJ, Leonetti DL, Kahn SE, Fujimoto WY. Visceral adiposity, not abdominal subcutaneous fat area, is associated with an increase in future insulin resistance in Japanese Americans. Diabetes. 2008;57(5):1269-75.
98. Fujimoto WY, Bergstrom RW, Boyko EJ, Chen K-W, Leonetti DL, Newell-Morris L, et al. Visceral adiposity and incident coronary heart disease in Japanese-American men. The 10-year follow-up results of the Seattle Japanese-American Community Diabetes Study. Diabetes Care. 1999;22(11):1808-12.
99. Lemieux S, Prud'homme D, Nadeau A, Tremblay A, Bouchard C, Després JP. Seven-year changes in body fat and visceral adipose tissue in women. Association with indexes of plasma glucose-insulin homeostasis. Diabetes Care. 1996;19(9):983-91.

100. Mohammed BS, Cohen S, Reeds D, Young VL, Klein S. Long‐term effects of large‐volume liposuction on metabolic risk factors for coronary heart disease. Obesity. 2008;16(12):2648-51.
101. Klein S, Fontana L, Young VL, Coggan AR, Kilo C, Patterson BW, et al. Absence of an effect of liposuction on insulin action and risk factors for coronary heart disease. N Engl J Med. 2004;350(25):2549-57.
102. Thörne A, Lönnqvist F, Apelman J, Hellers G, Arner P. A pilot study of long-term effects of a novel obesity treatment: omentectomy in connection with adjustable gastric banding. Int J Obes. 2002;26(2):193-9.
103. Tran TT, Yamamoto Y, Gesta S, Kahn CR. Beneficial effects of subcutaneous fat transplantation on metabolism. Cell Metab. 2008;7(5):410-20.
104. Hocking S, Chisholm D, James D. Studies of regional adipose transplantation reveal a unique and beneficial interaction between subcutaneous adipose tissue and the intra-abdominal compartment. Diabetologia. 2008;51(5):900-2.
105. Berg AH, Scherer PE. Adipose tissue, inflammation, and cardiovascular disease. Circ Res. 2005;96(9):939-49.
106. Kershaw EE, Flier JS. Adipose tissue as an endocrine organ. J Clin Endocrinol Metab. 2004;89(6):2548-56.
107. Mohamed-Ali V, Pinkney J, Coppack S. Adipose tissue as an endocrine and paracrine organ. Int J Obes. 1998;22(12):1145-58.
108. Tsigos C, Kyrou I, Chala E, Tsapogas P, Stavridis JC, Raptis SA, et al. Circulating tumor necrosis factor alpha concentrations are higher in abdominal versus peripheral obesity. Metabolism. 1999;48(10):1332-5.
109. Cartier A. The inflammatory profile associated with abdominal obesity. Official J International Chair on Cardiometabolic Risk. 2010;3(2):15-9.
110. Yu J-Y, Choi W-J, Lee H-S, Lee J-W. Relationship between inflammatory markers and visceral obesity in obese and overweight Korean adults: An observational study. Medicine (Baltimore). 2019;98(9):e14740.
111. Shimomura I, Funahasm T, Takahashi M, Maeda K, Kotani K, Nakamura T, et al. Enhanced expression of PAI–1 in visceral fat: Possible contributor to vascular disease in obeisty. Nat Med. 1996;2(7):800-3.
112. Côté M, Mauriège P, Bergeron J, Alméras N, Tremblay A, Lemieux I, et al. Adiponectinemia in visceral obesity: impact on glucose tolerance and plasma lipoprotein and lipid levels in men. J Clin Endocrinol Metab. 2005;90(3):1434-9.
113. Fontana L, Eagon JC, Trujillo ME, Scherer PE, Klein S. Visceral fat adipokine secretion is associated with systemic inflammation in obese humans. Diabetes. 2007;56(4):1010-3.
114. Eguchi Y, Eguchi T, Mizuta T, Ide Y, Yasutake T, Iwakiri R, et al. Visceral fat accumulation and insulin resistance are important factors in nonalcoholic fatty liver disease. J Gastroenterol. 2006;41(5):462-9.
115. Lee HW, Kim KJ, Jung KS, Chon YE, Huh JH, Park KH, et al. The relationship between visceral obesity and hepatic steatosis measured by controlled attenuation parameter. PLoS ONE. 2017;12(10):e0187066.
116. Bouchi R, Takeuchi T, Akihisa M, Ohara N, Nakano Y, Nishitani R, et al. Increased visceral adiposity with normal weight is associated with the prevalence of non‐alcoholic fatty liver disease in Japanese patients with type 2 diabetes. J Diabetes Investig. 2016;7(4):607-14.

117. van der Poorten D, Milner KL, Hui J, Hodge A, Trenell MI, Kench JG, et al. Visceral fat: a key mediator of steatohepatitis in metabolic liver disease. Hepatology. 2008;48(2):449-57.
118. Ebbert JO, Jensen MD. Fat depots, free fatty acids, and dyslipidemia. Nutrients. 2013;5(2):498-508.
119. Vanni E, Bugianesi E, Kotronen A, De Minicis S, Yki-Järvinen H, Svegliati-Baroni G. From the metabolic syndrome to NAFLD or vice versa? Dig Liver Dis. 2010;42(5):320-30.
120. Singh RG, Yoon HD, Wu LM, Lu J, Plank LD, Petrov MS. Ectopic fat accumulation in the pancreas and its clinical relevance: a systematic review, meta-analysis, and meta-regression. Metabolism. 2017;69:1-13.
121. Bi Y, Wang JL, Li ML, Zhou J, Sun XL. The association between pancreas steatosis and metabolic syndrome: A systematic review and meta‐analysis. Diabetes Metab Res Rev. 2019;35(5):e3142.
122. Saisho Y. Pancreas volume and fat deposition in diabetes and normal physiology: consideration of the interplay between endocrine and exocrine pancreas. The review of diabetic studies: RDS. 2016;13(2-3):132-47.
123. Majumder S, Philip NA, Takahashi N, Levy MJ, Singh VP, Chari ST. Fatty pancreas: should we be concerned? Pancreas. 2017;46(10):1251-8.
124. Heni M, Machann J, Staiger H, Schwenzer NF, Peter A, Schick F, et al. Pancreatic fat is negatively associated with insulin secretion in individuals with impaired fasting glucose and/or impaired glucose tolerance: a nuclear magnetic resonance study. Diabetes Metab Res Rev. 2010;26(3):200-5.
125. Tushuizen ME, Bunck MC, Pouwels PJ, Bontemps S, Van Waesberghe JHT, Schindhelm RK, et al. Pancreatic fat content and β-cell function in men with and without type 2 diabetes. Diabetes Care. 2007;30(11):2916-21.
126. Smits MM, Van Geenen EJ. The clinical significance of pancreatic steatosis. Nature reviews Gastroenterology & hepatology. 2011;8(3):169-77.
127. Takahashi M, Hori M, Ishigamori R, Mutoh M, Imai T, Nakagama H. Fatty pancreas: A possible risk factor for pancreatic cancer in animals and humans. Cancer Sci. 2018;109(10):3013-23.
128. van Raalte DH, van der Zijl NJ, Diamant M. Pancreatic steatosis in humans: cause or marker of lipotoxicity? Current Opinion in Clinical Nutrition & Metabolic Care. 2010;13(4):478-85.
129. Cnop M, Hannaert JC, Hoorens A, Eizirik DL, Pipeleers DG. Inverse relationship between cytotoxicity of free fatty acids in pancreatic islet cells and cellular triglyceride accumulation. Diabetes. 2001;50(8):1771-7.
130. Listenberger LL, Han X, Lewis SE, Cases S, Farese RV, Ory DS, et al. Triglyceride accumulation protects against fatty acid-induced lipotoxicity. Proceedings of the National Academy of Sciences. 2003;100(6):3077-82.
131. Oh YS, Bae GD, Baek DJ, Park E-Y, Jun H-S. Fatty acid-induced lipotoxicity in pancreatic beta-cells during development of type 2 diabetes. Frontiers in endocrinology. 2018;9:384.
132. Gerst F, Wagner R, Oquendo MB, Siegel-Axel D, Fritsche A, Heni M, et al. What role do fat cells play in pancreatic tissue? Molecular metabolism. 2019;25:1-10.
133. Gerst F, Wagner R, Kaiser G, Panse M, Heni M, Machann J, et al. Metabolic crosstalk between fatty pancreas and fatty liver: effects on local inflammation and insulin secretion. Diabetologia. 2017;60(11):2240-51.

134. Liu LF, Craig CM, Tolentino LL, Choi O, Morton J, Rivas H, et al. Adipose tissue macrophages impair preadipocyte differentiation in humans. PLoS ONE. 2017;12(2):e0170728.
135. Jaghutriz B, Wagner R, Machann J, Stefan N, Peter A, Siegel-Axel DI, et al. Association of Pancreas Fat with Impaired Insulin Secretion Depends on Liver Fat and Circulating Fatty Acids. Am Diabetes Assoc; 2018.
136. Junot C, Fenaille F, Colsch B, Bécher F. High resolution mass spectrometry based techniques at the crossroads of metabolic pathways. Mass Spectrom Rev. 2014;33(6):471-500.
137. Nicholson JK, Lindon JC. Metabonomics. Nature. 2008;455(7216):1054-6.
138. Misra BB, Langefeld C, Olivier M, Cox LA. Integrated omics: tools, advances and future approaches. J Mol Endocrinol. 2019;62(1):R21-R45.
139. Holmes E, Wilson ID, Nicholson JK. Metabolic phenotyping in health and disease. Cell. 2008;134(5):714-7.
140. Nicholson JK. Global systems biology, personalized medicine and molecular epidemiology. Mol Syst Biol. 2006;2(1):52.
141. Du F, Virtue A, Wang H, Yang X-F. Metabolomic analyses for atherosclerosis, diabetes, and obesity. Biomarker research. 2013;1(1):1-17.
142. Urpi-Sarda M, Almanza-Aguilera E, Tulipani S, Tinahones FJ, Salas-Salvadó J, Andres-Lacueva C. Metabolomics for biomarkers of type 2 diabetes mellitus: advances and nutritional intervention trends. Current cardiovascular risk reports. 2015;9(3):12.
143. Xie B, Waters MJ, Schirra HJ. Investigating potential mechanisms of obesity by metabolomics. BioMed Research International. 2012;2012.
144. Sas KM, Karnovsky A, Michailidis G, Pennathur S. Metabolomics and diabetes: analytical and computational approaches. Diabetes. 2015;64(3):718-32.
145. Dudley E, Yousef M, Wang Y, Griffiths W. Targeted metabolomics and mass spectrometry. Advances in protein chemistry and structural biology. 80: Elsevier; 2010. p. 45-83.
146. Vinayavekhin N, Saghatelian A. Untargeted metabolomics. Current protocols in molecular biology. 2010;90(1):30.1. 1-.1. 24.
147. Patti GJ. Separation strategies for untargeted metabolomics. J Sep Sci. 2011;34(24):3460-9.
148. Lu W, Su X, Klein MS, Lewis IA, Fiehn O, Rabinowitz JD. Metabolite measurement: pitfalls to avoid and practices to follow. Annu Rev Biochem. 2017;86:277-304.
149. Lu W, Bennett BD, Rabinowitz JD. Analytical strategies for LC–MS-based targeted metabolomics. Journal of chromatography B. 2008;871(2):236-42.
150. Azad RK, Shulaev V. Metabolomics technology and bioinformatics for precision medicine. Brief Bioinform. 2019;20(6):1957-71.
151. Rochat B. From targeted quantification to untargeted metabolomics: Why LC-high-resolution-MS will become a key instrument in clinical labs. TrAC Trends in Analytical Chemistry. 2016;84:151-64.
152. Theodoridis G, Gika HG, Wilson ID. Mass spectrometry‐based holistic analytical approaches for metabolite profiling in systems biology studies. Mass Spectrom Rev. 2011;30(5):884-906.

153. Ivanisevic J, Want EJ. From samples to insights into metabolism: Uncovering biologically relevant information in LC-HRMS metabolomics data. Metabolites. 2019;9(12):308.
154. Smith CA, Want EJ, O'Maille G, Abagyan R, Siuzdak G. XCMS: processing mass spectrometry data for metabolite profiling using nonlinear peak alignment, matching, and identification. Anal Chem. 2006;78(3):779-87.
155. Ni Y, Su M, Qiu Y, Jia W, Du X. ADAP-GC 3.0: improved peak detection and deconvolution of co-eluting metabolites from GC/TOF-MS data for metabolomics studies. Anal Chem. 2016;88(17):8802-11.
156. Giacomoni F, Le Corguillé G, Monsoor M, Landi M, Pericard P, Pétéra M, et al. Workflow4Metabolomics: a collaborative research infrastructure for computational metabolomics. Bioinformatics. 2015;31(9):1493-5.
157. Katajamaa M, Miettinen J, Orešič M. MZmine: toolbox for processing and visualization of mass spectrometry based molecular profile data. Bioinformatics. 2006;22(5):634-6.
158. Pang Z, Chong J, Li S, Xia J. MetaboAnalystR 3.0: Toward an Optimized Workflow for Global Metabolomics. Metabolites. 2020;10(5):186.
159. Tsugawa H, Cajka T, Kind T, Ma Y, Higgins B, Ikeda K, et al. MS-DIAL: data-independent MS/MS deconvolution for comprehensive metabolome analysis. Nat Methods. 2015;12(6):523-6.
160. Broadhurst D, Goodacre R, Reinke SN, Kuligowski J, Wilson ID, Lewis MR, et al. Guidelines and considerations for the use of system suitability and quality control samples in mass spectrometry assays applied in untargeted clinical metabolomic studies. Metabolomics. 2018;14(6):1-17.
161. Wishart DS, Feunang YD, Marcu A, Guo AC, Liang K, Vázquez-Fresno R, et al. HMDB 4.0: the human metabolome database for 2018. Nucleic Acids Res. 2018;46(D1):D608-D17.
162. Guijas C, Montenegro-Burke JR, Domingo-Almenara X, Palermo A, Warth B, Hermann G, et al. METLIN: a technology platform for identifying knowns and unknowns. Anal Chem. 2018;90(5):3156-64.
163. Fahy E, Sud M, Cotter D, Subramaniam S. LIPID MAPS online tools for lipid research. Nucleic Acids Res. 2007;35(suppl_2):W606-W12.
164. Rangel-Huerta OD, Pastor-Villaescusa B, Gil A. Are we close to defining a metabolomic signature of human obesity? A systematic review of metabolomics studies. Metabolomics. 2019;15(6):1-31.
165. Weir JM, Wong G, Barlow CK, Greeve MA, Kowalczyk A, Almasy L, et al. Plasma lipid profiling in a large population-based cohort. J Lipid Res. 2013;54(10):2898-908.
166. Anderson SG, Dunn WB, Banerjee M, Brown M, Broadhurst DI, Goodacre R, et al. Evidence that multiple defects in lipid regulation occur before hyperglycemia during the prodrome of type-2 diabetes. PLoS ONE. 2014;9(9):e103217.
167. Meikle PJ, Wong G, Barlow CK, Weir JM, Greeve MA, MacIntosh GL, et al. Plasma lipid profiling shows similar associations with prediabetes and type 2 diabetes. PLoS ONE. 2013;8(9):e74341.
168. Graessler J, Schwudke D, Schwarz PE, Herzog R, Shevchenko A, Bornstein SR. Top-down lipidomics reveals ether lipid deficiency in blood plasma of hypertensive patients. PLoS ONE. 2009;4(7):e6261.
169. Begum H, Torta F, Narayanaswamy P, Mundra PA, Ji S, Bendt AK, et al. Lipidomic profiling of plasma in a healthy Singaporean population to identify

ethnic specific differences in lipid levels and associations with disease risk factors. Clinical Mass Spectrometry. 2017;6:25-31.
170. Rai S, Bhatnagar S. Novel lipidomic biomarkers in hyperlipidemia and cardiovascular diseases: an integrative biology analysis. Omics: a journal of integrative biology. 2017;21(3):132-42.
171. Im S-S, Park HY, Shon JC, Chung I-S, Cho HC, Liu K-H, et al. Plasma sphingomyelins increase in pre-diabetic Korean men with abdominal obesity. PLoS ONE. 2019;14(3):e0213285.
172. Szymańska E, Bouwman J, Strassburg K, Vervoort J, Kangas AJ, Soininen P, et al. Gender-dependent associations of metabolite profiles and body fat distribution in a healthy population with central obesity: towards metabolomics diagnostics. Omics: a journal of integrative biology. 2012;16(12):652-67.
173. Orešič M, Hyötyläinen T, Kotronen A, Gopalacharyulu P, Nygren H, Arola J, et al. Prediction of non-alcoholic fatty-liver disease and liver fat content by serum molecular lipids. Diabetologia. 2013;56(10):2266-74.
174. Mayo R, Crespo J, Martínez‐Arranz I, Banales JM, Arias M, Mincholé I, et al. Metabolomic‐based noninvasive serum test to diagnose nonalcoholic steatohepatitis: Results from discovery and validation cohorts. Hepatology communications. 2018;2(7):807-20.
175. Rhee EP, Cheng S, Larson MG, Walford GA, Lewis GD, McCabe E, et al. Lipid profiling identifies a triacylglycerol signature of insulin resistance and improves diabetes prediction in humans. The Journal of clinical investigation. 2011;121(4):1402-11.
176. Stegemann C, Pechlaner R, Willeit P, Langley SR, Mangino M, Mayr U, et al. Lipidomics profiling and risk of cardiovascular disease in the prospective population-based Bruneck study. Circulation. 2014;129(18):1821-31.
177. Schwab U, Seppänen-Laakso T, Yetukuri L, Ågren J, Kolehmainen M, Laaksonen DE, et al. Triacylglycerol fatty acid composition in diet-induced weight loss in subjects with abnormal glucose metabolism–the GENOBIN study. PLoS ONE. 2008;3(7):e2630.
178. Gerl MJ, Klose C, Surma MA, Fernandez C, Melander O, Männistö S, et al. Machine learning of human plasma lipidomes for obesity estimation in a large population cohort. PLoS Biol. 2019;17(10):e3000443.
179. Bachlechner U, Floegel A, Steffen A, Prehn C, Adamski J, Pischon T, et al. Associations of anthropometric markers with serum metabolites using a targeted metabolomics approach: results of the EPIC-potsdam study. Nutrition & Diabetes. 2016;6(6):e215.
180. Bagheri M, Djazayery A, Farzadfar F, Qi L, Yekaninejad MS, Aslibekyan S, et al. Plasma metabolomic profiling of amino acids and polar lipids in Iranian obese adults. Lipids Health Dis. 2019;18(1):1-9.
181. Bagheri M, Farzadfar F, Qi L, Yekaninejad MS, Chamari M, Zeleznik OA, et al. Obesity-related metabolomic profiles and discrimination of metabolically unhealthy obesity. J Proteome Res. 2018;17(4):1452-62.
182. Yin X, Willinger CM, Keefe J, Liu J, Fernández-Ortiz A, Ibáñez B, et al. Lipidomic profiling identifies signatures of metabolic risk. EBioMedicine. 2020;51:102520.
183. Suhre K, Meisinger C, Döring A, Altmaier E, Belcredi P, Gieger C, et al. Metabolic footprint of diabetes: a multiplatform metabolomics study in an epidemiological setting. PLoS ONE. 2010;5(11):e13953.

184. Xu F, Tavintharan S, Sum CF, Woon K, Lim SC, Ong CN. Metabolic signature shift in type 2 diabetes mellitus revealed by mass spectrometry-based metabolomics. J Clin Endocrinol Metab. 2013;98(6):E1060-E5.
185. Yang SJ, Kwak S-Y, Jo G, Song T-J, Shin M-J. Serum metabolite profile associated with incident type 2 diabetes in Koreans: findings from the Korean Genome and Epidemiology Study. Scientific reports. 2018;8(1):1-10.
186. Floegel A, Stefan N, Yu Z, Mühlenbruch K, Drogan D, Joost H-G, et al. Identification of serum metabolites associated with risk of type 2 diabetes using a targeted metabolomic approach. Diabetes. 2013;62(2):639-48.
187. Suvitaival T, Bondia-Pons I, Yetukuri L, Pöhö P, Nolan JJ, Hyötyläinen T, et al. Lipidome as a predictive tool in progression to type 2 diabetes in Finnish men. Metabolism. 2018;78:1-12.
188. Zhao J, Zhu Y, Hyun N, Zeng D, Uppal K, Tran VT, et al. Novel metabolic markers for the risk of diabetes development in American Indians. Diabetes Care. 2015;38(2):220-7.
189. Razquin C, Toledo E, Clish CB, Ruiz-Canela M, Dennis C, Corella D, et al. Plasma lipidomic profiling and risk of type 2 diabetes in the PREDIMED trial. Diabetes Care. 2018;41(12):2617-24.
190. Wang C, Kong H, Guan Y, Yang J, Gu J, Yang S, et al. Plasma phospholipid metabolic profiling and biomarkers of type 2 diabetes mellitus based on high-performance liquid chromatography/electrospray mass spectrometry and multivariate statistical analysis. Anal Chem. 2005;77(13):4108-16.
191. Cole LK, Vance JE, Vance DE. Phosphatidylcholine biosynthesis and lipoprotein metabolism. Biochimica et biophysica acta Molecular and cell biology of lipids. 2012;1821(5):754-61.
192. Pickens CA, Jones D, Fenton JI. Obesity is associated with distinct changes in the human plasma phospholipidome. FASEB J. 2016;30(1 Supplement):271-7.
193. Pietiläinen KH, Róg T, Seppänen-Laakso T, Virtue S, Gopalacharyulu P, Tang J, et al. Association of lipidome remodeling in the adipocyte membrane with acquired obesity in humans. PLoS Biol. 2011;9(6):e1000623.
194. Tulipani S, Palau-Rodriguez M, Alonso AM, Cardona F, Marco-Ramell A, Zonja B, et al. Biomarkers of morbid obesity and prediabetes by metabolomic profiling of human discordant phenotypes. Clin Chim Acta. 2016;463:53-61.
195. Donovan EL, Pettine SM, Hickey MS, Hamilton KL, Miller BF. Lipidomic analysis of human plasma reveals ether-linked lipids that are elevated in morbidly obese humans compared to lean. Diabetol Metab Syndr. 2013;5(1):1-13.
196. Brosche T, Platt D. The biological significance of plasmalogens in defense against oxidative damage. Exp Gerontol. 1998;33(5):363-9.
197. Brosche T. Plasmalogen phospholipids—facts and theses to their antioxidative qualities. Arch Gerontol Geriatr. 1997;25(1):73-81.
198. Braverman NE, Moser AB. Functions of plasmalogen lipids in health and disease. Biochimica et biophysica acta Molecular basis of disease. 2012;1822(9):1442-52.
199. Garti N, Lichtenberg D, Silberstein T. The hydrolysis of phosphatidylcholine by phospholipase A2 in microemulsion as microreactor. Colloids and Surfaces A: Physicochemical and Engineering Aspects. 1997;128(1-3):17-25.
200. Goyal J, Wang K, Liu M, Subbaiah PV. Novel Function of Lecithin-Cholesterol Acyltransferase HYDROLYSIS OF OXIDIZED POLAR

PHOSPHOLIPIDS GENERATED DURING LIPOPROTEIN OXIDATION. J Biol Chem. 1997;272(26):16231-9.
201. Ha CY, Kim JY, Paik JK, Kim OY, Paik YH, Lee EJ, et al. The association of specific metabolites of lipid metabolism with markers of oxidative stress, inflammation and arterial stiffness in men with newly diagnosed type 2 diabetes. Clin Endocrinol (Oxf). 2012;76(5):674-82.
202. Ho JE, Larson MG, Ghorbani A, Cheng S, Chen M-H, Keyes M, et al. Metabolomic profiles of body mass index in the Framingham Heart Study reveal distinct cardiometabolic phenotypes. PLoS ONE. 2016;11(2):e0148361.
203. Heimerl S, Fischer M, Baessler A, Liebisch G, Sigruener A, Wallner S, et al. Alterations of plasma lysophosphatidylcholine species in obesity and weight loss. PLoS ONE. 2014;9(10):e111348.
204. Cirulli ET, Guo L, Swisher CL, Shah N, Huang L, Napier LA, et al. Profound perturbation of the metabolome in obesity is associated with health risk. Cell Metab. 2019;29(2):488-500.
205. Moore SC, Matthews CE, Sampson JN, Stolzenberg-Solomon RZ, Zheng W, Cai Q, et al. Human metabolic correlates of body mass index. Metabolomics. 2014;10(2):259-69.
206. Kim JY, Park JY, Kim OY, Ham BM, Kim H-J, Kwon DY, et al. Metabolic profiling of plasma in overweight/obese and lean men using ultra performance liquid chromatography and Q-TOF mass spectrometry (UPLC− Q-TOF MS). J Proteome Res. 2010;9(9):4368-75.
207. Stroeve JH, Saccenti E, Bouwman J, Dane A, Strassburg K, Vervoort J, et al. Weight loss predictability by plasma metabolic signatures in adults with obesity and morbid obesity of the D i OG enes study. Obesity. 2016;24(2):379-88.
208. Wang Y, Liu D, Li Y, Guo L, Cui Y, Zhang X, et al. Metabolomic analysis of serum from obese adults with hyperlipemia by UHPLC‐Q‐TOF MS/MS. Biomed Chromatogr. 2016;30(1):48-54.
209. Pietiläinen KH, Sysi-Aho M, Rissanen A, Seppänen-Laakso T, Yki-Järvinen H, Kaprio J, et al. Acquired obesity is associated with changes in the serum lipidomic profile independent of genetic effects–a monozygotic twin study. PLoS ONE. 2007;2(2):e218.
210. Heilbronn LK, Coster AC, Campbell LV, Greenfield JR, Lange K, Christopher MJ, et al. The effect of short‐term overfeeding on serum lipids in healthy humans. Obesity. 2013;21(12):E649-E59.
211. Wang‐Sattler R, Yu Z, Herder C, Messias AC, Floegel A, He Y, et al. Novel biomarkers for pre‐diabetes identified by metabolomics. Mol Syst Biol. 2012;8(1):615.
212. Ferrannini E, Natali A, Camastra S, Nannipieri M, Mari A, Adam K-P, et al. Early metabolic markers of the development of dysglycemia and type 2 diabetes and their physiological significance. Diabetes. 2013;62(5):1730-7.
213. Warensjö E, Rosell M, Hellenius M-L, Vessby B, De Faire U, Risérus U. Associations between estimated fatty acid desaturase activities in serum lipids and adipose tissue in humans: links to obesity and insulin resistance. Lipids Health Dis. 2009;8(1):1-6.
214. Pickens CA, Sordillo LM, Comstock SS, Harris WS, Hortos K, Kovan B, et al. Plasma phospholipids, non-esterified plasma polyunsaturated fatty acids and oxylipids are associated with BMI. Prostaglandins, Leukotrienes and Essential Fatty Acids. 2015;95:31-40.

215. Zhou YE, Kubow S, Dewailly E, Julien P, Egeland GM. Decreased activity of desaturase 5 in association with obesity and insulin resistance aggravates declining long-chain n-3 fatty acid status in Cree undergoing dietary transition. Br J Nutr. 2009;102(6):888-94.
216. Fekete K, Györei E, Lohner S, Verduci E, Agostoni C, Decsi T. Long‐chain polyunsaturated fatty acid status in obesity: a systematic review and meta‐analysis. Obes Rev. 2015;16(6):488-97.
217. Ni Y, Zhao L, Yu H, Ma X, Bao Y, Rajani C, et al. Circulating unsaturated fatty acids delineate the metabolic status of obese individuals. EBioMedicine. 2015;2(10):1513-22.
218. Newgard CB, An J, Bain JR, Muehlbauer MJ, Stevens RD, Lien LF, et al. A branched-chain amino acid-related metabolic signature that differentiates obese and lean humans and contributes to insulin resistance. Cell Metab. 2009;9(4):311-26.
219. Menni C, Migaud M, Glastonbury CA, Beaumont M, Nikolaou A, Small KS, et al. Metabolomic profiling to dissect the role of visceral fat in cardiometabolic health. Obesity. 2016;24(6):1380-8.
220. Galuszka J, Vostalova J, Cervena B, Galuszkova D, Simanek V, Holcapek M, et al. Omega‐3 fatty acid supplementation candidates can be selected using fatty acid profiling. European Journal of Lipid Science and Technology. 2015;117(5):601-7.
221. Bi X, Yeo PLQ, Loo YT, Henry CJ. Associations between circulating fatty acid levels and metabolic risk factors. Journal of Nutrition & Intermediary Metabolism. 2019;15:65-9.
222. Li X, Xu Z, Lu X, Yang X, Yin P, Kong H, et al. Comprehensive two-dimensional gas chromatography/time-of-flight mass spectrometry for metabonomics: Biomarker discovery for diabetes mellitus. Anal Chim Acta. 2009;633(2):257-62.
223. Menni C, Fauman E, Erte I, Perry JR, Kastenmüller G, Shin S-Y, et al. Biomarkers for type 2 diabetes and impaired fasting glucose using a nontargeted metabolomics approach. Diabetes. 2013;62(12):4270-6.
224. Fiehn O, Garvey WT, Newman JW, Lok KH, Hoppel CL, Adams SH. Plasma metabolomic profiles reflective of glucose homeostasis in non-diabetic and type 2 diabetic obese African-American women. PLoS ONE. 2010;5(12):e15234.
225. Mahendran Y, Cederberg H, Vangipurapu J, Kangas AJ, Soininen P, Kuusisto J, et al. Glycerol and fatty acids in serum predict the development of hyperglycemia and type 2 diabetes in Finnish men. Diabetes Care. 2013;36(11):3732-8.
226. Würtz P, Tiainen M, Mäkinen V-P, Kangas AJ, Soininen P, Saltevo J, et al. Circulating metabolite predictors of glycemia in middle-aged men and women. Diabetes Care. 2012;35(8):1749-56.
227. Perez-Cornago A, Brennan L, Ibero-Baraibar I, Hermsdorff HHM, O'Gorman A, Zulet M, et al. Metabolomics identifies changes in fatty acid and amino acid profiles in serum of overweight older adults following a weight loss intervention. J Physiol Biochem. 2014;70(2):593-602.
228. Lee YJ, Lee A, Yoo HJ, Kim M, Kim M, Jee SH, et al. Effect of weight loss on circulating fatty acid profiles in overweight subjects with high visceral fat area: a 12-week randomized controlled trial. Nutr J. 2018;17(1):1-14.

229. Mihalik SJ, Goodpaster BH, Kelley DE, Chace DH, Vockley J, Toledo FG, et al. Increased levels of plasma acylcarnitines in obesity and type 2 diabetes and identification of a marker of glucolipotoxicity. Obesity. 2010;18(9):1695-700.
230. Adams SH, Hoppel CL, Lok KH, Zhao L, Wong SW, Minkler PE, et al. Plasma acylcarnitine profiles suggest incomplete long-chain fatty acid β-oxidation and altered tricarboxylic acid cycle activity in type 2 diabetic African-American women. J Nutr. 2009;139(6):1073-81.
231. Koves TR, Ussher JR, Noland RC, Slentz D, Mosedale M, Ilkayeva O, et al. Mitochondrial overload and incomplete fatty acid oxidation contribute to skeletal muscle insulin resistance. Cell Metab. 2008;7(1):45-56.
232. Koves TR, Li P, An J, Akimoto T, Slentz D, Ilkayeva O, et al. Peroxisome proliferator-activated receptor-γ co-activator 1α-mediated metabolic remodeling of skeletal myocytes mimics exercise training and reverses lipid-induced mitochondrial inefficiency. J Biol Chem. 2005;280(39):33588-98.
233. Torretta E, Barbacini P, Al-Daghri NM, Gelfi C. Sphingolipids in Obesity and Correlated Co-Morbidities: The Contribution of Gender, Age and Environment. Int J Mol Sci. 2019;20(23):5901.
234. Larsen PJ, Tennagels N. On ceramides, other sphingolipids and impaired glucose homeostasis. Molecular metabolism. 2014;3(3):252-60.
235. Hanamatsu H, Ohnishi S, Sakai S, Yuyama K, Mitsutake S, Takeda H, et al. Altered levels of serum sphingomyelin and ceramide containing distinct acyl chains in young obese adults. Nutrition & diabetes. 2014;4(10):e141.
236. Mamtani M, Meikle PJ, Kulkarni H, Weir JM, Barlow CK, Jowett JB, et al. Plasma dihydroceramide species associate with waist circumference in Mexican American families. Obesity. 2014;22(3):950-6.
237. Yano M, Watanabe K, Yamamoto T, Ikeda K, Senokuchi T, Lu M, et al. Mitochondrial dysfunction and increased reactive oxygen species impair insulin secretion in sphingomyelin synthase 1-null mice. J Biol Chem. 2011;286(5):3992-4002.
238. Haus JM, Kashyap SR, Kasumov T, Zhang R, Kelly KR, DeFronzo RA, et al. Plasma ceramides are elevated in obese subjects with type 2 diabetes and correlate with the severity of insulin resistance. Diabetes. 2009;58(2):337-43.
239. Samad F, Hester KD, Yang G, Hannun YA, Bielawski J. Altered adipose and plasma sphingolipid metabolism in obesity: a potential mechanism for cardiovascular and metabolic risk. Diabetes. 2006;55(9):2579-87.
240. Chew WS, Torta F, Ji S, Choi H, Begum H, Sim X, et al. Large-scale lipidomics identifies associations between plasma sphingolipids and T2DM incidence. JCI insight. 2019;4(13):e126925.
241. Zheng W, Kollmeyer J, Symolon H, Momin A, Munter E, Wang E, et al. Ceramides and other bioactive sphingolipid backbones in health and disease: lipidomic analysis, metabolism and roles in membrane structure, dynamics, signaling and autophagy. Biochimica et Biophysica Acta (BBA)-Biomembranes. 2006;1758(12):1864-84.
242. Grösch S, Schiffmann S, Geisslinger G. Chain length-specific properties of ceramides. Prog Lipid Res. 2012;51(1):50-62.
243. Felig P, Marliss E, Cahill Jr GF. Plasma amino acid levels and insulin secretion in obesity. N Engl J Med. 1969;281(15):811-6.
244. Adeva MM, Calviño J, Souto G, Donapetry C. Insulin resistance and the metabolism of branched-chain amino acids in humans. Amino Acids. 2012;43(1):171-81.

245. Xie G, Ma X, Zhao A, Wang C, Zhang Y, Nieman D, et al. The metabolite profiles of the obese population are gender-dependent. J Proteome Res. 2014;13(9):4062-73.
246. Wang S, Yang R, Wang M, Ji F, Li H, Tang Y, et al. Identification of serum metabolites associated with obesity and traditional risk factors for metabolic disease in Chinese adults. Nutr Metab Cardiovasc Dis. 2018;28(2):112-8.
247. Foerster J, Hyötyläinen T, Oresic M, Nygren H, Boeing H. Serum Lipid and Serum Metabolite Components in relation to anthropometric parameters in EPIC-Potsdam participants. Metabolism. 2015;64(10):1348-58.
248. Pietzner M, Budde K, Homuth G, Kastenmüller G, Henning A-K, Artati A, et al. Hepatic steatosis is associated with adverse molecular signatures in subjects without diabetes. J Clin Endocrinol Metab. 2018;103(10):3856-68.
249. Neeland IJ, Boone SC, Mook‐Kanamori DO, Ayers C, Smit RA, Tzoulaki I, et al. Metabolomics Profiling of Visceral Adipose Tissue: Results From MESA and the NEO Study. J Am Heart Assoc. 2019;8(9):e010810.
250. Geidenstam N, Al-Majdoub M, Ekman M, Spégel P, Ridderstråle M. Metabolite profiling of obese individuals before and after a one year weight loss program. Int J Obes. 2017;41(9):1369-78.
251. Zheng Y, Ceglarek U, Huang T, Li L, Rood J, Ryan DH, et al. Weight-loss diets and 2-y changes in circulating amino acids in 2 randomized intervention trials–3. Am J Clin Nutr. 2016;103(2):505-11.
252. Wang TJ, Larson MG, Vasan RS, Cheng S, Rhee EP, McCabe E, et al. Metabolite profiles and the risk of developing diabetes. Nat Med. 2011;17(4):448-53.
253. Shah S, Crosslin D, Haynes C, Nelson S, Turer C, Stevens R, et al. Branched-chain amino acid levels are associated with improvement in insulin resistance with weight loss. Diabetologia. 2012;55(2):321-30.
254. Badoud F, Lam KP, DiBattista A, Perreault M, Zulyniak MA, Cattrysse B, et al. Serum and adipose tissue amino acid homeostasis in the metabolically healthy obese. J Proteome Res. 2014;13(7):3455-66.
255. Batch BC, Shah SH, Newgard CB, Turer CB, Haynes C, Bain JR, et al. Branched chain amino acids are novel biomarkers for discrimination of metabolic wellness. Metabolism. 2013;62(7):961-9.
256. Boulet MM, Chevrier G, Grenier-Larouche T, Pelletier M, Nadeau M, Scarpa J, et al. Alterations of plasma metabolite profiles related to adipose tissue distribution and cardiometabolic risk. American Journal of Physiology-Endocrinology and Metabolism. 2015;309(8):E736-E46.
257. Herman MA, She P, Peroni OD, Lynch CJ, Kahn BB. Adipose tissue branched chain amino acid (BCAA) metabolism modulates circulating BCAA levels. J Biol Chem. 2010;285(15):11348-56.
258. Butte NF, Liu Y, Zakeri IF, Mohney RP, Mehta N, Voruganti VS, et al. Global metabolomic profiling targeting childhood obesity in the Hispanic population. Am J Clin Nutr. 2015;102(2):256-67.
259. Tai E, Tan M, Stevens R, Low Y, Muehlbauer M, Goh D, et al. Insulin resistance is associated with a metabolic profile of altered protein metabolism in Chinese and Asian-Indian men. Diabetologia. 2010;53(4):757-67.
260. Yamada C, Kondo M, Kishimoto N, Shibata T, Nagai Y, Imanishi T, et al. Association between insulin resistance and plasma amino acid profile in non‐diabetic Japanese subjects. J Diabetes Investig. 2015;6(4):408-15.

261. Chen T, Ni Y, Ma X, Bao Y, Liu J, Huang F, et al. Branched-chain and aromatic amino acid profiles and diabetes risk in Chinese populations. Scientific reports. 2016;6(1):1-8.
262. Würtz P, Soininen P, Kangas AJ, Rönnemaa T, Lehtimäki T, Kähönen M, et al. Branched-chain and aromatic amino acids are predictors of insulin resistance in young adults. Diabetes Care. 2013;36(3):648-55.
263. Chen H, Tseng Y, Wang S, Tsai Y, Chang C, Kuo T, et al. The metabolome profiling and pathway analysis in metabolic healthy and abnormal obesity. Int J Obes. 2015;39(8):1241-8.
264. Fernstrom MH, Volk EA, Fernstrom JD. In vivo inhibition of tyrosine uptake into rat retina by large neutral but not acidic amino acids. American Journal of Physiology-Endocrinology and Metabolism. 1986;251(4):E393-E9.
265. Haufe S, Witt H, Engeli S, Kaminski J, Utz W, Fuhrmann J, et al. Branched-chain and aromatic amino acids, insulin resistance and liver specific ectopic fat storage in overweight to obese subjects. Nutr Metab Cardiovasc Dis. 2016;26(7):637-42.
266. Martin F-PJ, Montoliu I, Collino S, Scherer M, Guy P, Tavazzi I, et al. Topographical body fat distribution links to amino acid and lipid metabolism in healthy non-obese women. PLoS ONE. 2013;8(9):e73445.
267. Hargrove JL. Persulfide generated from L-cysteine inactivates tyrosine aminotransferase. Requirement for a protein with cysteine oxidase activity and gamma-cystathionase. J Biol Chem. 1988;263(33):17262-9.
268. Buckley WT, Milligan LP. Participation of cysteine and cystine in inactivation of tyrosine aminotransferase in rat liver homogenates. Biochem J. 1978;176(2):449-54.
269. Hargrove J, Wichman RD. A cystine-dependent inactivator of tyrosine aminotransferase co-purifies with gamma-cystathionase (cystine desulfurase). J Biol Chem. 1987;262(15):7351-7.
270. Yamanishi T, Tuboi S. The mechanism of the L-cystine cleavage reaction catalyzed by rat liver γ-cystathionase. The Journal of Biochemistry. 1981;89(6):1913-21.
271. Vitvitsky V, Mosharov E, Tritt M, Ataullakhanov F, Banerjee R. Redox regulation of homocysteine-dependent glutathione synthesis. Redox report. 2003;8(1):57-63.
272. de Castro NM, Yaqoob P, De la Fuente M, Baeza I, Claus SP. Premature impairment of methylation pathway and cardiac metabolic dysfunction in fa/fa obese zucker rats. J Proteome Res. 2013;12(4):1935-45.
273. Hargrove JL, Trotter JF, Ashline HC, Krishnamurti P. Experimental diabetes increases the formation of sulfane by transsulfuration and inactivation of tyrosine aminotransferase in cytosols from rat liver. Metabolism. 1989;38(7):666-72.
274. Jacobs RL, Stead LM, Brosnan ME, Brosnan JT. Hyperglucagonemia in rats results in decreased plasma homocysteine and increased flux through the transsulfuration pathway in liver. J Biol Chem. 2001;276(47):43740-7.
275. Swierczynski J, Sledzinski T, Slominska E, Smolenski R, Sledzinski Z. Serum phenylalanine concentration as a marker of liver function in obese patients before and after bariatric surgery. Obes Surg. 2009;19(7):883-9.
276. Goessling W, Massaro JM, Vasan RS, D'Agostino RB, Ellison RC, Fox CS. Aminotransferase levels and 20-year risk of metabolic syndrome, diabetes, and cardiovascular disease. Gastroenterology. 2008;135(6):1935-44.

277. Mohorko N, Petelin A, Jurdana M, Biolo G, Jenko-Pražnikar Z. Elevated serum levels of cysteine and tyrosine: early biomarkers in asymptomatic adults at increased risk of developing metabolic syndrome. BioMed research international. 2015;2015.
278. Elshorbagy AK, Kozich V, Smith AD, Refsum H. Cysteine and obesity: consistency of the evidence across epidemiologic, animal and cellular studies. Current Opinion in Clinical Nutrition & Metabolic Care. 2012;15(1):49-57.
279. Gall WE, Beebe K, Lawton KA, Adam K-P, Mitchell MW, Nakhle PJ, et al. α-Hydroxybutyrate is an early biomarker of insulin resistance and glucose intolerance in a nondiabetic population. PLoS ONE. 2010;5(5):e10883.
280. El-Khairy L, Ueland PM, Nygård O, Refsum H, Vollset SE. Lifestyle and cardiovascular disease risk factors as determinants of total cysteine in plasma: the Hordaland Homocysteine Study. Am J Clin Nutr. 1999;70(6):1016-24.
281. Elshorbagy AK, Refsum H, Smith AD, Graham IM. The Association of Plasma Cysteine and γ‐Glutamyltransferase With BMI and Obesity. Obesity. 2009;17(7):1435-40.
282. El-Khairy L, Vollset SE, Refsum H, Ueland PM. Predictors of change in plasma total cysteine: longitudinal findings from the Hordaland homocysteine study. Clin Chem. 2003;49(1):113-20.
283. Zhao Q, Zhu Y, Best LG, Umans JG, Uppal K, Tran VT, et al. Metabolic profiles of obesity in American Indians: the strong heart family study. PLoS ONE. 2016;11(7):e0159548.
284. Carayol M, Leitzmann MF, Ferrari P, Zamora-Ros R, Achaintre D, Stepien M, et al. Blood metabolic signatures of body mass index: a targeted metabolomics study in the EPIC cohort. J Proteome Res. 2017;16(9):3137-46.
285. Wang Y, Liu H, McKenzie G, Witting PK, Stasch J-P, Hahn M, et al. Kynurenine is an endothelium-derived relaxing factor produced during inflammation. Nat Med. 2010;16(3):279-85.
286. Wolowczuk I, Hennart B, Leloire A, Bessede A, Soichot M, Taront S, et al. Tryptophan metabolism activation by indoleamine 2, 3-dioxygenase in adipose tissue of obese women: an attempt to maintain immune homeostasis and vascular tone. American Journal of Physiology-Regulatory, Integrative and Comparative Physiology. 2012;303(2):R135-R43.
287. Favennec M, Hennart B, Caiazzo R, Leloire A, Yengo L, Verbanck M, et al. The kynurenine pathway is activated in human obesity and shifted toward kynurenine monooxygenase activation. Obesity. 2015;23(10):2066-74.
288. Jürgens B, Hainz U, Fuchs D, Felzmann T, Heitger A. Interferon-γ–triggered indoleamine 2, 3-dioxygenase competence in human monocyte-derived dendritic cells induces regulatory activity in allogeneic T cells. Blood, The Journal of the American Society of Hematology. 2009;114(15):3235-43.
289. Mangge H, Summers KL, Meinitzer A, Zelzer S, Almer G, Prassl R, et al. Obesity‐related dysregulation of the Tryptophan–Kynurenine metabolism: Role of age and parameters of the metabolic syndrome. Obesity. 2014;22(1):195-201.
290. Zhao H, Shen J, Djukovic D, Daniel‐MacDougall C, Gu H, Wu X, et al. Metabolomics‐identified metabolites associated with body mass index and prospective weight gain among Mexican American women. Obesity science & practice. 2016;2(3):309-17.
291. Kraus WE, Pieper CF, Huffman KM, Thompson DK, Kraus VB, Morey MC, et al. Association of plasma small-molecule intermediate metabolites with age

and body mass index across six diverse study populations. Journals of Gerontology Series A: Biomedical Sciences and Medical Sciences. 2016;71(11):1507-13.
292. Lustgarten MS, Price LL, Phillips EM, Fielding RA. Serum glycine is associated with regional body fat and insulin resistance in functionally-limited older adults. PLoS ONE. 2013;8(12):e84034.
293. Adeva-Andany M, Souto-Adeva G, Ameneiros-Rodriguez E, Fernandez-Fernandez C, Donapetry-Garcia C, Dominguez-Montero A. Insulin resistance and glycine metabolism in humans. Amino Acids. 2018;50(1):11-27.
294. Drogan D, Dunn WB, Lin W, Buijsse B, Schulze MB, Langenberg C, et al. Untargeted metabolic profiling identifies altered serum metabolites of type 2 diabetes mellitus in a prospective, nested case control study. Clin Chem. 2015;61(3):487-97.
295. Kalhan SC, Guo L, Edmison J, Dasarathy S, McCullough AJ, Hanson RW, et al. Plasma metabolomic profile in nonalcoholic fatty liver disease. Metabolism. 2011;60(3):404-13.
296. Shearer J, Duggan G, Weljie A, Hittel D, Wasserman D, Vogel H. Metabolomic profiling of dietary‐induced insulin resistance in the high fat‐fed C57BL/6J mouse. Diabetes Obes Metab. 2008;10(10):950-8.
297. Li H, Xie Z, Lin J, Song H, Wang Q, Wang K, et al. Transcriptomic and metabonomic profiling of obesity-prone and obesity-resistant rats under high fat diet. J Proteome Res. 2008;7(11):4775-83.
298. McGill JB, Cole TG, Nowatzke W, Houghton S, Ammirati EB, Gautille T, et al. Circulating 1, 5-anhydroglucitol levels in adult patients with diabetes reflect longitudinal changes of glycemia: a US trial of the GlycoMark assay. Diabetes Care. 2004;27(8):1859-65.
299. Al-Sulaiti H, Diboun I, Banu S, Al-Emadi M, Amani P, Harvey TM, et al. Triglyceride profiling in adipose tissues from obese insulin sensitive, insulin resistant and type 2 diabetes mellitus individuals. Journal of translational medicine. 2018;16(1):175.
300. Luukkonen PK, Zhou Y, Sädevirta S, Leivonen M, Arola J, Orešič M, et al. Hepatic ceramides dissociate steatosis and insulin resistance in patients with non-alcoholic fatty liver disease. J Hepatol. 2016;64(5):1167-75.
301. Böhm A, Halama A, Meile T, Zdichavsky M, Lehmann R, Weigert C, et al. Metabolic signatures of cultured human adipocytes from metabolically healthy versus unhealthy obese individuals. PLoS ONE. 2014;9(4):e93148.
302. Hanzu F, Vinaixa M, Papageorgiou A, Párrizas M, Correig X, Delgado S, et al. Obesity rather than regional fat depots marks the metabolomic pattern of adipose tissue: an untargeted metabolomic approach. Obesity. 2014;22(3):698-704.
303. Blachnio‐Zabielska AU, Koutsari C, Tchkonia T, Jensen MD. Sphingolipid content of human adipose tissue: relationship to adiponectin and insulin resistance. Obesity. 2012;20(12):2341-7.
304. Hellmuth C, Demmelmair H, Schmitt I, Peissner W, Blüher M, Koletzko B. Association between plasma nonesterified fatty acids species and adipose tissue fatty acid composition. PLoS ONE. 2013;8(10):e74927.
305. Walker CG, Browning LM, Stecher L, West AL, Madden J, Jebb SA, et al. Fatty acid profile of plasma NEFA does not reflect adipose tissue fatty acid profile. Br J Nutr. 2015;114(5):756-62.

306. Soeters MR, Sauerwein HP, Duran M, Wanders RJ, Ackermans MT, Fliers E, et al. Muscle acylcarnitines during short-term fasting in lean healthy men. Clin Sci. 2009;116(7):585-92.
307. Bélanger C, Hould F-S, Lebel S, Biron S, Brochu G, Tchernof A. Omental and subcutaneous adipose tissue steroid levels in obese men. Steroids. 2006;71(8):674-82.
308. Canelas AB, ten Pierick A, Ras C, Seifar RM, van Dam JC, van Gulik WM, et al. Quantitative evaluation of intracellular metabolite extraction techniques for yeast metabolomics. Anal Chem. 2009;81(17):7379-89.
309. Duportet X, Aggio RBM, Carneiro S, Villas-Bôas SG. The biological interpretation of metabolomic data can be misled by the extraction method used. Metabolomics. 2012;8(3):410-21.
310. Chang MS, Ji Q, Zhang J, El‐Shourbagy TA. Historical review of sample preparation for chromatographic bioanalysis: pros and cons. Drug Development Research. 2007;68(3):107-33.
311. Want EJ, O'Maille G, Smith CA, Brandon TR, Uritboonthai W, Qin C, et al. Solvent-dependent metabolite distribution, clustering, and protein extraction for serum profiling with mass spectrometry. Anal Chem. 2006;78(3):743-52.
312. Michopoulos F, Lai L, Gika H, Theodoridis G, Wilson I. UPLC-MS-based analysis of human plasma for metabonomics using solvent precipitation or solid phase extraction. J Proteome Res. 2009;8(4):2114-21.
313. Naz S, Moreira dos Santos DC, García A, Barbas C. Analytical protocols based on LC–MS, GC–MS and CE–MS for nontargeted metabolomics of biological tissues. Bioanalysis. 2014;6(12):1657-77.
314. Burden DW. Guide to the homogenization of biological samples. Random Primers. 2008;7:1-14.
315. Burden DW. Guide to the disruption of biological samples-2012. Random Primers. 2012;12(1):1-25.
316. Geier FM, Want EJ, Leroi AM, Bundy JG. Cross-platform comparison of Caenorhabditis elegans tissue extraction strategies for comprehensive metabolome coverage. Anal Chem. 2011;83(10):3730-6.
317. Liang X, Ubhayakar S, Liederer BM, Dean B, Ran-Ran Qin A, Shahidi-Latham S, et al. Evaluation of homogenization techniques for the preparation of mouse tissue samples to support drug discovery. Bioanalysis. 2011;3(17):1923-33.
318. Reis A, Rudnitskaya A, Blackburn GJ, Fauzi NM, Pitt AR, Spickett CM. A comparison of five lipid extraction solvent systems for lipidomic studies of human LDL. J Lipid Res. 2013;54(7):1812-24.
319. Lee DY, Kind T, Yoon Y-R, Fiehn O, Liu K-H. Comparative evaluation of extraction methods for simultaneous mass-spectrometric analysis of complex lipids and primary metabolites from human blood plasma. Anal Bioanal Chem. 2014;406(28):7275-86.
320. Folch J, Lees M, Sloane-Stanley G. A simple method for the isolation and purification of total lipids from animal tissues. J Biol Chem. 1957;226(1):497-509.
321. Bligh EG, Dyer WJ. A rapid method of total lipid extraction and purification. Canadian journal of biochemistry and physiology. 1959;37(8):911-7.
322. Le Belle J, Harris N, Williams S, Bhakoo K. A comparison of cell and tissue extraction techniques using high‐resolution 1H‐NMR spectroscopy. NMR Biomed. 2002;15(1):37-44.

323. Wheelock CE, Goto S, Hammock BD, Newman JW. Clofibrate-induced changes in the liver, heart, brain and white adipose lipid metabolome of Swiss-Webster mice. Metabolomics. 2007;3(2):137-45.
324. Williams J, Wood J, Pandarinathan L, Karanian DA, Bahr BA, Vouros P, et al. Quantitative method for the profiling of the endocannabinoid metabolome by LC-atmospheric pressure chemical ionization-MS. Anal Chem. 2007;79(15):5582-93.
325. Perrone CE, Mattocks DA, Plummer JD, Chittur SV, Mohney R, Vignola K, et al. Genomic and metabolic responses to methionine-restricted and methionine-restricted, cysteine-supplemented diets in Fischer 344 rat inguinal adipose tissue, liver and quadriceps muscle. Journal of nutrigenetics and nutrigenomics. 2012;5(3):132-57.
326. Masson P, Alves AC, Ebbels TM, Nicholson JK, Want EJ. Optimization and evaluation of metabolite extraction protocols for untargeted metabolic profiling of liver samples by UPLC-MS. Anal Chem. 2010;82(18):7779-86.
327. Matyash V, Liebisch G, Kurzchalia TV, Shevchenko A, Schwudke D. Lipid extraction by methyl-tert-butyl ether for high-throughput lipidomics. J Lipid Res. 2008;49(5):1137-46.
328. Chen S, Hoene M, Li J, Li Y, Zhao X, Häring H-U, et al. Simultaneous extraction of metabolome and lipidome with methyl tert-butyl ether from a single small tissue sample for ultra-high performance liquid chromatography/mass spectrometry. J Chromatogr A. 2013;1298:9-16.
329. Lindahl A, Sääf S, Lehtiö J, Nordström A. Tuning metabolome coverage in reversed phase LC–MS metabolomics of MeOH extracted samples using the reconstitution solvent composition. Anal Chem. 2017;89(14):7356-64.
330. Jové M, Moreno-Navarrete JM, Pamplona R, Ricart W, Portero-Otín M, Fernández-Real JM. Human omental and subcutaneous adipose tissue exhibit specific lipidomic signatures. The FASEB journal. 2014;28(3):1071-81.
331. Leseigneur-Meynier A, Gandemer G. Lipid composition of pork muscle in relation to the metabolic type of the fibres. Meat Science. 1991;29(3):229-41.
332. Römisch-Margl W, Prehn C, Bogumil R, Röhring C, Suhre K, Adamski J. Procedure for tissue sample preparation and metabolite extraction for high-throughput targeted metabolomics. Metabolomics. 2012;8(1):133-42.
333. Maekawa K, Hirayama A, Iwata Y, Tajima Y, Nishimaki-Mogami T, Sugawara S, et al. Global metabolomic analysis of heart tissue in a hamster model for dilated cardiomyopathy. J Mol Cell Cardiol. 2013;59:76-85.
334. McCombie G, Medina-Gomez G, Lelliott CJ, Vidal-Puig A, Griffin JL. Metabolomic and lipidomic analysis of the heart of peroxisome proliferator-activated receptor-γ coactivator 1-β knock out mice on a high fat diet. Metabolites. 2012;2(2):366-81.
335. Ashrafian H, Li JV, Spagou K, Harling L, Masson P, Darzi A, et al. Bariatric surgery modulates circulating and cardiac metabolites. J Proteome Res. 2013;13(2):570-80.
336. Clish CB. Metabolomics: an emerging but powerful tool for precision medicine. Molecular Case Studies. 2015;1(1):a000588.
337. Park S, Sadanala KC, Kim E-K. A metabolomic approach to understanding the metabolic link between obesity and diabetes. Mol Cells. 2015;38(7):587-96.
338. Orešič M. Metabolomics, a novel tool for studies of nutrition, metabolism and lipid dysfunction. Nutr Metab Cardiovasc Dis. 2009;19(11):816-24.

339. Roberts LD, Koulman A, Griffin JL. Towards metabolic biomarkers of insulin resistance and type 2 diabetes: progress from the metabolome. Lancet Diabetes Endocrinol. 2014;2(1):65-75.
340. Büscher JrM, Czernik D, Ewald JC, Sauer U, Zamboni N. Cross-platform comparison of methods for quantitative metabolomics of primary metabolism. Anal Chem. 2009;81(6):2135-43.
341. Gross RW, Han X. Lipidomics at the interface of structure and function in systems biology. Chemistry & biology. 2011;18(3):284-91.
342. Vorkas PA, Isaac G, Anwar MA, Davies AH, Want EJ, Nicholson JK, et al. Untargeted UPLC-MS profiling pipeline to expand tissue metabolome coverage: application to cardiovascular disease. Anal Chem. 2015;87(8):4184-93.
343. Alves RD, Dane AD, Harms A, Strassburg K, Seifar RM, Verdijk LB, et al. Global profiling of the muscle metabolome: method optimization, validation and application to determine exercise-induced metabolic effects. Metabolomics. 2015;11(2):271-85.
344. Anwar MA, Vorkas PA, Li JV, Shalhoub J, Want EJ, Davies AH, et al. Optimization of metabolite extraction of human vein tissue for ultra performance liquid chromatography-mass spectrometry and nuclear magnetic resonance-based untargeted metabolic profiling. Analyst. 2015;140(22):7586-97.
345. Sargent M. Guide to achieving reliable quantitative LC-MS measurements. RSC Analytical Methods Committee, United Kingdom. 2013.
346. Want EJ, Wilson ID, Gika H, Theodoridis G, Plumb RS, Shockcor J, et al. Global metabolic profiling procedures for urine using UPLC–MS. Nat Protoc. 2010;5(6):1005-18.
347. Luo X, Li L. Metabolomics of Small Numbers of Cells: Metabolomic Profiling of 100, 1000, and 10000 Human Breast Cancer Cells. Anal Chem. 2017;89(21):11664-71.
348. Cajka T, Smilowitz JT, Fiehn O. Validating Quantitative Untargeted Lipidomics Across Nine Liquid Chromatography–High-Resolution Mass Spectrometry Platforms. Anal Chem. 2017;89(22):12360-8.
349. Taylor PJ. Matrix effects: the Achilles heel of quantitative high-performance liquid chromatography–electrospray–tandem mass spectrometry. Clin Biochem. 2005;38(4):328-34.
350. Croixmarie V, Umbdenstock T, Cloarec O, Moreau Al, Pascussi J-M, Boursier-Neyret C, et al. Integrated comparison of drug-related and drug-induced ultra performance liquid chromatography/mass spectrometry metabonomic profiles using human hepatocyte cultures. Anal Chem. 2009;81(15):6061-9.
351. Duan L, Molnár I, Snyder JH, Shen G-a, Qi X. Discrimination and quantification of true biological signals in metabolomics analysis based on liquid chromatography-mass spectrometry. Molecular plant. 2016;9(8):1217-20.
352. Xu J, Begley P, Church SJ, Patassini S, Hollywood KA, Jüllig M, et al. Graded perturbations of metabolism in multiple regions of human brain in Alzheimer's disease: Snapshot of a pervasive metabolic disorder. Biochimica et biophysica acta Molecular basis of disease. 2016;1862(6):1084-92.
353. Samuelsson LM, Young W, Fraser K, Tannock GW, Lee J, Roy NC. Digestive-resistant carbohydrates affect lipid metabolism in rats. Metabolomics. 2016;12(5):79.
354. Fraser K, Harrison SJ, Lane GA, Otter DE, Hemar Y, Quek S-Y, et al. Non-targeted analysis of tea by hydrophilic interaction liquid chromatography and high resolution mass spectrometry. Food chemistry. 2012;134(3):1616-23.

355. Vuckovic D. Current trends and challenges in sample preparation for global metabolomics using liquid chromatography–mass spectrometry. Anal Bioanal Chem. 2012;403(6):1523-48.
356. Burla B, Arita M, Arita M, Bendt AK, Cazenave-Gassiot A, Dennis EA, et al. MS-based lipidomics of human blood plasma: A community-initiated position paper to develop accepted guidelines. J Lipid Res. 2018;59(10):2001-17.
357. Dettmer K, Aronov PA, Hammock BD. Mass spectrometry ‐ based metabolomics. Mass Spectrom Rev. 2007;26(1):51-78.
358. Waybright TJ, Van QN, Muschik GM, Conrads TP, Veenstra TD, Issaq HJ. LC ‐ MS in metabonomics: optimization of experimental conditions for the analysis of metabolites in human urine. Journal of liquid chromatography & related technologies. 2006;29(17):2475-97.
359. Ortega N, Romero M-P, Macià A, Reguant J, Anglès N, Morelló J-R, et al. Comparative study of UPLC–MS/MS and HPLC–MS/MS to determine procyanidins and alkaloids in cocoa samples. Journal of food composition and analysis. 2010;23(3):298-305.
360. Nordström A, O'Maille G, Qin C, Siuzdak G. Nonlinear data alignment for UPLC− MS and HPLC− MS based metabolomics: quantitative analysis of endogenous and exogenous metabolites in human serum. Anal Chem. 2006;78(10):3289-95.
361. Jankevics A, Merlo ME, de Vries M, Vonk RJ, Takano E, Breitling R. Separating the wheat from the chaff: a prioritisation pipeline for the analysis of metabolomics datasets. Metabolomics. 2012;8(1):29-36.
362. Berg M, Vanaerschot M, Jankevics A, Cuypers B, Breitling R, Dujardin J-C. LC-MS metabolomics from study design to data-analysis–using a versatile pathogen as a test case. Computational and structural biotechnology journal. 2013;4(5):1-8.
363. Want EJ, Masson P, Michopoulos F, Wilson ID, Theodoridis G, Plumb RS, et al. Global metabolic profiling of animal and human tissues via UPLC-MS. Nat Protoc. 2013;8(1):17-32.
364. Haid M, Muschet C, Wahl S, Römisch-Margl W, Prehn C, Möller G, et al. Long-term stability of human plasma metabolites during storage at− 80 C. J Proteome Res. 2017;17(1):203-11.
365. Furey A, Moriarty M, Bane V, Kinsella B, Lehane M. Ion suppression; a critical review on causes, evaluation, prevention and applications. Talanta. 2013;115:104-22.
366. Majors R. Sample preparation fundamentals for chromatography. Agilent Technologies, Mississauga, Canada. 2013.
367. Sandra K, dos Santos Pereira A, Vanhoenacker G, David F, Sandra P. Comprehensive blood plasma lipidomics by liquid chromatography/quadrupole time-of-flight mass spectrometry. J Chromatogr A. 2010;1217(25):4087-99.
368. Pati S, Nie B, Arnold RD, Cummings BS. Extraction, chromatographic and mass spectrometric methods for lipid analysis. Biomed Chromatogr. 2016;30(5):695-709.
369. Psychogios N, Hau DD, Peng J, Guo AC, Mandal R, Bouatra S, et al. The human serum metabolome. PLoS ONE. 2011;6(2):e16957.
370. Quehenberger O, Armando AM, Brown AH, Milne SB, Myers DS, Merrill AH, et al. Lipidomics reveals a remarkable diversity of lipids in human plasma. J Lipid Res. 2010;51(11):3299-305.

371. McGranaghan P, Saxena A, Rubens M, Radenkovic J, Bach D, Schleußner L, et al. Predictive value of metabolomic biomarkers for cardiovascular disease risk: a systematic review and meta-analysis. Biomarkers. 2020;25(2):101-11.
372. Carter TC, Rein D, Padberg I, Peter E, Rennefahrt U, David DE, et al. Validation of a metabolite panel for early diagnosis of type 2 diabetes. Metabolism. 2016;65(9):1399-408.
373. Gao X, Ke C, Liu H, Liu W, Li K, Yu B, et al. Large-scale metabolomic analysis reveals potential biomarkers for early stage coronary atherosclerosis. Scientific Reports. 2017;7(1):1-11.
374. Johnson CH, Ivanisevic J, Siuzdak G. Metabolomics: beyond biomarkers and towards mechanisms. Nature reviews Molecular cell biology. 2016;17(7):451-9.
375. Kotronen A, Seppänen‐Laakso T, Westerbacka J, Kiviluoto T, Arola J, Ruskeepää AL, et al. Comparison of lipid and fatty acid composition of the liver, subcutaneous and intra‐abdominal adipose tissue, and serum. Obesity. 2010;18(5):937-44.
376. Korsholm AS, Kjær TN, Ornstrup MJ, Pedersen SB. Comprehensive metabolomic analysis in blood, urine, fat, and muscle in men with metabolic syndrome: a randomized, placebo-controlled clinical trial on the effects of resveratrol after four months' treatment. Int J Mol Sci. 2017;18(3):554.
377. Diamanti K, Cavalli M, Pan G, Pereira MJ, Kumar C, Skrtic S, et al. Intra- and inter-individual metabolic profiling highlights carnitine and lysophosphatidylcholine pathways as key molecular defects in type 2 diabetes. Scientific reports. 2019;9(1):1-13.
378. Ruiz‐Canela M, Hruby A, Clish CB, Liang L, Martínez‐González MA, Hu FB. Comprehensive metabolomic profiling and incident cardiovascular disease: a systematic review. J Am Heart Assoc. 2017;6(10):e005705.
379. Wu ZE, Kruger MC, Cooper GJ, Poppitt SD, Fraser K. Tissue-Specific Sample Dilution: An Important Parameter to Optimise Prior to Untargeted LC-MS Metabolomics. Metabolites. 2019;9(7):124.
380. Chambers MC, Maclean B, Burke R, Amodei D, Ruderman DL, Neumann S, et al. A cross-platform toolkit for mass spectrometry and proteomics. Nat Biotechnol. 2012;30(10):918-20.
381. Van Der Kloet FM, Bobeldijk I, Verheij ER, Jellema RH. Analytical error reduction using single point calibration for accurate and precise metabolomic phenotyping. J Proteome Res. 2009;8(11):5132-41.
382. Fraser K, Roy NC, Goumidi L, Verdu A, Suchon P, Leal-Valentim F, et al. Plasma Biomarkers and Identification of Resilient Metabolic Disruptions in Patients With Venous Thromboembolism Using a Metabolic Systems Approach. Arterioscler Thromb Vasc Biol. 2020;40(10):2527-38.
383. Méndez-Sánchez N, Vítek L, Uribe M. Bilirubin as a biomarker in liver disease. Dordrecht: Springer; 2017. 281-304 p.
384. Kamath PS, Wiesner RH, Malinchoc M, Kremers W, Therneau TM, Kosberg CL, et al. A model to predict survival in patients with end‐stage liver disease. Hepatology. 2001;33(2):464-70.
385. De Mello V, Lankinen M, Schwab U, Kolehmainen M, Lehto S, Seppänen-Laakso T, et al. Link between plasma ceramides, inflammation and insulin resistance: association with serum IL-6 concentration in patients with coronary heart disease. Diabetologia. 2009;52(12):2612-5.

386. Wigger L, Cruciani-Guglielmacci C, Nicolas A, Denom J, Fernandez N, Fumeron F, et al. Plasma dihydroceramides are diabetes susceptibility biomarker candidates in mice and humans. Cell Reports. 2017;18(9):2269-79.
387. Kremer G, Atzpodien W, Schnellbacher E. Plasma glycosphingolipids in diabetics and normals. Klin Wochenschr. 1975;53(13):637-8.
388. Chaurasia B, Summers SA. Ceramides–lipotoxic inducers of metabolic disorders. Trends in Endocrinology & Metabolism. 2015;26(10):538-50.
389. Sui J, He M, Wang Y, Zhao X, He Y, Shi B. Sphingolipid metabolism in type 2 diabetes and associated cardiovascular complications. Experimental and therapeutic medicine. 2019;18(5):3603-14.
390. Riebeling C, Allegood JC, Wang E, Merrill AH, Futerman AH. Two mammalian longevity assurance gene (LAG1) family members, trh1 and trh4, regulate dihydroceramide synthesis using different fatty acyl-CoA donors. J Biol Chem. 2003;278(44):43452-9.
391. Laviad EL, Albee L, Pankova-Kholmyansky I, Epstein S, Park H, Merrill AH, et al. Characterization of Ceramide Synthase 2 Tissue distribution, substrate specificity, and inhibition by sphingosine 1-phosphate. J Biol Chem. 2008;283(9):5677-84.
392. Erion DM, Shulman GI. Diacylglycerol-mediated insulin resistance. Nat Med. 2010;16(4):400-2.
393. Itani SI, Ruderman NB, Schmieder F, Boden G. Lipid-induced insulin resistance in human muscle is associated with changes in diacylglycerol, protein kinase C, and IκB-α. Diabetes. 2002;51(7):2005-11.
394. Samuel VT, Liu Z-X, Qu X, Elder BD, Bilz S, Befroy D, et al. Mechanism of hepatic insulin resistance in non-alcoholic fatty liver disease. J Biol Chem. 2004;279(31):32345-53.
395. Dean JM, Lodhi IJ. Structural and functional roles of ether lipids. Protein & cell. 2018;9(2):196-206.
396. Li JB, Higgins JE, Jefferson LS. Changes in protein turnover in skeletal muscle in response to fasting. American Journal of Physiology-Endocrinology And Metabolism. 1979;236(3):E222.
397. Ruderman NB. Muscle amino acid metabolism and gluconeogenesis. Annu Rev Med. 1975;26(1):245-58.
398. De Blaauw I, Deutz N, Von Meyenfeldt M. In vivo amino acid metabolism of gut and liver during short and prolonged starvation. Am J Physiol Gastrointest Liver Physiol. 1996;270(2):G298-G306.
399. Pacana T, Cazanave S, Verdianelli A, Patel V, Min H-K, Mirshahi F, et al. Dysregulated hepatic methionine metabolism drives homocysteine elevation in diet-induced nonalcoholic fatty liver disease. PLoS ONE. 2015;10(8):e0136822.
400. Jung Y-S. Metabolism of sulfur-containing amino acids in the liver: a link between hepatic injury and recovery. Biol Pharm Bull. 2015;38(7):971-4.
401. Mato JM, Martinez-Chantar ML, Lu SC. Methionine metabolism and liver disease. Annu Rev Nutr. 2008;28:273-93.
402. Janeiro MH, Ramírez MJ, Milagro FI, Martínez JA, Solas M. Implication of trimethylamine N-oxide (TMAO) in disease: potential biomarker or new therapeutic target. Nutrients. 2018;10(10):1398.
403. Teft WA, Morse BL, Leake BF, Wilson A, Mansell SE, Hegele RA, et al. Identification and characterization of trimethylamine-N-oxide uptake and efflux transporters. Mol Pharm. 2017;14(1):310-8.
404. Federation ID. IDF Diabetes Atlas Eighth Edition. 2017.

405. Wang S, Marquez P, Langenbrunner J, Niessen L, Suhrcke M, Song F. Toward a healthy and harmonious life in China: stemming the rising tide of non-communicable diseases. Washington, DC: World Bank. 2011:1-48.
406. Popkin BM, Horton S, Kim S, Mahal A, Shuigao J. Trends in diet, nutritional status, and diet-related noncommunicable diseases in China and India: the economic costs of the nutrition transition. Nutr Rev. 2001;59(12):379-90.
407. Fujimoto WY, Boyko EJ, Hayashi T, Kahn SE, Leonetti DL, McNeely MJ, et al. Risk factors for type 2 diabetes: lessons learned from Japanese Americans in Seattle. J Diabetes Investig. 2012;3(3):212-24.
408. Sattar N, Gill JM. Type 2 diabetes as a disease of ectopic fat? BMC Med. 2014;12(1):1-6.
409. Hocking S, Samocha-Bonet D, Milner K-L, Greenfield JR, Chisholm DJ. Adiposity and insulin resistance in humans: the role of the different tissue and cellular lipid depots. Endocr Rev. 2013;34(4):463-500.
410. Kantartzis K, Totsikas C, Häring H-U, Stefan N. Role of ectopic fat in the pathogenesis of insulin resistance. Clin Lipidol. 2009;4(4):457-64.
411. Sniderman AD, Bhopal R, Prabhakaran D, Sarrafzadegan N, Tchernof A. Why might South Asians be so susceptible to central obesity and its atherogenic consequences? The adipose tissue overflow hypothesis. Int J Epidemiol. 2007;36(1):220-5.
412. Goossens GH. The metabolic phenotype in obesity: fat mass, body fat distribution, and adipose tissue function. Obes Facts. 2017;10(3):207-15.
413. Carpentier AC. The 2012 CDA-CIHR INMD Young Investigator Award Lecture: dysfunction of adipose tissues and the mechanisms of ectopic fat deposition in type 2 diabetes. Can J Diabetes. 2013;37(2):109-14.
414. Thomas EL, Parkinson JR, Frost GS, Goldstone AP, Doré CJ, McCarthy JP, et al. The missing risk: MRI and MRS phenotyping of abdominal adiposity and ectopic fat. Obesity. 2012;20(1):76-87.
415. Qiu G, Zheng Y, Wang H, Sun J, Ma H, Xiao Y, et al. Plasma metabolomics identified novel metabolites associated with risk of type 2 diabetes in two prospective cohorts of Chinese adults. Int J Epidemiol. 2016;45(5):1507-16.
416. Cobb J, Gall W, Adam K-P, Nakhle P, Button E, Hathorn J, et al. A novel fasting blood test for insulin resistance and prediabetes. J Diabetes Sci Technol. 2013;7(1):100-10.
417. Lu J, Xie G, Jia W, Jia W. Insulin resistance and the metabolism of branched-chain amino acids. Frontiers of medicine. 2013;7(1):53-9.
418. Sun L, Liang L, Gao X, Zhang H, Yao P, Hu Y, et al. Early prediction of developing type 2 diabetes by plasma acylcarnitines: a population-based study. Diabetes Care. 2016;39(9):1563-70.
419. Boone S, Mook-Kanamori D, Rosendaal F, den Heijer M, Lamb H, de Roos A, et al. Metabolomics: a search for biomarkers of visceral fat and liver fat content. Metabolomics. 2019;15(10):1-12.
420. Stats NZ Census. http://nzdotstat.stats.govt.nz/wbos/index.aspx (2018) [cited 2019 20 Dec].
421. Association AD. Diagnosis and classification of diabetes mellitus. Diabetes Care. 2013;36(Supplement 1):S67-S74.
422. Sequeira IR, Yip W, Lu L, Jiang Y, Murphy R, Plank L, et al. Visceral adiposity and glucoregulatory peptides are associated with susceptibility to type 2 diabetes: the TOFI_Asia study. Obesity. 2020;28(12):2368-78.

423. Myers OD, Sumner SJ, Li S, Barnes S, Du X. Detailed investigation and comparison of the XCMS and MZmine 2 chromatogram construction and chromatographic peak detection methods for preprocessing mass spectrometry metabolomics data. Anal Chem. 2017;89(17):8689-95.
424. Dalziel JE, Fraser K, Young W, McKenzie CM, Bassett SA, Roy NC. Gastroparesis and lipid metabolism-associated dysbiosis in Wistar-Kyoto rats. Am J Physiol Gastrointest Liver Physiol. 2017;313(1):G62-G72.
425. Benjamini Y, Hochberg Y. Controlling the false discovery rate: a practical and powerful approach to multiple testing. J R Stat Soc Series B Stat Methodol. 1995;57(1):289-300.
426. Breiman L. Random forests. Mach Learn. 2001;45(1):5-32.
427. Chong J, Soufan O, Li C, Caraus I, Li S, Bourque G, et al. MetaboAnalyst 4.0: towards more transparent and integrative metabolomics analysis. Nucleic Acids Res. 2018;46(W1):W486-W94.
428. Galaviz KI, Narayan KV, Lobelo F, Weber MB. Lifestyle and the prevention of Type 2 Diabetes: a status report. Am J Lifestyle Med. 2018;12(1):4-20.
429. Tabák AG, Herder C, Rathmann W, Brunner EJ, Kivimäki M. Prediabetes: a high-risk state for developing diabetes. Lancet. 2012;379(9833):2279-90.
430. Hu FB. Globalization of diabetes: the role of diet, lifestyle, and genes. Diabetes Care. 2011;34(6):1249-57.
431. Alshehry ZH, Mundra PA, Barlow CK, Mellett NA, Wong G, McConville MJ, et al. Plasma lipidomic profiles improve on traditional risk factors for the prediction of cardiovascular events in type 2 diabetes mellitus. Circulation. 2016;134(21):1637-50.
432. Chang W, Hatch GM, Wang Y, Yu F, Wang M. The relationship between phospholipids and insulin resistance: From clinical to experimental studies. J Cell Mol Med. 2019;23(2):702-10.
433. Han L-D, Xia J-F, Liang Q-L, Wang Y, Wang Y-M, Hu P, et al. Plasma esterified and non-esterified fatty acids metabolic profiling using gas chromatography–mass spectrometry and its application in the study of diabetic mellitus and diabetic nephropathy. Anal Chim Acta. 2011;689(1):85-91.
434. Steneberg P, Sykaras AG, Backlund F, Straseviciene J, Söderström I, Edlund H. Hyperinsulinemia enhances hepatic expression of the fatty acid transporter Cd36 and provokes hepatosteatosis and hepatic insulin resistance. J Biol Chem. 2015;290(31):19034-43.
435. Vatner DF, Majumdar SK, Kumashiro N, Petersen MC, Rahimi Y, Gattu AK, et al. Insulin-independent regulation of hepatic triglyceride synthesis by fatty acids. Proceedings of the National Academy of Sciences. 2015;112(4):1143-8.
436. Xin Y, Wang Y, Chi J, Zhu X, Zhao H, Zhao S, et al. Elevated free fatty acid level is associated with insulin-resistant state in nondiabetic Chinese people. Diabetes, metabolic syndrome and obesity: targets and therapy. 2019;12:139-47.
437. Jaworski K, Sarkadi-Nagy E, Duncan RE, Ahmadian M, Sul HS. Regulation of triglyceride metabolism. IV. Hormonal regulation of lipolysis in adipose tissue. Am J Physiol Gastrointest Liver Physiol. 2007;293(1):G1-G4.
438. Sonnweber T, Pizzini A, Nairz M, Weiss G, Tancevski I. Arachidonic acid metabolites in cardiovascular and metabolic diseases. Int J Mol Sci. 2018;19(11):3285.
439. Razquin C, Liang L, Toledo E, Clish CB, Ruiz-Canela M, Zheng Y, et al. Plasma lipidome patterns associated with cardiovascular risk in the PREDIMED trial: A case-cohort study. Int J Cardiol. 2018;253:126-32.

440. Gardner CD, Fortmann SP, Krauss RM. Association of small low-density lipoprotein particles with the incidence of coronary artery disease in men and women. JAMA. 1996;276(11):875-81.
441. Shepherd J, Caslake MJ, Lorimer AR, Vallance BD, Packard CJ. Fenofibrate reduces low density lipoprotein catabolism in hypertriglyceridemic subjects. Arteriosclerosis: An Official Journal of the American Heart Association, Inc. 1985;5(2):162-8.
442. Galeano NF, Al-Haideri M, Keyserman F, Rumsey SC, Deckelbaum RJ. Small dense low density lipoprotein has increased affinity for LDL receptor-independent cell surface binding sites: a potential mechanism for increased atherogenicity. J Lipid Res. 1998;39(6):1263-73.
443. Krauss RM, Blanche PJ, Rawlings RS, Fernstrom HS, Williams PT. Separate effects of reduced carbohydrate intake and weight loss on atherogenic dyslipidemia. Am J Clin Nutr. 2006;83(5):1025-31.
444. Hardy OT, Czech MP, Corvera S. What causes the insulin resistance underlying obesity? Curr Opin Endocrinol Diabetes Obes. 2012;19(2):81-7.
445. Poirier P, Giles TD, Bray GA, Hong Y, Stern JS, Pi-Sunyer FX, et al. Obesity and cardiovascular disease: pathophysiology, evaluation, and effect of weight loss: an update of the 1997 American Heart Association Scientific Statement on Obesity and Heart Disease from the Obesity Committee of the Council on Nutrition, Physical Activity, and Metabolism. Circulation. 2006;113(6):898-918.
446. Lee SY, Chang HJ, Sung J, Kim KJ, Shin S, Cho IJ, et al. The impact of obesity on subclinical coronary atherosclerosis according to the risk of cardiovascular disease. Obesity. 2014;22(7):1762-8.
447. Neeland IJ, Turer AT, Ayers CR, Powell-Wiley TM, Vega GL, Farzaneh-Far R, et al. Dysfunctional adiposity and the risk of prediabetes and type 2 diabetes in obese adults. JAMA. 2012;308(11):1150-9.
448. Shah RV, Murthy VL, Abbasi SA, Blankstein R, Kwong RY, Goldfine AB, et al. Visceral adiposity and the risk of metabolic syndrome across body mass index: the MESA Study. JACC Cardiovasc Imaging. 2014;7(12):1221-35.
449. Gitto S, Schepis F, Andreone P, Villa E. Study of the serum metabolomic profile in nonalcoholic fatty liver disease: research and clinical perspectives. Metabolites. 2018;8(1):17.
450. Jaghutriz BA, Wagner R, Heni M, Lehmann R, Machann J, Stefan N, et al. Metabolomic characteristics of fatty pancreas. Exp Clin Endocrinol Diabetes. 2020;128(12):804-10.
451. Sequeira IR, Yip W, Lu LW, Jiang Y, Murphy R, Plank LD, et al. Pancreas fat, a potential early marker of metabolic risk? A magnetic resonance study of Chinese and Caucasian women: the TOFI_Asia study. J Clin Endocrinol Metab. 2020;article in review.
452. Schneider CA, Rasband WS, Eliceiri KW. NIH Image to ImageJ: 25 years of image analysis. Nat Methods. 2012;9(7):671-5.
453. Al-Mrabeh A, Hollingsworth KG, Steven S, Tiniakos D, Taylor R. Quantification of intrapancreatic fat in type 2 diabetes by MRI. PLoS ONE. 2017;12(4):e0174660.
454. Crane JC, Olson MP, Nelson SJ. SIVIC: open-source, standards-based software for DICOM MR spectroscopy workflows. International journal of biomedical imaging. 2013;2013.

455. Cabrera D, Kruger M, Wolber FM, Roy NC, Totman JJ, Henry CJ, et al. Association of plasma lipids and polar metabolites with low bone mineral density in Singaporean-Chinese menopausal women: a pilot study. Int J Environ Res Public Health. 2018;15(5):1045.
456. D'agostino RB, Belanger A, D'Agostino Jr RB. A suggestion for using powerful and informative tests of normality. The American Statistician. 1990;44(4):316-21.
457. Shi L, Westerhuis JA, Rosén J, Landberg R, Brunius C. Variable selection and validation in multivariate modelling. Bioinformatics. 2019;35(6):972-80.
458. Hofmann AF. Detoxification of lithocholic acid, a toxic bile acid: relevance to drug hepatotoxicity. Drug Metab Rev. 2004;36(3-4):703-22.
459. Shapiro H, Kolodziejczyk AA, Halstuch D, Elinav E. Bile acids in glucose metabolism in health and disease. J Exp Med. 2018;215(2):383-96.
460. Browning MG, Pessoa BM, Khoraki J, Campos GM. Changes in bile acid metabolism, transport, and signaling as central drivers for metabolic improvements after bariatric surgery. Current obesity reports. 2019;8(2):175-84.
461. Nemati R, Lu J, Dokpuang D, Booth M, Plank LD, Murphy R. Increased bile acids and FGF19 after sleeve gastrectomy and Roux-en-Y gastric bypass correlate with improvement in type 2 diabetes in a randomized trial. Obes Surg. 2018;28(9):2672-86.
462. Chen Y, Lu J, Nemati R, Plank LD, Murphy R. Acute changes of bile acids and FGF19 after sleeve gastrectomy and Roux-en-Y gastric bypass. Obes Surg. 2019;29(11):3605-21.
463. Rauschert S, Uhl O, Koletzko B, Kirchberg F, Mori TA, Huang R-C, et al. Lipidomics reveals associations of phospholipids with obesity and insulin resistance in young adults. J Clin Endocrinol Metab. 2016;101(3):871-9.
464. Ahmad MS, Alsaleh M, Kimhofer T, Ahmad S, Jamal W, Wali SO, et al. Metabolic phenotype of obesity in a Saudi population. J Proteome Res. 2017;16(2):635-44.
465. Zarrati M, Aboutaleb N, Cheshmazar E, Shoormasti RS, Razmpoosh E, Nasirinezhad F. The association of obesity and serum leptin levels with complete blood count and some serum biochemical parameters in Iranian overweight and obese individuals. Medical journal of the Islamic Republic of Iran. 2019;33:72.
466. Yang R-x, Hu C-x, Sun W-l, Pan Q, Shen F, Yang Z, et al. Serum monounsaturated triacylglycerol predicts steatohepatitis in patients with non-alcoholic fatty liver disease and chronic hepatitis B. Scientific reports. 2017;7(1):1-11.
467. Horowitz JF, Ortega JF, Hinko A, Li M, Nelson RK, Mora-Rodriguez R. Changes in markers for cardio-metabolic disease risk after only 1-2 weeks of a high saturated fat diet in overweight adults. PLoS ONE. 2018;13(6):e0198372.
468. Lambert JE, Ramos–Roman MA, Browning JD, Parks EJ. Increased de novo lipogenesis is a distinct characteristic of individuals with nonalcoholic fatty liver disease. Gastroenterology. 2014;146(3):726-35.
469. Cohen JC, Horton JD, Hobbs HH. Human fatty liver disease: old questions and new insights. Science. 2011;332(6037):1519-23.
470. Tappy L, Lê K-A. Metabolic effects of fructose and the worldwide increase in obesity. Physiol Rev. 2010;90(1):23-46.
471. Sciacca MF, Brender JR, Lee D-K, Ramamoorthy A. Phosphatidylethanolamine enhances amyloid fiber-dependent membrane fragmentation. Biochemistry (Mosc). 2012;51(39):7676-84.

472. Chen Y, Varasteh B, Reaven G. Plasma lactate concentration in obesity and type 2 diabetes. Diabete & metabolisme. 1993;19(4):348-54.
473. Crawford SO, Hoogeveen RC, Brancati FL, Astor BC, Ballantyne CM, Schmidt MI, et al. Association of blood lactate with type 2 diabetes: the Atherosclerosis Risk in Communities Carotid MRI Study. Int J Epidemiol. 2010;39(6):1647-55.
474. Juraschek SP, Shantha GPS, Chu AY, Miller III ER, Guallar E, Hoogeveen RC, et al. Lactate and risk of incident diabetes in a case-cohort of the atherosclerosis risk in communities (ARIC) study. PLoS ONE. 2013;8(1):e55113.
475. Chondronikola M, Magkos F, Yoshino J, Okunade AL, Patterson BW, Muehlbauer MJ, et al. Effect of progressive weight loss on lactate metabolism: a randomized controlled trial. Obesity. 2018;26(4):683-8.
476. Ramakrishanan N, Denna T, Devaraj S, Adams-Huet B, Jialal I. Exploratory lipidomics in patients with nascent Metabolic Syndrome. J Diabetes Complications. 2018;32(8):791-4.
477. Tiwari-Heckler S, Gan-Schreier H, Stremmel W, Chamulitrat W, Pathil A. Circulating phospholipid patterns in NAFLD patients associated with a combination of metabolic risk factors. Nutrients. 2018;10(5):649.
478. Naughton SS, Mathai ML, Hryciw DH, McAinch AJ. Linoleic acid and the pathogenesis of obesity. Prostaglandins Other Lipid Mediat. 2016;125:90-9.
479. Kelli HM, Corrigan III FE, Heinl RE, Dhindsa DS, Hammadah M, Samman-Tahhan A, et al. Relation of changes in body fat distribution to oxidative stress. Am J Cardiol. 2017;120(12):2289-93.
480. Elshorbagy AK, Smith AD, Kozich V, Refsum H. Cysteine and obesity. Obesity. 2012;20(3):473-81.
481. Moriarty-Craige SE, Jones DP. Extracellular thiols and thiol/disulfide redox in metabolism. Annu Rev Nutr. 2004;24:481-509.
482. Lim S. Ectopic fat assessment focusing on cardiometabolic and renal risk. Endocrinology and Metabolism. 2014;29(1):1-4.
483. Iida M, Harada S, Takebayashi T. Application of Metabolomics to Epidemiological Studies of Atherosclerosis and Cardiovascular Disease. Journal of atherosclerosis and thrombosis. 2019:RV17036.
484. Petersen MC, Shulman GI. Roles of diacylglycerols and ceramides in hepatic insulin resistance. Trends Pharmacol Sci. 2017;38(7):649-65.
485. Lee Y, Lai HT, de Oliveira Otto MC, Lemaitre RN, McKnight B, King IB, et al. Serial Biomarkers of De Novo Lipogenesis Fatty Acids and Incident Heart Failure in Older Adults: The Cardiovascular Health Study. J Am Heart Assoc. 2020;9(4):e014119.
486. Fabbrini E, Magkos F, Mohammed BS, Pietka T, Abumrad NA, Patterson BW, et al. Intrahepatic fat, not visceral fat, is linked with metabolic complications of obesity. Proceedings of the National Academy of Sciences. 2009;106(36):15430-5.

9. Appendices

9.1 Appendix: Supplementary Figures

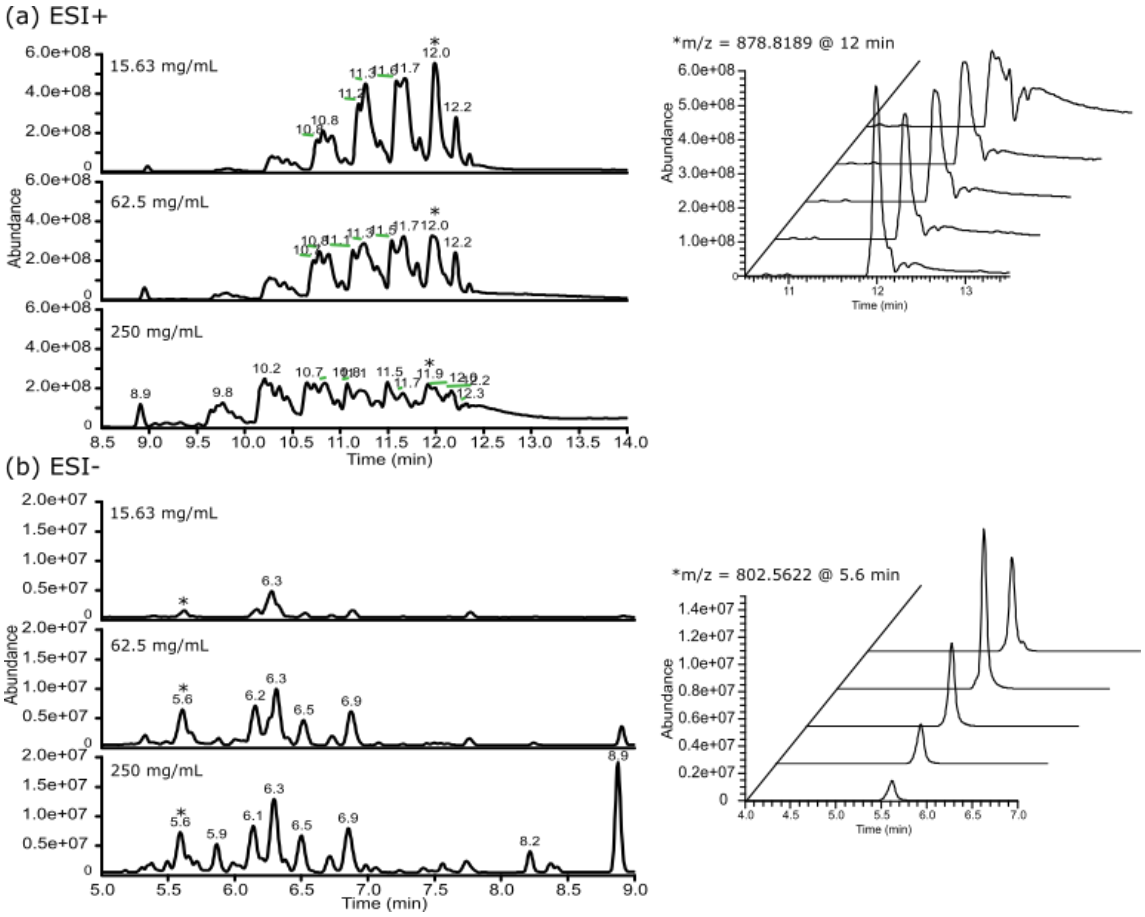

Figure 9.1: Total ion chromatogram (TIC) of lipid extracts from 50 mg adipose tissue at 15.63 mg/ml, 62.5 mg/ml and 250 mg/ml injected concentration and example for problematic extracted ion chromatogram (EIC) at this concentration range analysed by (a) ESI+ eluted between 8.5-14 min and (b) ESI- eluted between 5-9 min, on a fixed scale of absolute intensity. The EIC along the z-axis starts from the lowest injected concentration (15.63 mg/ml) at the front towards the highest concentration (250 mg/ml) at the back. The selected features for EIC examination were marked as * in the corresponding TIC.

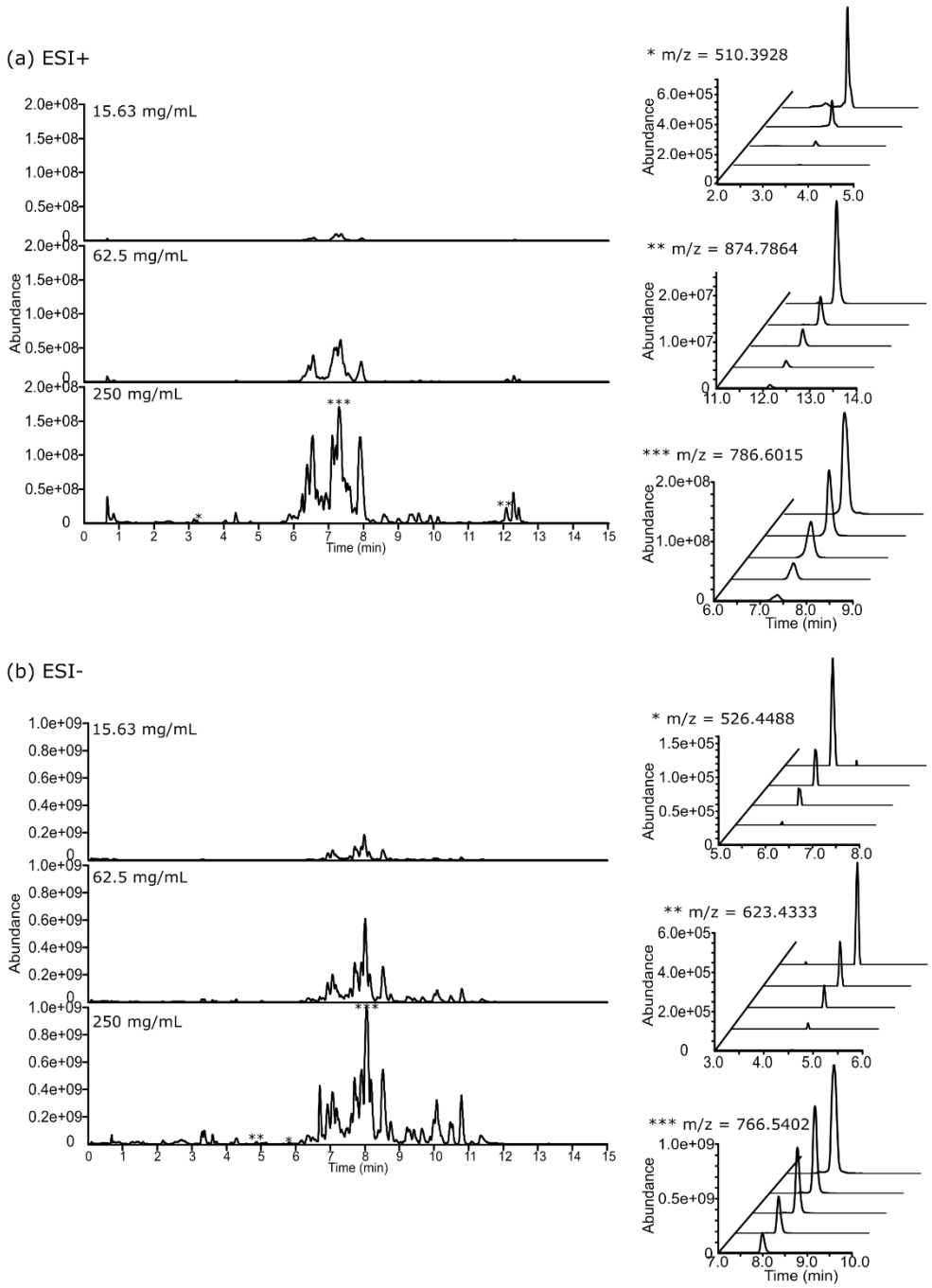

Figure 9.2: Total ion chromatogram (TIC) of lipid extracts from liver at low (15.63 mg/ml), intermediate (62.5 mg/ml) and high (250 mg/ml) injected concentration analysed by (a) ESI+ and (b) ESI-, and selected EIC of small (*), medium (**) and large (***) peaks representative of low, medium and high abundance features respectively on a fixed scale of absolute intensity to evaluate peak shape and the concentration-dependent response. The EIC along the z-axis starts from the lowest injected concentration at the front towards the highest concentration at the back.

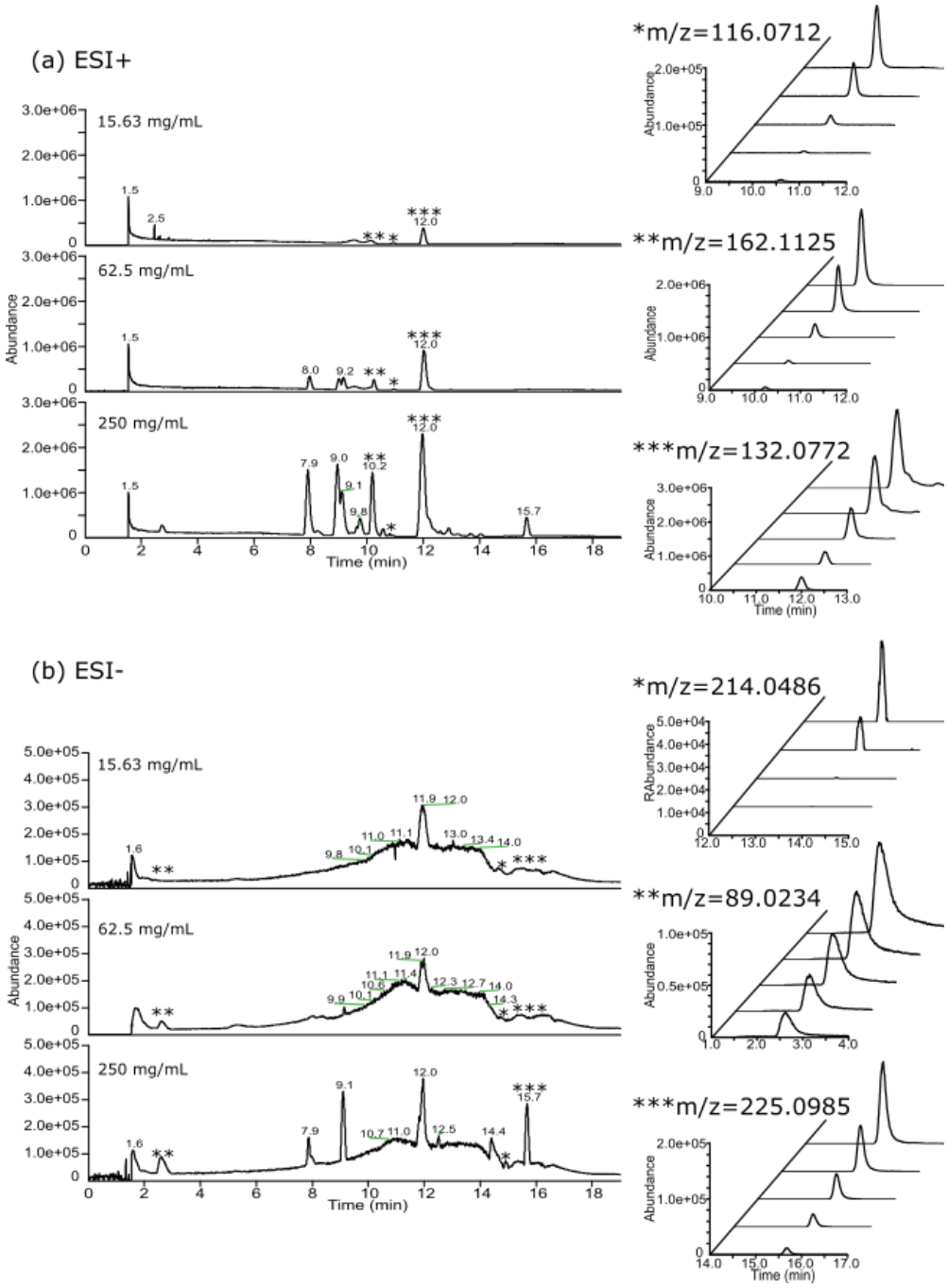

Figure 9.3: Total ion chromatogram (TIC) of polar extracts from adipose tissue at low (15.63 mg/ml), intermediate (62.5 mg/ml) and high (250 mg/ml) injected concentration analysed by (a) ESI+ and (b) ESI-, and selected EIC of small (*), medium (**) and large (***) peaks representative of low, medium and high abundance features respectively on a fixed scale of absolute intensity to evaluate peak shape and the concentration-dependent response. The EIC along the z-axis starts from the lowest injected concentration at the front towards the highest concentration at the back.

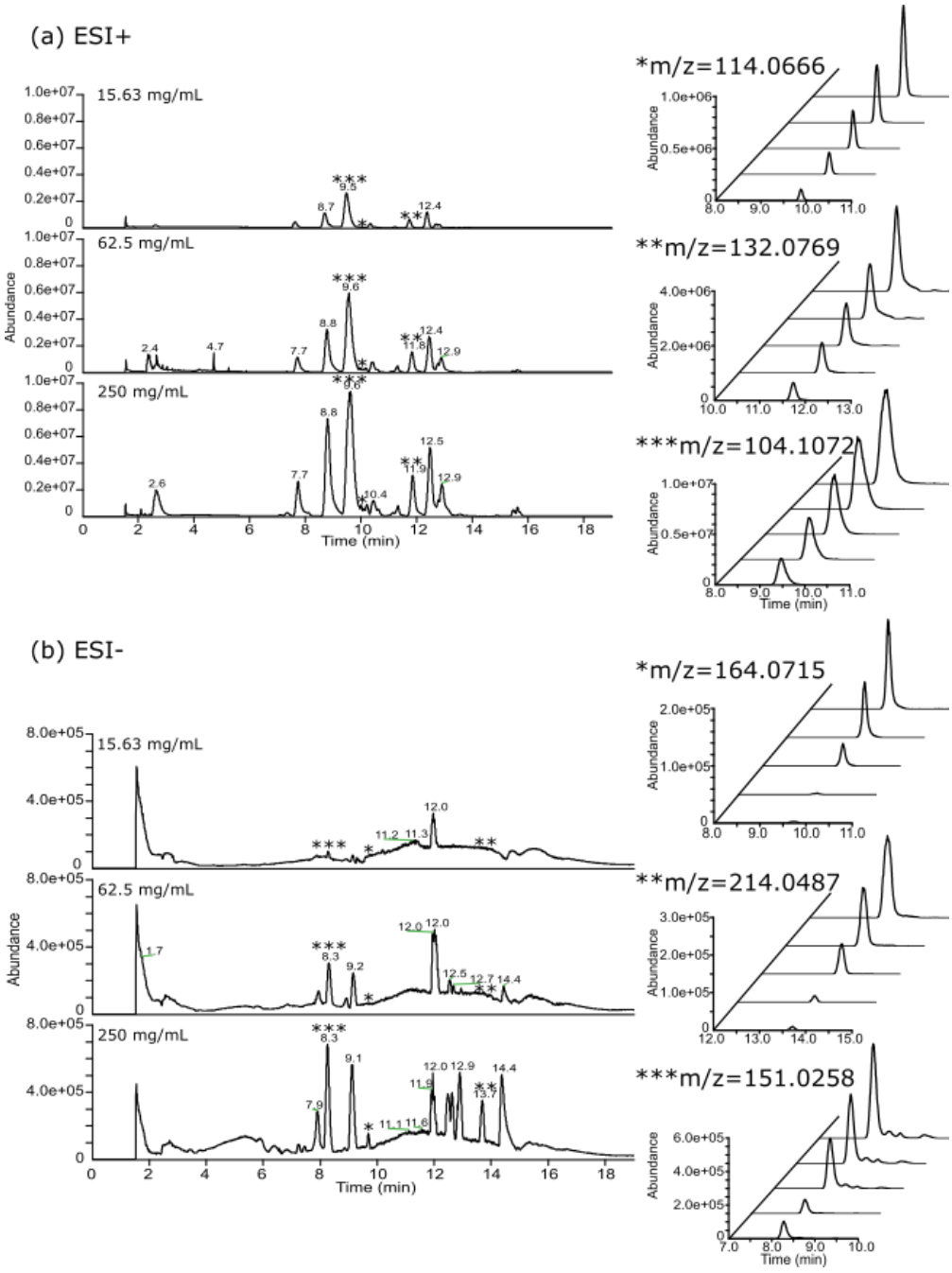

Figure 9.4: Total ion chromatogram (TIC) of polar extracts from liver at low (15.63 mg/ml), intermediate (62.5 mg/ml) and high (250 mg/ml) injected concentration analysed by (a) ESI+ and (b) ESI-, and selected EIC of small (*), medium (**) and large (***) peaks representative of low, medium and high abundance features respectively on a fixed scale of absolute intensity to evaluate peak shape and the concentration-dependent response. The EIC along the z-axis starts from the lowest injected concentration at the front towards the highest concentration at the back.

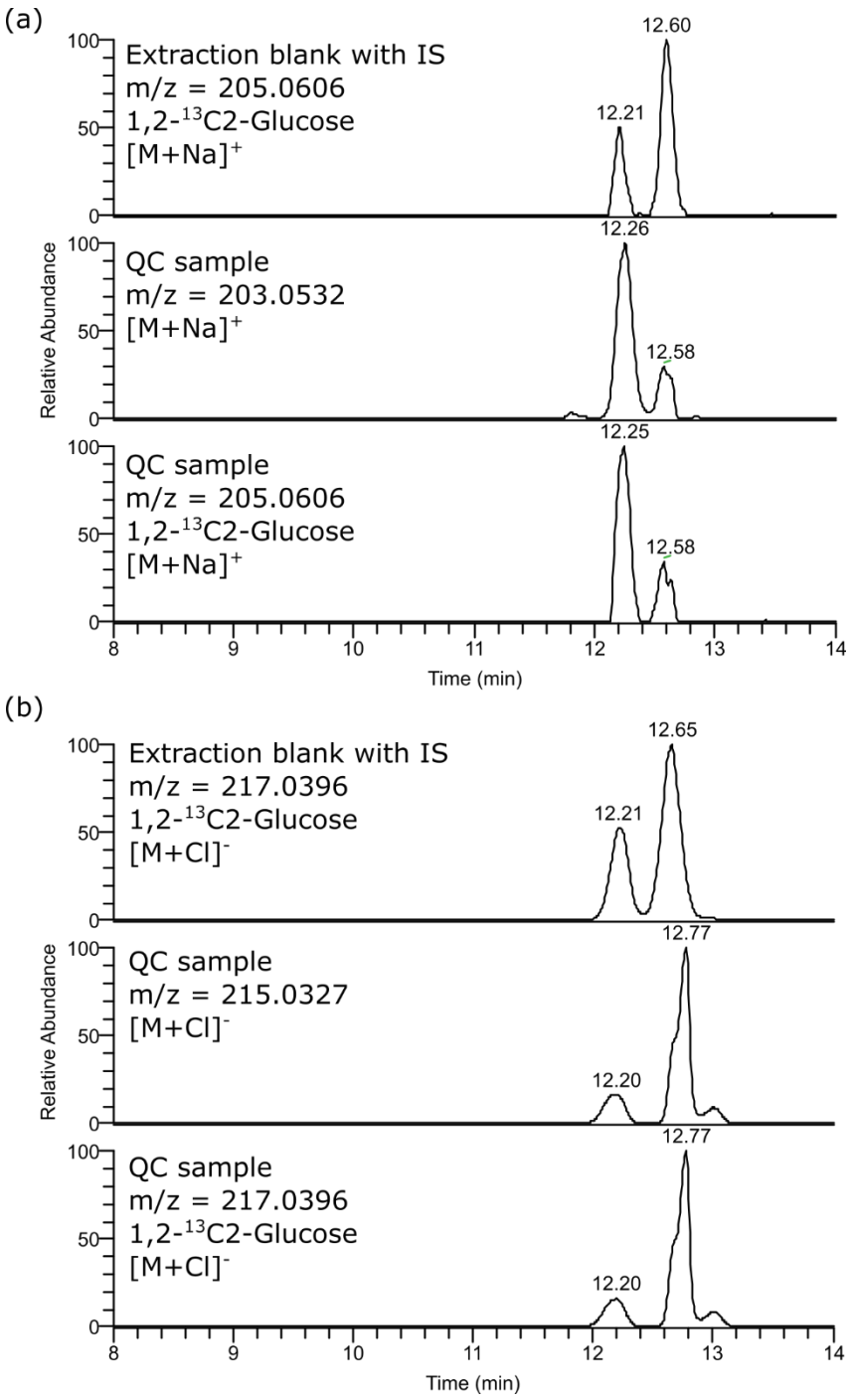

Figure 9.5: Annotation of glucose peak measured by ESI+ (a) and ESI- (b). Two peaks were eluted at 12.2 and 12.6 minutes respectively, confirmed by internal standard 1,2-^{13}C2-Glucose added in extraction solvent.

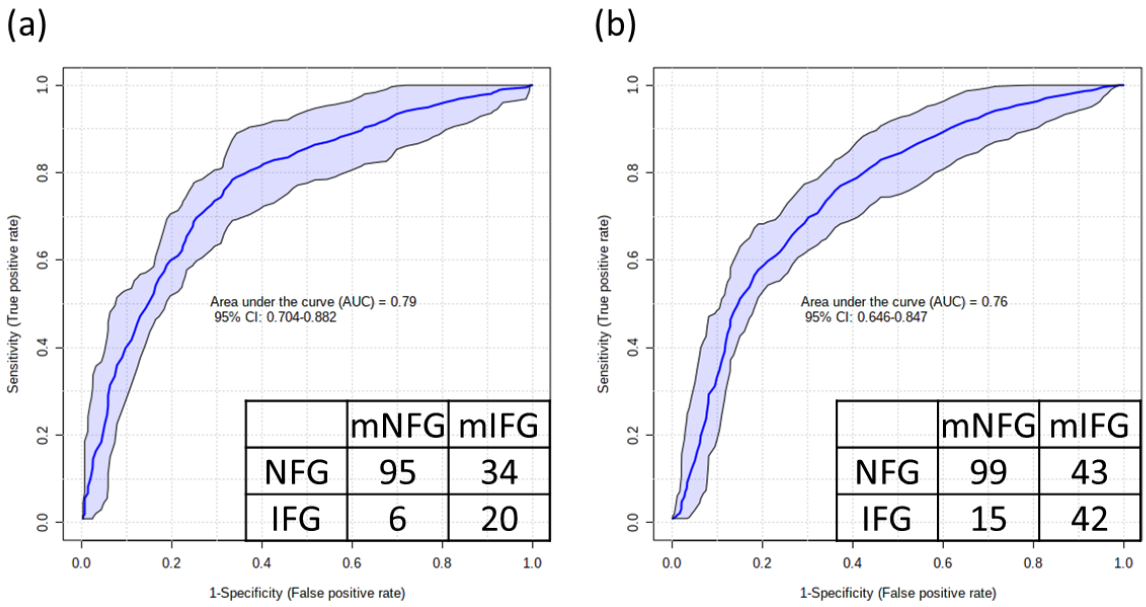

Figure 9.6: Receiver operating characteristic (ROC) curve of RF performed 100 most important variables among the pooled list of those associated with FPG or $\%VAT_{TBF}$ in (a) Caucasian and (b) Asian Chinese.

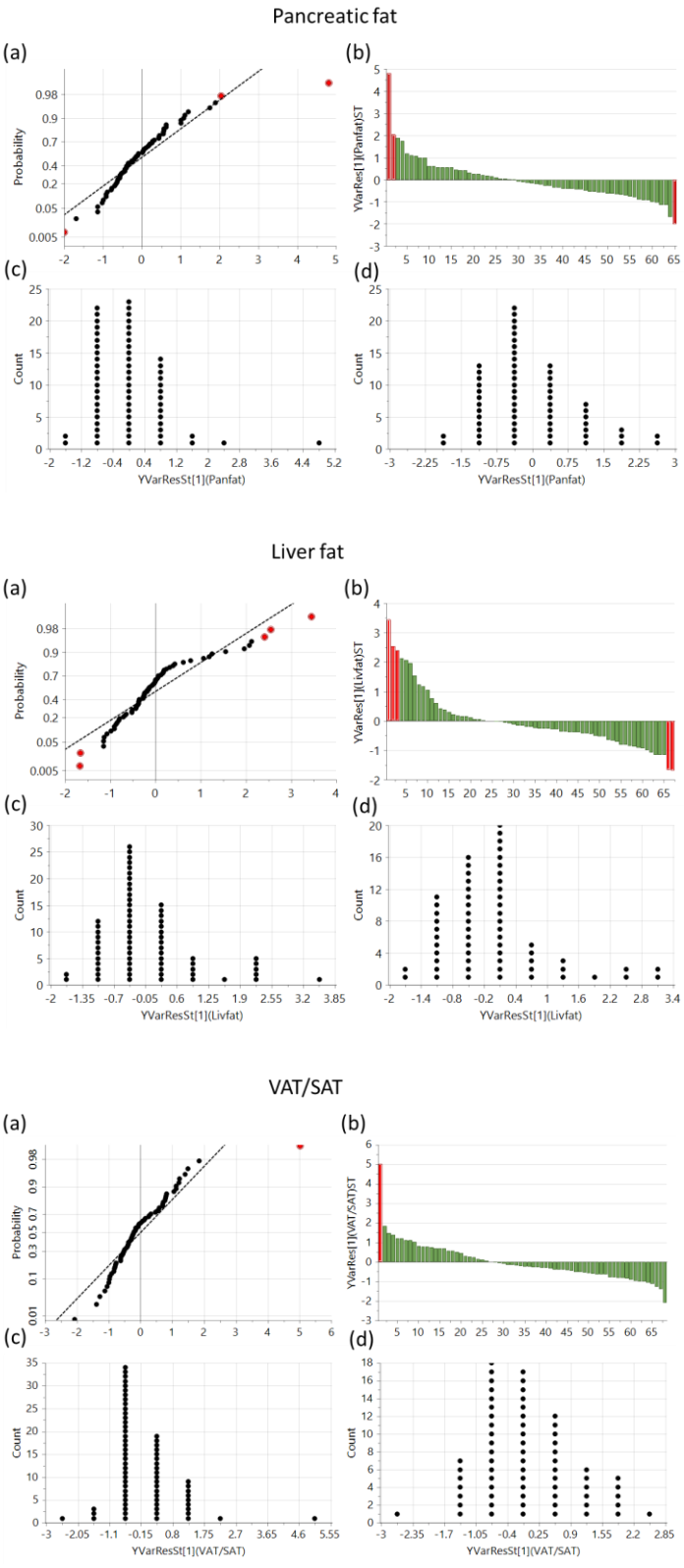

Figure 9.7: Y residual probability N-plot (a), bar plot showing Y residual expressed as unit of standard deviation (SD) (b), dot plot showing distribution of Y residual expressed as unit of SD before (c) and after (d) exclusion of outliers. The excluded outliers were highlighted in red in (a) and (b).

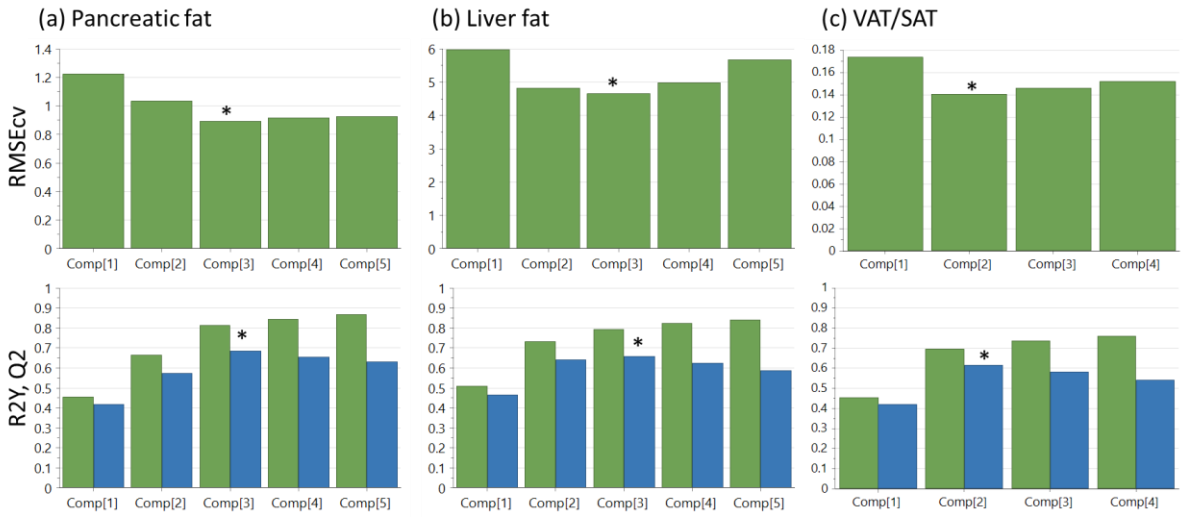

Figure 9.8: Barplot showing RMSEcv (top) and model performance (bottom) of up to 5 components in (a) pancreatic fat, (b) liver fat, (c) VAT/SAT. Number of components producing the lowest RMSEcv and highest Q2 (blue) was chosen as optimum (marked as *).

9.2 Appendix: Supplementary Tables

Table 9.1: Plasma lipid species showing significant correlation with concentrations in each of the 7 tissue site (BH-corrected p<0.05), with redundant features removed.

Plasma-tissue pair	ESI mode	peakID	MS1	MS2	Adduct	Class	mz	rt	r	CI	p(BH-corrected)
Plasma-STA	ESI+	LP_949.7275_596.91	TG 58:10		[M+Na]+	TG	949.7275	596.91	0.71	0.41, 0.87	3.56E-02
	ESI+	LP_970.7863_608.69	TG 60:11	TG(18:1/20:4/22:6)	[M+NH4]+	TG	970.7863	608.69	0.70	0.4, 0.87	3.56E-02
	ESI-	LN_666.6032_500.13	Cer 40:1;O2		[M+Formate]-	CER	666.6032	500.13	0.61	0.26, 0.82	4.45E-02
	ESI-	LN_676.6242_496.99	Cer 42:2;O		[M+Formate]-	CER	676.6242	496.99	0.69	0.37, 0.86	3.15E-02
	ESI-	LN_824.5439_310.62	PC 36:5	PC(16:0/20:5)	[M+Formate]-	PC	824.5439	310.62	0.63	0.28, 0.83	4.45E-02
	ESI-	LN_856.6052_390.9	PC 38:3	PC(18:0/20:3)	[M-H]-	PC	856.6052	390.90	0.61	0.26, 0.82	4.45E-02
Plasma-SSA	ESI+	LP_720.5905_396.22	PC O-32:0	PC(16:0e/16:0)	[M+H]+	ether-linked PC	720.5905	396.22	0.70	0.36, 0.88	4.83E-02
	ESI+	LP_851.7095_633.64	TG 50:3		[M+Na]+	TG	851.7095	633.64	0.75	0.44, 0.9	2.84E-02
	ESI+	LP_879.7402_661.87	TG 52:3		[M+Na]+	TG	879.7402	661.87	0.73	0.41, 0.89	3.05E-02
	ESI+	LP_877.7254_638.15	TG 52:4	TG(16:0/18:2/18:2)	[M+Na]+	TG	877.7254	638.15	0.74	0.43, 0.89	2.84E-02
	ESI-	LN_836.5799_353.31	PC O-38:6	PC(18:1p/20:4)	[M+Formate]-	ether-linked PC	836.5799	353.31	0.68	0.33, 0.87	4.49E-02
	ESI-	LN_838.5932_359.98	PC O-38:5	PC(18:0p/20:4)	[M+Formate]-	ether-linked PC	838.5932	359.98	0.69	0.34, 0.87	4.49E-02
Plasma-DSA	ESI+	LP_906.7554_604.48	TG 55:8		[M+NH4]+	TG	906.7554	604.48	0.66	0.37, 0.84	9.44E-03
	ESI+	LP_934.7864_627.48	TG 57:8		[M+NH4]+	TG	934.7864	627.48	0.76	0.53, 0.89	1.27E-03
	ESI+	LP_942.7567_574.03	TG 58:11		[M+NH4]+	TG	942.7567	574.03	0.76	0.52, 0.89	1.27E-03
	ESI+	LP_955.7725_651.61	TG 58:7		[M+Na]+	TG	955.7725	651.61	0.63	0.31, 0.82	2.19E-02
	ESI+	LP_1020.8956_651.92	TG 63:7		[M+NH4]+	TG	1020.8956	651.92	0.75	0.51, 0.89	1.27E-03
Plasma-IAA	ESI+	LP_894.7555_612.58	TG 54:7	TG(16:0/16:1/22:6)	[M+NH4]+	TG	894.7555	612.58	0.68	0.36, 0.85	1.20E-02
	ESI+	LP_892.7407_588.12	TG 54:8	TG(16:1/16:1/22:6)	[M+NH4]+	TG	892.7407	588.12	0.74	0.46, 0.89	2.65E-03
	ESI+	LP_910.7847_639.3	TG 55:6	TG(16:0/17:0/22:6)	[M+NH4]+	TG	910.7847	639.30	0.62	0.27, 0.82	3.14E-02
	ESI+	LP_908.77_626.68	TG 55:7	TG(15:0/18:1/22:6)	[M+NH4]+	TG	908.7700	626.68	0.69	0.39, 0.86	8.87E-03
	ESI+	LP_906.7554_604.48	TG 55:8		[M+NH4]+	TG	906.7554	604.48	0.76	0.5, 0.89	2.16E-03

	ESI+	LP_918.7559_591.89	TG 56:9	TG(16:1/18:2/22:6)	[M+NH4]+	TG	918.7559	591.89	0.76	0.5, 0.9	2.16E-03
	ESI+	LP_934.7864_627.48	TG 57:8		[M+NH4]+	TG	934.7864	627.48	0.75	0.48, 0.89	2.16E-03
	ESI+	LP_944.7717_598.16	TG 58:10	TG(18:1/18:3/22:6)	[M+NH4]+	TG	944.7717	598.16	0.79	0.55, 0.91	2.16E-03
	ESI+	LP_946.7863_618.34	TG 58:9	TG(18:1/18:2/22:6)	[M+NH4]+	TG	946.7863	618.34	0.75	0.49, 0.89	2.16E-03
	ESI+	LP_970.7863_608.69	TG 60:11	TG(18:1/20:4/22:6)	[M+NH4]+	TG	970.7863	608.69	0.68	0.36, 0.85	1.20E-02
	ESI+	LP_974.8164_618.07	TG 60:9		[M+NH4]+	TG	974.8164	618.07	0.65	0.31, 0.84	1.74E-02
	ESI+	LP_1020.8956_651.92	TG 63:7		[M+NH4]+	TG	1020.8956	651.92	0.66	0.33, 0.84	1.66E-02
	ESI-	LN_772.5275_352.83	PE O-40:8	PE(18:1p/22:6)	[M-H]-	Ether-linked PE	772.5275	352.83	0.74	0.47, 0.89	2.69E-03
	ESI-	LN_774.5429_389.66	PE O-40:7	PE(18:0p/22:6)	[M-H]-	Ether-linked PE	774.5429	389.66	0.81	0.58, 0.92	4.29E-04
	ESI-	LN_776.5436_334.52	PC 32:1	PC(16:0/16:1)	[M+Formate]-	PC	776.5436	334.52	0.62	0.26, 0.82	4.02E-02
	ESI-	LN_826.5593_334.9	PC 36:4	PC(16:0/20:4)	[M+Formate]-	PC	826.5593	334.90	0.64	0.3, 0.84	2.98E-02
Plasma-VL	ESI-	LN_327.2528_223.91	FA 18:1		[M+Formate]-	FFA and derivatives	327.2528	223.91	0.71	0.4, 0.88	1.12E-02
	ESI-	LN_826.5593_334.9	PC 36:4	PC(16:0/20:4)	[M+Formate]-	PC	826.5593	334.90	0.76	0.48, 0.9	5.06E-03
	ESI-	LN_824.5439_310.62	PC 36:5	PC(16:0/20:5)	[M+Formate]-	PC	824.5439	310.62	0.69	0.36, 0.87	1.35E-02
	ESI-	LN_850.5588_324.15	PC 38:6	PC(16:0/22:6)	[M-H]-	PC	850.5588	324.15	0.69	0.36, 0.87	1.35E-02
	ESI-	LN_788.58_391.91	PC O-34:2		[M+Formate]-	ether-linked PC	788.5800	391.91	0.64	0.28, 0.84	2.95E-02
	ESI-	LN_812.5801_360.51	PC O-36:4	PC(16:0e/20:4)	[M+Formate]-	ether-linked PC	812.5801	360.51	0.64	0.28, 0.84	2.95E-02
	ESI-	LN_810.5645_351.59	PC O-36:5	PC(16:0p/20:4)	[M+Formate]-	ether-linked PC	810.5645	351.59	0.69	0.35, 0.87	1.35E-02
	ESI-	LN_838.5932_359.98	PC O-38:5	PC(18:0p/20:4)	[M+Formate]-	ether-linked PC	838.5932	359.98	0.77	0.5, 0.9	5.06E-03
	ESI-	LN_836.5799_353.31	PC O-38:6	PC(18:1p/20:4)	[M+Formate]-	ether-linked PC	836.5799	353.31	0.76	0.47, 0.9	5.06E-03
	ESI-	LN_772.5275_352.83	PE O-40:8	PE(18:1p/22:6)	[M-H]-	ether-linked PE	772.5275	352.83	0.64	0.28, 0.84	2.95E-02
Plasma-RAM	ESI-	LN_748.5118_298.92	PC 30:1		[M+Formate]-	PC	748.5118	298.92	0.63	0.24, 0.84	4.96E-02
	ESI-	LN_804.5746_371.77	PC 34:1	PC(16:0/18:1)	[M+Formate]-	PC	804.5746	371.77	0.62	0.23, 0.84	4.96E-02
	ESI-	LN_826.5593_334.9	PC 36:4	PC(16:0/20:4)	[M+Formate]-	PC	826.5593	334.90	0.62	0.23, 0.84	4.96E-02
	ESI-	LN_824.5439_310.62	PC 36:5	PC(16:0/20:5)	[M+Formate]-	PC	824.5439	310.62	0.75	0.45, 0.9	6.32E-03
	ESI-	LN_850.5588_324.15	PC 38:6	PC(16:0/22:6)	[M-H]-	PC	850.5588	324.15	0.74	0.42, 0.89	6.32E-03
	ESI-	LN_760.5482_352.75	PC O-32:2		[M+Formate]-	ether-linked PC	760.5482	352.75	0.75	0.44, 0.9	6.32E-03

	ESI-	LN_810.5645_351.59	PC O-36:5	PC(16:0p/20:4)	[M+Formate]-	ether-linked PC	810.5645	351.59	0.74	0.42, 0.89	6.32E-03
	ESI-	LN_808.5492_325.55	PC O-36:6		[M+Formate]-	ether-linked PC	808.5492	325.55	0.86	0.67, 0.95	2.94E-04
	ESI-	LN_836.5799_353.31	PC O-38:6	PC(18:1p/20:4)	[M+Formate]-	ether-linked PC	836.5799	353.31	0.70	0.37, 0.88	1.29E-02
	ESI-	LN_834.5633_339.5	PC O-38:7		[M+Formate]-	ether-linked PC	834.5633	339.50	0.81	0.57, 0.93	1.46E-03
	ESI-	LN_746.5107_335.76	PE O-38:7		[M-H]-	ether-linked PE	746.5107	335.76	0.66	0.29, 0.86	3.21E-02
	ESI-	LN_774.5429_389.66	PE O-40:7	PE(18:0p/22:6)-H	[M-H]-	ether-linked PE	774.5429	389.66	0.75	0.45, 0.9	6.32E-03
Plasma-Liver	ESI+	LP_664.6037_640.54	CE 18:3	ChE(18:3)	[M+NH4]+	ChE	664.6037	640.54	0.59	0.25, 0.8	5.85E-03
	ESI+	LP_692.6347_670.97	CE 20:3	ChE(20:3)	[M+NH4]+	ChE	692.6347	670.97	0.63	0.31, 0.83	3.16E-03
	ESI+	LP_688.6039_623.34	CE 20:5	ChE(20:5)	[M+NH4]+	ChE	688.6039	623.34	0.66	0.35, 0.84	1.71E-03
	ESI+	LP_566.5516_418.5	Cer 36:1;O2		[M+H]+	CER	566.5516	418.50	0.63	0.3, 0.82	3.38E-03
	ESI+	LP_578.5884_459.05	Cer 38:1;O		[M+H]+	CER	578.5884	459.05	0.77	0.54, 0.9	6.62E-05
	ESI+	LP_594.5833_460.41	Cer 38:1;O2		[M+H]+	CER	594.5833	460.41	0.55	0.19, 0.78	1.22E-02
	ESI+	LP_590.5881_481.53	Cer 39:1;O2		[M+H-H2O]+	CER	590.5881	481.53	0.59	0.25, 0.8	5.88E-03
	ESI+	LP_622.6145_500.56	Cer 40:1;O2	Cer(d18:1/22:0)	[M+H]+	CER	622.6145	500.56	0.61	0.27, 0.81	4.98E-03
	ESI+	LP_620.5991_464.21	Cer 40:2;O2		[M+H]+	CER	620.5991	464.21	0.48	0.09, 0.74	3.27E-02
	ESI+	LP_636.6307_520.8	Cer 41:1;O2		[M+H]+	CER	636.6307	520.80	0.63	0.3, 0.82	3.35E-03
	ESI+	LP_634.6142_485.37	Cer 41:2;O2		[M+H]+	CER	634.6142	485.37	0.54	0.18, 0.78	1.37E-02
	ESI+	LP_634.6507_540.88	Cer 42:1;O		[M+H]+	CER	634.6507	540.88	0.72	0.45, 0.87	3.31E-04
	ESI+	LP_650.6453_540.52	Cer 42:1;O2	Cer(d18:1/24:0)	[M+H]+	CER	650.6453	540.52	0.57	0.21, 0.79	8.94E-03
	ESI+	LP_632.6352_497.82	Cer 42:2;O		[M+H]+	CER	632.6352	497.82	0.59	0.24, 0.8	6.56E-03
	ESI+	LP_664.6618_550.46	Cer 43:1;O2		[M+H]+	CER	664.6618	550.46	0.50	0.13, 0.75	2.43E-02
	ESI+	LP_558.51_408.49	DG 30:0		[M+NH4]+	DG	558.5100	408.49	0.54	0.17, 0.77	1.50E-02
	ESI+	LP_584.5259_411.82	DG 32:1	DG(16:0/16:1)	[M+NH4]+	DG	584.5259	411.82	0.78	0.55, 0.9	6.25E-05
	ESI+	LP_582.5103_375.12	DG 32:2	DG(14:0/18:2)	[M+NH4]+	DG	582.5103	375.12	0.74	0.48, 0.88	2.20E-04
	ESI+	LP_612.5571_449.26	DG 34:1	DG(16:0/18:1)	[M+NH4]+	DG	612.5571	449.26	0.66	0.34, 0.84	1.83E-03
	ESI+	LP_610.5414_417.15	DG 34:2	DG(16:1/18:1)	[M+NH4]+	DG	610.5414	417.15	0.49	0.11, 0.75	2.88E-02
	ESI+	LP_608.5261_380.6	DG 34:3		[M+NH4]+	DG	608.5261	380.60	0.58	0.23, 0.8	7.44E-03

	ESI+	LP_638.5728_451.57	DG 36:2	DG(18:1/18:1)	[M+NH4]+	DG	638.5728	451.57	0.60	0.27, 0.81	5.11E-03
	ESI+	LP_682.5415_365.11	DG 40:8		[M+NH4]+	DG	682.5415	365.11	0.62	0.29, 0.82	3.83E-03
	ESI+	LP_722.6668_452.3	DG 42:2		[M+NH4]+	DG	722.6668	452.30	0.52	0.15, 0.77	1.80E-02
	ESI+	LP_862.8233_715.51	DG 52:2		[M+NH4]+	DG	862.8233	715.51	0.48	0.1, 0.74	3.22E-02
	ESI+	LP_706.5385_329.87	PC 30:0	PC(16:0/14:0)	[M+H]+	PC	706.5385	329.87	0.85	0.69, 0.94	4.24E-06
	ESI+	LP_704.5236_298.44	PC 30:1		[M+H]+	PC	704.5236	298.44	0.88	0.75, 0.95	1.35E-06
	ESI+	LP_720.5544_348.62	PC 31:0		[M+H]+	PC	720.5544	348.62	0.54	0.17, 0.77	1.46E-02
	ESI+	LP_718.5382_316.3	PC 31:1		[M+H]+	PC	718.5382	316.30	0.81	0.6, 0.91	2.06E-05
	ESI+	LP_732.5543_334.27	PC 32:1	PC(16:0/16:1)	[M+H]+	PC	732.5543	334.27	0.79	0.56, 0.9	4.61E-05
	ESI+	LP_730.5389_305.29	PC 32:2	PC(16:1/16:1)	[M+H]+	PC	730.5389	305.29	0.79	0.56, 0.9	4.85E-05
	ESI+	LP_746.57_352.76	PC 33:1	PC(15:0/18:1)	[M+H]+	PC	746.5700	352.76	0.53	0.16, 0.77	1.73E-02
	ESI+	LP_744.5544_323.92	PC 33:2	PC(15:0/18:2)	[M+H]+	PC	744.5544	323.93	0.59	0.25, 0.8	5.88E-03
	ESI+	LP_782.567_372.13	PC 34:1	PC(16:0/18:1)	[M+Na]+	PC	782.5670	372.13	0.45	0.06, 0.72	4.97E-02
	ESI+	LP_780.5508_341.88	PC 34:2	PC(16:0/18:2)	[M+Na]+	PC	780.5508	341.88	0.72	0.44, 0.87	3.72E-04
	ESI+	LP_754.5379_298.64	PC 34:4	PC(16:1/18:3)	[M+H]+	PC	754.5379	298.64	0.74	0.47, 0.88	2.37E-04
	ESI+	LP_770.5697_331.02	PC 35:3	PC(17:1/18:2)	[M+H]+	PC	770.5697	331.02	0.73	0.46, 0.87	2.75E-04
	ESI+	LP_788.6172_417.13	PC 36:1	PC(18:0/18:1)	[M+H]+	PC	788.6172	417.13	0.71	0.44, 0.87	4.04E-04
	ESI+	LP_786.6011_382.65	PC 36:2	PC(18:0/18:2)	[M+H]+	PC	786.6011	382.65	0.45	0.06, 0.72	4.63E-02
	ESI+	LP_782.5665_314.67	PC 36:4		[M+H]+	PC	782.5665	314.67	0.72	0.44, 0.87	3.97E-04
	ESI+	LP_782.5701_334.8	PC 36:4	PC(16:0/20:4)	[M+H]+	PC	782.5701	334.80	0.59	0.25, 0.8	6.02E-03
	ESI+	LP_780.5546_310.94	PC 36:5	PC(16:1/20:4)	[M+H]+	PC	780.5546	310.94	0.77	0.53, 0.9	7.60E-05
	ESI+	LP_778.5393_289.57	PC 36:6		[M+H]+	PC	778.5393	289.58	0.59	0.25, 0.8	5.85E-03
	ESI+	LP_800.6178_400.83	PC 37:2		[M+H]+	PC	800.6178	400.83	0.48	0.09, 0.74	3.35E-02
	ESI+	LP_798.6011_369.38	PC 37:3	PC(19:1/18:2)	[M+H]+	PC	798.6011	369.38	0.63	0.3, 0.82	3.35E-03
	ESI+	LP_796.5842_351.22	PC 37:4	PC(17:0/20:4)	[M+H]+	PC	796.5842	351.22	0.60	0.25, 0.81	5.76E-03
	ESI+	LP_816.6488_451.55	PC 38:1		[M+H]+	PC	816.6488	451.55	0.62	0.3, 0.82	3.52E-03
	ESI+	LP_814.6329_416.87	PC 38:2	PC(20:0/18:2)	[M+H]+	PC	814.6329	416.87	0.66	0.36, 0.84	1.58E-03

	ESI+	LP_812.6169_391.28	PC 38:3	PC(20:1/18:2)	[M+H]+	PC	812.6169	391.28	0.74	0.47, 0.88	2.33E-04
	ESI+	LP_810.6_353.52	PC 38:4		[M+H]+	PC	810.6000	353.52	0.58	0.23, 0.8	7.10E-03
	ESI+	LP_810.6008_375.81	PC 38:4	PC(18:0/20:4)	[M+H]+	PC	810.6008	375.82	0.67	0.37, 0.85	1.32E-03
	ESI+	LP_806.57_325.14	PC 38:6	PC(16:0/22:6)	[M+H]+	PC	806.5700	325.14	0.58	0.24, 0.8	6.94E-03
	ESI+	LP_804.5545_294.07	PC 38:7	PC(16:1/22:6)	[M+H]+	PC	804.5545	294.07	0.58	0.23, 0.8	7.10E-03
	ESI+	LP_822.6001_351.83	PC 39:5		[M+H]+	PC	822.6001	351.83	0.62	0.29, 0.82	3.69E-03
	ESI+	LP_820.5842_338.9	PC 39:6	PC(17:0/22:6)	[M+H]+	PC	820.5842	338.90	0.63	0.3, 0.82	3.44E-03
	ESI+	LP_834.6012_362.35	PC 40:6	PC(18:0/22:6)	[M+H]+	PC	834.6012	362.35	0.49	0.11, 0.74	2.99E-02
	ESI+	LP_832.5852_328.98	PC 40:7	PC(18:1/22:6)	[M+H]+	PC	832.5852	328.98	0.52	0.15, 0.76	1.84E-02
	ESI+	LP_830.5702_301.29	PC 40:8	PC(16:1/24:7)	[M+H]+	PC	830.5702	301.29	0.65	0.33, 0.83	2.29E-03
	ESI+	LP_858.6005_329.89	PC 42:8		[M+H]+	PC	858.6005	329.89	0.51	0.13, 0.75	2.39E-02
	ESI+	LP_692.5612_354.2	PC O-30:0		[M+H]+	ether-linked PC	692.5612	354.20	0.48	0.1, 0.74	3.23E-02
	ESI+	LP_744.5894_366.48	PC O-34:2	PC(16:0e/18:2)	[M+H]+	ether-linked PC	744.5894	366.48	0.59	0.24, 0.8	6.56E-03
	ESI+	LP_764.5589_326.52	PC O-36:6	PC(16:1p/20:4)	[M+H]+	ether-linked PC	764.5589	326.52	0.80	0.59, 0.91	2.74E-05
	ESI+	LP_818.6055_348.66	PC O-40:7	PC(18:0p/22:6)	[M+H]+	ether-linked PC	818.6055	348.66	0.62	0.29, 0.82	3.55E-03
	ESI+	LP_878.7016_478.14	PC O-44:5		[M+H]+	ether-linked PC	878.7016	478.14	0.62	0.29, 0.82	3.58E-03
	ESI+	LP_790.6326_450.82	PE 36:0		[M+H]+	PC	790.6326	450.82	0.49	0.1, 0.74	3.03E-02
	ESI+	LP_746.5701_424.94	PE 36:1	PE(18:0/18:1)	[M+H]+	PE	746.5701	424.94	0.62	0.29, 0.82	3.73E-03
	ESI+	LP_744.5548_392.83	PE 36:2	PE(18:0/18:2)	[M+H]+	PE	744.5548	392.83	0.58	0.23, 0.8	7.27E-03
	ESI+	LP_742.5392_353.74	PE 36:3	PE(18:1/18:2)	[M+H]+	PE	742.5392	353.74	0.63	0.31, 0.82	3.19E-03
	ESI+	LP_700.5285_371.23	PE O-34:3	PE(16:0p/18:2)	[M+H]+	ether-linked PE	700.5285	371.23	0.46	0.07, 0.73	4.17E-02
	ESI+	LP_730.5751_444.56	PE O-36:2		[M+H]+	ether-linked PE	730.5751	444.56	0.51	0.13, 0.76	2.28E-02
	ESI+	LP_722.5135_336.23	PE O-36:6	PE(16:0p/20:5)	[M+H]+	ether-linked PE	722.5135	336.23	0.80	0.59, 0.91	3.11E-05
	ESI+	LP_776.56_390.19	PE O-40:7	PE(18:0p/22:6)	[M+H]+	ether-linked PE	776.5600	390.19	0.61	0.27, 0.81	4.90E-03
	ESI+	LP_733.6229_383.16	SM 36:0;O2	SM(d18:0/18:0)	[M+H]+	SM	733.6229	383.16	0.78	0.55, 0.9	5.74E-05
	ESI+	LP_761.654_427.35	SM 38:0;O2		[M+H]+	SM	761.6540	427.35	0.60	0.26, 0.81	5.17E-03
	ESI+	LP_773.6547_433.08	SM 39:1;O2	SM(d16:0/23:1)	[M+H]+	SM	773.6547	433.08	0.49	0.11, 0.75	2.88E-02

	ESI+	LP_789.6848_470.62	SM 40:0;O2		[M+H]+	SM	789.6848	470.62	0.60	0.26, 0.81	5.40E-03
	ESI+	LP_815.7009_495.68	SM 42:1;O2	SM(d16:0/26:1)	[M+H]+	SM	815.7009	495.68	0.52	0.15, 0.77	1.80E-02
	ESI+	LP_738.6613_572.31	TG 42:1	TG(18:1/12:0/12:0)	[M+NH4]+	TG	738.6613	572.31	0.68	0.38, 0.85	1.14E-03
	ESI+	LP_766.6925_603.01	TG 44:1	TG(18:1/12:0/14:0)	[M+NH4]+	TG	766.6925	603.01	0.80	0.58, 0.91	3.49E-05
	ESI+	LP_764.677_575.84	TG 44:2	TG(12:0/14:0/18:2)	[M+NH4]+	TG	764.6770	575.84	0.73	0.47, 0.88	2.45E-04
	ESI+	LP_780.708_616.75	TG 45:1	TG(15:0/12:0/18:1)	[M+NH4]+	TG	780.7080	616.75	0.63	0.3, 0.82	3.35E-03
	ESI+	LP_796.7391_658.39	TG 46:0	TG(16:0/14:0/16:0)	[M+NH4]+	TG	796.7391	658.39	0.85	0.68, 0.93	4.24E-06
	ESI+	LP_794.7238_630.73	TG 46:1	TG(16:0/14:0/16:1)	[M+NH4]+	TG	794.7238	630.73	0.81	0.61, 0.92	1.76E-05
	ESI+	LP_792.7083_605.14	TG 46:2	TG(16:1/12:0/18:1)	[M+NH4]+	TG	792.7083	605.14	0.77	0.54, 0.9	6.62E-05
	ESI+	LP_790.6927_579.26	TG 46:3	TG(16:1/14:1/16:1)	[M+NH4]+	TG	790.6927	579.26	0.71	0.42, 0.86	5.07E-04
	ESI+	LP_808.7393_644.59	TG 47:1	TG(15:0/16:0/16:1)	[M+NH4]+	TG	808.7393	644.59	0.75	0.5, 0.89	1.53E-04
	ESI+	LP_806.7237_618.38	TG 47:2	TG(15:0/16:1/16:1)	[M+NH4]+	TG	806.7237	618.38	0.72	0.45, 0.87	3.34E-04
	ESI+	LP_824.7705_684.75	TG 48:0	TG(16:0/16:0/16:0)	[M+NH4]+	TG	824.7705	684.75	0.88	0.74, 0.95	1.35E-06
	ESI+	LP_822.755_658.28	TG 48:1	TG(16:0/16:0/16:1)	[M+NH4]+	TG	822.7550	658.28	0.85	0.68, 0.93	4.91E-06
	ESI+	LP_820.7394_632.22	TG 48:2	TG(18:1/12:0/18:1)	[M+NH4]+	TG	820.7394	632.22	0.76	0.51, 0.89	1.33E-04
	ESI+	LP_818.7239_607.11	TG 48:3	TG(18:1/12:0/18:2)	[M+NH4]+	TG	818.7239	607.11	0.71	0.43, 0.86	5.00E-04
	ESI+	LP_816.7084_582.98	TG 48:4	TG(12:0/18:2/18:2)	[M+NH4]+	TG	816.7084	582.98	0.59	0.25, 0.8	5.85E-03
	ESI+	LP_838.786_630.24	TG 49:0		[M+NH4]+	TG	838.7860	630.24	0.73	0.46, 0.88	2.65E-04
	ESI+	LP_838.7861_694.97	TG 49:0	TG(16:0/16:0/17:0)	[M+NH4]+	TG	838.7861	694.97	0.83	0.63, 0.92	1.17E-05
	ESI+	LP_836.7701_603.74	TG 49:1		[M+NH4]+	TG	836.7701	603.74	0.74	0.48, 0.88	2.20E-04
	ESI+	LP_836.7708_671.03	TG 49:1	TG(15:0/16:0/18:1)	[M+NH4]+	TG	836.7708	671.04	0.78	0.54, 0.9	6.27E-05
	ESI+	LP_834.7551_645.8	TG 49:2	TG(15:0/16:0/18:2)	[M+NH4]+	TG	834.7551	645.80	0.70	0.41, 0.86	6.35E-04
	ESI+	LP_832.7398_620.85	TG 49:3	TG(15:0/16:1/18:2)	[M+NH4]+	TG	832.7398	620.85	0.64	0.33, 0.83	2.42E-03
	ESI+	LP_852.802_708.44	TG 50:0	TG(18:0/16:0/16:0)	[M+NH4]+	TG	852.8020	708.44	0.83	0.65, 0.93	9.31E-06
	ESI+	LP_850.7865_684.05	TG 50:1	TG(16:0/16:0/18:1)	[M+NH4]+	TG	850.7865	684.05	0.79	0.56, 0.9	4.61E-05
	ESI+	LP_848.7707_658.75	TG 50:2	TG(16:0/16:0/18:2)	[M+NH4]+	TG	848.7707	658.75	0.74	0.47, 0.88	2.33E-04
	ESI+	LP_846.7549_634.13	TG 50:3	TG(16:0/16:1/18:2)	[M+NH4]+	TG	846.7549	634.13	0.60	0.25, 0.81	5.84E-03

	ESI+	LP_844.7364_585.22	TG 50:4		[M+NH4]+	TG	844.7364	585.22	0.57	0.22, 0.79	8.27E-03
	ESI+	LP_844.7395_611.22	TG 50:4	TG(16:1/16:1/18:2)	[M+NH4]+	TG	844.7395	611.22	0.59	0.25, 0.81	5.85E-03
	ESI+	LP_842.7241_588.11	TG 50:5	TG(14:0/18:2/18:3)	[M+NH4]+	TG	842.7241	588.11	0.54	0.18, 0.78	1.31E-02
	ESI+	LP_866.8157_658.06	TG 51:0		[M+NH4]+	TG	866.8157	658.06	0.85	0.68, 0.93	4.24E-06
	ESI+	LP_864.801_630.65	TG 51:1		[M+NH4]+	TG	864.8010	630.65	0.82	0.63, 0.92	1.23E-05
	ESI+	LP_864.8023_694.83	TG 51:1	TG(16:0/17:0/18:1)	[M+NH4]+	TG	864.8023	694.83	0.80	0.59, 0.91	2.98E-05
	ESI+	LP_862.7859_606.24	TG 51:2		[M+NH4]+	TG	862.7859	606.24	0.74	0.49, 0.88	1.96E-04
	ESI+	LP_862.7863_692.49	TG 51:2	TG(16:0/17:1/18:1)	[M+NH4]+	TG	862.7863	692.49	0.78	0.55, 0.9	6.25E-05
	ESI+	LP_862.7865_671.61	TG 51:2	TG(16:1/17:0/18:1)	[M+NH4]+	TG	862.7865	671.61	0.69	0.4, 0.86	7.76E-04
	ESI+	LP_860.7708_648.15	TG 51:3	TG(16:1/17:1/18:1)	[M+NH4]+	TG	860.7708	648.15	0.51	0.14, 0.76	2.12E-02
	ESI+	LP_858.7552_624.79	TG 51:4	TG(16:1/17:1/18:2)	[M+NH4]+	TG	858.7552	624.79	0.49	0.11, 0.75	2.88E-02
	ESI+	LP_880.8348_727.76	TG 52:0	TG(18:0/16:0/18:0)	[M+NH4]+	TG	880.8348	727.76	0.53	0.16, 0.77	1.58E-02
	ESI+	LP_878.8179_707.82	TG 52:1	TG(18:0/16:0/18:1)	[M+NH4]+	TG	878.8179	707.82	0.82	0.62, 0.92	1.46E-05
	ESI+	LP_876.8021_683.58	TG 52:2	TG(16:0/18:1/18:1)	[M+NH4]+	TG	876.8021	683.58	0.69	0.4, 0.86	7.66E-04
	ESI+	LP_874.7861_661.22	TG 52:3	TG(16:0/18:1/18:2)	[M+NH4]+	TG	874.7861	661.22	0.47	0.08, 0.73	3.82E-02
	ESI+	LP_877.7254_638.15	TG 52:4	TG(16:0/18:2/18:2)	[M+Na]+	TG	877.7254	638.15	0.52	0.14, 0.76	1.99E-02
	ESI+	LP_875.7102_615.75	TG 52:5	TG(16:0/18:2/18:3)	[M+Na]+	TG	875.7102	615.75	0.49	0.11, 0.75	2.81E-02
	ESI+	LP_894.8476_684.46	TG 53:0		[M+NH4]+	TG	894.8476	684.46	0.87	0.71, 0.94	3.40E-06
	ESI+	LP_892.8315_658.07	TG 53:1		[M+NH4]+	TG	892.8315	658.07	0.83	0.64, 0.92	1.15E-05
	ESI+	LP_892.8332_714.55	TG 53:1	TG(18:0/17:0/18:1)	[M+NH4]+	TG	892.8332	714.55	0.82	0.63, 0.92	1.24E-05
	ESI+	LP_890.8167_632.05	TG 53:2		[M+NH4]+	TG	890.8167	632.05	0.73	0.46, 0.88	2.64E-04
	ESI+	LP_890.8175_695.42	TG 53:2	TG(17:0/18:1/18:1)	[M+NH4]+	TG	890.8175	695.42	0.72	0.45, 0.87	3.34E-04
	ESI+	LP_888.8017_672.84	TG 53:3	TG(17:0/18:1/18:2)	[M+NH4]+	TG	888.8017	672.84	0.56	0.21, 0.79	9.29E-03
	ESI+	LP_891.7415_649.95	TG 53:4		[M+Na]+	TG	891.7415	649.95	0.50	0.12, 0.75	2.45E-02
	ESI+	LP_911.8044_726.29	TG 54:1		[M+Na]+	TG	911.8044	726.29	0.84	0.66, 0.93	6.91E-06
	ESI+	LP_904.8319_631.37	TG 54:2		[M+NH4]+	TG	904.8319	631.37	0.78	0.55, 0.9	6.25E-05
	ESI+	LP_904.833_707.44	TG 54:2	TG(18:0/18:1/18:1)	[M+NH4]+	TG	904.8330	707.45	0.74	0.48, 0.88	2.20E-04

	ESI+	LP_902.8164_683.74	TG 54:3	TG(18:0/18:1/18:2)	[M+NH4]+	TG	902.8164	683.74	0.63	0.3, 0.82	3.42E-03
	ESI+	LP_894.7555_612.58	TG 54:7	TG(16:0/16:1/22:6)	[M+NH4]+	TG	894.7555	612.58	0.47	0.09, 0.74	3.63E-02
	ESI+	LP_922.8795_708.24	TG 55:0		[M+NH4]+	TG	922.8795	708.24	0.83	0.63, 0.92	1.18E-05
	ESI+	LP_920.8629_684.58	TG 55:1		[M+NH4]+	TG	920.8629	684.58	0.77	0.53, 0.89	8.28E-05
	ESI+	LP_918.8477_658.13	TG 55:2		[M+NH4]+	TG	918.8477	658.13	0.70	0.41, 0.86	6.35E-04
	ESI+	LP_916.8324_634.22	TG 55:3		[M+NH4]+	TG	916.8324	634.22	0.58	0.23, 0.8	7.10E-03
	ESI+	LP_934.8777_684.69	TG 56:1		[M+NH4]+	TG	934.8777	684.69	0.76	0.51, 0.89	1.13E-04
	ESI+	LP_932.8632_657.78	TG 56:2		[M+NH4]+	TG	932.8632	657.78	0.70	0.41, 0.86	6.79E-04
	ESI+	LP_937.8198_723.58	TG 56:2		[M+Na]+	TG	937.8198	723.58	0.58	0.24, 0.8	6.94E-03
	ESI+	LP_930.848_706.11	TG 56:3	TG(20:1/18:1/18:1)	[M+NH4]+	TG	930.8480	706.11	0.68	0.37, 0.85	1.18E-03
	ESI+	LP_948.8952_707.86	TG 57:1		[M+NH4]+	TG	948.8952	707.86	0.81	0.6, 0.91	2.32E-05
	ESI+	LP_946.8791_683.45	TG 57:2		[M+NH4]+	TG	946.8791	683.45	0.68	0.38, 0.85	1.14E-03
	ESI+	LP_960.8948_684.28	TG 58:2		[M+NH4]+	TG	960.8948	684.28	0.66	0.35, 0.84	1.73E-03
	ESI+	LP_950.8174_668.88	TG 58:7	TG(18:0/18:1/22:6)	[M+NH4]+	TG	950.8174	668.88	0.45	0.06, 0.72	4.76E-02
	ESI+	LP_946.7863_618.34	TG 58:9	TG(18:1/18:2/22:6)	[M+NH4]+	TG	946.7863	618.34	0.49	0.11, 0.75	2.88E-02
	ESI+	LP_974.911_707.44	TG 59:2		[M+NH4]+	TG	974.9110	707.44	0.74	0.47, 0.88	2.37E-04
	ESI+	LP_972.8951_684.74	TG 59:3		[M+NH4]+	TG	972.8951	684.74	0.61	0.27, 0.81	4.80E-03
	ESI+	LP_968.7715_649.52	TG 60:12		[M+NH4]+	TG	968.7715	649.52	0.65	0.33, 0.83	2.30E-03
	ESI+	LP_988.9268_707.46	TG 60:2		[M+NH4]+	TG	988.9268	707.46	0.73	0.46, 0.88	2.64E-04
	ESI+	LP_986.911_684.89	TG 60:3		[M+NH4]+	TG	986.9110	684.89	0.57	0.22, 0.79	8.16E-03
	ESI+	LP_1000.9266_705.56	TG 61:3	TG(25:1/18:1/18:1)	[M+NH4]+	TG	1000.9266	705.56	0.58	0.22, 0.79	7.79E-03
	ESI+	LP_1004.8663_617.46	TG 62:8		[M+NH4]+	TG	1004.8663	617.46	0.48	0.1, 0.74	3.23E-02
	ESI-	LN_583.2553_196	Bilirubin	Bilirubin	M-H	bile and derivatives	583.2553	196.00	0.69	0.39, 0.85	9.29E-04
	ESI-	LN_610.5409_417.26	Cer 36:1;O2		[M+Formate]-	CER	610.5409	417.26	0.61	0.27, 0.81	4.68E-03
	ESI-	LN_608.5247_380.04	Cer 36:2;O2		[M+Formate]-	CER	608.5247	380.04	0.56	0.21, 0.79	1.06E-02
	ESI-	LN_640.587_473.9	Cer 38:0;O2		[M+Formate]-	CER	640.5870	473.90	0.70	0.41, 0.86	7.19E-04
	ESI-	LN_638.5712_459.38	Cer 38:1;O2		[M+Formate]-	CER	638.5712	459.38	0.61	0.28, 0.81	4.57E-03

	ESI-	LN_636.5556_422.6	Cer 38:2;O2		[M+Formate]-	CER	636.5556	422.60	0.46	0.07, 0.73	4.65E-02
	ESI-	LN_652.5882_480.57	Cer 39:1;O2		[M+Formate]-	CER	652.5882	480.57	0.69	0.4, 0.86	8.24E-04
	ESI-	LN_652.6238_533.49	Cer 40:0;O		[M+Formate]-	CER	652.6238	533.49	0.84	0.63, 0.94	5.48E-05
	ESI-	LN_668.6192_513.54	Cer 40:0;O2		[M+Formate]-	CER	668.6192	513.54	0.78	0.55, 0.9	8.95E-05
	ESI-	LN_650.6083_499.49	Cer 40:1;O		[M+Formate]-	CER	650.6083	499.49	0.75	0.49, 0.88	2.05E-04
	ESI-	LN_666.6032_500.13	Cer 40:1;O2		[M+Formate]-	CER	666.6032	500.13	0.67	0.37, 0.85	1.32E-03
	ESI-	LN_664.5876_464.05	Cer 40:2;O2		[M+Formate]-	CER	664.5876	464.05	0.51	0.14, 0.76	2.29E-02
	ESI-	LN_682.6342_532	Cer 41:0;O2		[M+Formate]-	CER	682.6342	532.00	0.75	0.5, 0.89	2.02E-04
	ESI-	LN_680.6192_520.03	Cer 41:1;O2		[M+Formate]-	CER	680.6192	520.03	0.70	0.42, 0.86	6.71E-04
	ESI-	LN_678.6027_484.72	Cer 41:2;O2		[M+Formate]-	CER	678.6027	484.72	0.60	0.26, 0.81	5.79E-03
	ESI-	LN_680.6553_570.39	Cer 42:0;O		[M+Formate]-	CER	680.6553	570.39	0.82	0.59, 0.92	8.11E-05
	ESI-	LN_696.6503_551.31	Cer 42:0;O2		[M+Formate]-	CER	696.6503	551.31	0.82	0.61, 0.92	2.41E-05
	ESI-	LN_712.6455_517.86	Cer 42:0;O3		[M+Formate]-	CER	712.6455	517.86	0.76	0.52, 0.89	1.56E-04
	ESI-	LN_678.6398_538.3	Cer 42:1;O		[M+Formate]-	CER	678.6398	538.30	0.77	0.53, 0.9	1.10E-04
	ESI-	LN_694.6355_539.36	Cer 42:1;O2		[M+Formate]-	CER	694.6355	539.36	0.73	0.46, 0.87	3.34E-04
	ESI-	LN_676.6242_496.99	Cer 42:2;O		[M+Formate]-	CER	676.6242	496.99	0.76	0.51, 0.89	1.88E-04
	ESI-	LN_708.6503_550.13	Cer 43:1;O2		[M+Formate]-	CER	708.6503	550.13	0.69	0.4, 0.86	8.24E-04
	ESI-	LN_722.6661_573.29	Cer 44:1;O2		[M+Formate]-	CER	722.6661	573.29	0.57	0.22, 0.79	9.71E-03
	ESI-	LN_720.6505_533.63	Cer 44:2;O2		[M+Formate]-	CER	720.6505	533.63	0.45	0.06, 0.72	4.97E-02
	ESI-	LN_283.2634_257.52	FA 18:0		M-H	FFA and derivatives	283.2634	257.52	0.48	0.09, 0.74	3.84E-02
	ESI-	LN_301.2169_148.32	FA 20:5		M-H	FFA and derivatives	301.2169	148.32	0.66	0.34, 0.84	1.87E-03
	ESI-	LN_411.2046_224.06	FA 20:5;O4		[M+Formate]-	FFA and derivatives	411.2046	224.06	0.46	0.07, 0.73	4.73E-02
	ESI-	LN_934.6447_364.78	Hex2Cer 36:1;O2		[M+Formate]-	LacCer	934.6447	364.78	0.67	0.36, 0.84	1.35E-03
	ESI-	LN_962.6767_405.66	Hex2Cer 38:1;O2		[M+Formate]-	LacCer	962.6767	405.66	0.49	0.1, 0.75	3.59E-02
	ESI-	LN_990.707_445.7	Hex2Cer 40:1;O2		[M+Formate]-	LacCer	990.7070	445.70	0.59	0.25, 0.8	6.46E-03
	ESI-	LN_1018.7394_484.51	Hex2Cer 42:1;O2		[M+Formate]-	LacCer	1018.7394	484.51	0.60	0.26, 0.81	5.26E-03
	ESI-	LN_800.6241_421.74	HexCer 38:1;O2		[M+Formate]-	GlcCer	800.6241	421.74	0.54	0.17, 0.77	1.62E-02

	ESI-	LN_872.6814_490.81	HexCer 42:1;O3		[M+Formate]-	GlcCer	872.6814	490.81	0.72	0.45, 0.87	3.97E-04
	ESI-	LN_870.6634_448.81	HexCer 42:2;O3		[M+Formate]-	GlcCer	870.6634	448.81	0.45	0.06, 0.73	4.87E-02
	ESI-	LN_476.2776_84.02	LPE 18:2		[M-H]-	LPE	476.2776	84.02	0.53	0.16, 0.77	1.72E-02
	ESI-	LN_750.5287_330.11	PC 30:0		[M+Formate]-	PC	750.5287	330.11	0.89	0.75, 0.95	5.33E-07
	ESI-	LN_748.5118_298.92	PC 30:1		[M+Formate]-	PC	748.5118	298.92	0.91	0.81, 0.96	1.39E-07
	ESI-	LN_776.5436_334.52	PC 32:1	PC(16:0/16:1)	[M+Formate]-	PC	776.5436	334.52	0.91	0.79, 0.96	1.39E-07
	ESI-	LN_790.5615_352.77	PC 33:1	PC(15:0/18:1)	[M+Formate]-	PC	790.5615	352.77	0.75	0.5, 0.88	2.05E-04
	ESI-	LN_788.5439_322.81	PC 33:2		[M+Formate]-	PC	788.5439	322.81	0.73	0.46, 0.87	3.45E-04
	ESI-	LN_804.5746_371.77	PC 34:1	PC(16:0/18:1)	[M+Formate]-	PC	804.5746	371.77	0.48	0.09, 0.74	3.84E-02
	ESI-	LN_802.5591_341.48	PC 34:2	PC(16:0/18:2)	[M+Formate]-	PC	802.5591	341.48	0.58	0.23, 0.8	7.92E-03
	ESI-	LN_800.5437_314.18	PC 34:3	PC(16:1/18:2)	[M+Formate]-	PC	800.5437	314.18	0.49	0.11, 0.75	3.04E-02
	ESI-	LN_798.528_299.15	PC 34:4		[M+Formate]-	PC	798.5280	299.15	0.80	0.58, 0.91	4.51E-05
	ESI-	LN_818.5906_391.2	PC 35:1		[M+Formate]-	PC	818.5906	391.20	0.57	0.22, 0.79	9.53E-03
	ESI-	LN_816.5749_359.21	PC 35:2	PC(17:0/18:2)	[M+Formate]-	PC	816.5749	359.21	0.56	0.2, 0.79	1.12E-02
	ESI-	LN_812.5423_316.78	PC 35:4		[M+Formate]-	PC	812.5423	316.78	0.72	0.45, 0.87	3.99E-04
	ESI-	LN_810.5264_293.86	PC 35:5		[M+Formate]-	PC	810.5264	293.86	0.85	0.68, 0.93	6.90E-06
	ESI-	LN_834.62_450.49	PC 36:0		[M+Formate]-	PC	834.6200	450.49	0.61	0.27, 0.81	4.68E-03
	ESI-	LN_832.6068_413.93	PC 36:1		[M+Formate]-	PC	832.6068	413.93	0.82	0.62, 0.92	2.25E-05
	ESI-	LN_830.5903_380.54	PC 36:2	PC(18:1/18:1)	[M-H]-	PC	830.5903	380.54	0.73	0.46, 0.88	3.31E-04
	ESI-	LN_828.575_346.94	PC 36:3	PC(16:0/20:3)	[M+Formate]-	PC	828.5750	346.95	0.62	0.29, 0.82	3.90E-03
	ESI-	LN_826.5571_315.84	PC 36:4	PC(18:2/18:2)	[M-H]-	PC	826.5571	315.84	0.79	0.56, 0.9	7.05E-05
	ESI-	LN_826.5593_334.9	PC 36:4	PC(16:0/20:4)	[M+Formate]-	PC	826.5593	334.90	0.84	0.66, 0.93	8.88E-06
	ESI-	LN_824.5439_310.62	PC 36:5	PC(16:0/20:5)	[M+Formate]-	PC	824.5439	310.62	0.81	0.61, 0.92	2.62E-05
	ESI-	LN_844.6046_400.39	PC 37:2		[M+Formate]-	PC	844.6046	400.39	0.67	0.36, 0.84	1.40E-03
	ESI-	LN_842.5874_367.11	PC 37:3		[M+Formate]-	PC	842.5874	367.11	0.79	0.56, 0.9	6.71E-05
	ESI-	LN_840.572_352.3	PC 37:4		[M+Formate]-	PC	840.5720	352.30	0.83	0.63, 0.92	1.73E-05
	ESI-	LN_838.5576_322.31	PC 37:5		[M+Formate]-	PC	838.5576	322.31	0.84	0.67, 0.93	8.88E-06

	ESI-	LN_836.542_307.13	PC 37:6		[M+Formate]-	PC	836.5420	307.13	0.75	0.5, 0.89	2.05E-04
	ESI-	LN_860.6355_450.77	PC 38:1		[M+Formate]-	PC	860.6355	450.77	0.75	0.5, 0.89	2.02E-04
	ESI-	LN_858.6201_417	PC 38:2		[M+Formate]-	PC	858.6201	417.01	0.75	0.49, 0.88	2.05E-04
	ESI-	LN_856.6052_390.9	PC 38:3	PC(18:0/20:3)	[M-H]-	PC	856.6052	390.90	0.89	0.76, 0.95	4.47E-07
	ESI-	LN_854.5898_353.88	PC 38:4	PC(16:0/22:4)	[M+Formate]-	PC	854.5898	353.88	0.75	0.49, 0.88	2.05E-04
	ESI-	LN_854.59_373.51	PC 38:4		[M+Formate]-	PC	854.5900	373.51	0.83	0.65, 0.93	1.09E-05
	ESI-	LN_852.5741_337.48	PC 38:5	PC(16:0/22:5)	[M+Formate]-	PC	852.5741	337.48	0.66	0.35, 0.84	1.59E-03
	ESI-	LN_850.5587_308.16	PC 38:6	PC(18:2/20:4)	[M-H]-	PC	850.5587	308.16	0.71	0.43, 0.87	5.24E-04
	ESI-	LN_850.5588_324.15	PC 38:6	PC(16:0/22:6)	[M-H]-	PC	850.5588	324.15	0.74	0.47, 0.88	2.66E-04
	ESI-	LN_864.5719_340.41	PC 39:6		[M+Formate]-	PC	864.5719	340.41	0.84	0.66, 0.93	8.88E-06
	ESI-	LN_882.6204_401.91	PC 40:4		[M+Formate]-	PC	882.6204	401.92	0.73	0.46, 0.88	3.23E-04
	ESI-	LN_878.5871_340.46	PC 40:6		[M+Formate]-	PC	878.5871	340.46	0.50	0.12, 0.75	2.92E-02
	ESI-	LN_878.5898_361.84	PC 40:6	PC(22:6/18:0)	[M-H]-	PC	878.5898	361.84	0.68	0.38, 0.85	1.15E-03
	ESI-	LN_876.5722_327.08	PC 40:7	PC(22:6/18:1)	[M-H]-	PC	876.5722	327.08	0.69	0.4, 0.86	8.24E-04
	ESI-	LN_874.5583_301.4	PC 40:8		[M+Formate]-	PC	874.5583	301.40	0.70	0.42, 0.86	6.71E-04
	ESI-	LN_898.5577_293.38	PC 42:10		[M+Formate]-	PC	898.5577	293.38	0.68	0.37, 0.85	1.16E-03
	ESI-	LN_788.5765_365.53	PC O-34:2	PC(16:0e/18:2)	[M+Formate]-	PC	788.5765	365.53	0.52	0.15, 0.76	2.14E-02
	ESI-	LN_836.5799_353.31	PC O-38:6	PC(18:1p/20:4)	[M+Formate]-	PC	836.5799	353.31	0.58	0.23, 0.8	7.74E-03
	ESI-	LN_862.5949_348.86	PC O-40:7		[M+Formate]-	PC	862.5949	348.86	0.79	0.56, 0.9	6.68E-05
	ESI-	LN_922.689_477.48	PC O-44:5		[M+Formate]-	PC	922.6890	477.48	0.65	0.33, 0.83	2.25E-03
	ESI-	LN_716.5224_381.74	PE 34:1	PE(16:0/18:1)	[M-H]-	PE	716.5224	381.74	0.50	0.12, 0.75	2.94E-02
	ESI-	LN_714.507_350.58	PE 34:2	PE(16:0/18:2)	[M-H]-	PE	714.5070	350.58	0.53	0.16, 0.77	1.87E-02
	ESI-	LN_744.5544_423.23	PE 36:1	PE(18:0/18:1)	[M-H]-	PE	744.5544	423.23	0.60	0.26, 0.81	5.23E-03
	ESI-	LN_742.5383_390.18	PE 36:2	PE(18:1/18:1)	[M-H]-	PE	742.5383	390.18	0.68	0.38, 0.85	1.03E-03
	ESI-	LN_740.5209_354.11	PE 36:3	PE(18:1/18:2)	[M-H]-	PE	740.5209	354.11	0.59	0.25, 0.8	6.28E-03
	ESI-	LN_736.4897_318.58	PE 36:5	PE(16:0/20:5)	[M-H]-	PE	736.4897	318.58	0.47	0.08, 0.74	3.98E-02
	ESI-	LN_768.5524_400.17	PE 38:3	PE(18:0/20:3)	[M-H]-	PE	768.5524	400.17	0.81	0.61, 0.91	2.72E-05

	ESI-	LN_844.5875_366.95	PE 44:7		[M-H]-	PE	844.5875	366.95	0.54	0.17, 0.77	1.56E-02
	ESI-	LN_698.5119_370.02	PE O-34:3	PE(16:0p/18:2)	[M-H]-	PE	698.5119	370.02	0.57	0.22, 0.79	9.42E-03
	ESI-	LN_728.5595_444.36	PE O-36:2		[M-H]-	PE	728.5595	444.36	0.50	0.12, 0.75	2.76E-02
	ESI-	LN_726.5437_410.82	PE O-36:3	PE(18:0p/18:2)	[M-H]-	PE	726.5437	410.82	0.46	0.07, 0.73	4.72E-02
	ESI-	LN_720.4963_335.18	PE O-36:6	PE(16:0p/20:5)	[M-H]-	PE	720.4963	335.18	0.74	0.49, 0.88	2.14E-04
	ESI-	LN_752.5595_420.98	PE O-38:4		[M-H]-	PE	752.5595	420.98	0.50	0.13, 0.75	2.73E-02
	ESI-	LN_784.5093_381.74	PE O-38:6		[M+Cl]-	PE	784.5093	381.74	0.55	0.19, 0.78	1.36E-02
	ESI-	LN_746.5119_349.91	PE O-38:7	PE(16:0p/22:6)	[M-H]-	PE	746.5119	349.91	0.68	0.39, 0.85	9.60E-04
	ESI-	LN_776.5586_402.84	PE O-40:6		[M-H]-	PE	776.5586	402.84	0.48	0.09, 0.74	3.78E-02
	ESI-	LN_774.5429_389.66	PE O-40:7	PE(18:0p/22:6)	[M-H]-	PE	774.5429	389.66	0.75	0.49, 0.88	2.05E-04
	ESI-	LN_772.5275_352.83	PE O-40:8	PE(18:1p/22:6)	[M-H]-	PE	772.5275	352.83	0.64	0.31, 0.83	2.73E-03
	ESI-	LN_772.582_412.47	PE-NMe2(36:1)		M-H	PE-NMe2	772.5820	412.47	0.49	0.11, 0.75	3.12E-02
	ESI-	LN_770.5668_379.98	PE-NMe2(36:2)		M-H	PE-NMe2	770.5668	379.98	0.74	0.47, 0.88	2.66E-04
	ESI-	LN_766.5368_334.9	PE-NMe2(36:4)		M-H	PE-NMe2	766.5368	334.90	0.65	0.33, 0.83	2.25E-03
	ESI-	LN_764.5209_310.97	PE-NMe2(36:5)		M-H	PE-NMe2	764.5209	310.97	0.70	0.41, 0.86	7.55E-04
	ESI-	LN_790.536_324.09	PE-NMe2(38:6)		M-H	PE-NMe2	790.5360	324.09	0.65	0.34, 0.84	1.90E-03
	ESI-	LN_719.534_288.29	SM 32:1;O2	SM(d16:1/16:0)	[M+Formate]-	SM	719.5340	288.29	0.50	0.12, 0.75	2.76E-02
	ESI-	LN_749.5797_341.66	SM 34:0;O2	SM(d16:0/18:0)	[M+Formate]-	SM	749.5797	341.66	0.48	0.09, 0.74	3.66E-02
	ESI-	LN_777.6095_383.23	SM 36:0;O2	SM(d18:0/18:0)	[M+Formate]-	SM	777.6095	383.23	0.85	0.68, 0.93	7.34E-06
	ESI-	LN_773.5799_333.24	SM 36:2;O2	SM(d18:2/18:0)	[M+Formate]-	SM	773.5799	333.24	0.46	0.07, 0.73	4.70E-02
	ESI-	LN_805.6421_426.51	SM 38:0;O2		[M+Formate]-	SM	805.6421	426.51	0.65	0.34, 0.84	1.97E-03
	ESI-	LN_803.628_411.76	SM 38:1;O2	SM(d22:1/16:0)	[M+Formate]-	SM	803.6280	411.76	0.54	0.18, 0.78	1.47E-02
	ESI-	LN_801.61_372.8	SM 38:2;O2	SM(d20:0/18:2)	[M+Formate]-	SM	801.6100	372.80	0.46	0.07, 0.73	4.72E-02
	ESI-	LN_817.6425_432.17	SM 39:1;O2	SM(d16:0/23:1)	[M+Formate]-	SM	817.6425	432.17	0.63	0.3, 0.82	3.36E-03
	ESI-	LN_833.673_469.15	SM 40:0;O2		[M+Formate]-	SM	833.6730	469.15	0.63	0.31, 0.82	3.08E-03
	ESI-	LN_831.6592_454.62	SM 40:1;O2	SM(d22:1/18:0)	[M+Formate]-	SM	831.6592	454.62	0.56	0.2, 0.78	1.22E-02
	ESI-	LN_845.6749_475.01	SM 41:1;O2	SM(d16:0/25:1)	[M+Formate]-	SM	845.6749	475.01	0.56	0.2, 0.78	1.22E-02

	ESI-	LN_859.691_495.35	SM 42:1;O2	SM(d18:1/24:0)	[M+Formate]-	SM	859.6910	495.35	0.64	0.32, 0.83	2.65E-03
	ESI-	LN_873.7063_506.92	SM 43:1;O2		[M+Formate]-	SM	873.7063	506.92	0.51	0.13, 0.76	2.53E-02

Table 9.2: Plasma polar metabolites showing significant correlation with concentrations in each of the 7 tissue site (BH-corrected p<0.05), with redundant features removed.

Plasma-tissue pair	ESI mode	peakID	Metabolite	Adduct	mz	rt	r	CI	p (BH-corrected)
Plasma-STA	ESI+	HP_76.0764_618.2	Trimethylamine N-oxide	M+H+	76.0764	618.20	0.76	0.49, 0.89	1.66E-03
	ESI+	HP_129.0667_759.1	Dihydrothymine	M+H+	129.0667	759.10	0.63	0.29, 0.83	2.05E-02
	ESI+	HP_230.0965_761.56	Ergothioneine	M+H+	230.0965	761.56	0.64	0.29, 0.83	2.05E-02
	ESI-	LN_187.0068_130.14	p-Cresol sulfate	M-H-	187.0068	130.14	0.78	0.54, 0.91	9.26E-05
Plasma-SAA	ESI+	HP_118.087_672.87	L-Valine	M+H+	118.0870	672.87	0.71	0.38, 0.88	1.98E-02
Plasma-DSA	ESI+	HP_90.0557_764.62	L-Alanine	M+H+	90.0557	764.62	0.55	0.2, 0.77	2.19E-02
	ESI+	HP_118.087_672.87	L-Valine	M+H+	118.0870	672.87	0.54	0.2, 0.77	2.19E-02
	ESI+	HP_118.087_569.29	Betaine	M+H+	118.0870	569.29	0.60	0.28, 0.8	1.90E-02
	ESI+	HP_137.0713_681.06	Trigonellinamide (1-Methylnicotinamide)	M+H+	137.0713	681.06	0.58	0.24, 0.79	1.90E-02
	ESI+	HP_150.0588_650.57	L-Methionine	M+H+	150.0588	650.57	0.57	0.23, 0.78	1.90E-02
	ESI+	HP_162.1128_652.07	L-Carnitine	M+H+	162.1128	652.07	0.58	0.25, 0.79	1.90E-02
Plasma-IAA	ESI+	HP_76.0764_618.2	Trimethylamine N-oxide	M+H+	76.0764	618.20	0.81	0.6, 0.92	1.49E-04
	ESI+	HP_129.0667_759.1	Dihydrothymine	M+H+	129.0667	759.10	0.79	0.55, 0.91	2.70E-04
	ESI+	HP_230.0965_761.56	Ergothioneine	M+H+	230.0965	761.56	0.76	0.49, 0.89	5.96E-04
Plasma-VL	ESI+	HP_76.0401_805.67	Glycine	M+H+	76.0401	805.67	0.56	0.15, 0.81	4.05E-02
	ESI+	HP_76.0764_618.2	Trimethylamine N-oxide	M+H+	76.0764	618.20	0.72	0.39, 0.88	4.51E-03
	ESI+	HP_104.1077_636.65	Choline	M+H+	104.1077	636.65	0.59	0.18, 0.82	3.30E-02
	ESI+	HP_106.0507_829.31	L-Serine	M+H+	106.0507	829.31	0.70	0.37, 0.88	4.59E-03
	ESI+	HP_118.087_672.87	L-Valine	M+H+	118.0870	672.87	0.69	0.34, 0.87	5.81E-03
	ESI+	HP_118.087_569.29	Betaine	M+H+	118.0870	569.29	0.65	0.27, 0.85	1.19E-02
	ESI+	HP_132.1027_610.27	L-Leucine	M+H+	132.1027	610.27	0.82	0.59, 0.93	2.04E-04
	ESI+	HP_138.0553_605.76	Trigonelline	M+H+	138.0553	605.76	0.75	0.44, 0.9	2.22E-03
	ESI+	HP_161.1289_931.5	N(6)-Methyllysine	M+H+	161.1289	931.50	0.83	0.61, 0.93	1.89E-04
	ESI+	HP_166.0869_608.34	L-Phenylalanine	M+H+	166.0869	608.34	0.81	0.56, 0.92	3.15E-04

	ESI+	HP_176.1034_840.7	L-Citrulline	M+H+	176.1034	840.70	0.66	0.29, 0.86	9.70E-03
	ESI+	HP_176.1285_558.16	3-Oxooctanoic acid	M+NH4+	176.1285	558.16	0.95	0.87, 0.98	2.36E-08
	ESI+	HP_182.0819_705.36	L-Tyrosine	M+H+	182.0819	705.36	0.71	0.38, 0.88	4.55E-03
	ESI+	HP_185.0329_806.49	L-Glutamine	M+K+	185.0329	806.49	0.69	0.34, 0.87	5.81E-03
	ESI+	HP_205.0978_643.22	L-Tryptophan	M+H+	205.0978	643.22	0.57	0.16, 0.82	3.70E-02
	ESI+	HP_247.1447_504.71	Lenticin	M+H+	247.1447	504.71	0.90	0.76, 0.96	4.00E-06
	ESI-	LN_103.0393_136.89	Hydroxy butyric acid	M-H-	103.0393	136.89	0.70	0.35, 0.87	6.14E-03
	ESI-	LN_187.0068_130.14	p-Cresol sulfate	M-H-	187.0068	130.14	0.80	0.55, 0.92	4.75E-04
Plasma-RAM	ESI+	HP_61.0403_452.59	Urea	M+H+	61.0403	452.59	0.67	0.32, 0.86	1.17E-02
	ESI+	HP_76.0401_805.67	Glycine	M+H+	76.0401	805.67	0.75	0.45, 0.9	2.34E-03
	ESI+	HP_76.0764_618.2	Trimethylamine N-oxide	M+H+	76.0764	618.20	0.73	0.42, 0.89	3.19E-03
	ESI+	HP_118.087_672.87	L-Valine	M+H+	118.0870	672.87	0.63	0.25, 0.84	1.78E-02
	ESI+	HP_120.0663_780.21	L-Threonine	M+H+	120.0663	780.21	0.59	0.19, 0.82	2.82E-02
	ESI+	HP_129.0667_759.1	Dihydrothymine	M+H+	129.0667	759.10	0.64	0.27, 0.85	1.64E-02
	ESI+	HP_132.1027_628.47	L-Isoleucine	M+H+	132.1027	628.47	0.60	0.2, 0.83	2.82E-02
	ESI+	HP_132.1027_610.27	L-Leucine	M+H+	132.1027	610.27	0.59	0.19, 0.82	2.82E-02
	ESI+	HP_138.0553_605.76	Trigonelline	M+H+	138.0553	605.76	0.67	0.3, 0.86	1.17E-02
	ESI+	HP_138.0553_482.34	p-Aminobenzoic acid	M+H+	138.0553	482.34	0.98	0.94, 0.99	2.69E-11
	ESI+	HP_156.0772_941.88	L-Histidine	M+H+	156.0772	941.88	0.66	0.3, 0.86	1.17E-02
	ESI+	HP_157.0611_761.66	4-Imidazolone-5-propionic acid	M+H+	157.0611	761.66	0.80	0.55, 0.92	4.67E-04
	ESI+	HP_160.1336_579.28	DL-2-Aminooctanoic acid	M+H+	160.1336	579.28	0.60	0.2, 0.83	2.82E-02
	ESI+	HP_176.1285_558.16	3-Oxooctanoic acid	M+NH4+	176.1285	558.16	0.95	0.88, 0.98	6.27E-09
	ESI+	HP_247.1447_504.71	Lenticin	M+H+	247.1447	504.71	0.98	0.94, 0.99	2.69E-11
Plasma-Liver	ESI+	HP_61.0403_452.59	Urea	M+H+	61.0403	452.59	0.57	0.22, 0.79	1.22E-02
	ESI+	HP_76.0401_805.67	Glycine	M+H+	76.0401	805.67	0.62	0.29, 0.82	5.46E-03
	ESI+	HP_76.0764_618.2	Trimethylamine N-oxide	M+H+	76.0764	618.20	0.92	0.83, 0.97	2.15E-09
	ESI+	HP_104.0713_722.71	L-a-Amino-n-butyric acid	M+H+	104.0713	722.71	0.56	0.2, 0.79	1.43E-02

ESI+	HP_114.067_657	L-Creatinine	M+H+	114.0670	657.00	0.49	0.1, 0.74	4.16E-02
ESI+	HP_116.0714_663.92	L-Proline	M+H+	116.0714	663.92	0.72	0.44, 0.87	4.22E-04
ESI+	HP_118.087_672.87	L-Valine	M+H+	118.0870	672.87	0.57	0.21, 0.79	1.34E-02
ESI+	HP_118.087_569.29	Betaine	M+H+	118.0870	569.29	0.72	0.45, 0.87	4.18E-04
ESI+	HP_120.0663_780.21	L-Threonine	M+H+	120.0663	780.21	0.54	0.17, 0.77	2.00E-02
ESI+	HP_129.0667_759.1	Dihydrothymine	M+H+	129.0667	759.10	0.90	0.79, 0.96	1.87E-08
ESI+	HP_138.0553_605.76	Trigonelline	M+H+	138.0553	605.76	0.88	0.73, 0.94	2.38E-07
ESI+	HP_138.0553_482.34	p-Aminobenzoic acid	M+H+	138.0553	482.34	0.98	0.96, 0.99	8.18E-16
ESI+	HP_146.1178_604.33	4-Trimethylammoniobutanoic acid	M+H+	146.1178	604.33	0.49	0.11, 0.75	3.89E-02
ESI+	HP_147.0769_807.33	L-Glutamine	M+H+	147.0769	807.33	0.65	0.33, 0.83	2.76E-03
ESI+	HP_150.0588_650.57	L-Methionine	M+H+	150.0588	650.57	0.54	0.17, 0.77	2.00E-02
ESI+	HP_156.0772_941.88	L-Histidine	M+H+	156.0772	941.88	0.59	0.25, 0.8	9.32E-03
ESI+	HP_160.1336_579.28	DL-2-Aminooctanoic acid	M+H+	160.1336	579.28	0.83	0.64, 0.92	4.42E-06
ESI+	HP_161.1289_931.5	N(6)-Methyllysine	M+H+	161.1289	931.50	0.78	0.55, 0.9	4.20E-05
ESI+	HP_162.1128_652.07	L-Carnitine	M+H+	162.1128	652.07	0.58	0.23, 0.8	1.16E-02
ESI+	HP_166.0869_608.34	L-Phenylalanine	M+H+	166.0869	608.34	0.48	0.09, 0.74	4.56E-02
ESI+	HP_176.1285_558.16	3-Oxooctanoic acid	M+NH4+	176.1285	558.16	0.98	0.95, 0.99	5.33E-15
ESI+	HP_185.0329_806.49	L-Glutamine	M+K+	185.0329	806.49	0.48	0.1, 0.74	4.22E-02
ESI+	HP_205.0978_643.22	L-Tryptophan	M+H+	205.0978	643.22	0.70	0.42, 0.86	6.23E-04
ESI+	HP_230.0965_761.56	Ergothioneine	M+H+	230.0965	761.56	0.83	0.64, 0.92	4.42E-06
ESI+	HP_247.1447_504.71	Lenticin	M+H+	247.1447	504.71	0.96	0.92, 0.98	7.50E-13
ESI+	HP_258.1109_783.38	sn-Glycero-3-phosphocholine	M+H+	258.1109	783.38	0.53	0.17, 0.77	2.03E-02
ESI+	HP_265.1189_359.88	Phenylacetylglutamine	M+H+	265.1189	359.88	0.80	0.58, 0.91	2.37E-05
ESI-	LN_103.0393_136.89	Hydroxy butyric acid	M-H-	103.0393	136.89	0.62	0.29, 0.82	1.20E-02

Table 9.3: Internal standard added to extraction solvent for monitoring signal variation during instrumental analysis

Compound	Concentration (mg/L)
d_2-tyrosine	1.6
d_5-tryptophan	1.6
d_4-citric acid	1.6
d_{10}-leucine	2
d_4-alanine	4
^{13}C-glucose	16

Table 9.4: Data pre-processing parameters for lipidomic profile (XCMS)

ESI mode	pos	neg
method	centWave	centWave
noise	20000	20000
ppm	15	15
mzdiff	0.001	0.001
peakwidth	(5,30)	(5,30)
prefilter	c(5,30000)	c(5,30000)
snthresh	10	10
integrate	1	1
bw	5	5
mzwid	0.015	0.015
minfrac	0.8	0.8

Table 9.5: Data pre-processing parameters HILIC profile (ADAP)

ESI mode		pos	neg
mass detection	method	centroid	centroid
	noise level	200	200
chromatogram builder	method	ADAP	ADAP
	Min scans	5	5
	Min highest intensity	300	300
	m/z tol	0.001,15ppm	0.001,15ppm
chromatogram deconvolution	method	wavelets ADAP	wavelets ADAP
	snthresh	7	7
	coef/area threshold	60	60
	min height	300	300
	peak duration range	0.05-2	0.05-2
	RT wavelet scale	0.05-0.14	0.05-0.14
deisotope	*m/z* tol	0.001, 5ppm	0.001, 5ppm
	RT tolerance	1% relative	1% relative
	max charge	1	1
	rep isotope	lowest *m/z*	lowest *m/z*
dulicate peak filter		0.001, 5ppm, 0.15 min	0.001, 5ppm, 0.15 min
RT correction	RT normaliser	0.001,15ppm, 0.5min, 20000	0.001,15ppm, 0.5min, 10000
peak alignment	Join aligner	0.001, 15ppm, 85, 0.5min, 85	0.001, 15ppm, 85, 0.5min, 85
peak filter	peak filter	100% (QC)	100% (QC)

Table 9.6: Differentially expressed lipid species between Caucasian and Asian Chinese

MS1	*MS2*	*mz*	*rt(min)*	*Lipid Subclass*	*Odds ratio*	*CI Lower*	*CI Upper*	*p*
FA(20:4)		303.2331	3.03	Fatty Acyls	1.47	1.12	1.96	1.30E-02
FA(22:6)		327.2330	2.86	Fatty Acyls	2.13	1.56	3.00	2.83E-05
FA(18:2)		279.2330	3.16	Fatty Acyls	3.22	2.23	4.85	4.63E-08
DG(38:3)		664.5878	7.27	Diacylglycerol	1.58	1.10	2.37	3.34E-02
DG(40:7)		684.5559	6.83	Diacylglycerol	1.60	1.14	2.46	3.15E-02
DG(36:4)	DG(18:2/18:2)	634.5399	6.67	Diacylglycerol	1.87	1.29	2.81	3.57E-03
DG(40:8)		682.5406	6.25	Diacylglycerol	2.02	1.42	3.06	9.60E-04
TG(50:2)		853.7244	11.35	Triacylglycerol	0.23	0.15	0.34	1.20E-10
TG(47:1)	TG(14:0/15:0/18:1)	808.7382	11.13	Triacylglycerol	0.25	0.16	0.39	2.90E-08
TG(48:2)		825.6942	10.92	Triacylglycerol	0.26	0.17	0.37	2.70E-10
TG(50:3)		851.7090	10.95	Triacylglycerol	0.35	0.23	0.52	1.86E-06
TG(49:1)	TG(15:0/16:0/18:1)	836.7700	11.59	Triacylglycerol	0.37	0.26	0.51	9.69E-08
TG(55:2)		918.8467	11.39	Triacylglycerol	0.40	0.28	0.55	6.63E-07
TG(49:2)	TG(15:0/16:0/18:2)	834.7541	11.17	Triacylglycerol	0.41	0.29	0.56	1.44E-06
TG(47:0)		810.7539	11.59	Triacylglycerol	0.42	0.29	0.59	1.19E-05
TG(44:1)	TG(12:0/14:0/18:1)	766.6920	10.39	Triacylglycerol	0.44	0.30	0.62	4.33E-05
TG(48:1)	TG(14:0/16:0/18:1)	822.7541	11.36	Triacylglycerol	0.42	0.30	0.58	2.26E-06
TG(51:1)	TG(16:0/17:0/18:1)	864.8011	11.99	Triacylglycerol	0.43	0.31	0.58	9.34E-07
TG(58:9)		946.7852	11.92	Triacylglycerol	0.51	0.32	0.78	6.37E-03
TG(46:0)	TG(14:0/16:0/16:0)	796.7383	11.37	Triacylglycerol	0.48	0.33	0.68	2.32E-04
TG(46:1)	TG(12:0/16:0/18:1)	794.7230	10.91	Triacylglycerol	0.48	0.34	0.66	8.67E-05
TG(44:0)	TG(14:0/14:0/16:0)	768.7071	10.90	Triacylglycerol	0.50	0.34	0.71	6.54E-04
TG(49:0)	TG(16:0/16:0/17:0)	838.7855	12.01	Triacylglycerol	0.49	0.36	0.66	3.87E-05
TG(44:2)	TG(12:0/14:0/18:2)	764.6763	9.92	Triacylglycerol	0.51	0.36	0.69	1.26E-04
TG(66:9)		1058.9097	11.92	Triacylglycerol	0.56	0.38	0.80	4.61E-03
TG(50:1)		855.7408	11.80	Triacylglycerol	0.57	0.42	0.75	4.86E-04

TG(56:7)	TG(16:0/18:1/22:6)	922.7849	11.06	Triacylglycerol	1.41	1.05	1.95	4.52E-02
TG(52:4)		877.7245	11.03	Triacylglycerol	1.59	1.08	2.43	4.46E-02
TG(60:4)		984.8928	11.41	Triacylglycerol	1.48	1.10	2.04	2.36E-02
TG(57:3)		944.8622	11.41	Triacylglycerol	1.64	1.12	2.48	2.83E-02
TG(52:3)	TG(16:0/18:1/18:2)	874.7847	11.41	Triacylglycerol	1.75	1.20	2.64	1.14E-02
TG(58:4)		956.8625	11.03	Triacylglycerol	1.75	1.22	2.58	7.02E-03
TG(60:5)		982.8783	11.05	Triacylglycerol	1.76	1.24	2.58	5.64E-03
TG(54:5)		903.7405	11.07	Triacylglycerol	1.83	1.26	2.72	4.54E-03
TG(58:3)		958.8779	11.40	Triacylglycerol	1.97	1.34	2.98	2.10E-03
TG(59:5)		968.8629	11.04	Triacylglycerol	2.05	1.40	3.13	1.22E-03
TG(52:5)	TG(16:0/18:2/18:3)	870.7544	10.67	Triacylglycerol	2.09	1.41	3.25	1.50E-03
TG(59:4)		970.8780	11.41	Triacylglycerol	1.98	1.43	2.81	2.47E-04
TG(58:9)'	TG(18:1/18:2/22:6)	946.7853	10.69	Triacylglycerol	2.20	1.51	3.41	4.56E-04
TG(56:8)	TG(16:0/18:2/22:6)	920.7700	10.66	Triacylglycerol	2.31	1.54	3.67	4.71E-04
TG(54:6)		901.7250	10.64	Triacylglycerol	2.15	1.54	3.07	5.69E-05
TG(58:8)	TG(18:1/18:1/22:6)	948.8002	11.09	Triacylglycerol	2.62	1.76	4.10	3.42E-05
TG(57:4)		942.8472	11.03	Triacylglycerol	2.93	1.85	4.91	6.73E-05
TG(54:4)	TG(18:1/18:1/18:2)	900.7992	11.41	Triacylglycerol	2.84	1.87	4.46	1.40E-05
TG(58:10)		944.7702	10.28	Triacylglycerol	2.80	1.88	4.44	1.40E-05
TG(57:5)		940.8325	10.66	Triacylglycerol	4.25	2.49	7.69	3.06E-06
LPC(20:3)		590.3465	1.50	Lysophosphatidylcholine	0.53	0.40	0.70	5.71E-05
LPC(18:1)		566.3464	1.76	Lysophosphatidylcholine	0.74	0.56	0.96	4.39E-02
LPE(20:4)		500.2782	1.24	Lysophosphatidylethanolamine	0.63	0.47	0.82	2.96E-03
PC(31:0)		720.5529	5.98	Phosphatidylcholine	0.14	0.09	0.23	3.62E-12
PC(30:1)		748.5140	5.06	Phosphatidylcholine	0.16	0.09	0.26	2.61E-10
PC(33:1)	PC(15:0/18:1)	790.5606	6.10	Phosphatidylcholine	0.16	0.09	0.24	2.05E-12
PC(28:0)		722.4981	4.97	Phosphatidylcholine	0.19	0.10	0.32	1.94E-07
PC(35:1)	PC(17:0/18:1)	818.5920	6.83	Phosphatidylcholine	0.18	0.11	0.27	1.33E-11

PC(30:0)		750.5294	5.67	Phosphatidylcholine	0.22	0.14	0.33	2.70E-10
PC(32:1)	PC(16:0/16:1)	776.5440	5.76	Phosphatidylcholine	0.23	0.15	0.34	2.52E-10
PC(33:2)	PC(15:0/18:2)	788.5444	5.52	Phosphatidylcholine	0.25	0.16	0.35	3.74E-11
PC(33:0)		748.5856	6.62	Phosphatidylcholine	0.27	0.18	0.39	1.64E-09
PC(34:1)	PC(16:0/18:1)	804.5753	6.45	Phosphatidylcholine	0.36	0.25	0.50	5.23E-08
PC(34:4)		798.5298	5.07	Phosphatidylcholine	0.36	0.26	0.50	3.18E-08
PC(35:3)		814.5605	5.71	Phosphatidylcholine	0.37	0.26	0.51	3.74E-08
PC(36:1)	PC(18:0/18:1)	832.6075	7.23	Phosphatidylcholine	0.39	0.28	0.53	8.38E-08
PC(35:4)		812.5449	5.41	Phosphatidylcholine	0.41	0.29	0.55	2.02E-07
PC(37:3)		842.5909	6.38	Phosphatidylcholine	0.41	0.30	0.55	1.17E-07
PC(37:5)		838.5603	5.51	Phosphatidylcholine	0.43	0.31	0.59	2.65E-06
PC(40:4)		838.6318	6.99	Phosphatidylcholine	0.44	0.32	0.60	1.86E-06
PC(38:5)	PC(16:0/22:5)	852.5749	5.79	Phosphatidylcholine	0.44	0.32	0.59	5.00E-07
PC(32:2)	PC(14:0/18:2)	774.5294	5.19	Phosphatidylcholine	0.46	0.33	0.62	4.71E-06
PC(38:3)	PC(18:0/20:3)	856.6074	6.82	Phosphatidylcholine	0.48	0.35	0.63	4.65E-06
PC(36:3)	PC(16:0/20:3)	828.5756	6.05	Phosphatidylcholine	0.48	0.36	0.64	3.45E-06
PC(37:4)		840.5751	6.11	Phosphatidylcholine	0.52	0.39	0.69	3.96E-05
PC(35:2)	PC(17:0/18:2)	816.5758	6.24	Phosphatidylcholine	0.54	0.40	0.73	1.85E-04
PC(37:2)		800.6163	6.97	Phosphatidylcholine	0.56	0.41	0.75	5.97E-04
PC(38:4)	PC(18:1/20:3)	854.5908	6.13	Phosphatidylcholine	0.54	0.41	0.70	4.18E-05
PC(32:0)	PC(16:0/16:0)	778.5600	6.39	Phosphatidylcholine	0.56	0.42	0.75	3.18E-04
PC(35:5)		766.5374	4.94	Phosphatidylcholine	0.57	0.42	0.75	4.09E-04
PC(38:2)		814.6315	7.27	Phosphatidylcholine	0.61	0.46	0.80	1.38E-03
PC(34:3)	PC(16:1/18:2)	800.5445	5.38	Phosphatidylcholine	0.64	0.49	0.83	2.44E-03
PC(34:0)		806.5920	7.18	Phosphatidylcholine	0.65	0.49	0.84	4.00E-03
PC(36:6)		822.5296	4.89	Phosphatidylcholine	0.67	0.50	0.89	1.24E-02
PC(34:2)	PC(16:0/18:2)	780.5497	5.88	Phosphatidylcholine	0.67	0.50	0.87	8.93E-03
PC(38:6)	PC(18:2/20:4)	850.5602	5.28	Phosphatidylcholine	0.69	0.51	0.91	1.79E-02

PC(37:6)		836.5449	5.22	Phosphatidylcholine	0.69	0.52	0.91	1.81E-02
PC(36:4)	PC(16:0/20:4)	826.5597	5.76	Phosphatidylcholine	0.70	0.54	0.90	1.38E-02
PC(36:5)	PC(16:0/20:5)	802.5349	5.27	Phosphatidylcholine	0.72	0.55	0.95	3.64E-02
PC(36:0)		790.6314	7.89	Phosphatidylcholine	0.74	0.56	0.94	3.38E-02
PC(38:1)		860.6390	7.94	Phosphatidylcholine	0.74	0.56	0.96	4.72E-02
PC(40:6)	PC(18:0/22:6)	878.5915	6.28	Phosphatidylcholine	1.50	1.15	1.98	7.95E-03
PC(O-30:0)		692.5597	6.09	Phosphatidylcholine (Ether-linked)	0.20	0.12	0.30	7.79E-11
PC(P-30:0)		690.5438	5.98	Phosphatidylcholine (Ether-linked)	0.20	0.12	0.31	1.53E-10
PC(O-34:1)		790.5966	6.95	Phosphatidylcholine (Ether-linked)	0.31	0.21	0.45	5.18E-08
PC(P-34:1)		788.5811	6.83	Phosphatidylcholine (Ether-linked)	0.37	0.25	0.54	4.71E-06
PC(P-42:4)		850.6684	7.66	Phosphatidylcholine (Ether-linked)	0.39	0.26	0.56	5.60E-06
PC(P-32:1)		716.5584	6.08	Phosphatidylcholine (Ether-linked)	0.41	0.28	0.58	9.42E-06
PC(O-34:0)		748.6217	7.66	Phosphatidylcholine (Ether-linked)	0.44	0.31	0.60	4.94E-06
PC(O-32:0)		764.5816	6.91	Phosphatidylcholine (Ether-linked)	0.47	0.34	0.64	1.48E-05
PC(P-40:4)		866.6285	6.96	Phosphatidylcholine (Ether-linked)	0.50	0.36	0.68	7.31E-05
PC(O-32:2)		760.5588	5.65	Phosphatidylcholine (Ether-linked)	0.50	0.36	0.67	3.99E-05
PC(P-32:0)		762.5662	6.78	Phosphatidylcholine (Ether-linked)	0.53	0.38	0.71	1.81E-04
PC(P-38:3)		840.6128	6.97	Phosphatidylcholine (Ether-linked)	0.62	0.47	0.82	2.51E-03
PC(O-32:1)		718.5733	6.22	Phosphatidylcholine (Ether-linked)	0.66	0.49	0.86	7.59E-03
PC(P-38:6)		834.5641	5.83	Phosphatidylcholine (Ether-linked)	1.76	1.32	2.40	5.22E-04
PC(P-40:6)		862.5960	6.01	Phosphatidylcholine (Ether-linked)	3.27	2.34	4.72	5.39E-10
PE(34:1)		716.5233	6.65	Phosphatidylethanolamine	0.47	0.31	0.67	3.42E-04
PE(36:1)		744.5555	7.40	Phosphatidylethanolamine	0.49	0.35	0.66	3.99E-05
PE(36:4)		738.5071	5.93	Phosphatidylethanolamine	0.62	0.45	0.81	2.82E-03
PE(36:5)		736.4920	5.45	Phosphatidylethanolamine	0.64	0.48	0.84	4.07E-03
PE(38:5)		764.5215	5.99	Phosphatidylethanolamine	0.66	0.50	0.86	5.87E-03
PE(P-38:3)		752.5605	7.37	Phosphatidylethanolamine (Ether-linked)	0.69	0.52	0.89	9.98E-03
PE(P-34:1)		702.5432	7.00	Phosphatidylethanolamine (Ether-linked)	0.72	0.54	0.93	2.85E-02

PE(P-36:1)		728.5606	7.79	Phosphatidylethanolamine (Ether-linked)	0.73	0.55	0.95	3.50E-02
PE(O-36:4)		724.5266	6.42	Phosphatidylethanolamine (Ether-linked)	1.52	1.15	2.05	8.68E-03
PE(P-34:2)	PE(P-16:0/18:2)	698.5124	6.41	Phosphatidylethanolamine (Ether-linked)	1.62	1.22	2.20	3.37E-03
PE(P-38:5)	PE(P-18:1/20:4)	748.5284	6.31	Phosphatidylethanolamine (Ether-linked)	1.72	1.27	2.37	1.89E-03
PE(P-36:4)	PE(P-16:0/20:4)	722.5127	6.26	Phosphatidylethanolamine (Ether-linked)	1.85	1.36	2.58	5.35E-04
PE(P-40:6)	PE(P-18:0/22:6)	774.5442	6.79	Phosphatidylethanolamine (Ether-linked)	1.90	1.42	2.61	1.11E-04
PE(P-38:6)	PE(P-16:0/22:6)	746.5125	6.04	Phosphatidylethanolamine (Ether-linked)	2.73	1.95	3.95	1.84E-07
PE(P-40:7)	PE(P-18:1/22:6)	772.5283	6.10	Phosphatidylethanolamine (Ether-linked)	2.92	2.11	4.17	1.08E-08
PI(34:1)	PI(16:0/18:1)	835.5357	5.64	Phosphatidylinositol	0.34	0.22	0.51	3.06E-06
PI(36:1)		863.5652	6.32	Phosphatidylinositol	0.49	0.34	0.67	8.60E-05
Cer(d39:1)		652.5891	8.44	Ceramide	0.31	0.21	0.45	1.56E-08
Cer(d41:2)		678.6050	8.47	Ceramide	0.42	0.30	0.57	6.29E-07
Cer(d43:1)		708.6520	9.65	Ceramide	0.44	0.32	0.59	1.23E-06
Cer(d38:1)		638.5728	8.06	Ceramide	0.45	0.33	0.61	3.17E-06
Cer(d41:1)		680.6204	9.11	Ceramide	0.54	0.40	0.72	1.20E-04
Cer(d40:1)		604.6027	8.72	Ceramide	0.55	0.41	0.73	2.08E-04
Cer(d42:3)		690.6046	8.09	Ceramide	0.61	0.47	0.80	1.24E-03
Cer(d34:1)		582.5092	6.49	Ceramide	0.62	0.47	0.81	1.84E-03
LacCer(d34:1)		906.6163	5.60	Glycosphingolipids	0.54	0.40	0.71	1.14E-04
HexCer(d34:1)		700.5708	5.83	Glycosphingolipids	0.68	0.51	0.88	9.96E-03
HexCer(d41:1)		842.6739	8.48	Glycosphingolipids	0.69	0.52	0.90	1.49E-02
SM(d32:0)		721.5505	5.15	Sphingomyelin	0.14	0.08	0.23	2.82E-12
SM(d32:2)		717.5192	4.27	Sphingomyelin	0.14	0.09	0.23	2.05E-12
SM(d30:1)		691.5036	4.17	Sphingomyelin	0.18	0.11	0.29	2.70E-10
SM(d39:1)	SM(d17:1/22:0)	817.6452	7.60	Sphingomyelin	0.20	0.12	0.30	4.90E-11
SM(d33:1)	SM(d17:1/16:0)	733.5503	5.24	Sphingomyelin	0.21	0.13	0.32	1.20E-10
SM(d32:1)	SM(d16:1/16:0)	719.5348	4.88	Sphingomyelin	0.21	0.13	0.32	5.93E-11
SM(d37:1)		789.6145	6.78	Sphingomyelin	0.26	0.17	0.38	9.48E-10

SM(d39:2)		815.6321	6.89	Sphingomyelin	0.26	0.17	0.40	1.70E-08
SM(d39:0)		797.6537	6.83	Sphingomyelin	0.28	0.17	0.42	1.94E-07
SM(d38:1)	SM(d18:1/20:0)	803.6286	7.19	Sphingomyelin	0.35	0.24	0.48	2.90E-08
SM(d36:3)		771.5659	5.14	Sphingomyelin	0.37	0.25	0.52	4.24E-07
SM(d35:2)		759.5653	5.35	Sphingomyelin	0.39	0.27	0.55	1.09E-06
SM(d37:2)		743.6080	6.07	Sphingomyelin	0.40	0.28	0.56	1.70E-06
SM(d40:3)		827.6283	6.49	Sphingomyelin	0.44	0.31	0.60	4.73E-06
SM(d43:2)		871.6925	8.14	Sphingomyelin	0.43	0.31	0.58	9.47E-07
SM(d38:0)		761.6530	7.48	Sphingomyelin	0.46	0.33	0.62	6.92E-06
SM(d41:2)	SM(d17:1/24:1)	843.6605	7.64	Sphingomyelin	0.47	0.34	0.64	1.88E-05
SM(d38:2)		757.6224	6.47	Sphingomyelin	0.51	0.37	0.69	7.31E-05
SM(d40:2)	SM(d18:2/22:0)	829.6442	7.25	Sphingomyelin	0.52	0.38	0.70	1.02E-04
SM(d35:1)		761.5810	5.98	Sphingomyelin	0.53	0.39	0.71	1.50E-04
SM(d41:1)	SM(d18:1/23:0)	845.6762	8.32	Sphingomyelin	0.54	0.40	0.72	1.72E-04
SM(d34:1)	SM(d18:1/16:0)	747.5653	5.56	Sphingomyelin	0.55	0.41	0.72	7.09E-05
SM(d36:1)	SM(d18:1/18:0)	775.5968	6.38	Sphingomyelin	0.62	0.47	0.82	2.44E-03
SM(d36:0)		777.6125	6.70	Sphingomyelin	0.66	0.49	0.88	1.30E-02
SM(d31:1)		661.5286	5.71	Sphingomyelin	0.65	0.49	0.85	5.16E-03
SM(d43:1)		873.7087	8.92	Sphingomyelin	0.67	0.51	0.87	6.80E-03
SM(d42:2)		813.6844	7.88	Sphingomyelin	0.67	0.51	0.87	7.24E-03
SM(d34:2)		701.5590	4.95	Sphingomyelin	0.68	0.51	0.89	1.43E-02
SM(d40:1)	SM(d18:1/22:0)	831.6600	7.95	Sphingomyelin	0.72	0.55	0.94	3.32E-02
SM(d36:2)	SM(d18:2/18:0)	773.5809	5.75	Sphingomyelin	0.73	0.55	0.95	3.94E-02
SM(d42:3)		811.6678	7.20	Sphingomyelin	0.74	0.56	0.96	4.19E-02
CDCA sulfate		453.2342	5.64	Cholesterol and bile derivatives	0.68	0.52	0.87	6.02E-03
Hydroxycholesterol		447.3477	3.66	Cholesterol and bile derivatives	1.44	1.09	1.93	2.09E-02
7-Ketocholesterol		445.3322	3.57	Cholesterol and bile derivatives	2.25	1.65	3.15	3.95E-06
Cholesteryl acetate		473.3636	3.82	Cholesterol and bile derivatives	3.15	2.19	4.74	4.90E-08

CE(20:3)	692.6333	11.57	Cholesteryl Esters	0.29	0.19	0.43	4.73E-08
CE(18:1)	668.6334	11.93	Cholesteryl Esters	0.58	0.35	0.89	3.80E-02
CE(18:3)	664.6022	11.02	Cholesteryl Esters	0.55	0.40	0.74	4.56E-04
CE(21:0)	712.6961	11.96	Cholesteryl Esters	0.63	0.44	0.86	1.49E-02
Unknown	397.3687	4.15		0.49	0.33	0.69	3.67E-04
Unknown	411.3844	4.47		0.48	0.33	0.68	2.82E-04
Unknown	425.3638	4.01		0.58	0.43	0.78	9.29E-04
Unknown	537.4884	5.39		0.73	0.55	0.95	3.99E-02
Unknown	557.4572	5.30		1.60	1.20	2.17	4.28E-03
Unknown	595.4945	4.40		0.46	0.31	0.66	1.93E-04
Unknown	671.5956	9.07		0.51	0.37	0.68	3.99E-05
Unknown	707.6135	9.43		0.62	0.47	0.81	1.48E-03
Unknown	736.5280	6.62		1.50	1.13	2.03	1.39E-02
Unknown	750.5367	6.33		1.64	1.24	2.20	1.87E-03
Unknown	760.5278	6.36		1.75	1.30	2.43	1.23E-03
Unknown	790.5018	6.27		1.99	1.45	2.80	1.30E-04
Unknown	816.5195	6.32		2.02	1.48	2.81	6.51E-05
Unknown	818.5328	7.03		1.69	1.25	2.36	3.04E-03
Unknown	820.5989	6.84		0.49	0.36	0.66	2.05E-05
Unknown	824.5811	6.33		0.65	0.48	0.86	7.12E-03
Unknown	841.6474	6.86		0.25	0.16	0.39	2.55E-08
Unknown	869.6783	7.59		0.23	0.15	0.36	1.28E-09
Unknown	885.6331	7.60		0.18	0.11	0.27	4.04E-12
Unknown	886.5202	7.03		1.83	1.36	2.53	4.27E-04
Unknown	894.6605	7.69		0.42	0.30	0.58	2.25E-06
Unknown	922.6920	8.38		0.71	0.53	0.93	2.60E-02
Unknown	967.6351	7.98		0.61	0.46	0.79	8.38E-04
Unknown	981.6513	8.33		0.44	0.32	0.59	9.44E-07

Unknown	995.6667	8.68		0.71	0.54	0.91	1.73E-02

Odds ratio >1 indicated higher level in Asian Chinese; odds ratio <1 indicated higher level in Caucasian.

Table 9.7: Differentially expressed metabolites between Caucasian and Asian Chinese

Metabolite ID	*m/z*	*RT (min)*	*Pathway*	*Detail*	*Odds ratio*	*CI Lower*	*CI Upper*	*p*
L-kynurenine	209.0931	10.28	AA metabolism	Tryptophan metabolism	0.30	0.21	0.43	3.06E-08
5-Hydroxyindoleacetic acid	192.0666	10.27	AA metabolism	Tryptophan metabolism	0.34	0.24	0.47	9.06E-08
4-Imidazolone-5-propionic acid	157.0617	12.54	AA metabolism	AA catabolic product; Histidine	0.37	0.26	0.52	1.44E-06
Glutarylcarnitine	276.1457	9.26	AA metabolism	AA catabolic product; Lysine	0.38	0.27	0.51	1.47E-07
L-Homocitrulline	190.1195	13.48	AA metabolism	non-proteinogenic AA metabolism; Urea cycle; Proline and arginine;	0.47	0.34	0.63	1.45E-05
Indolelactic acid	188.0716	8.24	AA metabolism	Tryptophan metabolism	0.58	0.43	0.76	8.51E-04
2-Pyrrolidinone	86.0609	2.39	AA metabolism	AA catabolic product; GABA	0.61	0.46	0.80	2.37E-03
Phenylacetylglutamine	265.1198	5.85	AA metabolism	Urea cycle	0.63	0.48	0.81	3.04E-03
2-Keto-6-aminocaproate Peak A	146.0820	2.39	AA metabolism	AA catabolic product; Lysine	0.63	0.48	0.82	3.52E-03
5-Amino-2-oxopentanoic acid	130.0500	2.75	AA metabolism	AA catabolic product; Proline;	0.64	0.48	0.83	4.74E-03
5-Hydroxy-L-tryptophan	221.0934	10.33	AA metabolism	Tryptophan metabolism	0.65	0.49	0.86	9.98E-03
Putreanine	161.1293	11.76	AA metabolism	non-proteinogenic AA metabolism	0.68	0.52	0.88	1.32E-02
Dopaquinone	196.0606	12.67	AA metabolism		1.44	1.08	1.99	4.79E-02
Diaminohexanoate peak B	147.1136	15.32	AA metabolism	AA catabolic product; Lysine	1.60	1.16	2.27	1.83E-02
Hydroxy-L-proline	132.0666	12.57	AA metabolism	non-proteinogenic AA metabolism; Proline; Collagen-derived residue	1.81	1.36	2.47	6.95E-04
L-Serine	104.0343	13.86	AA metabolism	Proteinogenic AA	1.89	1.43	2.55	1.07E-04
4-Acetamidobutanal	130.0873	9.81	AA metabolism	non-proteinogenic AA metabolism; Proline and arginine; Polyamine metabolism;	2.87	1.93	4.48	1.10E-05
Lithocholic acid	376.3203	12.18	Bile acid metabolism		1.41	1.09	1.86	3.28E-02
Erythronic acid	135.0290	12.22	CHO metabolism	Protein glycation potential	0.46	0.33	0.61	7.49E-06
Erythrulose/Erythrose	119.0340	7.23	CHO metabolism	Protein glycation potential	0.56	0.40	0.78	3.83E-03
Unknown Hexose	215.0320	12.95	CHO metabolism	Sugar	0.58	0.43	0.76	7.53E-04
Glucose peak A	203.0537	12.18	CHO metabolism	Sugar	0.61	0.45	0.81	3.90E-03
L-Creatinine	114.0671	10.86	Energy production		0.43	0.30	0.60	1.49E-05
Creatine	132.0776	12.52	Energy production		1.42	1.09	1.88	3.21E-02
Gluconic acid	195.0500	13.47	Exogenous	Sugar-related	0.38	0.27	0.52	4.57E-07

Trigonelline	138.0557	10.01	Exogenous	Niacin-related	0.41	0.28	0.57	1.45E-05
Ribonic acid	165.0396	12.88	Exogenous	Sugar-related	0.44	0.32	0.60	2.58E-06
L-Xylonate	165.0396	12.99	Exogenous	Sugar-related	0.48	0.35	0.65	4.12E-05
Theophylline	181.0730	2.32	Exogenous	Purine-related	0.51	0.37	0.68	7.00E-05
5-Acetylamino-6-amino-3-methyluracil	199.0834	8.9	Exogenous	Purine-related	0.53	0.38	0.71	4.12E-04
Lenticin	247.1454	8.24	Exogenous	Tryptophan-related	0.61	0.45	0.79	2.70E-03
DL-2-Aminooctanoic acid	160.1341	9.24	FA metabolism	MCFA metabolism and derivatives;	0.42	0.29	0.58	4.90E-06
N-Heptanoylglycine (was 8-Amino-7-oxononanoate)	188.1291	10.14	FA metabolism	MCFA metabolism and derivatives; acylglycine	0.43	0.30	0.59	9.09E-06
Hydroxy butyric acid	103.0390	2.06	FA metabolism		1.42	1.10	1.85	2.51E-02
L-Carnitine	162.1133	10.75	FA metabolism		1.42	1.08	1.89	3.89E-02
3-Oxooctanoic acid Peak A	176.1291	8.98	FA metabolism	MCFA metabolism and derivatives;	1.88	1.33	2.81	4.28E-03
Propionic acid	73.0285	2.24	FA metabolism	SCFA;	1.96	1.45	2.71	1.65E-04
3-Oxooctanoic acid Peak B	176.1291	10.15	FA metabolism	MCFA metabolism and derivatives;	7.82	4.43	14.76	5.87E-09
(alpha-keto-dimethyl-delta-N,N-Dimethylguanidynol) valeric acid	202.1197	9.81	Guanidino compound	Guanidino compound; NO regulation	0.36	0.25	0.50	2.67E-07
5-Methylthioribose	181.0539	7.91	Gut microbical metabolite	Methionine	0.42	0.30	0.58	2.87E-06
p-Cresol sulfate	187.0063	2.22	Gut microbical metabolite	Aromatic AA	0.59	0.45	0.77	7.47E-04
Phenol sulphate	172.9906	2.44	Gut microbical metabolite	Aromatic AA	1.78	1.31	2.52	2.70E-03
N(6)-Methyllysine	161.1293	15.32	Methyl transfer		0.45	0.33	0.60	2.58E-06
Ne,Ne-Dimethyllysine	175.1450	15.22	Methyl transfer		0.45	0.34	0.60	1.53E-06
Sarcosine	90.0559	12.14	Methyl transfer		0.62	0.46	0.82	4.16E-03
1-Methyl-L-histidine	170.0933	15.21	Methyl transfer		0.62	0.47	0.82	4.43E-03
3-Methyl-L-histidine	170.0934	15.66	Methyl transfer		0.72	0.54	0.94	4.57E-02
Betaine	118.0872	9.41	Methyl transfer		1.65	1.25	2.21	2.70E-03
L-Homocysteine	136.0434	11.37	Methyl transfer	non-proteinogenic AA metabolism; Sulfur-containing compound metabolism	1.74	1.32	2.34	7.47E-04
Dihydrothymine (was pyroglutamine)	129.0669	12.59	Nucleotide metabolism	Pyrimidine metabolism	0.30	0.20	0.44	1.47E-07
Allantoin	157.0358	10.91	Nucleotide metabolism	Purine metabolism	0.50	0.37	0.67	5.77E-05
Methylguanine	166.0733	8.89	Nucleotide metabolism	Purine methylation	0.60	0.45	0.78	1.29E-03

N-a-Acetyl-L-arginine	217.1303	12.63	Protein and AA acetylation		0.41	0.29	0.57	4.27E-06
Acetylglycine	116.0344	4.76	Protein and AA acetylation		0.57	0.40	0.80	6.22E-03
N-Acetylornithine	175.1087	12.38	Protein and AA acetylation		0.62	0.40	0.87	4.18E-02
N-Acetylisoleucine	174.1134	10.09	Protein and AA acetylation		3.67	2.35	6.12	2.25E-06
Isoleucylproline	229.1559	9.24	Protein degradation		0.50	0.36	0.70	4.60E-04
Glycyl-Threonine/Alanyl-Serine	177.0879	14.58	Protein degradation		0.63	0.47	0.83	4.50E-03
Prolylhydroxyproline	229.1195	13.47	Protein degradation	Collagen-derived dipeptides	0.63	0.48	0.83	4.39E-03
Glutamylthreonine	249.1093	13.31	Protein degradation		0.71	0.54	0.92	3.28E-02
3-Hydroxypyridine	96.0453	2.6			0.43	0.31	0.58	2.58E-06
Phosphonic acid	80.9739	12.84			1.53	1.18	1.99	5.25E-03
Unknown	86.9095	14.52			0.42	0.30	0.57	2.30E-06
Unknown	84.9121	14.52			0.44	0.32	0.59	2.58E-06
Unknown	122.9255	15.02			0.68	0.52	0.88	1.40E-02

Odds ratio >1 indicated higher level in Asian Chinese; odds ratio <1 indicated higher level in Caucasian.

Table 9.8: Metabolites associated with FPG in Caucasian and/or Asian Chinese analysed by multiple linear regression adjusted for gender, age and BMI (BH-corrected p<0.05)

					Caucasian				*Asian Chinese*			
MS1	MS2	mz	rt(min)	Marker in	β	CI 2.5%	CI 97.5%	p	β	CI 2.5%	CI 97.5%	p
DG(36:2)	DG(18:1/18:1)	638.5719	7.85	Both	0.27	0.12	0.42	3.15E-02	0.23	0.13	0.33	3.41E-04
DG(38:2)		666.6024	7.85	Both	0.23	0.08	0.38	4.71E-02	0.26	0.16	0.36	5.77E-05
DG(38:5)		660.5564	7.07	Both	0.29	0.16	0.42	1.19E-02	0.18	0.07	0.29	1.08E-02
DG(38:6)		658.5416	6.52	Both	0.25	0.12	0.38	2.65E-02	0.15	0.04	0.26	4.92E-02
Hexose A(glucose)	Hexose A(glucose)	215.0320	12.19	Both	0.31	0.21	0.41	5.46E-07	0.32	0.19	0.45	3.01E-04
Hexose B(glucose)	Hexose B(glucose)	215.0320	12.71	Both	0.33	0.21	0.44	2.87E-06	0.23	0.11	0.35	4.82E-03
TG(53:3)	TG(17:0/18:1/18:2)	888.8011	11.62	Both	0.27	0.10	0.44	4.22E-02	0.25	0.14	0.36	3.10E-04
TG(54:2)	TG(18:0/18:1/18:1)	904.8321	12.14	Both	0.24	0.10	0.38	3.46E-02	0.20	0.09	0.31	4.29E-03
TG(54:3)	TG(18:0/18:1/18:2)	902.8151	11.82	Both	0.27	0.09	0.44	4.84E-02	0.30	0.18	0.42	7.39E-05
TG(55:3)'		916.8322	12.02	Both	0.24	0.08	0.40	4.84E-02	0.27	0.16	0.38	2.07E-04
TG(56:2)		932.8613	11.79	Both	0.26	0.11	0.42	3.49E-02	0.22	0.11	0.33	1.19E-03
TG(56:3)	TG(18:1/18:1/20:1)	930.8473	12.14	Both	0.26	0.10	0.42	3.49E-02	0.26	0.16	0.36	5.77E-05
TG(56:6)	TG(16:0/18:1/22:5)	924.7993	11.25	Both	0.44	0.23	0.66	1.19E-02	0.16	0.06	0.26	1.14E-02
TG(57:2)		946.8780	11.79	Both	0.27	0.12	0.42	3.15E-02	0.20	0.09	0.31	3.83E-03
TG(58:2)		960.8935	11.79	Both	0.28	0.11	0.44	3.46E-02	0.19	0.07	0.31	1.42E-02
TG(58:3)	TG(18:1/18:2/22:0)	958.8793	12.34	Both	0.25	0.10	0.40	3.46E-02	0.21	0.11	0.31	1.17E-03
TG(58:3)'		958.8779	11.40	Both	0.33	0.13	0.52	3.46E-02	0.26	0.14	0.37	5.37E-04
TG(58:6)		952.8318	11.64	Both	0.22	0.08	0.35	3.49E-02	0.21	0.09	0.33	6.86E-03
TG(59:2)		974.9101	12.14	Both	0.26	0.11	0.41	3.46E-02	0.22	0.12	0.33	6.76E-04
TG(59:3)		972.8936	11.81	Both	0.23	0.08	0.39	4.84E-02	0.27	0.16	0.37	5.77E-05
TG(60:2)		988.9260	12.14	Both	0.26	0.11	0.42	3.46E-02	0.23	0.13	0.34	4.33E-04
TG(60:3)	TG(20:1/18:1/22:1)	986.9093	11.81	Both	0.25	0.10	0.40	3.49E-02	0.25	0.13	0.36	5.96E-04
CE(18:2)	CE(18:2)	666.6175	11.46	Asian Chinese	-0.07	-0.24	0.10	6.31E-01	-0.20	-0.34	-0.05	4.42E-02
CE(22:4)	CE(22:4)	718.6488	11.18	Asian Chinese	0.09	-0.08	0.27	5.40E-01	-0.24	-0.40	-0.08	2.25E-02

Cer(d39:1)		652.5891	8.44	Asian Chinese	0.02	-0.12	0.15	9.18E-01	0.20	0.05	0.35	4.92E-02
Cer(d40:1)	Cer(d18:1/22:0)	666.6046	8.77	Asian Chinese	0.09	-0.05	0.23	4.64E-01	0.19	0.07	0.31	1.14E-02
Cer(d40:2)		664.5891	8.10	Asian Chinese	0.07	-0.07	0.21	5.39E-01	0.25	0.13	0.37	5.96E-04
Cer(d41:1)		680.6204	9.11	Asian Chinese	0.09	-0.06	0.23	4.76E-01	0.17	0.05	0.29	3.71E-02
Cer(d41:2)		678.6050	8.47	Asian Chinese	-0.05	-0.18	0.09	7.03E-01	0.20	0.07	0.33	2.07E-02
Cer(d42:1)		711.6263	9.42	Asian Chinese	0.05	-0.09	0.19	6.89E-01	0.16	0.04	0.28	3.69E-02
DG(34:1)	DG(16:0/18:1)	612.5564	7.82	Asian Chinese	0.18	0.04	0.32	1.05E-01	0.18	0.08	0.29	7.71E-03
DG(34:2)	DG(16:0/18:2)	610.5405	7.20	Asian Chinese	0.22	0.07	0.37	5.64E-02	0.20	0.10	0.30	2.07E-03
DG(34:3)		608.5254	6.56	Asian Chinese	0.18	0.03	0.32	1.15E-01	0.20	0.09	0.30	3.83E-03
DG(36:3)	DG(18:1/18:2)	636.5563	7.26	Asian Chinese	0.24	0.05	0.43	1.04E-01	0.25	0.15	0.34	5.77E-05
DG(36:4)	DG(18:2/18:2)	634.5399	6.67	Asian Chinese	0.15	-0.05	0.35	3.56E-01	0.22	0.12	0.32	3.44E-04
DG(38:3)		664.5878	7.27	Asian Chinese	0.25	0.04	0.46	1.31E-01	0.25	0.15	0.34	5.77E-05
FA(16:0)		255.2328	3.56	Asian Chinese	0.07	-0.06	0.21	5.28E-01	-0.15	-0.26	-0.04	4.56E-02
FA(18:2)		279.2330	3.16	Asian Chinese	-0.01	-0.21	0.19	9.72E-01	-0.14	-0.25	-0.04	4.14E-02
HexCer(d42:2)	HexCer(d42:2)	854.6735	8.09	Asian Chinese	-0.14	-0.27	-0.02	1.47E-01	-0.16	-0.28	-0.04	4.56E-02
Hexose C	Hexose C	215.0320	12.95	Asian Chinese	0.17	0.05	0.28	1.19E-01	0.29	0.17	0.42	3.01E-04
L-Acetylcarnitine	L-Acetylcarnitine	204.1241	8.57	Asian Chinese	-0.01	-0.14	0.12	9.75E-01	-0.20	-0.32	-0.09	1.20E-02
PC(36:4)	PC(18:2/18:2)	826.5601	5.39	Asian Chinese	-0.06	-0.20	0.08	6.44E-01	0.18	0.07	0.29	1.37E-02
PC(36:5)		780.5532	4.91	Asian Chinese	-0.03	-0.15	0.10	8.18E-01	0.21	0.09	0.32	7.80E-03
PC(38:4)	PC(18:1/20:3)	854.5908	6.13	Asian Chinese	0.03	-0.10	0.15	8.38E-01	0.18	0.05	0.30	3.01E-02
PC(38:6)	PC(18:2/20:4)	850.5602	5.28	Asian Chinese	0.00	-0.13	0.14	9.74E-01	0.18	0.05	0.30	3.08E-02
PC(O-44:5)		922.6920	8.38	Asian Chinese	-0.08	-0.21	0.05	4.88E-01	-0.20	-0.32	-0.08	1.14E-02
PC(P-42:4)		850.6684	7.66	Asian Chinese	-0.05	-0.19	0.09	6.99E-01	-0.25	-0.41	-0.10	1.30E-02
PE(36:1)		744.5555	7.40	Asian Chinese	0.05	-0.07	0.17	6.20E-01	0.20	0.07	0.34	2.09E-02
PE(36:2)	PE(18:0/18:2)	744.5542	6.77	Asian Chinese	0.03	-0.09	0.15	7.82E-01	0.21	0.08	0.34	1.39E-02
PE(36:3)	PE(18:1/18:2)	740.5233	6.12	Asian Chinese	-0.04	-0.16	0.09	7.63E-01	0.20	0.07	0.33	1.37E-02
SM(d36:1)	SM(d18:1/18:0)	753.5887	6.36	Asian Chinese	0.11	-0.04	0.26	3.71E-01	-0.17	-0.29	-0.04	4.92E-02
SM(d36:2)	SM(d18:2/18:0)	773.5809	5.75	Asian Chinese	0.05	-0.09	0.19	6.95E-01	-0.20	-0.33	-0.08	1.11E-02

SM(d40:1)'		809.6511	6.58	Asian Chinese	0.05	-0.09	0.19	7.01E-01	-0.20	-0.34	-0.06	2.87E-02
SM(d40:3)		827.6283	6.49	Asian Chinese	-0.07	-0.20	0.05	4.73E-01	-0.26	-0.42	-0.10	9.96E-03
SM(d42:2)	SM(d18:1/24:1)	857.6755	7.90	Asian Chinese	-0.05	-0.19	0.08	6.68E-01	-0.19	-0.30	-0.07	1.14E-02
SM(d42:3)	SM(d18:2/24:1)	811.6678	7.20	Asian Chinese	0.08	-0.05	0.21	4.81E-01	-0.23	-0.37	-0.09	1.31E-02
SM(d43:2)		871.6925	8.14	Asian Chinese	0.01	-0.14	0.16	9.48E-01	-0.17	-0.29	-0.04	4.92E-02
SM(t34:1)		763.5609	5.38	Asian Chinese	-0.04	-0.18	0.09	7.45E-01	-0.20	-0.31	-0.09	3.83E-03
TG(48:2)	TG(14:0/16:0/18:2)	820.7387	10.95	Asian Chinese	0.12	0.00	0.24	2.42E-01	0.18	0.06	0.31	2.56E-02
TG(48:3)	TG(12:0/18:1/18:2)	818.7233	10.48	Asian Chinese	0.13	-0.01	0.27	2.66E-01	0.18	0.08	0.29	7.96E-03
TG(48:4)	TG(12:0/18:2/18:2)	816.7078	10.05	Asian Chinese	0.13	-0.02	0.28	3.09E-01	0.18	0.07	0.28	7.80E-03
TG(49:1)	TG(15:0/16:0/18:1)	836.7700	11.59	Asian Chinese	0.09	-0.04	0.22	3.86E-01	0.20	0.07	0.33	1.71E-02
TG(49:2)	TG(15:0/16:0/18:2)	834.7541	11.17	Asian Chinese	0.12	-0.01	0.25	2.90E-01	0.20	0.07	0.33	1.47E-02
TG(49:3)	TG(15:0/16:1/18:2)	832.7387	10.73	Asian Chinese	0.11	-0.02	0.25	3.25E-01	0.17	0.06	0.29	2.52E-02
TG(50:2)	TG(16:0/16:1/18:1)	848.7697	11.37	Asian Chinese	0.18	0.05	0.32	8.40E-02	0.19	0.07	0.32	1.21E-02
TG(50:3)	TG(16:0/16:1/18:2)	846.7543	10.97	Asian Chinese	0.21	0.06	0.36	6.62E-02	0.20	0.09	0.31	5.46E-03
TG(50:4)	TG(14:0/18:2/18:2)	844.7389	10.56	Asian Chinese	0.17	-0.01	0.34	2.66E-01	0.22	0.13	0.32	3.08E-04
TG(50:5)	TG(14:0/18:2/18:3)	842.7234	10.15	Asian Chinese	0.12	-0.05	0.29	3.86E-01	0.19	0.09	0.29	2.21E-03
TG(51:1)	TG(16:0/17:0/18:1)	864.8011	11.99	Asian Chinese	0.15	0.01	0.29	1.82E-01	0.20	0.08	0.33	9.02E-03
TG(51:2)	TG(16:0/17:1/18:1)	862.7856	11.61	Asian Chinese	0.18	0.03	0.34	1.42E-01	0.21	0.09	0.33	6.86E-03
TG(51:3)	TG(15:0/18:1/18:2)	860.7699	11.20	Asian Chinese	0.23	0.06	0.40	9.20E-02	0.23	0.12	0.34	5.96E-04
TG(51:4)	TG(15:0/18:2/18:2)	858.7545	10.80	Asian Chinese	0.13	-0.07	0.34	4.35E-01	0.21	0.11	0.31	7.30E-04
TG(52:2)	TG(16:0/18:1/18:1)	876.8011	11.79	Asian Chinese	0.22	0.05	0.40	9.52E-02	0.22	0.09	0.34	8.06E-03
TG(52:3)	TG(16:0/18:1/18:2)	874.7847	11.41	Asian Chinese	0.31	0.10	0.51	5.17E-02	0.26	0.15	0.37	2.71E-04
TG(52:4)	TG(16:0/18:2/18:2)	872.7698	11.03	Asian Chinese	0.31	0.05	0.56	1.30E-01	0.25	0.14	0.36	2.17E-04
TG(52:5)	TG(16:0/18:2/18:3)	870.7544	10.67	Asian Chinese	0.22	-0.02	0.45	2.66E-01	0.23	0.14	0.33	1.51E-04
TG(52:6)	TG(16:1/18:2/18:3)	868.7391	10.23	Asian Chinese	0.07	-0.08	0.23	5.76E-01	0.17	0.06	0.28	1.36E-02
TG(53:2)	TG(17:0/18:1/18:1)	890.8166	11.99	Asian Chinese	0.22	0.06	0.39	8.40E-02	0.25	0.13	0.37	5.96E-04
TG(53:2)'		890.8166	10.95	Asian Chinese	0.12	-0.01	0.24	2.65E-01	0.20	0.08	0.32	1.06E-02
TG(53:4)	TG(17:1/18:1/18:2)	886.7855	11.23	Asian Chinese	0.25	0.07	0.44	8.40E-02	0.26	0.15	0.37	1.26E-04

TG(53:5)	TG(17:0/18:2/18:3)	884.7700	10.86	Asian Chinese	0.15	-0.04	0.34	3.36E-01	0.23	0.13	0.34	2.71E-04
TG(54:4)	TG(18:1/18:1/18:2)	900.7992	11.41	Asian Chinese	0.23	0.01	0.45	2.03E-01	0.28	0.18	0.38	5.77E-05
TG(54:5)	TG(18:1/18:2/18:2)	898.7843	11.05	Asian Chinese	0.10	-0.10	0.30	5.50E-01	0.28	0.17	0.38	5.77E-05
TG(54:6)	TG(18:1/18:2/18:3)	896.7697	10.66	Asian Chinese	0.09	-0.14	0.32	6.65E-01	0.22	0.13	0.32	2.13E-04
TG(54:6)'		896.7637	10.23	Asian Chinese	0.17	-0.07	0.41	3.91E-01	0.19	0.09	0.28	2.07E-03
TG(55:3)		916.8316	10.98	Asian Chinese	0.20	0.04	0.36	1.04E-01	0.21	0.10	0.32	1.59E-03
TG(56:4)	TG(18:1/18:2/20:1)	928.8293	11.83	Asian Chinese	0.15	-0.01	0.31	2.66E-01	0.26	0.15	0.38	3.35E-04
TG(56:8)	TG(16:0/18:2/22:6)	920.7700	10.66	Asian Chinese	0.18	-0.03	0.38	3.19E-01	0.16	0.06	0.26	1.36E-02
TG(57:3)		944.8622	11.41	Asian Chinese	0.28	0.07	0.49	8.62E-02	0.26	0.13	0.38	1.09E-03
TG(57:4)		942.8472	11.03	Asian Chinese	0.32	0.07	0.57	1.05E-01	0.22	0.12	0.32	5.30E-04
TG(57:5)		940.8325	10.66	Asian Chinese	0.27	-0.04	0.58	3.09E-01	0.21	0.12	0.31	3.49E-04
TG(58:1)	TG(16:0/18:1/24:0)	962.9098	12.59	Asian Chinese	0.20	0.07	0.34	5.09E-02	0.23	0.12	0.34	5.96E-04
TG(58:10)		944.7702	10.28	Asian Chinese	0.14	-0.05	0.32	3.74E-01	0.15	0.04	0.25	3.69E-02
TG(58:4)		956.8625	11.03	Asian Chinese	0.20	0.00	0.40	2.17E-01	0.23	0.12	0.33	5.96E-04
TG(58:8)	TG(18:1/18:1/22:6)	948.8002	11.09	Asian Chinese	0.22	0.02	0.42	1.68E-01	0.15	0.04	0.25	2.99E-02
TG(58:9)	TG(18:1/18:2/22:6)	946.7853	10.69	Asian Chinese	0.14	-0.04	0.31	3.56E-01	0.17	0.07	0.27	1.14E-02
TG(59:4)		970.8780	11.41	Asian Chinese	0.15	-0.03	0.34	3.26E-01	0.21	0.10	0.32	3.38E-03
TG(59:5)		968.8629	11.04	Asian Chinese	0.22	0.00	0.44	2.42E-01	0.26	0.17	0.36	5.77E-05
TG(60:4)		984.8928	11.41	Asian Chinese	0.07	-0.10	0.24	6.68E-01	0.17	0.05	0.28	2.77E-02
TG(60:5)		982.8783	11.05	Asian Chinese	0.17	-0.03	0.37	3.26E-01	0.26	0.16	0.36	5.77E-05
TG(61:6)		994.8788	11.26	Asian Chinese	0.24	0.07	0.42	6.71E-02	0.19	0.09	0.29	3.28E-03
Erythronic acid	Erythronic acid	135.0290	12.22	Caucasian	0.18	0.07	0.29	3.64E-02	0.20	0.04	0.35	1.93E-01
PC(36:4)'	PC(16:0/20:4)	782.5692	5.72	Caucasian	0.23	0.11	0.35	2.65E-02	0.04	-0.10	0.18	8.04E-01
PC(36:5)"		780.5537	5.61	Caucasian	0.23	0.09	0.38	3.94E-02	0.06	-0.06	0.18	5.45E-01
PC(38:4)'	PC(18:0/20:4)	810.5993	6.47	Caucasian	0.20	0.08	0.33	3.54E-02	-0.02	-0.15	0.11	9.19E-01
PC(O-36:4)	PC(O-16:0/20:4)	768.5889	6.19	Caucasian	0.24	0.10	0.38	3.46E-02	-0.04	-0.16	0.09	7.76E-01
PC(O-38:5)		795.6088	6.80	Caucasian	0.22	0.08	0.36	4.76E-02	-0.03	-0.17	0.10	8.13E-01
PE(P-36:1)		730.5747	7.76	Caucasian	0.25	0.13	0.38	1.40E-02	0.10	-0.03	0.23	3.17E-01

PE(P-36:4)	PE(P-16:0/20:4)	724.5274	6.24	Caucasian	0.37	0.19	0.55	1.19E-02	-0.02	-0.14	0.09	8.56E-01
PE(P-38:4)	PE(P-18:0/20:4)	752.5598	6.98	Caucasian	0.30	0.15	0.44	1.19E-02	0.06	-0.07	0.20	5.54E-01
PE(P-38:5)	PE(P-18:1/20:4)	750.5427	6.29	Caucasian	0.27	0.12	0.41	3.15E-02	-0.01	-0.13	0.11	9.62E-01
TG(56:1)		934.8692	11.37	Caucasian	0.22	0.09	0.35	3.49E-02	0.16	0.03	0.30	7.01E-02

β: beta-coefficient of individual metabolites as indepedent variable in the linear regression model adjusting for age, gender and BMI. p: adjusted p-value using Benjamin-Hochberg multiple testing correction (cut-off value 0.05). Cer: ceramide; DG: diacylglycerol; TG: triacylglycerol; CE: cholesteryl ester; HexCer: hexosylceramide; FA: fatty acid; PC: phosphatidylcholine; PE: phosphatidylethanolamine; SM: sphingomyelin; Only annotated metabolites are displayed.

Table 9.9: Metabolites associated with %VAT$_{TBF}$ in Caucasian and/or Asian Chinese analysed by multiple linear regression adjusted for gender, age and BMI (BH-corrected p<0.05)

					Caucasian				*Asian Chinese*			
MS1	MS2	mz	rt(min)	Marker in	β	CI 2.5%	CI 97.5%	p	β	CI 2.5%	CI 97.5%	p
Cer(d40:0)		668.6207	9.01	Both	0.16	0.06	0.26	1.09E-02	0.11	0.04	0.19	2.55E-02
DG(34:1)	DG(16:0/18:1)	612.5564	7.82	Both	0.20	0.11	0.29	4.53E-04	0.14	0.06	0.22	7.77E-03
DG(34:2)	DG(16:0/18:2)	610.5405	7.20	Both	0.24	0.15	0.33	5.26E-05	0.17	0.09	0.25	9.16E-04
DG(34:3)		608.5254	6.56	Both	0.17	0.08	0.26	4.28E-03	0.16	0.08	0.24	1.45E-03
DG(36:2)	DG(18:1/18:1)	638.5719	7.85	Both	0.24	0.15	0.34	5.16E-05	0.12	0.05	0.20	1.53E-02
DG(36:3)	DG(18:1/18:2)	636.5563	7.26	Both	0.25	0.13	0.37	1.14E-03	0.15	0.08	0.23	1.28E-03
DG(36:4)	DG(18:2/18:2)	634.5399	6.67	Both	0.19	0.07	0.32	2.26E-02	0.15	0.08	0.23	1.45E-03
DG(38:2)		666.6024	7.85	Both	0.24	0.15	0.33	4.53E-05	0.10	0.02	0.18	4.76E-02
DG(38:3)		664.5878	7.27	Both	0.24	0.11	0.38	4.68E-03	0.16	0.08	0.23	1.13E-03
PC(38:3)	PC(18:0/20:3)	856.6074	6.82	Both	0.15	0.05	0.25	2.89E-02	0.11	0.02	0.19	4.94E-02
PC(P-34:1)		788.5811	6.83	Both	-0.13	-0.21	-0.04	2.93E-02	-0.25	-0.37	-0.14	6.98E-04
PC(P-34:2)	PC(P-16:0/18:2)	786.5653	6.22	Both	-0.14	-0.24	-0.04	3.07E-02	-0.19	-0.27	-0.10	9.16E-04
PE(34:1)		716.5233	6.65	Both	0.11	0.04	0.19	2.02E-02	0.18	0.05	0.31	3.62E-02
PE(36:1)		744.5555	7.40	Both	0.15	0.07	0.23	3.20E-03	0.15	0.04	0.25	3.55E-02
PE(36:2)	PE(18:0/18:2)	742.5392	6.80	Both	0.14	0.05	0.23	1.40E-02	0.13	0.05	0.22	1.68E-02
SM(d36:0)		769.5583	6.99	Both	0.13	0.04	0.21	3.04E-02	0.13	0.04	0.22	3.02E-02
TG(48:1)	TG(14:0/16:0/18:1)	822.7541	11.36	Both	0.15	0.07	0.22	3.33E-03	0.15	0.05	0.25	2.44E-02
TG(48:2)	TG(14:0/16:0/18:2)	820.7387	10.95	Both	0.16	0.08	0.24	1.10E-03	0.15	0.06	0.25	1.62E-02
TG(48:3)	TG(12:0/18:1/18:2)	818.7233	10.48	Both	0.16	0.07	0.25	4.96E-03	0.12	0.04	0.20	2.98E-02
TG(49:1)	TG(15:0/16:0/18:1)	836.7700	11.59	Both	0.16	0.07	0.24	3.47E-03	0.14	0.04	0.24	2.98E-02
TG(49:2)	TG(15:0/16:0/18:2)	834.7541	11.17	Both	0.16	0.08	0.25	2.04E-03	0.16	0.07	0.26	1.01E-02
TG(49:3)	TG(15:0/16:1/18:2)	832.7387	10.73	Both	0.15	0.07	0.24	6.04E-03	0.14	0.05	0.23	2.16E-02
TG(50:1)	TG(16:0/16:0/18:1)	850.7856	11.80	Both	0.16	0.06	0.25	1.66E-02	0.15	0.07	0.24	5.32E-03
TG(50:2)	TG(16:0/16:1/18:1)	848.7697	11.37	Both	0.22	0.13	0.30	5.26E-05	0.18	0.09	0.27	1.73E-03

TG(50:3)	TG(16:0/16:1/18:2)	846.7543	10.97	Both	0.24	0.15	0.33	4.53E-05	0.19	0.10	0.27	6.98E-04
TG(50:4)	TG(14:0/18:2/18:2)	844.7389	10.56	Both	0.24	0.13	0.35	6.44E-04	0.14	0.06	0.21	4.22E-03
TG(51:1)	TG(16:0/17:0/18:1)	864.8011	11.99	Both	0.20	0.11	0.29	2.86E-04	0.15	0.06	0.24	1.06E-02
TG(51:2)	TG(16:0/17:1/18:1)	862.7856	11.61	Both	0.23	0.13	0.33	1.99E-04	0.16	0.07	0.26	5.03E-03
TG(51:3)	TG(15:0/18:1/18:2)	860.7699	11.20	Both	0.24	0.13	0.35	5.24E-04	0.18	0.10	0.26	8.48E-04
TG(51:4)	TG(15:0/18:2/18:2)	858.7545	10.80	Both	0.25	0.12	0.38	1.90E-03	0.15	0.07	0.23	2.11E-03
TG(52:1)	TG(16:0/18:0/18:1)	878.8169	12.15	Both	0.15	0.06	0.23	9.00E-03	0.12	0.03	0.21	3.80E-02
TG(52:2)	TG(16:0/18:1/18:1)	876.8011	11.79	Both	0.25	0.15	0.36	1.95E-04	0.19	0.10	0.29	1.45E-03
TG(52:3)	TG(16:0/18:1/18:2)	874.7847	11.41	Both	0.33	0.21	0.46	4.53E-05	0.21	0.13	0.30	6.87E-05
TG(52:4)	TG(16:0/18:2/18:2)	872.7698	11.03	Both	0.36	0.20	0.52	3.70E-04	0.22	0.14	0.30	1.42E-05
TG(52:5)	TG(16:0/18:2/18:3)	870.7544	10.67	Both	0.26	0.11	0.41	5.83E-03	0.15	0.08	0.23	1.21E-03
TG(53:1)		892.8307	11.37	Both	0.15	0.07	0.22	3.11E-03	0.15	0.05	0.25	2.54E-02
TG(53:2)	TG(17:0/18:1/18:1)	890.8166	11.99	Both	0.24	0.14	0.35	1.95E-04	0.15	0.06	0.24	1.11E-02
TG(53:2)'		890.8166	10.95	Both	0.16	0.08	0.24	1.78E-03	0.14	0.05	0.23	1.85E-02
TG(53:3)	TG(17:0/18:1/18:2)	888.8011	11.62	Both	0.26	0.15	0.37	1.41E-04	0.17	0.09	0.25	1.45E-03
TG(53:4)	TG(17:1/18:1/18:2)	886.7855	11.23	Both	0.26	0.14	0.38	4.11E-04	0.18	0.10	0.26	6.98E-04
TG(53:5)	TG(17:0/18:2/18:3)	884.7700	10.86	Both	0.17	0.05	0.30	3.29E-02	0.14	0.06	0.22	4.90E-03
TG(54:2)	TG(18:0/18:1/18:1)	904.8321	12.14	Both	0.21	0.12	0.30	3.13E-04	0.15	0.06	0.23	6.32E-03
TG(54:3)	TG(18:0/18:1/18:2)	902.8151	11.82	Both	0.24	0.13	0.36	5.24E-04	0.16	0.07	0.25	7.33E-03
TG(54:4)	TG(18:1/18:1/18:2)	900.7992	11.41	Both	0.21	0.07	0.36	2.90E-02	0.16	0.08	0.24	1.45E-03
TG(55:1)		920.8618	11.80	Both	0.14	0.06	0.23	7.40E-03	0.17	0.08	0.26	4.68E-03
TG(55:2)		918.8467	11.39	Both	0.23	0.15	0.32	1.71E-05	0.20	0.10	0.30	1.73E-03
TG(55:3)		916.8316	10.98	Both	0.23	0.14	0.33	1.83E-04	0.18	0.10	0.25	8.48E-04
TG(55:3)'		916.8322	12.02	Both	0.21	0.11	0.31	7.98E-04	0.14	0.06	0.23	1.12E-02
TG(56:1)		934.8692	11.37	Both	0.23	0.15	0.31	1.01E-05	0.20	0.10	0.30	1.67E-03
TG(56:2)		932.8613	11.79	Both	0.30	0.20	0.40	4.29E-06	0.17	0.09	0.25	1.28E-03
TG(56:3)	TG(18:1/18:1/20:1)	930.8473	12.14	Both	0.23	0.12	0.33	3.91E-04	0.11	0.03	0.19	3.78E-02
TG(56:6)	TG(16:0/18:1/22:5)	924.7993	11.25	Both	0.28	0.13	0.42	2.08E-03	0.13	0.05	0.20	8.39E-03

TG(57:1)		948.8946	12.15	Both	0.19	0.10	0.29	7.54E-04	0.11	0.02	0.19	4.76E-02
TG(57:2)		946.8780	11.79	Both	0.26	0.16	0.35	3.40E-05	0.16	0.08	0.25	1.77E-03
TG(57:3)		944.8622	11.41	Both	0.34	0.21	0.46	4.53E-05	0.26	0.17	0.35	1.06E-05
TG(57:4)		942.8472	11.03	Both	0.33	0.17	0.49	7.98E-04	0.19	0.12	0.26	7.66E-05
TG(57:5)		940.8325	10.66	Both	0.36	0.16	0.56	4.31E-03	0.14	0.07	0.21	2.03E-03
TG(58:1)'		962.9101	12.15	Both	0.22	0.12	0.32	3.02E-04	0.11	0.04	0.19	2.81E-02
TG(58:2)		960.8935	11.79	Both	0.31	0.21	0.41	4.29E-06	0.19	0.10	0.28	1.13E-03
TG(58:3)'		958.8779	11.40	Both	0.29	0.17	0.42	1.81E-04	0.25	0.17	0.34	1.06E-05
TG(58:4)		956.8625	11.03	Both	0.25	0.13	0.38	1.74E-03	0.21	0.13	0.29	2.80E-05
TG(58:6)		952.8318	11.64	Both	0.12	0.04	0.21	3.97E-02	0.17	0.08	0.26	2.64E-03
TG(59:2)		974.9101	12.14	Both	0.22	0.13	0.32	1.84E-04	0.12	0.04	0.20	3.06E-02
TG(59:3)		972.8936	11.81	Both	0.22	0.13	0.32	2.86E-04	0.14	0.06	0.22	5.98E-03
TG(59:5)		968.8629	11.04	Both	0.20	0.06	0.35	3.79E-02	0.15	0.08	0.23	1.45E-03
TG(60:2)		988.9260	12.14	Both	0.25	0.16	0.35	4.53E-05	0.14	0.06	0.22	9.10E-03
TG(60:3)	TG(20:1/18:1/22:1)	986.9093	11.81	Both	0.21	0.11	0.31	5.87E-04	0.14	0.05	0.23	1.27E-02
CE(18:1)	CE(18:1)	668.6334	11.93	Asian Chinese	0.03	-0.12	0.17	8.60E-01	-0.25	-0.44	-0.06	4.82E-02
CE(22:4)	CE(22:4)	718.6488	11.18	Asian Chinese	-0.05	-0.16	0.07	6.63E-01	-0.17	-0.29	-0.04	3.97E-02
Cer(d40:1)	Cer(d18:1/22:0)	666.6046	8.77	Asian Chinese	0.06	-0.04	0.15	4.94E-01	0.12	0.03	0.21	4.10E-02
Cer(d42:1)	Cer(d18:1/24:0)	694.6359	9.41	Asian Chinese	0.07	-0.02	0.16	2.78E-01	0.12	0.03	0.22	4.49E-02
Cer(d42:2)	Cer(d18:1/24:1)	692.6203	8.73	Asian Chinese	0.03	-0.05	0.12	6.76E-01	0.12	0.03	0.22	4.98E-02
DG(38:5)		660.5564	7.07	Asian Chinese	0.12	0.03	0.21	5.31E-02	0.13	0.04	0.21	2.15E-02
DG(38:6)		658.5416	6.52	Asian Chinese	0.07	-0.02	0.17	2.76E-01	0.14	0.05	0.22	1.30E-02
PC(38:7)		804.5534	4.94	Asian Chinese	0.01	-0.07	0.10	8.70E-01	-0.13	-0.23	-0.03	4.23E-02
PC(O-30:0)		692.5597	6.09	Asian Chinese	-0.04	-0.13	0.05	6.55E-01	-0.21	-0.36	-0.06	3.78E-02
PC(O-34:1)		746.6055	6.92	Asian Chinese	0.00	-0.09	0.08	9.55E-01	-0.17	-0.29	-0.06	2.55E-02
PC(O-36:3)		770.6036	6.39	Asian Chinese	0.05	-0.04	0.14	5.01E-01	-0.12	-0.21	-0.03	3.78E-02
PC(P-30:0)		690.5438	5.98	Asian Chinese	-0.05	-0.14	0.04	4.66E-01	-0.30	-0.44	-0.16	9.16E-04
PC(P-32:1)		716.5584	6.08	Asian Chinese	-0.03	-0.12	0.05	7.00E-01	-0.22	-0.35	-0.10	5.64E-03

PC(P-34:3)		740.5578	5.64	Asian Chinese	-0.09	-0.19	0.01	2.49E-01	-0.21	-0.31	-0.12	8.48E-04
PC(P-36:2)		814.5975	6.99	Asian Chinese	-0.12	-0.21	-0.02	8.68E-02	-0.17	-0.26	-0.08	3.48E-03
PC(P-36:5)		808.5500	5.55	Asian Chinese	-0.05	-0.15	0.05	5.82E-01	-0.11	-0.20	-0.03	4.22E-02
PC(P-38:3)'		818.6026	6.57	Asian Chinese	-0.13	-0.24	-0.02	8.74E-02	-0.15	-0.25	-0.05	2.06E-02
PC(P-38:6)		834.5641	5.83	Asian Chinese	-0.11	-0.20	-0.02	8.72E-02	-0.11	-0.19	-0.02	4.99E-02
PC(P-40:7)		816.5895	5.87	Asian Chinese	-0.11	-0.20	-0.01	1.26E-01	-0.14	-0.22	-0.05	1.55E-02
PE(34:2)		714.5075	6.06	Asian Chinese	0.11	0.03	0.19	5.99E-02	0.13	0.03	0.23	4.23E-02
PE(36:4)	PE(16:0/20:4)	738.5071	5.93	Asian Chinese	0.10	0.02	0.18	9.74E-02	0.17	0.06	0.28	1.77E-02
PE(38:4)	PE(18:0/20:4)	766.5387	6.68	Asian Chinese	0.03	-0.05	0.12	7.03E-01	0.15	0.06	0.24	8.24E-03
PE(40:5)		792.5521	6.69	Asian Chinese	0.12	0.03	0.22	5.31E-02	0.11	0.03	0.20	3.80E-02
PE(40:6)	PE(18:0/22:6)	790.5384	6.44	Asian Chinese	0.11	0.01	0.21	1.09E-01	0.15	0.06	0.23	1.09E-02
PE(P-36:1)		730.5747	7.76	Asian Chinese	0.01	-0.08	0.10	9.00E-01	-0.13	-0.22	-0.03	4.23E-02
SM(d31:1)		661.5286	5.71	Asian Chinese	-0.08	-0.17	0.01	2.47E-01	-0.14	-0.25	-0.04	4.23E-02
SM(d32:0)		721.5505	5.15	Asian Chinese	-0.03	-0.12	0.07	7.89E-01	-0.19	-0.33	-0.04	4.58E-02
SM(d32:1)	SM(d16:1/16:0)	675.5435	4.85	Asian Chinese	-0.01	-0.11	0.08	8.71E-01	-0.18	-0.31	-0.05	3.98E-02
SM(d34:1)	SM(d18:1/16:0)	1406.1409	5.60	Asian Chinese	-0.07	-0.17	0.03	3.85E-01	-0.15	-0.26	-0.05	2.26E-02
SM(d35:1)		717.5891	5.93	Asian Chinese	-0.05	-0.15	0.04	5.01E-01	-0.15	-0.26	-0.04	4.23E-02
SM(d35:2)		715.5749	5.33	Asian Chinese	-0.05	-0.13	0.03	4.73E-01	-0.17	-0.30	-0.05	4.11E-02
SM(d40:0)		833.6753	8.25	Asian Chinese	0.09	-0.01	0.20	2.33E-01	0.12	0.03	0.20	3.06E-02
SM(d42:3)	SM(d18:2/24:1)	811.6678	7.20	Asian Chinese	-0.03	-0.12	0.06	7.60E-01	-0.15	-0.25	-0.04	3.78E-02
SM(d43:2)		827.7008	8.09	Asian Chinese	-0.03	-0.09	0.03	5.25E-01	-0.44	-0.77	-0.10	4.94E-02
SM(t34:1)		719.5698	5.35	Asian Chinese	-0.04	-0.13	0.06	6.70E-01	-0.15	-0.25	-0.05	1.88E-02
TG(50:5)	TG(14:0/18:2/18:3)	842.7234	10.15	Asian Chinese	0.14	0.04	0.25	5.21E-02	0.13	0.05	0.21	1.09E-02
TG(54:5)	TG(18:1/18:2/18:2)	898.7843	11.05	Asian Chinese	0.13	0.00	0.26	1.75E-01	0.19	0.11	0.27	3.17E-04
TG(54:6)	TG(18:1/18:2/18:3)	896.7697	10.66	Asian Chinese	0.13	-0.02	0.28	2.49E-01	0.12	0.04	0.19	1.50E-02
TG(56:8)	TG(16:0/18:2/22:6)	920.7700	10.66	Asian Chinese	0.10	-0.04	0.24	3.66E-01	0.11	0.03	0.18	3.53E-02
TG(59:4)		970.8780	11.41	Asian Chinese	0.13	0.01	0.25	1.32E-01	0.15	0.07	0.24	3.89E-03
TG(60:4)		984.8928	11.41	Asian Chinese	0.12	0.01	0.23	1.32E-01	0.12	0.03	0.20	4.23E-02

TG(60:5)		982.8783	11.05	Asian Chinese	0.17	0.04	0.30	6.19E-02	0.16	0.09	0.24	1.21E-03
TG(61:6)		994.8788	11.26	Asian Chinese	0.12	0.00	0.23	1.59E-01	0.13	0.05	0.20	1.03E-02
PC(31:1)		735.5634	5.71	Caucasian	0.11	0.03	0.19	3.21E-02	0.08	-0.08	0.23	5.01E-01
PC(32:1)	PC(16:0/16:1)	776.5440	5.76	Caucasian	0.11	0.04	0.19	3.27E-02	0.08	-0.05	0.22	3.98E-01
PC(36:3)	PC(16:0/20:3)	784.5835	6.01	Caucasian	0.14	0.05	0.23	1.76E-02	0.04	-0.07	0.14	6.47E-01
PE(40:6)	PE(18:0/22:6)	792.5529	6.44	Caucasian	0.16	0.06	0.25	1.40E-02	0.10	0.01	0.20	9.44E-02
SM(d42:3)	SM(d18:2/24:1)	855.6596	7.23	Caucasian	-0.12	-0.21	-0.03	4.47E-02	-0.06	-0.15	0.04	4.00E-01
SM(t42:1)		875.6874	7.54	Caucasian	-0.15	-0.23	-0.06	6.61E-03	-0.08	-0.17	0.01	1.74E-01
TG(46:2)	TG(12:0/16:1/18:1)	792.7077	10.45	Caucasian	0.12	0.04	0.20	2.32E-02	0.09	0.00	0.19	1.63E-01
TG(47:1)	TG(14:0/15:0/18:1)	808.7382	11.13	Caucasian	0.10	0.03	0.17	4.81E-02	0.17	0.03	0.30	6.44E-02
TG(48:4)	TG(12:0/18:2/18:2)	816.7078	10.05	Caucasian	0.17	0.08	0.27	4.14E-03	0.08	0.00	0.16	1.31E-01
TG(49:0)	TG(16:0/16:0/17:0)	838.7855	12.01	Caucasian	0.12	0.04	0.20	2.23E-02	0.13	0.03	0.23	5.64E-02
TG(51:0)	TG(18:0/16:0/17:0)	866.8169	12.26	Caucasian	0.15	0.07	0.23	5.85E-03	0.08	-0.01	0.17	2.19E-01
TG(52:6)	TG(16:1/18:2/18:3)	868.7391	10.23	Caucasian	0.16	0.06	0.26	1.09E-02	0.08	0.00	0.16	1.49E-01
TG(54:1)	TG(18:0/18:0/18:1)	906.8482	12.35	Caucasian	0.22	0.12	0.32	5.30E-04	0.06	-0.01	0.14	2.49E-01
TG(54:1)'		906.8468	11.37	Caucasian	0.18	0.10	0.26	5.24E-04	0.09	0.00	0.19	1.45E-01
TG(58:3)	TG(18:1/18:2/22:0)	958.8793	12.34	Caucasian	0.13	0.04	0.23	4.89E-02	0.07	-0.01	0.15	1.95E-01

β: beta-coefficient of individual metabolites as indepedent variable in the linear regression model adjusting for age, gender and BMI. p: adjusted p-value using Benjamin-Hochberg multiple testing correction (cut-off value 0.05). Cer: ceramide; DG: diacylglycerol; PC: phosphatidylcholine; PE: phosphatidylethanolamine; SM: sphingomyelin; TG: triacylglycerol; CE: cholesteryl ester; Only annotated metabolites are displayed.

Table 9.10: Table S7: Metabolites associated with FPG and/or %VATTBF in Caucasian analysed by multiple linear regression adjusted for gender, age and BMI (BH-corrected p<0.05). The list of metabolites is ordered by the variable importance in ramdon forest, and the top 100 variables (from unknown X160_HP_241.0719_12.18 to unknown LP_802.5932_348.16) were selected for sample restratification.

			FPG				*%VAT$_{TBF}$*				
MS1	MS2	Marker of	β	CI 2.5%	CI 97.5%	p	β	CI 2.5%	CI 97.5%	p	Importance
HP_241.0719_12.18		FPG	0.53	0.40	0.65	2.97E-12	0.11	0.01	0.21	3.70E-01	4.54
TG(56:6)	TG(16:0/18:1/22:5)	Both	0.44	0.23	0.66	1.19E-02	0.28	0.13	0.42	2.08E-03	2.45
TG(52:3)	TG(16:0/18:1/18:2)	%VAT$_{TBF}$	0.31	0.10	0.51	5.17E-02	0.33	0.21	0.46	4.53E-05	1.96
TG(55:1)		%VAT$_{TBF}$	0.11	-0.02	0.24	3.28E-01	0.14	0.06	0.23	7.40E-03	1.80
TG(58:3)'		Both	0.33	0.13	0.52	3.46E-02	0.29	0.17	0.42	1.81E-04	1.66
PC(36:5)''		FPG	0.23	0.09	0.38	3.94E-02	0.06	-0.04	0.16	5.01E-01	1.63
TG(57:3)		%VAT$_{TBF}$	0.28	0.07	0.49	8.62E-02	0.34	0.21	0.46	4.53E-05	1.59
TG(56:1)		Both	0.22	0.09	0.35	3.49E-02	0.23	0.15	0.31	1.01E-05	1.57
TG(50:2)	TG(16:0/16:1/18:1)	%VAT$_{TBF}$	0.18	0.05	0.32	8.40E-02	0.22	0.13	0.30	5.26E-05	1.48
TG(51:1)	TG(16:0/17:0/18:1)	%VAT$_{TBF}$	0.15	0.01	0.29	1.82E-01	0.20	0.11	0.29	2.86E-04	1.45
LP_933.8665_739.69		Both	0.23	0.09	0.38	3.49E-02	0.15	0.06	0.24	1.34E-02	1.44
HN_88.014_12.55		FPG	0.20	0.07	0.32	4.72E-02	0.08	0.00	0.16	4.71E-01	1.41
TG(50:3)	TG(16:0/16:1/18:2)	%VAT$_{TBF}$	0.21	0.06	0.36	6.62E-02	0.24	0.15	0.33	4.53E-05	1.36
LP_893.8359_735.23		%VAT$_{TBF}$	0.17	0.03	0.32	1.40E-01	0.21	0.12	0.30	3.91E-04	1.34
TG(50:1)	TG(16:0/16:0/18:1)	%VAT$_{TBF}$	0.12	-0.03	0.27	3.50E-01	0.16	0.06	0.25	1.66E-02	1.32
TG(53:2)	TG(17:0/18:1/18:1)	%VAT$_{TBF}$	0.22	0.06	0.39	8.40E-02	0.24	0.14	0.35	1.95E-04	1.32
TG(55:2)		%VAT$_{TBF}$	0.19	0.06	0.33	6.62E-02	0.23	0.15	0.32	1.71E-05	1.29
TG(57:2)		Both	0.27	0.12	0.42	3.15E-02	0.26	0.16	0.35	3.40E-05	1.25
TG(58:2)		Both	0.28	0.11	0.44	3.46E-02	0.31	0.21	0.41	4.29E-06	1.21
TG(48:1)	TG(14:0/16:0/18:1)	%VAT$_{TBF}$	0.10	-0.02	0.22	3.26E-01	0.15	0.07	0.22	3.33E-03	1.18

TG(54:2)	TG(18:0/18:1/18:1)	Both	0.24	0.10	0.38	3.46E-02	0.21	0.12	0.30	3.13E-04	1.18
TG(52:5)	TG(16:0/18:2/18:3)	%VAT$_{TBF}$	0.22	-0.02	0.45	2.66E-01	0.26	0.11	0.41	5.83E-03	1.14
TG(52:4)	TG(16:0/18:2/18:2)	%VAT$_{TBF}$	0.31	0.05	0.56	1.30E-01	0.36	0.20	0.52	3.70E-04	1.13
TG(53:3)	TG(17:0/18:1/18:2)	Both	0.27	0.10	0.44	4.22E-02	0.26	0.15	0.37	1.41E-04	1.12
TG(54:1)'		%VAT$_{TBF}$	0.12	-0.01	0.25	2.66E-01	0.18	0.10	0.26	5.24E-04	1.11
TG(57:1)		%VAT$_{TBF}$	0.19	0.05	0.34	9.20E-02	0.19	0.10	0.29	7.54E-04	1.10
PE(34:1)		%VAT$_{TBF}$	0.03	-0.08	0.14	7.66E-01	0.11	0.04	0.19	2.02E-02	1.09
Erythronic acid	M-H-	FPG	0.18	0.07	0.29	3.64E-02	0.07	0.00	0.14	4.71E-01	1.07
TG(53:1)		%VAT$_{TBF}$	0.10	-0.02	0.22	3.34E-01	0.15	0.07	0.22	3.11E-03	1.00
TG(49:2)	TG(15:0/16:0/18:2)	%VAT$_{TBF}$	0.12	-0.01	0.25	2.90E-01	0.16	0.08	0.25	2.04E-03	0.99
DG(38:6)		FPG	0.25	0.12	0.38	2.65E-02	0.07	-0.02	0.17	2.76E-01	0.98
TG(51:4)	TG(15:0/18:2/18:2)	%VAT$_{TBF}$	0.13	-0.07	0.34	4.35E-01	0.25	0.12	0.38	1.90E-03	0.98
TG(52:1)	TG(16:0/18:0/18:1)	%VAT$_{TBF}$	0.14	0.00	0.27	2.07E-01	0.15	0.06	0.23	9.00E-03	0.98
DG(34:2)	DG(16:0/18:2)	%VAT$_{TBF}$	0.22	0.07	0.37	5.64E-02	0.24	0.15	0.33	5.26E-05	0.97
TG(49:0)	TG(16:0/16:0/17:0)	%VAT$_{TBF}$	0.07	-0.04	0.19	4.64E-01	0.12	0.04	0.20	2.23E-02	0.97
TG(48:2)	TG(14:0/16:0/18:2)	%VAT$_{TBF}$	0.12	0.00	0.24	2.42E-01	0.16	0.08	0.24	1.10E-03	0.96
TG(59:3)		Both	0.23	0.08	0.39	4.84E-02	0.22	0.13	0.32	2.86E-04	0.94
TG(49:1)	TG(15:0/16:0/18:1)	%VAT$_{TBF}$	0.09	-0.04	0.22	3.86E-01	0.16	0.07	0.24	3.47E-03	0.90
PE(P-36:4)	PE(P-16:0/20:4)	FPG	0.37	0.19	0.55	1.19E-02	0.06	-0.07	0.18	5.92E-01	0.89
TG(47:1)	TG(14:0/15:0/18:1)	%VAT$_{TBF}$	0.06	-0.05	0.17	5.01E-01	0.10	0.03	0.17	4.81E-02	0.89
TG(52:2)	TG(16:0/18:1/18:1)	%VAT$_{TBF}$	0.22	0.05	0.40	9.52E-02	0.25	0.15	0.36	1.95E-04	0.85
TG(53:5)	TG(17:0/18:2/18:3)	%VAT$_{TBF}$	0.15	-0.04	0.34	3.36E-01	0.17	0.05	0.30	3.29E-02	0.81
PC(38:4)'	PC(18:0/20:4)	FPG	0.20	0.08	0.33	3.54E-02	0.03	-0.05	0.12	7.00E-01	0.77
TG(51:3)	TG(15:0/18:1/18:2)	%VAT$_{TBF}$	0.23	0.06	0.40	9.20E-02	0.24	0.13	0.35	5.24E-04	0.75
TG(55:3)'		Both	0.24	0.08	0.40	4.84E-02	0.21	0.11	0.31	7.98E-04	0.75
LP_739.5445_394.48		FPG	0.24	0.08	0.39	4.78E-02	-0.01	-0.12	0.09	9.00E-01	0.75

TG(59:2)		Both	0.26	0.11	0.41	3.46E-02	0.22	0.13	0.32	1.84E-04	0.72
TG(51:2)	TG(16:0/17:1/18:1)	$\%VAT_{TBF}$	0.18	0.03	0.34	1.42E-01	0.23	0.13	0.33	1.99E-04	0.71
TG(58:1)'		$\%VAT_{TBF}$	0.20	0.04	0.35	1.03E-01	0.22	0.12	0.32	3.02E-04	0.70
TG(49:3)	TG(15:0/16:1/18:2)	$\%VAT_{TBF}$	0.11	-0.02	0.25	3.25E-01	0.15	0.07	0.24	6.04E-03	0.70
DG(38:5)		FPG	0.29	0.16	0.42	1.19E-02	0.12	0.03	0.21	5.31E-02	0.69
TG(56:2)		Both	0.26	0.11	0.42	3.49E-02	0.30	0.20	0.40	4.29E-06	0.63
TG(55:3)		$\%VAT_{TBF}$	0.20	0.04	0.36	1.04E-01	0.23	0.14	0.33	1.83E-04	0.58
DG(36:2)	DG(18:1/18:1)	Both	0.27	0.12	0.42	3.15E-02	0.24	0.15	0.34	5.16E-05	0.56
TG(56:3)	TG(18:1/18:1/20:1)	Both	0.26	0.10	0.42	3.49E-02	0.23	0.12	0.33	3.91E-04	0.55
TG(50:4)	TG(14:0/18:2/18:2)	$\%VAT_{TBF}$	0.17	-0.01	0.34	2.66E-01	0.24	0.13	0.35	6.44E-04	0.54
TG(53:2)'		$\%VAT_{TBF}$	0.12	-0.01	0.24	2.65E-01	0.16	0.08	0.24	1.78E-03	0.53
TG(51:0)	TG(18:0/16:0/17:0)	$\%VAT_{TBF}$	0.11	-0.02	0.24	3.24E-01	0.15	0.07	0.23	5.85E-03	0.53
TG(60:2)		Both	0.26	0.11	0.42	3.46E-02	0.25	0.16	0.35	4.53E-05	0.52
PC(O-36:4)	PC(O-16:0/20:4)	FPG	0.24	0.10	0.38	3.46E-02	0.00	-0.09	0.10	9.76E-01	0.52
TG(54:1)	TG(18:0/18:0/18:1)	$\%VAT_{TBF}$	0.21	0.05	0.37	9.71E-02	0.22	0.12	0.32	5.30E-04	0.52
TG(58:3)	TG(18:1/18:2/22:0)	Both	0.25	0.10	0.40	3.46E-02	0.13	0.04	0.23	4.89E-02	0.49
TG(48:3)	TG(12:0/18:1/18:2)	$\%VAT_{TBF}$	0.13	-0.01	0.27	2.66E-01	0.16	0.07	0.25	4.96E-03	0.47
TG(54:3)	TG(18:0/18:1/18:2)	Both	0.27	0.09	0.44	4.84E-02	0.24	0.13	0.36	5.24E-04	0.44
DG(34:1)	DG(16:0/18:1)	$\%VAT_{TBF}$	0.18	0.04	0.32	1.05E-01	0.20	0.11	0.29	4.53E-04	0.42
TG(46:2)	TG(12:0/16:1/18:1)	$\%VAT_{TBF}$	0.09	-0.04	0.21	3.86E-01	0.12	0.04	0.20	2.32E-02	0.42
PE(40:6)	PE(18:0/22:6)	$\%VAT_{TBF}$	0.19	0.04	0.33	9.87E-02	0.16	0.06	0.25	1.40E-02	0.41
TG(53:4)	TG(17:1/18:1/18:2)	$\%VAT_{TBF}$	0.25	0.07	0.44	8.40E-02	0.26	0.14	0.38	4.11E-04	0.41
LP_883.684_344.19		FPG	0.20	0.08	0.32	3.46E-02	0.04	-0.04	0.12	6.00E-01	0.40
PE(36:1)		$\%VAT_{TBF}$	0.05	-0.07	0.17	6.20E-01	0.15	0.07	0.23	3.20E-03	0.39
PE(P-38:4)	PE(P-18:0/20:4)	FPG	0.30	0.15	0.44	1.19E-02	0.02	-0.08	0.12	8.61E-01	0.38
PC(36:4)'	PC(16:0/20:4)	FPG	0.23	0.11	0.35	2.65E-02	0.07	-0.01	0.15	2.66E-01	0.37

PE(P-38:5)	PE(P-18:1/20:4)	FPG	0.27	0.12	0.41	3.15E-02	0.01	-0.09	0.11	9.26E-01	0.29
TG(59:5)		%VAT$_{TBF}$	0.22	0.00	0.44	2.42E-01	0.20	0.06	0.35	3.79E-02	0.24
PE(P-36:1)		FPG	0.25	0.13	0.38	1.40E-02	0.01	-0.08	0.10	9.00E-01	0.21
PC(O-38:5)		FPG	0.22	0.08	0.36	4.76E-02	-0.02	-0.12	0.07	8.14E-01	0.17
LP_869.6727_344.17		FPG	0.20	0.08	0.32	3.49E-02	0.05	-0.04	0.13	5.24E-01	0.16
TG(57:4)		%VAT$_{TBF}$	0.32	0.07	0.57	1.05E-01	0.33	0.17	0.49	7.98E-04	0.16
DG(36:3)	DG(18:1/18:2)	%VAT$_{TBF}$	0.24	0.05	0.43	1.04E-01	0.25	0.13	0.37	1.14E-03	0.12
DG(34:3)		%VAT$_{TBF}$	0.18	0.03	0.32	1.15E-01	0.17	0.08	0.26	4.28E-03	0.12
TG(58:6)		Both	0.22	0.08	0.35	3.49E-02	0.12	0.04	0.21	3.97E-02	0.09
TG(60:3)	TG(20:1/18:1/22:1)	Both	0.25	0.10	0.40	3.49E-02	0.21	0.11	0.31	5.87E-04	0.09
PC(P-34:2)	PC(P-16:0/18:2)	%VAT$_{TBF}$	-0.03	-0.18	0.11	8.14E-01	-0.14	-0.24	-0.04	3.07E-02	0.09
LP_796.6117_373.29		FPG	0.20	0.08	0.33	3.63E-02	0.03	-0.05	0.12	7.09E-01	0.07
PC(32:1)	PC(16:0/16:1)	%VAT$_{TBF}$	0.00	-0.12	0.12	9.96E-01	0.11	0.04	0.19	3.27E-02	0.03
DG(38:2)		Both	0.23	0.08	0.38	4.71E-02	0.24	0.15	0.33	4.53E-05	0.01
TG(48:4)	TG(12:0/18:2/18:2)	%VAT$_{TBF}$	0.13	-0.02	0.28	3.09E-01	0.17	0.08	0.27	4.14E-03	-0.01
PC(38:3)	PC(18:0/20:3)	%VAT$_{TBF}$	0.04	-0.11	0.20	7.81E-01	0.15	0.05	0.25	2.89E-02	-0.02
PE(36:2)	PE(18:0/18:2)	%VAT$_{TBF}$	0.04	-0.09	0.17	7.52E-01	0.14	0.05	0.23	1.40E-02	-0.04
TG(58:4)		%VAT$_{TBF}$	0.20	0.00	0.40	2.17E-01	0.25	0.13	0.38	1.74E-03	-0.07
PC(P-34:1)		%VAT$_{TBF}$	-0.02	-0.16	0.11	8.75E-01	-0.13	-0.21	-0.04	2.93E-02	-0.15
TG(57:5)		%VAT$_{TBF}$	0.27	-0.04	0.58	3.09E-01	0.36	0.16	0.56	4.31E-03	-0.17
SM(d42:3)	SM(d18:2/24:1)	%VAT$_{TBF}$	-0.12	-0.25	0.02	3.11E-01	-0.12	-0.21	-0.03	4.47E-02	-0.21
DG(36:4)	DG(18:2/18:2)	%VAT$_{TBF}$	0.15	-0.05	0.35	3.56E-01	0.19	0.07	0.32	2.26E-02	-0.27
PC(31:1)		%VAT$_{TBF}$	0.04	-0.08	0.15	7.60E-01	0.11	0.03	0.19	3.21E-02	-0.28
DG(38:3)		%VAT$_{TBF}$	0.25	0.04	0.46	1.31E-01	0.24	0.11	0.38	4.68E-03	-0.29
SM(t42:1)		%VAT$_{TBF}$	-0.10	-0.23	0.04	3.86E-01	-0.15	-0.23	-0.06	6.61E-03	-0.46
TG(54:4)	TG(18:1/18:1/18:2)	%VAT$_{TBF}$	0.23	0.01	0.45	2.03E-01	0.21	0.07	0.36	2.90E-02	-0.51

SM(d36:0)		$\%VAT_{TBF}$	0.03	-0.10	0.16	8.43E-01	0.13	0.04	0.21	3.04E-02	-0.53
LP_802.5932_348.16		$\%VAT_{TBF}$	-0.05	-0.21	0.10	7.21E-01	-0.16	-0.26	-0.07	1.06E-02	-0.67
Cer(d40:0)		$\%VAT_{TBF}$	0.22	0.07	0.36	5.62E-02	0.16	0.06	0.26	1.09E-02	-0.68
PC(36:3)	PC(16:0/20:3)	$\%VAT_{TBF}$	0.11	-0.02	0.25	3.26E-01	0.14	0.05	0.23	1.76E-02	-0.76
TG(52:6)	TG(16:1/18:2/18:3)	$\%VAT_{TBF}$	0.07	-0.08	0.23	5.76E-01	0.16	0.06	0.26	1.09E-02	-1.17
Hexose A(glucose)	M+Cl-	FPG	0.31	0.21	0.41	5.46E-07	0.05	-0.03	0.12	6.91E-01	NA
Hexose B(glucose)	M+Cl-	FPG	0.33	0.21	0.44	2.87E-06	0.09	0.00	0.17	3.91E-01	NA

β: beta-coefficient of individual metabolites as indepedent variable in the linear regression model adjusting for age, gender and BMI. p: adjusted p-value using Benjamin-Hochberg multiple testing correction (cut-off value 0.05). Importance: decreases in accuracy of each metabolite in the random forest model for the prediction of FPG state. Cer: ceramide; DG: diacylglycerol; PC: phosphatidylcholine; PE: phosphatidylethanolamine; SM: sphingomyelin; TG: triacylglycerol.Unknown ID is displayed in the form of "platform, ESI mode, m/z and retention time" in seconds for lipid or in minutes for polar metabolites. LP: lipidomics ESI+; HP: HILIC ESI+; HN: HILIC ESI-.

Table 9.11: Metabolites associated with FPG and/or %VATTBF in Asian Chinese analysed by multiple linear regression adjusted for gender, age and BMI (BH-corrected p<0.05). The list of metabolites is ordered by the variable importance in ramdon forest, and the top 100 variables (from unknown X160_HP_241.0719_12.18 to PE(P-36:1)) were selected for sample restratification.

			FPG				*%VAT$_{TBF}$*				
MS1	MS2	Marker of	β	CI 2.5%	CI 97.5%	p	β	CI 2.5%	CI 97.5%	p	Importance
HP_241.0719_12.18		FPG	0.22	0.12	0.33	1.77E-03	0.01	-0.07	0.10	9.10E-01	3.69
Hexose C		FPG	0.29	0.17	0.42	3.01E-04	0.00	-0.09	0.10	9.92E-01	2.85
SM(d40:1)'		FPG	-0.20	-0.34	-0.06	2.87E-02	-0.13	-0.24	-0.03	6.17E-02	2.61
TG(59:2)		Both	0.22	0.12	0.33	6.76E-04	0.12	0.04	0.20	3.06E-02	2.40
TG(59:3)		Both	0.27	0.16	0.37	5.77E-05	0.14	0.06	0.22	5.98E-03	2.35
TG(56:3)	TG(18:1/18:1/20:1)	Both	0.26	0.16	0.36	5.77E-05	0.11	0.03	0.19	3.78E-02	2.30
TG(54:3)	TG(18:0/18:1/18:2)	Both	0.30	0.18	0.42	7.39E-05	0.16	0.07	0.25	7.33E-03	2.10
TG(60:3)	TG(20:1/18:1/22:1)	Both	0.25	0.13	0.36	5.96E-04	0.14	0.05	0.23	1.27E-02	2.06
TG(60:2)		Both	0.23	0.13	0.34	4.33E-04	0.14	0.06	0.22	9.10E-03	1.97
PC(P-34:1)		%VAT$_{TBF}$	-0.18	-0.33	-0.02	1.08E-01	-0.25	-0.37	-0.14	6.98E-04	1.96
SM(d42:3)	SM(d18:2/24:1)	Both	-0.23	-0.37	-0.09	1.31E-02	-0.15	-0.25	-0.04	3.78E-02	1.93
TG(54:4)	TG(18:1/18:1/18:2)	Both	0.28	0.18	0.38	5.77E-05	0.16	0.08	0.24	1.45E-03	1.77
LN_853.6434_394.8		FPG	-0.22	-0.34	-0.09	7.00E-03	-0.09	-0.19	0.00	1.63E-01	1.75
TG(59:5)		Both	0.26	0.17	0.36	5.77E-05	0.15	0.08	0.23	1.45E-03	1.66
TG(55:3)'		Both	0.27	0.16	0.38	2.07E-04	0.14	0.06	0.23	1.12E-02	1.65
LN_923.6473_433.94		FPG	-0.28	-0.39	-0.16	2.77E-04	-0.09	-0.19	0.00	1.52E-01	1.65
TG(53:4)	TG(17:1/18:1/18:2)	Both	0.26	0.15	0.37	1.26E-04	0.18	0.10	0.26	6.98E-04	1.65
TG(56:2)		Both	0.22	0.11	0.33	1.19E-03	0.17	0.09	0.25	1.28E-03	1.60
TG(59:4)		Both	0.21	0.10	0.32	3.38E-03	0.15	0.07	0.24	3.89E-03	1.59
TG(54:5)	TG(18:1/18:2/18:2)	Both	0.28	0.17	0.38	5.77E-05	0.19	0.11	0.27	3.17E-04	1.58
TG(58:1)	TG(16:0/18:1/24:0)	FPG	0.23	0.12	0.34	5.96E-04	0.06	-0.02	0.15	2.96E-01	1.56
LP_802.5932_348.16		FPG	-0.20	-0.34	-0.07	1.97E-02	-0.11	-0.21	-0.01	1.13E-01	1.54

TG(58:3)'		Both	0.26	0.14	0.37	5.37E-04	0.25	0.17	0.34	1.06E-05	1.51
TG(53:3)	TG(17:0/18:1/18:2)	Both	0.25	0.14	0.36	3.10E-04	0.17	0.09	0.25	1.45E-03	1.46
TG(57:1)		$\%VAT_{TBF}$	0.13	0.02	0.24	7.47E-02	0.11	0.02	0.19	4.76E-02	1.46
TG(60:5)		Both	0.26	0.16	0.36	5.77E-05	0.16	0.09	0.24	1.21E-03	1.42
TG(54:6)	TG(18:1/18:2/18:3)	Both	0.22	0.13	0.32	2.13E-04	0.12	0.04	0.19	1.50E-02	1.40
TG(53:2)	TG(17:0/18:1/18:1)	Both	0.25	0.13	0.37	5.96E-04	0.15	0.06	0.24	1.11E-02	1.37
TG(54:2)	TG(18:0/18:1/18:1)	Both	0.20	0.09	0.31	4.29E-03	0.15	0.06	0.23	6.32E-03	1.35
TG(52:2)	TG(16:0/18:1/18:1)	Both	0.22	0.09	0.34	8.06E-03	0.19	0.10	0.29	1.45E-03	1.34
TG(60:4)		Both	0.17	0.05	0.28	2.77E-02	0.12	0.03	0.20	4.23E-02	1.31
TG(58:2)		Both	0.19	0.07	0.31	1.42E-02	0.19	0.10	0.28	1.13E-03	1.28
DG(36:3)	DG(18:1/18:2)	Both	0.25	0.15	0.34	5.77E-05	0.15	0.08	0.23	1.28E-03	1.25
TG(52:5)	TG(16:0/18:2/18:3)	Both	0.23	0.14	0.33	1.51E-04	0.15	0.08	0.23	1.21E-03	1.24
TG(58:3)	TG(18:1/18:2/22:0)	FPG	0.21	0.11	0.31	1.17E-03	0.07	-0.01	0.15	1.95E-01	1.22
SM(d40:3)		FPG	-0.26	-0.42	-0.10	9.96E-03	-0.04	-0.16	0.08	6.51E-01	1.20
TG(52:3)	TG(16:0/18:1/18:2)	Both	0.26	0.15	0.37	2.71E-04	0.21	0.13	0.30	6.87E-05	1.18
TG(57:5)		Both	0.21	0.12	0.31	3.49E-04	0.14	0.07	0.21	2.03E-03	1.17
TG(51:3)	TG(15:0/18:1/18:2)	Both	0.23	0.12	0.34	5.96E-04	0.18	0.10	0.26	8.48E-04	1.12
SM(d42:2)	SM(d18:1/24:1)	FPG	-0.19	-0.30	-0.07	1.14E-02	-0.03	-0.12	0.06	6.80E-01	1.10
TG(52:1)	TG(16:0/18:0/18:1)	$\%VAT_{TBF}$	0.12	0.01	0.24	1.37E-01	0.12	0.03	0.21	3.80E-02	1.09
LP_933.8665_739.69		FPG	0.22	0.11	0.32	1.14E-03	0.08	0.00	0.16	1.36E-01	1.05
SM(d36:2)	SM(d18:2/18:0)	FPG	-0.20	-0.33	-0.08	1.11E-02	-0.02	-0.12	0.07	7.76E-01	1.03
L-Acetylcarnitine		FPG	-0.20	-0.32	-0.09	1.20E-02	-0.10	-0.18	-0.01	3.33E-01	0.99
DG(36:2)	DG(18:1/18:1)	Both	0.23	0.13	0.33	3.41E-04	0.12	0.05	0.20	1.53E-02	0.97
LP_961.8984_748.8		FPG	0.24	0.13	0.35	5.96E-04	0.06	-0.02	0.15	3.01E-01	0.96
TG(57:4)		Both	0.22	0.12	0.32	5.30E-04	0.19	0.12	0.26	7.66E-05	0.96
TG(57:3)		Both	0.26	0.13	0.38	1.09E-03	0.26	0.17	0.35	1.06E-05	0.94
TG(51:1)	TG(16:0/17:0/18:1)	Both	0.20	0.08	0.33	9.02E-03	0.15	0.06	0.24	1.06E-02	0.91
TG(48:4)	TG(12:0/18:2/18:2)	FPG	0.18	0.07	0.28	7.80E-03	0.08	0.00	0.16	1.31E-01	0.88

DG(38:2)		Both	0.26	0.16	0.36	5.77E-05	0.10	0.02	0.18	4.76E-02	0.87
TG(58:1)'		%VAT$_{TBF}$	0.13	0.03	0.24	6.70E-02	0.11	0.04	0.19	2.81E-02	0.87
DG(38:5)		Both	0.18	0.07	0.29	1.08E-02	0.13	0.04	0.21	2.15E-02	0.87
TG(57:2)		Both	0.20	0.09	0.31	3.83E-03	0.16	0.08	0.25	1.77E-03	0.86
Cer(d40:2)		FPG	0.25	0.13	0.37	5.96E-04	0.10	0.01	0.19	8.50E-02	0.81
TG(55:3)		Both	0.21	0.10	0.32	1.59E-03	0.18	0.10	0.25	8.48E-04	0.80
TG(53:5)	TG(17:0/18:2/18:3)	Both	0.23	0.13	0.34	2.71E-04	0.14	0.06	0.22	4.90E-03	0.80
TG(48:2)	TG(14:0/16:0/18:2)	Both	0.18	0.06	0.31	2.56E-02	0.15	0.06	0.25	1.62E-02	0.76
TG(54:6)'		FPG	0.19	0.09	0.28	2.07E-03	0.09	0.02	0.16	6.45E-02	0.76
DG(38:6)		Both	0.15	0.04	0.26	4.92E-02	0.14	0.05	0.22	1.30E-02	0.75
HexCer(d42:2)		FPG	-0.16	-0.28	-0.04	4.56E-02	-0.05	-0.14	0.04	4.72E-01	0.74
TG(53:1)		%VAT$_{TBF}$	0.14	0.00	0.27	1.44E-01	0.15	0.05	0.25	2.54E-02	0.72
TG(52:4)	TG(16:0/18:2/18:2)	Both	0.25	0.14	0.36	2.17E-04	0.22	0.14	0.30	1.42E-05	0.72
TG(49:1)	TG(15:0/16:0/18:1)	Both	0.20	0.07	0.33	1.71E-02	0.14	0.04	0.24	2.98E-02	0.71
TG(48:1)	TG(14:0/16:0/18:1)	%VAT$_{TBF}$	0.13	-0.01	0.26	1.79E-01	0.15	0.05	0.25	2.44E-02	0.70
TG(55:1)		%VAT$_{TBF}$	0.13	0.01	0.26	1.20E-01	0.17	0.08	0.26	4.68E-03	0.70
LP_988.9264_755.24		FPG	0.23	0.12	0.34	5.69E-04	0.05	-0.04	0.13	4.57E-01	0.69
Cer(d41:1)		FPG	0.17	0.05	0.29	3.71E-02	0.10	0.01	0.19	1.13E-01	0.68
TG(53:2)'		Both	0.20	0.08	0.32	1.06E-02	0.14	0.05	0.23	1.85E-02	0.67
PE(36:1)		Both	0.20	0.07	0.34	2.09E-02	0.15	0.04	0.25	3.55E-02	0.65
FA(18:2)		FPG	-0.14	-0.25	-0.04	4.14E-02	0.03	-0.05	0.11	6.77E-01	0.63
DG(34:1)	DG(16:0/18:1)	Both	0.18	0.08	0.29	7.71E-03	0.14	0.06	0.22	7.77E-03	0.62
TG(55:2)		%VAT$_{TBF}$	0.17	0.04	0.30	5.40E-02	0.20	0.10	0.30	1.73E-03	0.62
TG(50:4)	TG(14:0/18:2/18:2)	Both	0.22	0.13	0.32	3.08E-04	0.14	0.06	0.21	4.22E-03	0.61
Cer(d40:1)	Cer(d18:1/22:0)	Both	0.19	0.07	0.31	1.14E-02	0.12	0.03	0.21	4.10E-02	0.60
TG(58:6)		Both	0.21	0.09	0.33	6.86E-03	0.17	0.08	0.26	2.64E-03	0.59
LN_808.6137_565.18		%VAT$_{TBF}$	0.10	0.00	0.21	1.74E-01	0.11	0.03	0.19	3.78E-02	0.59

TG(56:1)		%VAT$_{TBF}$	0.16	0.03	0.30	7.01E-02	0.20	0.10	0.30	1.67E-03	0.58
PE(40:5)		%VAT$_{TBF}$	0.08	-0.03	0.19	3.56E-01	0.11	0.03	0.20	3.80E-02	0.58
TG(50:1)	TG(16:0/16:0/18:1)	%VAT$_{TBF}$	0.12	0.00	0.23	1.41E-01	0.15	0.07	0.24	5.32E-03	0.57
SM(t34:1)		Both	-0.20	-0.31	-0.09	3.83E-03	-0.15	-0.25	-0.05	1.88E-02	0.51
DG(38:3)		Both	0.25	0.15	0.34	5.77E-05	0.16	0.08	0.23	1.13E-03	0.50
PC(P-36:5)		%VAT$_{TBF}$	-0.01	-0.12	0.11	9.55E-01	-0.11	-0.20	-0.03	4.22E-02	0.48
TG(51:2)	TG(16:0/17:1/18:1)	Both	0.21	0.09	0.33	6.86E-03	0.16	0.07	0.26	5.03E-03	0.48
PC(O-44:5)		FPG	-0.20	-0.32	-0.08	1.14E-02	-0.05	-0.14	0.05	5.10E-01	0.47
Cer(d40:0)		%VAT$_{TBF}$	0.12	0.02	0.23	9.18E-02	0.11	0.04	0.19	2.55E-02	0.44
LP_568.4274_230.27		%VAT$_{TBF}$	-0.06	-0.19	0.07	5.75E-01	-0.19	-0.28	-0.10	1.45E-03	0.44
Cer(d42:1)	Cer(d18:1/24:0)	Both	0.16	0.04	0.28	3.69E-02	0.12	0.03	0.22	4.49E-02	0.42
DG(36:4)	DG(18:2/18:2)	Both	0.22	0.12	0.32	3.44E-04	0.15	0.08	0.23	1.45E-03	0.41
TG(56:6)	TG(16:0/18:1/22:5)	Both	0.16	0.06	0.26	1.14E-02	0.13	0.05	0.20	8.39E-03	0.40
TG(48:3)	TG(12:0/18:1/18:2)	Both	0.18	0.08	0.29	7.96E-03	0.12	0.04	0.20	2.98E-02	0.40
TG(50:5)	TG(14:0/18:2/18:3)	Both	0.19	0.09	0.29	2.21E-03	0.13	0.05	0.21	1.09E-02	0.39
CE(18:2)		FPG	-0.20	-0.34	-0.05	4.42E-02	-0.09	-0.20	0.02	2.43E-01	0.37
FA(16:0)		FPG	-0.15	-0.26	-0.04	4.56E-02	0.06	-0.02	0.14	3.21E-01	0.37
TG(49:2)	TG(15:0/16:0/18:2)	Both	0.20	0.07	0.33	1.47E-02	0.16	0.07	0.26	1.01E-02	0.37
TG(50:3)	TG(16:0/16:1/18:2)	Both	0.20	0.09	0.31	5.46E-03	0.19	0.10	0.27	6.98E-04	0.36
TG(56:4)	TG(18:1/18:2/20:1)	FPG	0.26	0.15	0.38	3.35E-04	0.11	0.02	0.20	6.18E-02	0.35
PC(38:4)	PC(18:1/20:3)	FPG	0.18	0.05	0.30	3.01E-02	0.04	-0.06	0.14	5.85E-01	0.34
DG(34:2)	DG(16:0/18:2)	Both	0.20	0.10	0.30	2.07E-03	0.17	0.09	0.25	9.16E-04	0.33
PE(P-36:1)		%VAT$_{TBF}$	0.10	-0.03	0.23	3.17E-01	-0.13	-0.22	-0.03	4.23E-02	0.31
SM(d32:0)		%VAT$_{TBF}$	-0.13	-0.32	0.06	3.74E-01	-0.19	-0.33	-0.04	4.58E-02	0.28
TG(58:4)		Both	0.23	0.12	0.33	5.96E-04	0.21	0.13	0.29	2.80E-05	0.27
PC(P-30:0)		%VAT$_{TBF}$	-0.13	-0.32	0.06	3.75E-01	-0.30	-0.44	-0.16	9.16E-04	0.26
TG(61:6)		Both	0.19	0.09	0.29	3.28E-03	0.13	0.05	0.20	1.03E-02	0.26

PE(36:4)	PE(16:0/20:4)	%VAT$_{TBF}$	-0.04	-0.18	0.10	7.76E-01	0.17	0.06	0.28	1.77E-02	0.21
LP_536.438_558.95		%VAT$_{TBF}$	-0.02	-0.14	0.09	8.71E-01	-0.17	-0.26	-0.09	1.21E-03	0.20
PE(38:4)	PE(18:0/20:4)	%VAT$_{TBF}$	0.02	-0.10	0.13	9.19E-01	0.15	0.06	0.24	8.24E-03	0.18
SM(d31:1)		%VAT$_{TBF}$	-0.10	-0.24	0.05	4.01E-01	-0.14	-0.25	-0.04	4.23E-02	0.17
TG(51:4)	TG(15:0/18:2/18:2)	Both	0.21	0.11	0.31	7.30E-04	0.15	0.07	0.23	2.11E-03	0.17
Cer(d41:2)		FPG	0.20	0.07	0.33	2.07E-02	0.07	-0.03	0.17	3.10E-01	0.17
PC(O-34:1)		%VAT$_{TBF}$	-0.12	-0.28	0.04	3.22E-01	-0.17	-0.29	-0.06	2.55E-02	0.17
PC(P-42:4)		FPG	-0.25	-0.41	-0.10	1.30E-02	-0.08	-0.20	0.04	3.54E-01	0.13
SM(d36:1)	SM(d18:1/18:0)	FPG	-0.17	-0.29	-0.04	4.92E-02	-0.04	-0.14	0.06	5.85E-01	0.13
TG(49:3)	TG(15:0/16:1/18:2)	Both	0.17	0.06	0.29	2.52E-02	0.14	0.05	0.23	2.16E-02	0.12
TG(50:2)	TG(16:0/16:1/18:1)	Both	0.19	0.07	0.32	1.21E-02	0.18	0.09	0.27	1.73E-03	0.11
PC(P-34:2)	PC(P-16:0/18:2)	%VAT$_{TBF}$	-0.07	-0.19	0.04	4.25E-01	-0.19	-0.27	-0.10	9.16E-04	0.10
SM(d40:0)		%VAT$_{TBF}$	-0.02	-0.13	0.09	9.02E-01	0.12	0.03	0.20	3.06E-02	0.07
CE(22:4)		Both	-0.24	-0.40	-0.08	2.25E-02	-0.17	-0.29	-0.04	3.97E-02	0.05
LP_901.7254_652.19		%VAT$_{TBF}$	0.15	0.02	0.28	1.14E-01	0.16	0.06	0.26	1.33E-02	0.05
LN_869.6783_455.69		%VAT$_{TBF}$	-0.24	-0.43	-0.04	7.23E-02	-0.21	-0.35	-0.07	2.55E-02	0.05
PC(P-32:1)		%VAT$_{TBF}$	-0.10	-0.27	0.07	4.74E-01	-0.22	-0.35	-0.10	5.64E-03	0.05
SM(d35:2)		%VAT$_{TBF}$	-0.08	-0.25	0.10	6.06E-01	-0.17	-0.30	-0.05	4.11E-02	0.04
LP_924.8006_638.38		Both	0.21	0.10	0.31	1.94E-03	0.10	0.02	0.18	4.90E-02	0.02
TG(56:8)	TG(16:0/18:2/22:6)	Both	0.16	0.06	0.26	1.36E-02	0.11	0.03	0.18	3.53E-02	0.00
SM(d32:1)	SM(d16:1/16:0)	%VAT$_{TBF}$	-0.01	-0.19	0.17	9.67E-01	-0.18	-0.31	-0.05	3.98E-02	0.00
PC(P-38:6)		%VAT$_{TBF}$	-0.06	-0.17	0.06	5.43E-01	-0.11	-0.19	-0.02	4.99E-02	-0.02
TG(58:10)		FPG	0.15	0.04	0.25	3.69E-02	0.05	-0.03	0.13	3.48E-01	-0.03
PE(36:3)	PE(18:1/18:2)	FPG	0.20	0.07	0.33	1.37E-02	0.07	-0.03	0.18	3.09E-01	-0.04
SM(d43:2)		Both	-0.17	-0.29	-0.04	4.92E-02	-0.44	-0.77	-0.10	4.94E-02	-0.06
PC(O-36:3)		%VAT$_{TBF}$	-0.05	-0.17	0.07	6.11E-01	-0.12	-0.21	-0.03	3.78E-02	-0.07

PC(36:5)		FPG	0.21	0.09	0.32	7.80E-03	-0.05	-0.14	0.04	4.76E-01	-0.08
TG(52:6)	TG(16:1/18:2/18:3)	FPG	0.17	0.06	0.28	1.36E-02	0.08	0.00	0.16	1.49E-01	-0.08
PC(P-36:2)		$\%VAT_{TBF}$	-0.06	-0.18	0.06	5.45E-01	-0.17	-0.26	-0.08	3.48E-03	-0.08
TG(58:8)	TG(18:1/18:1/22:6)	FPG	0.15	0.04	0.25	2.99E-02	0.07	-0.01	0.15	1.98E-01	-0.09
LP_902.6995_486.7		FPG	-0.20	-0.34	-0.06	3.69E-02	-0.13	-0.24	-0.02	6.75E-02	-0.09
SM(d34:1)	SM(d18:1/16:0)	$\%VAT_{TBF}$	-0.15	-0.29	-0.01	1.20E-01	-0.15	-0.26	-0.05	2.26E-02	-0.14
PC(P-40:7)		$\%VAT_{TBF}$	-0.05	-0.17	0.07	6.16E-01	-0.14	-0.22	-0.05	1.55E-02	-0.15
TG(58:9)	TG(18:1/18:2/22:6)	FPG	0.17	0.07	0.27	1.14E-02	0.10	0.02	0.17	6.93E-02	-0.16
PC(36:4)	PC(18:2/18:2)	FPG	0.18	0.07	0.29	1.37E-02	-0.04	-0.13	0.05	5.25E-01	-0.17
PE(36:2)	PE(18:0/18:2)	Both	0.21	0.08	0.34	1.39E-02	0.13	0.05	0.22	1.68E-02	-0.19
DG(34:3)		Both	0.20	0.09	0.30	3.83E-03	0.16	0.08	0.24	1.45E-03	-0.20
PC(P-38:3)'		$\%VAT_{TBF}$	-0.10	-0.24	0.03	3.27E-01	-0.15	-0.25	-0.05	2.06E-02	-0.21
SM(d35:1)		$\%VAT_{TBF}$	-0.09	-0.24	0.05	4.22E-01	-0.15	-0.26	-0.04	4.23E-02	-0.25
LP_776.58_338.34		$\%VAT_{TBF}$	-0.08	-0.24	0.09	5.85E-01	-0.22	-0.34	-0.09	6.10E-03	-0.26
PE(34:1)		$\%VAT_{TBF}$	0.04	-0.11	0.20	7.82E-01	0.18	0.05	0.31	3.62E-02	-0.27
PC(38:7)		$\%VAT_{TBF}$	0.10	-0.03	0.23	3.31E-01	-0.13	-0.23	-0.03	4.23E-02	-0.28
PC(O-30:0)		$\%VAT_{TBF}$	-0.11	-0.32	0.09	4.94E-01	-0.21	-0.36	-0.06	3.78E-02	-0.34
PE(34:2)		$\%VAT_{TBF}$	0.05	-0.08	0.18	6.51E-01	0.13	0.03	0.23	4.23E-02	-0.35
LP_756.5894_387.1		$\%VAT_{TBF}$	-0.06	-0.19	0.06	5.38E-01	-0.18	-0.27	-0.09	2.11E-03	-0.36
SM(d36:0)		$\%VAT_{TBF}$	0.12	0.01	0.24	1.24E-01	0.13	0.04	0.22	3.02E-02	-0.37
Cer(d42:2)	Cer(d18:1/24:1)	$\%VAT_{TBF}$	0.13	0.00	0.25	1.60E-01	0.12	0.03	0.22	4.98E-02	-0.38
LP_536.438_504.2		$\%VAT_{TBF}$	-0.06	-0.22	0.09	6.21E-01	-0.21	-0.32	-0.09	4.22E-03	-0.46
PC(P-34:3)		$\%VAT_{TBF}$	-0.03	-0.16	0.11	8.58E-01	-0.21	-0.31	-0.12	8.48E-04	-0.48
CE(18:1)		$\%VAT_{TBF}$	-0.08	-0.34	0.18	7.60E-01	-0.25	-0.44	-0.06	4.82E-02	-0.48
Cer(d39:1)		FPG	0.20	0.05	0.35	4.92E-02	0.04	-0.07	0.16	6.24E-01	-0.67
PC(38:3)	PC(18:0/20:3)	$\%VAT_{TBF}$	0.07	-0.04	0.18	4.46E-01	0.11	0.02	0.19	4.94E-02	-0.69

PE(40:6)	PE(18:0/22:6)	$\%VAT_{TBF}$	0.05	-0.06	0.17	6.02E-01	0.15	0.06	0.23	1.09E-02	-0.74
PC(38:6)	PC(18:2/20:4)	FPG	0.18	0.05	0.30	3.08E-02	0.01	-0.08	0.11	8.73E-01	-0.79
Hexose A(glucose)		FPG	0.32	0.19	0.45	3.01E-04	-0.03	-0.13	0.07	8.60E-01	NA
Hexose B(glucose)		FPG	0.23	0.11	0.35	4.82E-03	0.00	-0.09	0.09	9.95E-01	NA

β: beta-coefficient of individual metabolites as indepedent variable in the linear regression model adjusting for age, gender and BMI. p: adjusted p-value using Benjamin-Hochberg multiple testing correction (cut-off value 0.05). Importance: decreases in accuracy of each metabolite in the random forest model for the prediction of FPG state. CE: cholesteryl ester; Cer: ceramide; DG: diacylglycerol; FA: fatty acid; HexCer: hexosylceramide; PC: phosphatidylcholine; PE: phosphatidylethanolamine; SM: sphingomyelin; TG: triacylglycerol.Unknown ID is displayed in the form of "platform, ESI mode, m/z and retention time" in seconds for lipid or in minutes for polar metabolites. LP: lipidomics ESI+; LN: lipidomics ESI-; HP: HILIC ESI+.

Table 9.12: Performances of PLS models before and after exclusion of outliers

	entire dataset					excluding outliers					
	n	R2Y	Q2	Kurtosis test (p)	$P_{CV\text{-}ANOVA}$	n	R2Y	Q2	Kurtosis test (p)	$P_{CV\text{-}ANOVA}$	excluded ID
Pancreatic fat	n=65	0.27	0.07	0.0000	1.02E-01	n=62	0.39	0.25	0.2745	2.43E-04	41261; 41244; 41378
Liver fat	n=67	0.34	0.08	0.0122	6.57E-02	n=62	0.52	0.33	0.0557	6.86E-06	41038; 41319; 41167; 41128; 41378
VAT/SAT	n=68	0.38	0.17	0.0000	2.10E-03	n=67	0.47	0.30	0.9512	1.32E-05	41370

n: number of samples; nComp: number of components; R2Y: goodness of model fit; Q2: predictivity; Pcv-anova: statistical significance of the PLS model

Table 9.13: Model performances of PLS-rdCV before and after variable selection by MUVR.

	Pancreatic fat		Liver fat		VAT/SAT	
	Full metabolome	post-selection	Full metabolome	post-selection	Full metabolome	post-selection
nVar	910	61	910	69	910	35
nComp	2	4	2	3	2	3
R2Y	0.656	0.865	0.665	0.791	0.646	0.748
Q2	0.214	0.698	0.311	0.657	0.243	0.628
r	0.496	0.838	0.576	0.811	0.523	0.794
p	4.11E-05	< 2.2e-16	9.69E-07	1.41E-15	5.59E-06	1.11E-15
pPerm	2.75E-04	2.75E-09	1.94E-04	4.01E-11	1.59E-04	2.22E-16
δ(Perm Q2, Actual Q2)	0.923	0.703	0.718	0.873	0.629	0.736

nVar: number of variables; nComp: number of components; R2Y: goodness of model fit; Q2: predictivity; r: Pearson correlation coefficient; p: significance of Pearson correlation; Perm: 100 permutation tests; δ(Perm Q2, Actual Q2) difference between permuted Q2 and actual Q2 value, and the p-value (pPerm) of permutation tests.

Table 9.14: Variable parameters of metabolites associated with pancreatic fat.

ID	*M1 (ethnicity)*		*M2 (ethnicity + BMI + %TBF)*		*M3 (ethnicity + BMI + %TBF + VAT/SAT)*		*PLS*			
	β (CI 2.5%-97.5%)	p	β (CI 2.5%-97.5%)	p	β (CI 2.5%-97.5%)	p	CoeffCS	CoeffCScvSE	CI 2.5%	CI 97.5%
CE(20:3)	0.62 (0.38-0.86)	1.22E-03	0.42 (0.18-0.66)	2.74E-02	0.24 (-0.01-0.49)	3.01E-01	0.04	0.03	-0.02	0.09
DG(16:0/18:1)	0.46 (0.22-0.69)	5.80E-03	0.32 (0.11-0.53)	4.20E-02	0.16 (-0.05-0.38)	4.18E-01	0.01	0.01	-0.02	0.04
DG(16:0/18:2)	0.5 (0.26-0.73)	2.61E-03	0.35 (0.13-0.56)	3.69E-02	0.19 (-0.03-0.4)	3.73E-01	0.04	0.02	0.01	0.07
FA(16:1)	0.35 (0.1-0.59)	3.66E-02	0.15 (-0.08-0.39)	3.95E-01	0.15 (-0.05-0.35)	4.41E-01	0.08	0.07	-0.06	0.22
Glucose	0.18 (-0.08-0.43)	3.52E-01	0.11 (-0.11-0.32)	5.16E-01	0.15 (-0.03-0.34)	3.94E-01	0.15	0.07	0.01	0.28
Kynurenic acid	-0.33 (-0.58--0.08)	5.36E-02	-0.24 (-0.45--0.02)	1.34E-01	-0.2 (-0.38--0.01)	2.65E-01	0.00	0.04	-0.08	0.08
L-Asparagine	-0.42 (-0.67--0.17)	1.47E-02	-0.22 (-0.45-0.02)	2.16E-01	-0.11 (-0.32-0.11)	6.05E-01	-0.04	0.03	-0.10	0.02
L-Isoleucine	-0.27 (-0.52--0.02)	1.30E-01	-0.18 (-0.39-0.04)	2.80E-01	-0.11 (-0.3-0.08)	5.44E-01	-0.02	0.03	-0.08	0.04
L-Leucine	-0.24 (-0.5-0.01)	1.79E-01	-0.14 (-0.36-0.08)	4.00E-01	-0.1 (-0.29-0.09)	6.03E-01	0.02	0.03	-0.03	0.07
LN_557.4572_317.72	0.15 (-0.12-0.43)	4.83E-01	0.08 (-0.16-0.33)	6.93E-01	0 (-0.21-0.22)	9.93E-01	0.15	0.04	0.06	0.23
LN_814.5418_298.91	0.38 (0.13-0.62)	2.47E-02	0.2 (-0.03-0.43)	2.47E-01	0.08 (-0.13-0.29)	7.14E-01	0.08	0.03	0.02	0.14
LP_847.6864_385.63	0.52 (0.28-0.77)	2.61E-03	0.39 (0.16-0.61)	2.80E-02	0.25 (0.03-0.47)	2.37E-01	-0.01	0.03	-0.07	0.05
LP_871.6894_361.17	0.53 (0.28-0.77)	2.61E-03	0.39 (0.17-0.6)	2.73E-02	0.24 (0.02-0.46)	2.39E-01	0.02	0.04	-0.06	0.11
LPA(22:5)	-0.22 (-0.47-0.04)	2.36E-01	-0.16 (-0.37-0.05)	3.26E-01	-0.21 (-0.39--0.03)	2.37E-01	-0.13	0.07	-0.27	0.01
LPC(22:6)	-0.18 (-0.44-0.08)	3.42E-01	0.05 (-0.18-0.28)	8.01E-01	0.07 (-0.14-0.27)	7.53E-01	-0.11	0.06	-0.23	0.02
L-Phenylalanine	-0.25 (-0.5-0)	1.66E-01	-0.14 (-0.35-0.08)	4.07E-01	-0.13 (-0.32-0.05)	4.59E-01	0.04	0.02	0.01	0.07
L-Tryptophan	-0.28 (-0.53--0.03)	1.16E-01	-0.13 (-0.35-0.09)	4.32E-01	-0.12 (-0.31-0.07)	5.19E-01	-0.02	0.03	-0.08	0.04
Methionyl-Methionine	0.41 (0.17-0.65)	1.27E-02	0.37 (0.17-0.56)	1.93E-02	0.32 (0.15-0.49)	7.54E-02	0.14	0.07	0.01	0.26
PC(31:1)	0.59 (0.34-0.85)	1.91E-03	0.35 (0.07-0.62)	8.65E-02	0.27 (0.03-0.51)	2.37E-01	0.00	0.03	-0.06	0.06
PC(32:1)	0.63 (0.37-0.88)	1.29E-03	0.39 (0.12-0.66)	5.74E-02	0.31 (0.07-0.55)	2.37E-01	0.01	0.03	-0.04	0.07
PC(16:0/18:1)	0.28 (0.01-0.55)	1.38E-01	0.14 (-0.1-0.38)	4.39E-01	0.03 (-0.18-0.25)	9.01E-01	-0.09	0.02	-0.14	-0.05
PC(16:0/20:3)	0.54 (0.31-0.78)	1.96E-03	0.42 (0.21-0.62)	1.75E-02	0.27 (0.06-0.49)	2.37E-01	0.06	0.04	-0.01	0.13
PC(18:1/20:3)	0.55 (0.3-0.79)	2.13E-03	0.36 (0.12-0.6)	4.33E-02	0.25 (0.03-0.47)	2.37E-01	0.07	0.03	0.00	0.12
PC(O-32:0)	-0.12 (-0.39-0.14)	5.62E-01	-0.14 (-0.35-0.08)	4.12E-01	-0.11 (-0.3-0.07)	5.37E-01	-0.13	0.06	-0.25	-0.01
Phosphorylcholine	-0.43 (-0.67--0.18)	1.23E-02	-0.25 (-0.48--0.03)	1.33E-01	-0.16 (-0.37-0.05)	4.13E-01	-0.09	0.02	-0.12	-0.04

PI(40:6)	-0.05 (-0.32-0.21)	8.23E-01	0.11 (-0.12-0.34)	5.49E-01	0.12 (-0.08-0.32)	5.33E-01	-0.11	0.07	-0.25	0.03
SM(d18:2/18:0)	0.38 (0.13-0.63)	2.47E-02	0.15 (-0.09-0.39)	4.11E-01	0.08 (-0.14-0.29)	7.13E-01	0.09	0.05	0.00	0.18
SM(d36:3)	0.57 (0.3-0.84)	2.88E-03	0.37 (0.09-0.64)	7.15E-02	0.3 (0.06-0.54)	2.37E-01	0.06	0.03	0.00	0.13
SM(d40:1)'	0.41 (0.17-0.65)	1.30E-02	0.28 (0.06-0.51)	8.93E-02	0.24 (0.04-0.44)	2.37E-01	0.08	0.06	-0.04	0.19
Sulfolithocholic acid	0.37 (0.13-0.61)	2.65E-02	0.42 (0.23-0.61)	1.75E-02	0.36 (0.19-0.53)	3.87E-02	0.16	0.07	0.02	0.29
TG(47:0)	0.49 (0.26-0.72)	2.61E-03	0.37 (0.16-0.57)	2.40E-02	0.26 (0.07-0.45)	2.24E-01	0.03	0.03	-0.03	0.10
TG(14:0/15:0/18:1)	0.53 (0.3-0.77)	2.02E-03	0.39 (0.19-0.6)	1.90E-02	0.29 (0.09-0.49)	2.02E-01	0.03	0.03	-0.04	0.09
TG(14:0/16:0/18:1)	0.49 (0.26-0.72)	2.61E-03	0.34 (0.13-0.55)	3.54E-02	0.22 (0.01-0.42)	2.65E-01	0.00	0.01	-0.01	0.02
TG(48:2)	0.49 (0.25-0.73)	3.61E-03	0.34 (0.12-0.55)	4.20E-02	0.22 (0.02-0.43)	2.55E-01	-0.01	0.02	-0.05	0.04
TG(15:0/16:0/18:1)	0.51 (0.28-0.74)	2.13E-03	0.4 (0.2-0.6)	1.75E-02	0.3 (0.11-0.48)	1.58E-01	0.03	0.03	-0.02	0.08
TG(15:0/16:0/18:2)	0.54 (0.32-0.76)	1.29E-03	0.42 (0.22-0.61)	1.75E-02	0.31 (0.12-0.5)	1.37E-01	0.04	0.02	-0.01	0.08
TG(15:0/16:1/18:2)	0.47 (0.24-0.7)	4.30E-03	0.37 (0.17-0.57)	1.90E-02	0.27 (0.08-0.45)	2.17E-01	0.03	0.02	-0.01	0.07
TG(16:0/16:0/18:1)	0.5 (0.27-0.72)	2.52E-03	0.35 (0.15-0.56)	2.80E-02	0.2 (-0.01-0.41)	3.01E-01	0.01	0.02	-0.04	0.05
TG(50:2)	0.54 (0.31-0.77)	1.91E-03	0.36 (0.13-0.58)	4.12E-02	0.26 (0.06-0.47)	2.37E-01	0.00	0.02	-0.04	0.04
TG(50:3)	0.51 (0.28-0.73)	2.13E-03	0.36 (0.15-0.56)	2.80E-02	0.26 (0.07-0.45)	2.37E-01	0.02	0.02	-0.02	0.07
TG(16:0/17:0/18:1)	0.45 (0.22-0.69)	5.80E-03	0.35 (0.15-0.55)	2.74E-02	0.22 (0.02-0.42)	2.37E-01	0.01	0.02	-0.04	0.05
TG(16:0/17:1/18:1)	0.51 (0.28-0.73)	2.13E-03	0.41 (0.22-0.6)	1.75E-02	0.29 (0.1-0.48)	1.58E-01	0.03	0.02	-0.01	0.08
TG(15:0/18:1/18:2)	0.47 (0.23-0.7)	5.33E-03	0.38 (0.18-0.58)	1.90E-02	0.25 (0.04-0.45)	2.37E-01	0.05	0.03	-0.01	0.11
TG(16:0/18:0/18:1)	0.45 (0.21-0.68)	7.57E-03	0.31 (0.1-0.52)	4.98E-02	0.15 (-0.06-0.37)	4.50E-01	-0.01	0.02	-0.05	0.04
TG(16:0/18:1/18:1)	0.49 (0.26-0.72)	2.61E-03	0.38 (0.18-0.58)	1.90E-02	0.23 (0.03-0.44)	2.37E-01	0.02	0.02	-0.02	0.07
TG(53:1)	0.48 (0.26-0.71)	2.65E-03	0.34 (0.14-0.55)	3.36E-02	0.22 (0.02-0.42)	2.37E-01	0.00	0.01	-0.02	0.02
TG(53:2)'	0.47 (0.24-0.7)	3.55E-03	0.35 (0.14-0.55)	2.80E-02	0.22 (0.03-0.42)	2.37E-01	0.01	0.01	0.00	0.03
TG(54:1)'	0.48 (0.25-0.71)	2.83E-03	0.35 (0.15-0.55)	2.80E-02	0.23 (0.03-0.43)	2.37E-01	0.02	0.02	-0.02	0.06
TG(55:1)	0.49 (0.27-0.72)	2.61E-03	0.36 (0.16-0.56)	2.73E-02	0.2 (-0.01-0.42)	3.05E-01	0.02	0.02	-0.02	0.05
TG(55:2)	0.57 (0.36-0.78)	1.22E-03	0.41 (0.21-0.62)	1.75E-02	0.28 (0.08-0.49)	2.24E-01	0.05	0.02	0.02	0.08
TG(56:1)	0.55 (0.33-0.77)	1.22E-03	0.39 (0.18-0.6)	1.90E-02	0.25 (0.04-0.46)	2.37E-01	0.04	0.02	0.00	0.07
TG(56:2)	0.43 (0.19-0.67)	1.04E-02	0.3 (0.09-0.51)	5.80E-02	0.13 (-0.08-0.35)	5.35E-01	0.00	0.04	-0.08	0.08
TG(57:2)	0.47 (0.23-0.7)	5.24E-03	0.35 (0.15-0.55)	2.80E-02	0.19 (-0.03-0.4)	3.67E-01	0.03	0.03	-0.02	0.09

TG(58:2)	0.52 (0.3-0.75)	1.91E-03	0.4 (0.2-0.6)	1.77E-02	0.25 (0.04-0.46)	2.37E-01	0.04	0.02	0.00	0.08
Urea	-0.42 (-0.65--0.18)	1.14E-02	-0.23 (-0.46--0.01)	1.70E-01	-0.17 (-0.37-0.03)	3.67E-01	-0.07	0.05	-0.16	0.03
HP_96.0817_11.19	-0.42 (-0.66--0.18)	1.27E-02	-0.27 (-0.49--0.06)	8.79E-02	-0.19 (-0.39-0)	2.96E-01	-0.07	0.06	-0.20	0.06

p: adjusted p-value using Benjamin-Hochberg multiple testing correction (cut-off value 0.05). CE: cholesteryl ester; DG: diacylglycerol; FA: fatty acid; LPA: lysophosphatidic acid; LPC: lysophosphatidylcholine; PC: phosphatidylcholine; SM: sphingomyelin; TG: triacylglycerol. Unknown ID is displayed in the form of "platform, ESI mode, m/z and retention time" in seconds for lipid or in minutes for polar metabolites. LP: lipidomics ESI+; LN: lipidomics ESI-; HP: HILIC ESI+.

Table 9.15: Variable parameters of metabolites associated with liver fat.

ID	*M1 (ethnicity)*		*M2 (ethnicity + BMI + %TBF)*		*M3 (ethnicity + BMI + %TBF + VAT/SAT)*		*PLS*			
	β (CI 2.5%-97.5%)	p	β (CI 2.5%-97.5%)	p	β (CI 2.5%-97.5%)	p	CoeffCS	CoeffCScvSE	CI 2.5%	CI 97.5%
DG(16:0/18:1)	0.64 (0.45-0.84)	5.76E-07	0.59 (0.39-0.8)	1.05E-05	0.58 (0.35-0.8)	1.17E-04	0.01	0.01	-0.02	0.03
DG(16:0/18:2)	0.63 (0.43-0.83)	1.67E-06	0.58 (0.37-0.79)	4.11E-05	0.56 (0.32-0.79)	3.73E-04	0.02	0.02	-0.03	0.06
DG(34:3)	0.6 (0.39-0.8)	7.27E-06	0.54 (0.33-0.76)	1.04E-04	0.51 (0.28-0.74)	9.37E-04	0.03	0.03	-0.03	0.08
DG(18:1/18:1)	0.5 (0.28-0.73)	3.50E-04	0.45 (0.23-0.67)	2.10E-03	0.41 (0.16-0.66)	2.10E-02	-0.02	0.02	-0.06	0.01
DG(38:2)	0.52 (0.3-0.74)	2.01E-04	0.48 (0.26-0.69)	7.67E-04	0.44 (0.2-0.67)	5.86E-03	-0.01	0.02	-0.05	0.03
FA(16:0)	0.18 (-0.08-0.43)	4.73E-01	0.09 (-0.17-0.35)	8.11E-01	0.02 (-0.24-0.28)	9.78E-01	0.02	0.03	-0.03	0.07
FA(18:0)	0.19 (-0.06-0.45)	4.07E-01	0.12 (-0.14-0.37)	7.42E-01	0.03 (-0.24-0.29)	9.73E-01	0.00	0.02	-0.04	0.04
FA(18:1)	0.12 (-0.14-0.39)	6.68E-01	0.06 (-0.21-0.32)	8.79E-01	0.01 (-0.24-0.27)	9.86E-01	0.05	0.02	0.01	0.08
FA(18:2)	0.13 (-0.16-0.42)	6.84E-01	0.1 (-0.18-0.38)	8.09E-01	0.03 (-0.25-0.31)	9.73E-01	0.05	0.03	-0.01	0.10
FA(22:5)	0.22 (-0.03-0.47)	2.96E-01	0.22 (-0.01-0.46)	2.76E-01	0.22 (-0.01-0.45)	3.19E-01	0.08	0.07	-0.07	0.22
LacCer(d34:1)	-0.28 (-0.53--0.03)	1.26E-01	-0.3 (-0.53--0.07)	7.72E-02	-0.25 (-0.48--0.01)	2.44E-01	-0.11	0.03	-0.17	-0.04
Lactic acid	0.47 (0.23-0.72)	2.55E-03	0.4 (0.14-0.66)	2.61E-02	0.33 (0.06-0.61)	1.31E-01	0.10	0.03	0.04	0.16
L-Homocitrulline	-0.15 (-0.43-0.12)	5.87E-01	-0.08 (-0.35-0.2)	8.39E-01	-0.08 (-0.35-0.18)	8.76E-01	-0.11	0.03	-0.18	-0.04
LN_355.1585_213.13	0.16 (-0.09-0.42)	5.25E-01	0.08 (-0.18-0.34)	8.21E-01	0.01 (-0.25-0.27)	9.86E-01	0.01	0.03	-0.04	0.07
LP_624.6401_404.17	0.2 (-0.06-0.45)	4.07E-01	0.11 (-0.15-0.37)	7.55E-01	0.04 (-0.22-0.3)	9.57E-01	-0.11	0.09	-0.28	0.06
LP_894.8462_708.86	0.78 (0.62-0.94)	2.99E-11	0.75 (0.58-0.91)	7.19E-10	0.72 (0.56-0.89)	6.08E-09	0.09	0.03	0.04	0.14
PC(16:0/18:2)	0.38 (0.14-0.62)	1.48E-02	0.34 (0.11-0.57)	3.58E-02	0.29 (0.05-0.53)	1.40E-01	0.08	0.05	-0.02	0.18
PE(34:1)	0.6 (0.39-0.8)	9.22E-06	0.54 (0.32-0.77)	1.76E-04	0.5 (0.28-0.73)	8.95E-04	0.03	0.06	-0.08	0.15
PE(34:2)	0.52 (0.3-0.74)	1.91E-04	0.48 (0.26-0.7)	7.46E-04	0.45 (0.23-0.66)	2.16E-03	0.04	0.05	-0.06	0.13
PE(18:0/18:2)	0.53 (0.31-0.74)	1.58E-04	0.5 (0.29-0.71)	2.43E-04	0.46 (0.25-0.68)	1.51E-03	0.05	0.04	-0.03	0.13
PI(40:6)	0.05 (-0.21-0.32)	8.77E-01	0.13 (-0.13-0.39)	7.03E-01	0.09 (-0.16-0.34)	8.47E-01	-0.10	0.03	-0.16	-0.04
SM(d36:0)	0.6 (0.39-0.8)	7.27E-06	0.55 (0.35-0.76)	4.11E-05	0.52 (0.31-0.73)	2.31E-04	0.04	0.04	-0.04	0.11
TG(14:0/14:0/16:0)	0.58 (0.37-0.8)	1.85E-05	0.53 (0.32-0.75)	1.04E-04	0.53 (0.32-0.73)	1.09E-04	0.05	0.05	-0.06	0.15
TG(14:0/16:0/16:0)	0.73 (0.55-0.9)	6.00E-09	0.68 (0.5-0.86)	6.37E-08	0.66 (0.48-0.83)	1.48E-07	0.07	0.03	0.00	0.13
TG(12:0/16:0/18:1)	0.65 (0.46-0.85)	4.82E-07	0.61 (0.41-0.81)	4.25E-06	0.58 (0.38-0.78)	1.28E-05	0.05	0.03	-0.02	0.11

TG(47:0)	0.65 (0.45-0.85)	8.61E-07	0.6 (0.41-0.8)	4.25E-06	0.58 (0.39-0.77)	8.77E-06	0.04	0.05	-0.06	0.14
TG(14:0/16:0/18:0)	0.76 (0.6-0.92)	1.69E-10	0.73 (0.55-0.9)	6.01E-09	0.7 (0.52-0.88)	5.20E-08	0.07	0.02	0.04	0.11
TG(14:0/16:0/18:1)	0.7 (0.52-0.89)	4.18E-08	0.66 (0.47-0.85)	7.14E-07	0.63 (0.43-0.82)	3.94E-06	0.03	0.02	0.00	0.06
TG(14:0/16:0/18:2)	0.65 (0.45-0.84)	5.76E-07	0.6 (0.4-0.8)	7.88E-06	0.57 (0.36-0.77)	4.95E-05	0.02	0.02	-0.01	0.06
TG(12:0/18:1/18:2)	0.58 (0.38-0.79)	1.12E-05	0.54 (0.33-0.74)	6.00E-05	0.5 (0.29-0.71)	3.74E-04	0.03	0.02	-0.01	0.07
TG(16:0/16:0/17:0)	0.66 (0.47-0.85)	2.48E-07	0.62 (0.43-0.81)	1.19E-06	0.59 (0.41-0.78)	3.94E-06	0.04	0.04	-0.03	0.12
TG(15:0/16:0/18:1)	0.61 (0.4-0.82)	7.27E-06	0.56 (0.35-0.77)	4.11E-05	0.53 (0.32-0.74)	1.20E-04	-0.01	0.04	-0.08	0.07
TG(15:0/16:0/18:2)	0.6 (0.4-0.81)	7.27E-06	0.55 (0.34-0.77)	6.16E-05	0.52 (0.3-0.73)	2.75E-04	-0.01	0.03	-0.07	0.05
TG(15:0/16:1/18:2)	0.59 (0.39-0.8)	9.18E-06	0.55 (0.34-0.75)	5.27E-05	0.51 (0.31-0.72)	1.75E-04	0.01	0.02	-0.04	0.06
TG(16:0/16:0/18:0)	0.73 (0.56-0.91)	1.81E-09	0.7 (0.52-0.87)	2.27E-08	0.68 (0.49-0.86)	1.89E-07	0.06	0.02	0.03	0.09
TG(16:0/16:0/18:1)	0.66 (0.47-0.85)	2.48E-07	0.62 (0.41-0.82)	6.71E-06	0.59 (0.37-0.81)	7.81E-05	0.01	0.02	-0.03	0.05
TG(16:0/16:1/18:1)	0.61 (0.41-0.81)	3.54E-06	0.56 (0.35-0.78)	7.60E-05	0.53 (0.3-0.76)	7.04E-04	-0.01	0.03	-0.07	0.06
TG(16:0/16:1/18:2)	0.6 (0.4-0.81)	6.79E-06	0.55 (0.33-0.76)	8.60E-05	0.52 (0.28-0.75)	8.95E-04	0.01	0.02	-0.03	0.06
TG(16:0/17:0/18:1)	0.6 (0.39-0.8)	8.55E-06	0.55 (0.34-0.76)	4.51E-05	0.51 (0.3-0.73)	2.58E-04	0.00	0.04	-0.08	0.07
TG(16:0/17:1/18:1)	0.54 (0.33-0.76)	7.90E-05	0.49 (0.28-0.71)	4.38E-04	0.45 (0.23-0.68)	2.46E-03	-0.04	0.02	-0.08	0.01
TG(15:0/18:1/18:2)	0.55 (0.33-0.76)	7.14E-05	0.5 (0.29-0.71)	2.74E-04	0.46 (0.24-0.69)	2.22E-03	-0.01	0.01	-0.03	0.01
TG(16:0/18:0/18:1)	0.68 (0.49-0.87)	8.19E-08	0.64 (0.44-0.84)	1.27E-06	0.62 (0.41-0.82)	1.30E-05	0.05	0.02	0.01	0.09
TG(16:0/18:1/18:1)	0.47 (0.24-0.7)	1.24E-03	0.41 (0.18-0.64)	8.05E-03	0.36 (0.1-0.61)	5.86E-02	-0.04	0.03	-0.10	0.02
TG(53:1)	0.69 (0.51-0.88)	6.40E-08	0.65 (0.45-0.84)	9.40E-07	0.62 (0.42-0.81)	3.94E-06	0.03	0.02	-0.01	0.06
TG(17:0/18:1/18:1)	0.51 (0.28-0.73)	3.48E-04	0.47 (0.25-0.68)	8.73E-04	0.43 (0.2-0.65)	4.79E-03	-0.02	0.02	-0.07	0.02
TG(53:2)'	0.65 (0.46-0.84)	4.56E-07	0.6 (0.4-0.8)	5.85E-06	0.57 (0.37-0.77)	3.54E-05	0.03	0.02	-0.01	0.06
TG(17:0/18:1/18:2)	0.47 (0.24-0.7)	1.44E-03	0.44 (0.22-0.66)	2.80E-03	0.39 (0.15-0.63)	2.19E-02	-0.03	0.02	-0.06	0.00
TG(54:1)'	0.68 (0.49-0.87)	1.05E-07	0.63 (0.44-0.83)	1.19E-06	0.6 (0.41-0.8)	7.15E-06	0.03	0.02	-0.01	0.07
TG(18:0/18:1/18:1)	0.53 (0.31-0.75)	1.85E-04	0.47 (0.25-0.7)	1.11E-03	0.43 (0.19-0.67)	8.96E-03	-0.03	0.02	-0.07	0.01
TG(55:0)	0.68 (0.5-0.87)	7.93E-08	0.65 (0.46-0.83)	6.11E-07	0.62 (0.43-0.81)	3.94E-06	0.06	0.01	0.03	0.09
TG(55:1)	0.69 (0.5-0.87)	6.35E-08	0.65 (0.45-0.85)	1.19E-06	0.65 (0.43-0.87)	1.30E-05	0.03	0.02	-0.01	0.06
TG(55:2)	0.61 (0.41-0.82)	3.47E-06	0.57 (0.35-0.79)	7.60E-05	0.53 (0.3-0.76)	6.70E-04	0.00	0.02	-0.04	0.04
TG(55:3)	0.61 (0.41-0.82)	4.76E-06	0.56 (0.35-0.77)	5.14E-05	0.54 (0.3-0.77)	5.44E-04	0.02	0.03	-0.03	0.08

TG(55:3)'	0.45 (0.22-0.68)	2.34E-03	0.43 (0.21-0.65)	2.81E-03	0.39 (0.15-0.62)	1.87E-02	-0.04	0.02	-0.09	0.01
TG(56:1)	0.59 (0.38-0.8)	1.00E-05	0.54 (0.31-0.77)	2.74E-04	0.5 (0.25-0.75)	2.50E-03	-0.02	0.03	-0.07	0.04
TG(56:2)	0.65 (0.46-0.84)	4.45E-07	0.6 (0.4-0.8)	7.42E-06	0.58 (0.36-0.81)	8.54E-05	0.02	0.01	0.00	0.03
TG(56:2)'	0.59 (0.38-0.79)	9.18E-06	0.56 (0.35-0.76)	2.90E-05	0.55 (0.32-0.77)	2.90E-04	0.02	0.03	-0.04	0.08
TG(57:1)	0.66 (0.47-0.86)	2.48E-07	0.63 (0.44-0.82)	1.27E-06	0.6 (0.4-0.8)	1.28E-05	0.05	0.01	0.03	0.08
TG(57:2)	0.51 (0.29-0.73)	2.89E-04	0.45 (0.22-0.68)	2.80E-03	0.41 (0.15-0.67)	2.86E-02	-0.03	0.02	-0.07	0.02
TG(16:0/18:1/24:0)	0.66 (0.47-0.86)	4.47E-07	0.64 (0.46-0.83)	6.54E-07	0.61 (0.42-0.81)	3.94E-06	0.07	0.02	0.02	0.12
TG(58:1)'	0.67 (0.48-0.86)	1.49E-07	0.63 (0.44-0.83)	1.17E-06	0.61 (0.41-0.81)	8.96E-06	0.05	0.01	0.02	0.07
TG(58:2)	0.47 (0.24-0.7)	1.23E-03	0.41 (0.17-0.64)	9.74E-03	0.35 (0.09-0.61)	7.41E-02	-0.04	0.03	-0.09	0.01
TG(59:2)	0.58 (0.37-0.8)	1.85E-05	0.55 (0.34-0.76)	5.97E-05	0.53 (0.29-0.76)	6.79E-04	0.01	0.02	-0.02	0.04
TG(60:2)	0.56 (0.34-0.78)	6.42E-05	0.52 (0.31-0.74)	1.67E-04	0.5 (0.26-0.73)	1.80E-03	0.00	0.02	-0.04	0.04

p: adjusted p-value using Benjamin-Hochberg multiple testing correction (cut-off value 0.05). DG: diacylglycerol; FA: fatty acid; LacCer: lactosylceramide; PC: phosphatidylcholine; PE: phosphatidylethanolamine; PI: phosphatidylinositol; SM: sphingomyelin; TG: triacylglycerol. Unknown ID is displayed in the form of "platform, ESI mode, m/z and retention time" in seconds for lipid. LP: lipidomics ESI+; LN: lipidomics ESI-.

Table 9.16: Variable parameters of metabolites associated with VAT/SAT

ID	*M1 (ethnicity)*		*M2 (ethnicity + BMI + %TBF)*		*PLS*			
	β (CI 2.5%-97.5%)	p	β (CI 2.5%-97.5%)	p	CoeffCS	CoeffCScvSE	CI 2.5%	CI 97.5%
Cer(d41:1)	0.61 (0.4-0.81)	4.73E-05	0.57 (0.36-0.78)	1.09E-04	0.11	0.04	0.03	0.19
DG(18:1/18:1)	0.48 (0.27-0.7)	7.18E-04	0.46 (0.24-0.67)	1.76E-03	0.00	0.02	-0.04	0.04
DG(18:1/18:2)	0.52 (0.3-0.75)	5.81E-04	0.5 (0.27-0.72)	1.27E-03	0.01	0.02	-0.02	0.04
DG(38:2)	0.43 (0.21-0.65)	3.68E-03	0.41 (0.19-0.63)	6.58E-03	-0.02	0.02	-0.07	0.03
FA(16:0)	0.24 (0.01-0.48)	1.71E-01	0.19 (-0.06-0.44)	3.32E-01	0.12	0.03	0.06	0.17
FA(18:0)	0.36 (0.14-0.59)	2.10E-02	0.31 (0.08-0.55)	6.91E-02	0.15	0.04	0.07	0.22
FA(18:2)	0.28 (0.04-0.52)	1.14E-01	0.24 (-0.01-0.48)	2.02E-01	0.13	0.02	0.09	0.16
L-Cystine	0.54 (0.33-0.75)	1.52E-04	0.51 (0.3-0.72)	3.37E-04	0.17	0.08	0.02	0.32
PC(O-38:6)	0.32 (0.09-0.55)	5.06E-02	0.32 (0.1-0.55)	5.11E-02	0.15	0.05	0.05	0.24
TG(14:0/18:2/18:3)	0.23 (-0.01-0.48)	2.01E-01	0.22 (-0.01-0.46)	2.23E-01	-0.07	0.05	-0.17	0.04
TG(16:0/18:1/18:2)	0.55 (0.31-0.79)	5.79E-04	0.51 (0.26-0.76)	2.33E-03	0.02	0.02	-0.02	0.05
TG(16:0/18:2/18:2)	0.63 (0.39-0.87)	1.38E-04	0.59 (0.35-0.84)	3.37E-04	0.03	0.03	-0.02	0.09
TG(17:0/18:1/18:2)	0.5 (0.29-0.71)	4.27E-04	0.48 (0.27-0.69)	6.77E-04	0.01	0.01	-0.02	0.03
TG(17:1/18:1/18:2)	0.53 (0.31-0.75)	2.95E-04	0.51 (0.3-0.73)	4.42E-04	0.01	0.02	-0.02	0.04
TG(17:0/18:2/18:3)	0.34 (0.1-0.58)	4.85E-02	0.32 (0.09-0.56)	5.77E-02	-0.05	0.02	-0.09	-0.01
TG(54:2)	0.56 (0.35-0.76)	7.03E-05	0.54 (0.34-0.74)	1.14E-04	0.05	0.02	0.00	0.10
TG(18:0/18:1/18:2)	0.6 (0.39-0.81)	4.73E-05	0.6 (0.39-0.8)	6.49E-05	0.06	0.02	0.02	0.10
TG(18:1/18:2/18:2)	0.64 (0.4-0.88)	1.30E-04	0.64 (0.4-0.87)	1.14E-04	0.05	0.03	0.00	0.10
TG(55:3)	0.45 (0.24-0.67)	1.92E-03	0.42 (0.19-0.64)	7.11E-03	-0.01	0.01	-0.04	0.01
TG(56:2)	0.54 (0.34-0.74)	8.92E-05	0.52 (0.32-0.72)	2.05E-04	0.03	0.01	0.00	0.06
TG(18:1/18:1/20:1)	0.57 (0.37-0.77)	4.73E-05	0.57 (0.37-0.76)	6.49E-05	0.06	0.02	0.03	0.09
TG(57:2)	0.56 (0.37-0.76)	4.73E-05	0.53 (0.33-0.74)	1.55E-04	0.04	0.03	-0.01	0.10
TG(57:4)	0.65 (0.42-0.87)	4.73E-05	0.61 (0.39-0.84)	1.14E-04	0.05	0.01	0.02	0.07
TG(18:1/18:2/22:0)	0.58 (0.37-0.78)	4.73E-05	0.57 (0.37-0.77)	6.88E-05	0.07	0.05	-0.02	0.17
TG(58:4)	0.65 (0.42-0.87)	4.73E-05	0.62 (0.39-0.85)	1.14E-04	0.05	0.02	0.01	0.08

TG(59:2)	0.53 (0.32-0.74)	1.85E-04	0.5 (0.29-0.71)	4.17E-04	0.03	0.03	-0.03	0.09
TG(59:3)	0.58 (0.37-0.78)	4.97E-05	0.58 (0.38-0.78)	6.49E-05	0.04	0.02	0.01	0.08
TG(59:5)	0.64 (0.41-0.87)	4.73E-05	0.63 (0.41-0.85)	6.88E-05	0.05	0.01	0.03	0.07
TG(60:2)	0.53 (0.32-0.74)	1.82E-04	0.51 (0.3-0.72)	3.70E-04	0.03	0.03	-0.03	0.08
TG(20:1/18:1/22:1)	0.53 (0.32-0.73)	1.85E-04	0.55 (0.35-0.75)	1.01E-04	0.04	0.02	0.00	0.08
TG(60:5)	0.58 (0.34-0.82)	2.66E-04	0.58 (0.35-0.81)	2.19E-04	0.03	0.02	-0.01	0.08

p: adjusted p-value using Benjamin-Hochberg multiple testing correction (cut-off value 0.05). Cer: ceramide; FA: fatty acid; PC: phosphatidylcholine; TG: triacylglycerol.